Investigating c-FLIP Suppression and TRAIL Treatment in Breast Cancer

Andreia M. Silva

A dissertation submitted to Cardiff University in accordance with the requirements of the degree of Doctor of Philosophy (Ph.D)

School of Biosciences

September 2017

TABLE OF CONTENTS

DECLARATION

This work has not been submitted in substance for any other degree or award at this or any other university or place of learning, nor is being submitted concurrently in candidature for any degree or other award.

Signed …… (candidate) Date ……

STATEMENT 1

This thesis is being submitted in partial fulfillment of the requirements for the degree of PhD

Signed …… (candidate) Date ……

STATEMENT 2

This thesis is the result of my own independent work/investigation, except where otherwise stated. Other sources are acknowledged by explicit references. The views expressed are my own.

Signed …… (candidate) Date ……

STATEMENT 3

I hereby give consent for my thesis, if accepted, to be available for photocopying and for inter-library loan, and for the title and summary to be made available to outside organisations.

Signed …… (candidate) Date ……

STATEMENT 4: PREVIOUSLY APPROVED BAR ON ACCESS

I hereby give consent for my thesis, if accepted, to be available for photocopying and for inter-library loans **after expiry of a bar on access previously approved by the Academic Standards & Quality Committee.**

Signed …… (candidate) Date ……

DEDICATION

The most special thank you goes to my Mum, the strongest and most amazing woman I will ever meet. During my PhD, breast cancer took your life. You fought till the very end. I wish I could have spent more time with you. I think about you every day and I wish you to be proud of me as I am of you.

My work is dedicated to you and in your memory.

Breast cancer takes the life of 500000 women every year around the world.

AKNOWLEDGEMENTS

First and foremost I thank my supervisor, Dr. Richard Clarkson for the opportunity to conduct my thesis within his research group. Richard is a great group leader and being part of this group was a huge achievement for me and an opportunity I was very grateful to be offered. Thank you for all your support, guidance, patience and enthusiasm – it has been immeasurable. I also would like to thank Dr. Luke Piggott for his supervision, help collecting all the samples received during this study and help with the animal work.

I am grateful to *Tenovus*, the cancer charity who funded this study and my PhD, for all the support given over the last years and for being an incredible cancer charity. Also, thanks to the doctors and patients at Llandough Hospital for providing the breast biopsies for this study.

I would like to thank Dr. Bruno Simões and Dr. Robert Clarke for their invaluable collaboration on providing the metastatic breast samples provided for this work.

Thanks to Liv Hayward and Rhiannon French for listening my doubts, for the help and contributions on this study. I would like to thank all the other group members: Dan Turnham; Will Yang, Tim Robinson and Aleks Grupka for always helping me and for the great team ethos where we were all able to flourish. I cannot forget to thank all the ECSCRI members, for the enjoyable lab environment and of course the unforgettable pub nights after work.

During the last four years, I've had an unforgettable time in Cardiff and naturally, met some amazing people. A special mention goes to Guy for his love, patience and for always being there. I met friends for life and (should you ever read this) then to Sarah, Katie, Kristine, Sara, Penny, Maria, Kayla, Bex and Fen I thank you for the friendship and for making great memories with me.

Thanks to all my friends home in Portugal, during the last few years there were moments difficult for us to keep in touch, however; I hope you all know that I will always be there for you.

Very special thanks go to my Dad, my Sister and family for the love and for always supporting me. You made me who I am today.

ABSTRACT

Breast cancer mortality is invariably due to metastasis, the dissemination of cancer cells from the primary tumour to distant organs. This process is proposed to arise from the breast cancer stem cells (bCSCs), the minority of cells within a tumour that are capable of propagating new tumour growth. bCSCs are also associated with potentiating endocrine therapy resistance and therefore relapse after tamoxifen or anastrozole treatments. Tumour necrosis factor -related apoptosis inducing ligand (TRAIL) is an anti-cancer agent that induces apoptosis in bCSCs and has almost no toxicity to normal cells. However, there is an inherent resistance to TRAIL *in vitro* in a large proportion of breast cancer cell types due to the expression of the survival factor cellular FLICE-Like Inhibitory Protein (c-FLIP). It has been shown that siRNA-mediated suppression of the gene for c-FLIP combined with TRAIL is effective *in vitro* at sensitising bCSCs to apoptosis in breast cancer cell lines.

To test whether these findings have direct clinical relevance for breast cancer patients, diagnostic biopsies; surgical breast resections and pleural effusions were collected from the clinic. Testing TRAIL alone in breast samples resulted in a decrease in the number of tumourspheres in 82% of tumours that have acquired endocrine resistance to tamoxifen and anastrozole. Importantly, TRAIL was efficient *in vivo* at decreasing primary tumour size in tumours that have acquired resistance to tamoxifen *in vivo* and number of metastases of an anastrozole-resistant sample. Additionally, TRAIL was also effective at decreasing bCSCs in triple negative metastatic tumours, corroborating studies supporting a relationship between a mesenchymal phenotype and TRAIL sensitivity. However, there was no correlation between TRAIL response and either ER or HER2 status in primary breast samples.

Furthermore, c-FLIP was suppressed, either genetically (siRNA) or pharmacologically (OH14) and combined with TRAIL treatment sensitised bulk and bCSCs to TRAIL in breast tumours from patients with metastatic disease irrespective of their estrogen receptor (ER)/HER2 status.

As the tumour microenvironment can modulate drug responses, TRAIL treatment was investigated on breast cancer epithelial cells in the presence of cancer associated fibroblasts (CAFs) and CAFs-conditioned medium (CM). Short exposure to CAFs and CM sensitised MCF-7 and primary metastatic cells to TRAIL whereas a longer exposure to CM conferred resistance to TRAIL potentially due to an induction of epithelial-mesenchymal transition.

With these results in primary cells, TRAIL could be a valuable treatment to the clinic for patients that have acquired resistance to endocrine treatments. Additionally, c-FLIP suppression and TRAIL treatment could be a promising therapeutic treatment at eliminating bCSCs in patients with metastatic disease. We hypothesise that a partial EMT confers resistance to TRAIL but a full EMT state is associated with resistance to TRAIL.

LIST OF ABBREVIATONS

ACTB β-actin

Akt Protein kinase B

ALDH1 Aldehyde Dehydrogenase 1

BC Breast Cancer

bCSC breast Cancer Stem Cells

BRCA-1 Breast cancer 1

c-FLIP Cellular FLICE-Like Inhibitory Protein

CM Conditioned Medium

CSC Cancer Stem Cell

DCIS Ductal Carcinoma *in situ*

DcR Decoy receptor

DED Dead Effector Domain

DISC Death Inducing Signalling Complex

DR4 Death receptor 4

DR5 Death receptor 5

ECM Extracellular matrix

EGFR Epidermal Growth Factor Receptor

EMT Epithelial Mesenchymal Transition

ER Estrogen Receptor

ErbB2 Erythroblastic leukemia viral oncogene homolog

ERK Extracellular signal-regulated kinase

FACS Fluorescence Activated Cell Sorting

FADD Fas Associated Death Domain

FasL Fas Ligand

FBS Fetal Bovine Serum

FEC Fluorouracil, Epirubicin; Cyclophosphamide

FGF Fibroblast Growth Factor

HDAC Histone Deacetylase

HER2 Human Epidermal Receptor 2

HIF Hypoxia-Inducible Factor

HMECs Human Mammary epithelial cells

HRT Hormonal Replacement Therapy

iFLIP inhibition of c-FLIP

iFLIP/TRAIL inhibition of c-FLIP/TRAIL treatment

IGFR Insulin-like Growth Factor Receptor

IL-6 Interleukin 6

IL8 Interleukin 8

JNK c-jun N-termina Kinase

KD knock-down

LCIS Lobular Carcinoma *in situ*

MAC Molecular Apocrine

MaSCs Mammary stem cells

MPBC Metaplastic Breast Cancer

MAPK Mitogen-activated Protein Kinase

MDR1 Multidrug Resistance protein 1

MFU Mammosphere Forming Unit

MMPs Matrix Metalloproteinase

MMTV Mouse Mammary Tumour Virus

N-cadherin Neural-cadherin

NF-Kb Nuclear factor binding kappa-lighchain enhancer element

OH14 Olivia Hayward 14 – c-FLIP inhibitor

PBS Phosphate-buffered Saline

PCR Polymerase Chain Reaction

PI3K Phosphatidylinositol 3-kinase

PgR Progesterone Receptor

qRT-PCR Quantative Reverse Transcription PCR

PDX Patient derived xenograft

PgR Progesterone Receptor

RNA Ribonucleotid Nucleic Acid

Snail Zinc finger protein SNAI1 gene

siRNA small interfering RNA

siFLIP Inhibiton of c-FLIP using siRNA

shRNA short hairpin RNA

TFU Tumoursphere-forming unit

TGF-β Transforming Growth Factor-β

TNBC Triple Negative Breast Cancer

TNF-α Tumour necrosis factor- α

TRAIL TNF-related apoptosis inducing ligand

ZEB1 Zinc finger E-box-binding homeobox 1

ZEB2 Zinc finger E-box-binding homeobox 1

LIST OF FIGURES

Chapter 1

Chapter 3

Chapter 4

Chapter 5

Chapter 6

Chapter 7

LIST OF TABLES

Chapter 1

Chapter 2

Chapter 3

Chapter 5

Chapter 6

CHAPTER 1

General Introduction

1. General Introduction

Breast cancer is the most commonly diagnosed cancer in women around the world. It is also the main cause of death from cancer among women. In 2012, almost 1.7 million new cases of breast cancer were diagnosed (second most frequent cancer overall) representing roughly 12% of all new cancer cases and 25% of all cancers in women (Breast Cancer Statistics Worldwide, 2012; Jemal *et al*., 2011). In the UK during 2014, there were 11,433 female and 75 male deaths from invasive breast cancer (Cancer research UK, 2017).

Normal development and cancer progression have obvious parallels, evident even at the molecular level. In order to accomplish normal human development, complex signalling pathways have developed to allows cells to communicate with each other and their surrounding environment. Unsurprisingly, many of the same signalling pathways are (mis)used by tumours and cancer stem cells (Malhotra *et al.*, 2011).

1.1. Mammary gland

The mammary gland derives from the apocrine glands and is a glandular organ that, during the lifetime of a female, undergoes many changes in function and structure. These changes include hormonal changes influenced by the menstrual cycle and the changes during pregnancy, lactation and involution of a functional mammary gland. During these different phases, the cells within the mammary gland proliferate, differentiate or apoptose in response to stimuli, due the reorganisation of the glandular tissue (Inman *et al*., 2015).

1.1.1. Mammary Gland Development

The human breast consists of parenchymal and stromal cells such as: epithelial, adipose, fibroblasts, immune, lymphatic and vascular cells which, are important at specific phases of the mammary gland development. The parenchyma forms a structure of branching ducts responsible for the secretory ductules or acini (branching morphogenesis) development, whilst the stroma consists

mainly of adipose tissue that provides the environment for the development of the parenchyma (Inman *et al*., 2015). The primary ducts that reach the nipple form a complex of segmental and sub-segmental ducts. These sub-segmental ducts lead to terminal duct formation, which further subdivides to form several terminal acini. A collection of acini arising from one terminal duct along with the surrounding introlobular stroma is named alveoli (secretory cells) (Javed and Lteif, 2013; Imnan, 2015). The mammary gland is then formed by a final arboreal, bi-layered ductal structure that is composed of an outer contractile myoepithelial cells layer and an inner apically oriented luminal epithelial cells layer that can be divided further into ductal luminal cells, coating the inside of the ducts, and alveolar luminal cells, which secrete milk during lactation (Javed and Lteif, 2013). Therefore, the cap cells (multipotent stem cells) at the tip of the terminal end buds (TEBs) generate transit cells of a myoepithelial/basal lineage on the outer side of the TEB and generate transit cells (body cells) of a luminal epithelial lineage to form the central TEB mass. The ductal lumen is formed as central body cells apoptose and outer cells differentiate into luminal epithelial cells (Figure 1.1).

The mammary epithelium that forms the nipple remains inactive until puberty. Hormones and other factors trigger the invasion of the ductal epithelium and acini development into the mammary fat pad. Enzymes of the extracellular-matrix degrade the stroma in front of the TEB to enable it to move through the fat pad, however this movement is not fully understood. This movement could potentially be explained by progressive cell division build up, causing cell bulk in front of the mass of body cells. Combining this with progressive apoptosis degrading cell bulk at the back of the mass of body cells, can create the impression of movement (Smalley and Ashworth, 2003).

The invading front of the TEB high proliferative epithelial cells and exhibit some features of mesenchymal cells, suggesting that some degree of epithelial-to-mesenchymal transition (EMT) occurs at the TEB. However, unlike tumour cells, EMT genes involved during branching morphogenesis are highly regulated. When the fat pad is filled, this process stops when endogenous cytokine transforming growth factor – beta (TGF-β) is activated. This cytokine is responsible for cell growth,

proliferation and differentiation (Inman., 2015; Kalluri and Weinberg, 2009). Ductal elongation and complex branching originated at the site of the TEB, specifically at the site of the mammary stem cells in the cap cell layer.

During puberty, there is no further breast development in males due to increasing levels of testosterone. However, 40% of these males may develop transient gynecomastia that is a transient enlargement of glandular and adipose tissue caused by a higher proportion of estrogen (Javed and Lfeit., 2013; Vandeven and Pensler, 2017). Other hormones implicated in prenatal and pubertal breast development are: placental hormones progesterone, growth hormone, insulin-like growth factors, prolactin, adrenal corticoids, and triiodothyronine (Javed and Lteif, 2013).

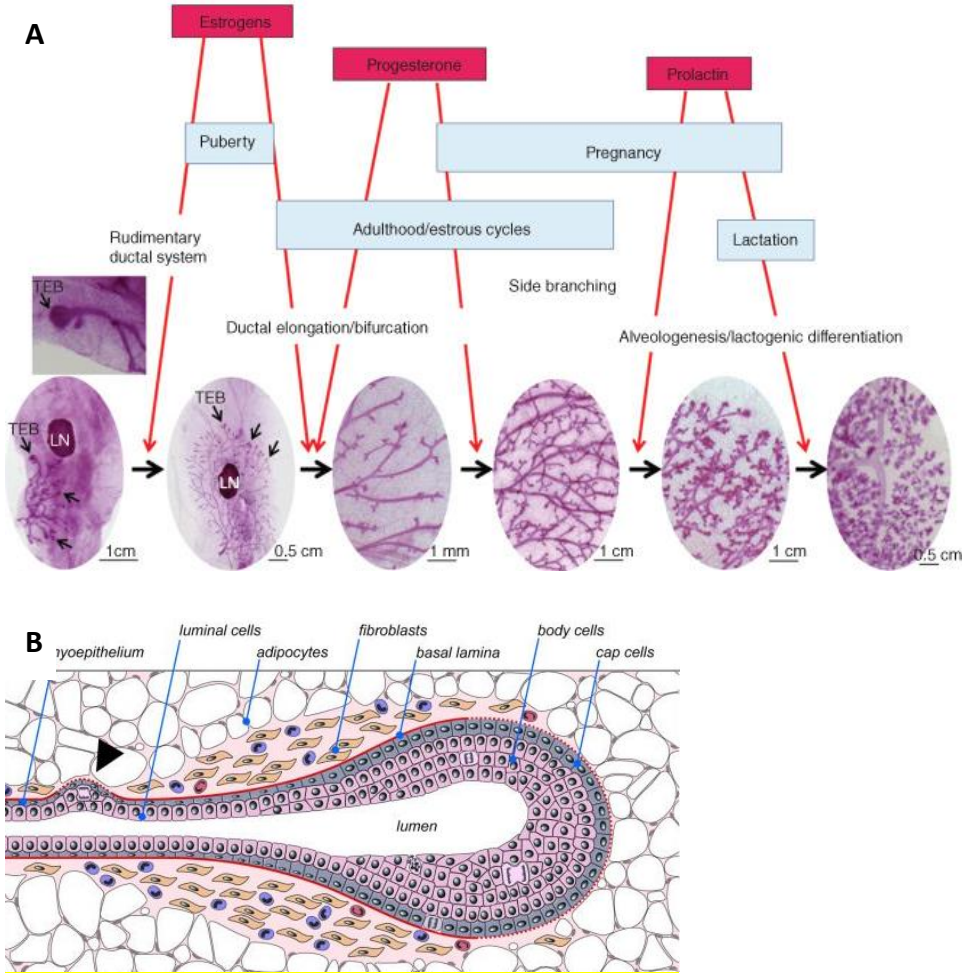

Figure 1.1. Mammary gland development. A. Hormones involved in mammary gland development and formation and elongation of the terminal end bud (TEB) *(adapted from* Brisken and Ataca, 2015). | **B.** Cells composing the mammary gland (*adapted from* Sternlicht, 2006).

1.1.2. Progenitor and Mammary Stem Cells

The ground-breaking work of DeOme's laboratory (DeOme *et al*., 1959) showed that small fragments or hyperplastic mouse mammary epithelium are able to generate similar patterns when transplanted into de-epitheliased mammary fat pads. Additionally, these patterns were able to produce similar secondary patterns when re-transplanted, confirming the existence of cells within the mammary epithelium, which have: (i) the ability to self-renew; (ii) multipotency and (iii) perform cell-autonomous actions which are all the features of stem cells (Reya *et al*., 2001). In the normal tissue, cell turnover is a characteristic of tissue maintenance. Stem cells give rise to transit-amplifying cells that are differentiating to produce mature cells that are incapable of further division (Valent *et al*., 2012). Stem cells are present in many different somatic tissues and are important participants in their normal physiology. It is crucial to understand whether the origin is in the progenitor cells (with lineage restriction that form the mammary gland) or in a mammary stem cell (MaSC) that is able to give rise to an entire mammary epithelium. Studies using the mouse mammary tumour virus (MMTV) allowed the investigation of the clonal origins of the mammary gland and demonstrated that the entire mammary epithelium is derived from a multipotent and self-renewing stem cell (Kordon and Smith, 1998). In the adult mammary gland, the stem cell compartment is heterogeneous and is composed by both multipotent, long-term and short-term repopulating cells. These cells produce committed progenitor cells for the myoepithelial and luminal (ductal and alveolar) epithelial lineages. Luminal progenitors only produce ductal or alveolar cells. These ductal progenitors possibly comprise both hormone receptor (HR)-positive and HR-negative cells, while the early and late alveolar-restricted progenitors are likely to be HR-negative. Moreover, there may be a common luminal progenitor for these sub-lineages (Figure 1.2). Isolation of cellular populations from mouse and human mammary tissue corroborated hierarchical organisation. It is worth to mentioning two types of unipotent MaSCs (lum-SC and myo-SC) may exist (*reviewed* in Visvader and Stingl, 2014).

Isolation of MaSCs and progenitor cells, using antibodies and fluorescence activated cell sorting (FACS) allowed the discovery that both luminal epithelial (epithelial membrane antigen [EMA/25.5/MUC1] positive-population) and myoepithelial (common lymphoblastic leukemia antigen [CALLA/NEP/gp100]) populations are enriched with heterogeneous cellular identities (Mahendran *et al*., 1989; Dundas, *et al*. 1991). As previously mentioned neither MaSCs nor progenitors express receptors for hormones, and HR-positive cells generally do not proliferate. Thus, hormones provoke morphological changes by acting on a complex regulatory network of paracrine signals and transcription factors to modulate the activity of MaSCs. Study of human breast development is crucial to understand breast cancer progression and diagnosis, in particular acquired disorders that often have a basis in normal development (Smalley and Ashworth, 2003).

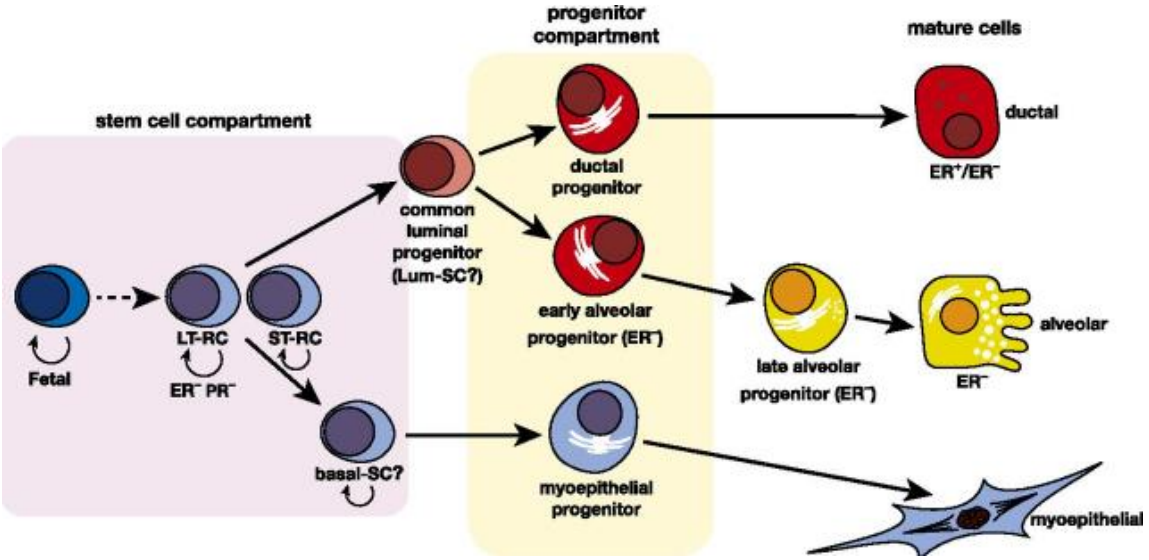

Figure 1.2. Hypothetical model of the mammary epithelial hierarchy. Stem cell compartment is composed by multipotent long-term (LT-RCs) and short-term repopulating cells (ST-RCs). These produces committed progenitor cells for the myoepithelial and luminal (ductal and alveolar) epithelial lineages. Luminal progenitors only produce ductal or alveolar cells (Visvader and Stingl, 2014).

1.1.3. Progression into Breast Cancer

Studies have reported evidence showing additional signalling pathways and transcription factors which regulate specific aspects of the mammary cellular specification. Lineage specification

and homeostasis of mammary stem and progenitor cells is maintained by interactions among; steroid hormone-signalling pathways; lineage-specific transcription factors and signals derived from the surrounding microenvironment. Stem cells are thought to be the cell of cancer origin, due to their self-renewing, long-lived and hence are likely to accumulate mutations during their lifetime (Smalley and Ashworth, 2003; Magee *et al*., 2012). It is hypothesised that tumours could arise from committed progenitor cells, with multipotent capacity to produce heterogeneity within the tumour. Stem cells may be the first cells to acquire the first genetic aberration and give rise to giving a predisposition to further mutations and triggering the disease (Dontu *et al*., 2003). Within the tumour, there are hormone-responsive and hormone-non-responsive cells, where expression of estrogen and progesterone is variable within each intrinsic molecular subtype. Whether tumours arise from transformed MaSCs (that acquire heterogeneity through clonal evolution) or can arise from committed progenitors or transit-amplifying cells, is still unknown. It is likely both mechanisms coexist with different propositions in each breast cancer subtype (Smalley and Ashworth, 2003).

In more detail, cancer models propose that cancer stem cells (CSCs) arise from normal stem cells during cancer initiation. Mutations and/or epigenetic changes will induce alterations that deregulate cell production and then give rise to clonal expansion producing a malignant clone. These cells have acquired several aberrations and lack of normal differentiation features (Figure 1.3 A) (Valent *et al*., 2012). Other models propose that CSCs derive from an initially mutated or epigenetically altered progenitor cell thereby acquiring a proliferative advantage over the normal cells which is enough to create a persistent cancer clone. This mutated clone gives rise to several sub-clones that are controlled by the natural immune system and/or the environment of the surrounding tissue/organ and hence these do not produce an apparent malignancy. In a pre-malignant stage, cancer stem cells are pre-malignant stem cells. However, if one or more sub-clones acquires certain mutations and or/ epigenetic changes (indicated by colour changes), they produce a cancer phenotype. At that time, in a malignant stage, the cancer stem cells become cancer-initiating cells and can thus be called cancer

CSCs (indicated by black outlines) (Figure 3). However, the other cancer subclones and their stem cells stay and produce "pre-malignant" and/or malignant subclones. The term pre-malignant cancer stem cells are thus best confined to cells shown or experimentally shown to be indicators of malignant stem cells, whereas those that may never transform further are more accurately defined as pre-malignant (Figure 1.3 B) (*reviewed in* Visvader and Stingl, 2014).

A

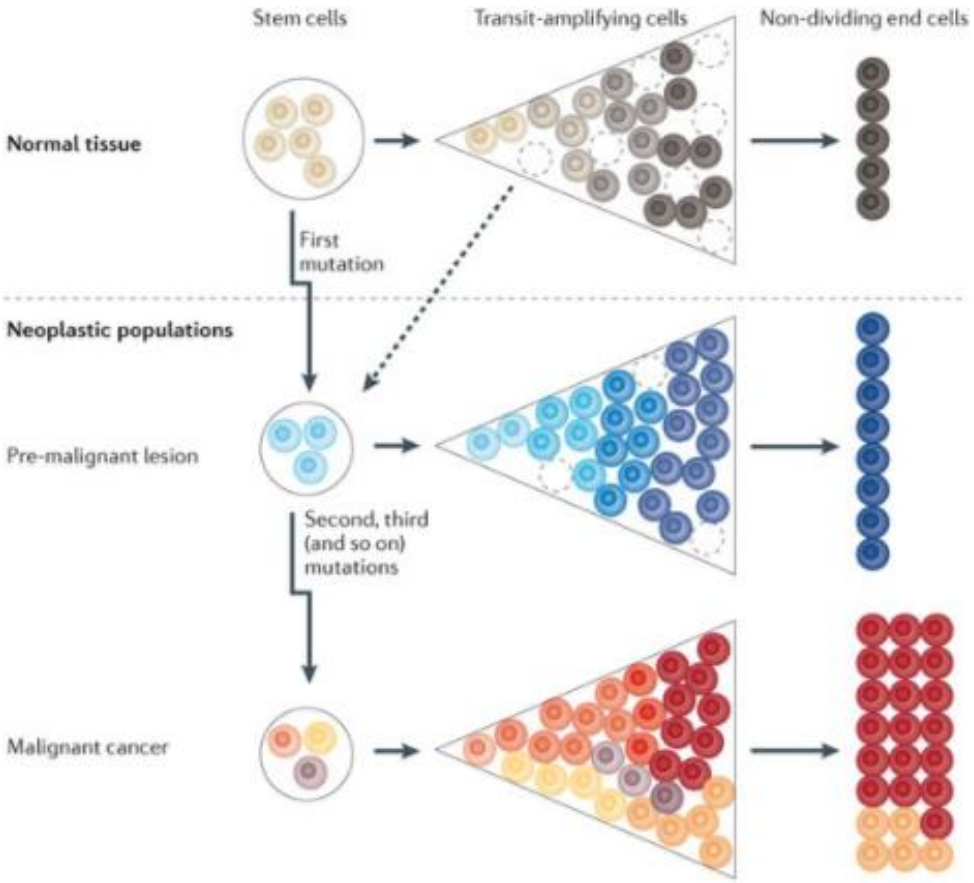

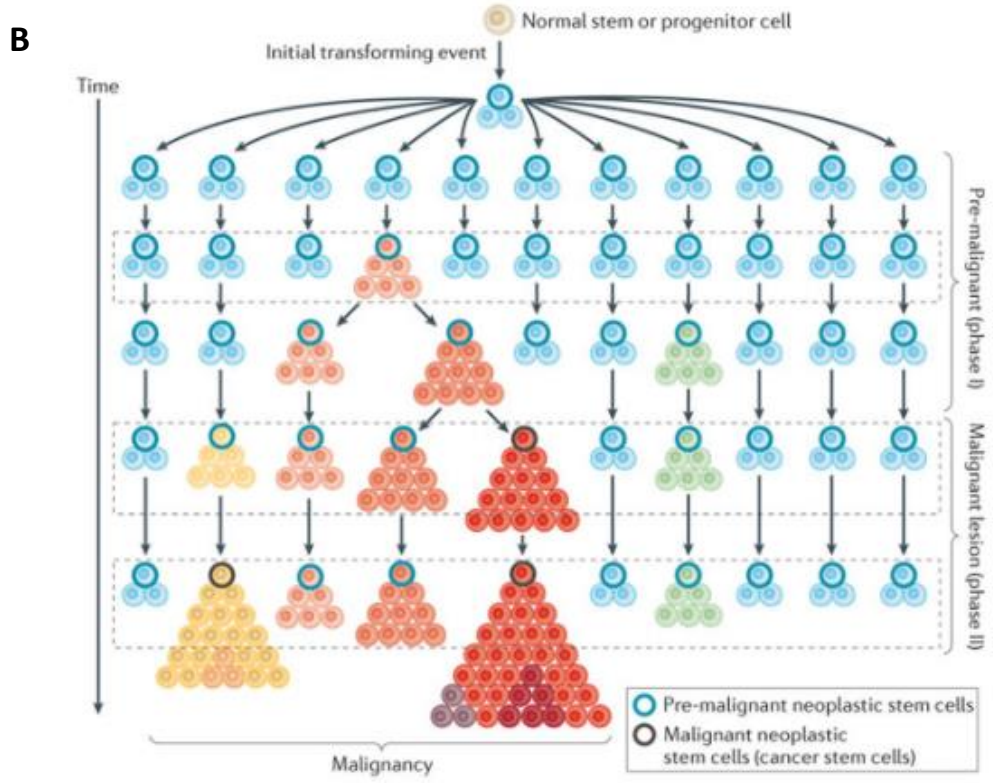

Figure 1.3. Models of cancer stem cell evolution | **A.** Theory that cancer stem cells derive from normal stem cells. | **B.** Theory that cancer stem cells derive from stem or progenitor cells (Valent *et al*., 2012).

1.2. Breast Cancer

Breast cancer is a highly heterogeneous disease. This heterogeneity can be defined as either inter-tumour heterogeneity, which relates to the different breast cancer clinical entities, or as intra tumour heterogeneity, which relates to the heterogeneous cellular composition of individual tumours (Smalley *et al*., 2012). Biological information (including morphological features, protein and gene expression), genetic information and the molecular techniques have both changed our understanding of the basic biology of breast cancer, and provided the platform for new methods of personalised prognostic and predictive testing. While traditional staging on the basis of tumour size and lymph node status remains the initial indicator, it has become clear that not all breast cancers presenting at the same stage have the same underlying biology or clinical behaviour. The knowledge of new biological markers has catapulted the development of many successful anti-cancer treatments. In fact, there are

some successful examples in breast cancer. However, there is still a need to develop more effective treatments to improve patient survival rate. This goal can only be achieved by gaining a greater understanding of the biology of the disease, in order to drive the development of more effective and more specific targeted therapies.

1.2.1. Aetiology of Breast Cancer

Most established risk factors for breast cancer in humans are thought to induce risk through hormone-related pathways. Epidemiological and experimental evidence implicates estrogens in the aetiology of this disease (Pike *et al*., 1993).

Estrogens mediate the relationship between breast cancer and many established risk factors through prolonged exposure to endogenous estrogen and progesterone, such as; early menarche and late menopause, exogenous estrogen and progesterone (the oral contraceptive pill) and hormone replacement therapy (Garcia-Closas *et al*., 2006, Collaborative Group on Hormonal Factors in Breast Cancer [CGHFBC], 1997; Beral, 2003).

Additionally, estrogen replacement has been shown effective to treat vasomotor symptoms of menopause, with good improvements in symptom frequency and severity within weeks after starting with the hormone replacement therapy (HRT). However, HRT in postmenopausal women is clearly connected with an increased risk of breast cancer, which is higher for combined estrogen/progesterone therapy than for unopposed estrogen therapy alone (Shah and Wong, 2009).

Furthermore, risk for breast cancer increases with age, being higher in the postmenopausal women (Key *et al*., 2002). Epidemiological studies have also firmly established associations with other reproductive factors, including nulliparity or low parity, late age at first birth, and breast feeding (Key *et al*., 2001). It has been proposed that there is a greater reduction in risk when giving birth at a young age compared giving births at an older age, meaning women who have their first before the age of 20 years have a 30% lower risk than women whose first birth is after the age of 35 years (Choudhury *et*

al., 2013). The very high serum levels of estrogens and progesterone during pregnancy stimulate growth of the mammary epithelium, promoting its differentiation and reducing the number of epithelial structures that are most vulnerable to malignant transformation (Russo *et al*., 1979). Breast-feeding is also associated with a modest decrease in risk for breast cancer, above and beyond that which is associated with multiple pregnancies. This effect might be due to the suppression of ovulation, reducing the exposure to ovarian hormones (CGHFBC, 2002).

Family history is also a known risk factor for developing breast cancer, although over 85% of patients with breast cancer have no family history of this disease (CGHFBC, 2001). Roughly 10%–30% of breast cancer cases are associated to hereditary factors. However, only 5%–10% of breast cancer cases are identified with a strong inherited component, while just a small fraction of these cases (4%-5%) is explained by mutations in high dominant genes that are transmitted in an autosomal dominant manner. Lifetime risks of breast cancer are 80% higher among women carrying *BRCA1* (breast cancer subtype 1, early onset) mutations, which are characterised by elevated cancer risk at younger ages. Female *BRCA2* (breast cancer subtype 2, susceptibility protein) mutation carriers also face a lifetime risk around 26%–84% for breast cancer. The Checkpoint kinase 2 (*CHEK2*) gene is associated with increased risks of breast cancer. Another gene frequently mutated is *ATM,* it's mutation heterozygotes are twice as likely to contract breast cancer risk compared to the general population. This risk is elevated by five times in women under the age of 50 (Apostolou *et al*., 2013).

The histologic architecture of the benign breast lesions is strongly associated with the risk of breast cancer. Biopsies with nonproliferative features have a lower risk of breast cancer compared to histological features of biopsies with proliferative changes but no atypia or atpypcal hyperplasia. Histologic features, the age at biopsy, and the degree of family history are highly related with the risk of breast cancer after the diagnosis of benign breast disease. Women with nonproliferative lesions have no increased preposition to breast cancer. However, this risk increases if they present a strong family history. The high risk of cancer in the ipsilateral breast in the first 10 years after the diagnosis

of the benign breast condition (especially in women with atypia) corroborates the presence of precursors in some women (Hartmann et al., 2005).

A high amount of adipose tissue within the mammary gland is linked to a higher cancer progression due to the increased expression of the Hypoxia-Induced Factor-1α (HIF-1α). HIF-1 and HIF-2) are responsible for the adaptation to decreased oxigen availability in breast cancer tumours. HIF-1α leads to a loss of ER α protein and the high activation of HIF's seems to increase metastasis and worsen the prognosis of patient survival due to an increase in tumour angiogenesis (Rausch *et al.,* 2017).

Furthermore, benign ovarian cysts (including mainly seromucinous, functional cysts, and endometriomas) can affect women during their reproductive age. These conditions have been linked to infertility and irregular and anovulatory menstrual cycles. Therefore, ovarian cysts reflect hormonal abnormalities, particularly impaired levels of female steroid hormones, which may also influence breast cancer risk. Additionally, it is known that bilateral oophorectomy reduces breast cancer risk (Swerdlow and Jones, 2007).

More recent studies have attributed various lifestyle-related factors to an increased risk for breast cancer, such as moderate alcohol consumption and obesity (Baan *et al*., 2007; Parkin *et al*., 2011). This association is probably due to the relationship between body mass index and endogenous estrogen concentrations, since, in postmenopausal women, circulating estrogen concentrations are dependent on the extraglandular production of estrogen in the adipose tissue. Physical activity has also been correlated with a reduced risk for breast cancer in both premenopausal and postmenopausal women (Baan *et al*., 2007; Parkin *et al*., 2011; Vainio & Bianchini, 2002).

1.2.2. Breast Cancer Molecular Subtypes

Morphologically and biologically, breast cancer is a heterogeneous disease that comprises a number of molecular subtypes (Simpson *et al*., 2005). This inter-heterogeneity can be hypothesised

using three models: (1) “mutation-of-origin” model; (2) “cell-of-origin model and (3) both models combined. The first model suggest that all tumour subtypes arise from a common precursor cell, a bipotent MaCSC (Figure 1.3). This MaCSC had specific genetic/epigenetic alterations acquired during tumourigenesis that affects cell capacity to commit to a luminal or basal lineage. In this model, common and recurrent mutations would be expected in each subtype. In fact, gene sequencing has shown basal and luminal tumours show specific and generally non-overlapping mutations (Koboldt *et al.,* 2012). The second model proposes that cell differentiation is firmly encoded during tumourigenesis. Therefore, luminal progenitors would give rise to luminal-type tumours and basal/myoepithelial progenitor cells would give rise to basal-like tumours. Studies corroborate with this demonstrating that luminal-like tumours show characteristics of normal luminal epithelial cells (cytokeratins 8, 18, 19 ,7; MUC1; EPCAM; CD24 and ERα) and basal tumours shows characteristics or normal basal progenitors (cytokeratins 5,6, and 17; CD44, CD49f; laminin and p63). Furthermore, this model is supported by *in vitro* experiments where transforming different cell lines with the same panel of oncogenes develop tumours with different features and phenotypes that are reminiscent of the cell-of-origin (Visvader*,* 2009; Perou *et al.,* 2010). Taking this, a third model mixing both theories has been proposed. It is likely that both models coexist with different propositions in each breast cancer subtype. (Smalley and Ashworth, 2003; Gross *et al.,* 2016)

Actually, numerous gene expression clusters representing genes associated with these different breast cancer subtypes have been described. With the support of hierarchical clustering analyses, five classical distinct molecular subgroups of invasive breast cancer based on these genetic signatures were reported: normal breast-like; basal-like, luminal A, luminal B, human epidermal growth factor receptor 2 (HER2) and normal breast-like (*Sørlie et al*., 2001).

Normal breast-like subtype tumours are poorly characterised and have been grouped into the classification of intrinsic subtypes with fibroadenomas and normal breast samples. These tumours express gene characteristics of adipose tissue presenting an intermediate prognosis between luminal

and basal-like cancers and usually do not respond to neoadjuvant chemotherapy. Despite these tumours not expressing ER, PR and HER2 they are not included in the triple-negative subtype because they are negative for CK5 and EGFR. The normal breast-like remains inexact, since it is believed that they could be a technical artifact from high contamination with normal tissue during the microarrays (Weigelt *et al*., 2010).

Estrogen is the most important and dominant biomarker for breast cancer classification. ER positive tumours comprise up to 75% of all breast cancer patients, and constitute 65% and 80%, , patients under and above 50 years, respectively (Anderson *et al*., 2002). Luminal A is the most prevalent subtype and is characterised by the expression of estrogen receptor (ER) and progesterone receptor (PgR) in cancer cells, whereas the luminal B subtype is characterized by lower levels of ER and PgR expression and can have HER2 overexpression. Progesterone is an ovarian steroid hormone that is important for normal breast development during puberty but also for lactation and breastfeeding. Progesterone functions are mainly mediated by classical PgR-A and -B isoforms expressed in the breast and reproductive organs but also in the brain where progesterone controls reproductive behavior progesterone/PgR isoforms are responsible for the development of the TEBs or acini located at the ends of ducts that will become the milk-producing structures in the lactating mammary gland. Interestingly, PgR isoform expression can not be induced in response to estrogen unless EGF is present, suggesting the existence of important cross talk between EGFR and/or HER2 family members and both hormone receptors (Daniel *et al*., 2011).

The major biological distinction between luminal A and B is the proliferation signature, including genes such as *CCNB1*, *MKI67*, and *MYBL2*, which have higher expression in luminal B tumours than in luminal A tumours. MKI67 encodes the nuclear marker of proliferation Ki67 which is heavily used to distinguish between luminal A and B. Ki67 is associated with worse prognosis for breast cancer patients (Cheang *et al*., 2009).

The association of HER2 in breast cancer was first discovered in 1987 (Slamon *et al.*, 1987). The HER family proteins are type I transmembrane growth factor receptors that function to activate intracellular signalling pathways in response to extracellular signals. HER2 is formed by an extracellular ligand binding domain, a transmembrane domain, and an intracellular tyrosine kinase domain (*reviewed* in Moasser, 2007). The growth stimuli including ligands bind to EGFR an HER2 activating a cascade of intracellular signals mainly via the PI3K/Akt/mTOR and the MAPK/ERK pathways. The mTOR phosphorylates downstream kinases including the S6 kinase, which phosphorylates and activates ER, which can regulate the transcription of many genes including GFR ligands, cyclin, VEGF and PARP (Metha and Tripathy, 2014). Overall, HER2 is absent or expressed at low-levels in benign breast conditions. However, HER2 is amplified and over-expressed in high-grade ductal carcinoma *in situ* (DCIS), particularly of the comedo type, and in high-grade inflammatory breast cancer. In addition, HER2 expression is kept during progression to invasive cancer, nodal metastasis and distant metastasis. *HER2* amplification/over-expression and aneuploidy are considered downstream mechanisms of p53 dysfunction. Therefore, HER2 overexpressing cells have significantly prolonged activation of downstream MAPK and c-jun following stimulation with EGFR or HER3 ligands compared with low HER2 cells (reviewed in Moasser, 2007). Furthermore, HER2 is also involved in metastasis through the cross-talk between HER2 and CXCR4 signalling pathways. CXCR4 contributes to invasiveness through increasing migration and adhesion activity (Freudenberg *et al.,* 2009). Moreover, several studies correlate HER2 gene amplification or protein over-expression with poor prognosis and positive clinical results receiving systemic chemotherapy treatment (Dai *et al*., 2009). These amplification/over-expression events occur in 13% to 20% of invasive ductal breast cancer and around 55% of this subtype is ER negative (ER -ve) and PgR negative (PgR -ve). HER2 tumours are negative for HR and overexpress HER2 protein, which is highly associated with gene HER2/neu amplification.

Basal-like tumours are mainly characterised by the absence of ER, PgR and HER2 expression (triple negative tumours), and constitutes a heterogeneous group of tumours expressing distinct basal

markers. Within the triple-negative subtype a novel subgroup has been described, which was designated claudin-low and is characterised by comparatively high expression of mesenchymal markers, such as vimentin, and low expression of epithelial markers, notably claudins and E-cadherin (*Sørlie et al*., 2003; Herschkowitz, *et al*., 2007; Prat *et al*., 2010). The interferon-rich subtype was recognised from triple negative tumours, which is characterised by the over-expression of interferon-regulated genes (Teschendorff *et al*., 2007). Within these interferon-regulated genes, STAT1 and SP110 are the most important and help differentiate tumours of this subtype. STAT1 is the transcription factor mediating interferon-regulated gene expression and SP110 is associated with prognosis (Dai *et al*., 2016). Additionally, metaplastic breast cancers (MPBC) with a triple-negative profile and overexpression of programmed death (PD)-ligand 1 (PD-L1) are rare and very aggressive tumours comprising ~1% of all breast cancers. MPBC prognosis is worse than the other triple negative cancers due to a low response to systemic therapy, and a median survival of 8 months after growth of metastases (Weigelt *et al*., 2014). Recently, besides ER, PgR and HER2, androgen receptor (AR) has also been used in molecular classifications. AR is expressed in 90% of the ER positive (ER +ve) and in 55% of the ER negative tumours (Hu *et al*., 2011). AR was considered a potential prognostic marker and therapeutic target in breast cancer playing a similar role as HER2. Studies conducted by Lakis *et al*., (2014) have classified ER-ve/PgR-ve tumours into ER -ve/ PgR -ve/ AR +ve (molecular apocrine, called MAC) and HR-ve tumours. MAC accounts for 13.2% of all the breast cancer cases and is commonly characterised by Ki67 expression.

These different subtypes result in different clinical outcomes and can respond differently to the same treatment; triple negative tumours have the worst prognosis, with luminal A tumours having the best (Simpson *et al*., 2005; Sørlie *et al*., 2006) (Table 1.1).

Table 1.1. Molecular and histological types of breast cancer (reviewed in Day *et al*., 2016).

Molecular Subtype	Biomarker status	Grade	Outcome	Common histological type	%
Luminal A	ER+; PgR+; HER2-; Ki67-	1/2	Good	IDC; Lobular; Tubular; Mucinous; Neuroendocrine; Cribiform	23.7%
Luminal B	ER+; PgR+; HER2-; Ki67+ ER+; PgR+; HER2+; Ki67+	2/3	Intermediate Poor	IDC; Micropapillary	38.8% 14%
HER2 overexpression	ER-; PgR-; HER2+	2/3	Poor	IDC; Apocrine; Micropapillary; Pleomorphic lobular	11.2%
TNBC - Basal	ER-; PgR-; HER2-; basal marker+	3	Poor	IDC; Medullary; Metaplastic; Adenoid cystic; Secretory	10-25%
TNBC - Claudin-low	ER-; PgR-; HER2-; EMT marker+; stem cell marker+; claudin-	3	Poor	IDC; Medullary; Metapladtic	7-14%
TNBC – Metaplastic breast cancer	ER-; PgR-; HER2-; EMT marker+; stem cell marker+; PD-L1	3	Poor		1%
TNBC – Interferon-rich	ER-; PgR-; HER2-; interferon regulated genes+	3	Intermediate	IDC; Medullary; Metaplatic	~10%

1.2.3. Breast Cancer Histological Subtypes

Breast cancers can be categorised into biologically and clinically subgroups according to histological grade (Elston and Ellis, 1991) and histological type (Ellis *et al*., 1992). Grade is an evaluation of the degree of differentiation (tubule formation and nuclear pleomorphism) and proliferative activity (mitotic changes) of a tumour. Grade is therefore related to tumour aggressiveness and identifies prognostic subgroups (Elston and Ellis, 1991, Mallotra *et al*., 2010). Tumours present a wide histological diversity with specific morphological and cytological patterns that can be associated with individual clinical characteristics and outcomes, such patterns are called 'histological types'. Breast cancer can be broadly categorised into *in situ* carcinoma and invasive (infiltrating) carcinoma (Malhotra *et al*., 2010). Carcinoma *in situ* is further sub-classified into ductal carcinoma *in situ* (DCIS) or lobular carcinoma *in situ* (LCIS). DCIS was primarily sub-classified based on the architectural features of the tumour into: comedo, cribiform, micropapillary, papillary and solid white. The main invasive tumour types include invasive ductal, invasive lobular, ductal/lobular, mucinous (colloid), tubular,

medullary and papillary carcinomas. Of these, invasive ductal carcinoma is the most frequent subtype accounting for 70–80% of all invasive lesions. Invasive ductal carcinomas are further sub-classified as well-differentiated (grade 1), moderately differentiated (grade 2) or poorly differentiated (grade 3) (Ellis *et al*., 2003). Moreover, a recent histological classification has been created with a new subgroup of breast cancer special types. These special types represent around 25% of all breast cancers and the latest edition of the World Health Organisation classification recognises the existence of at least 17 distinct histological special types (Ellis *et al*., 2003.) Within these histological special types of breast cancer, some are preferentially estrogen receptor positive: tubular carcinoma, cribriform carcinoma, classic invasive lobular carcinoma, pleomorphic invasive lobular carcinoma, mucinous carcinoma, neuroendocrine carcinoma, micropapillary carcinoma, papillary carcinoma and low grade invasive ductal carcinoma with osteoclast-like giant cells. In addition, the other histological special types of breast cancer preferentially estrogen receptor negative: adenoid cystic carcinoma, secretory carcinoma, acinic-cell carcinoma, apocrine carcinoma, medullary carcinoma, metaplastic carcinoma with heterogenous elements, metaplastic carcinoma with squamous metaplasia, metaplastic spindle cell carcinoma, metaplastic matrix-producing carcinoma (Weigelt *et al.*, 2010).

1.3. Estrogens, Estrogen Receptor and Endocrine Therapies in Breast Cancer

1.3.1. Estrogens and Estrogen Receptor

The hormone estrogen works as a chemical messenger in the body. It is essential for normal sexual development and function of female organs (ovaries, uterus, breasts) that are important for childbearing (Yager and Davidson, 2006). The three maim estrogens in women are estrone, estradiol and estriol. The release of estrogen from the ovaries causes a systemic effect that is mediated by the ER (Tsai and O'Malley, 1994). ER is a ligand-dependent nuclear transcription factor, which regulates downstream gene expression and transcription when activated by ligand binding (Bocchinfuso & Korach, 1997).

Since Jensen *et al*., described the ER, in 1960, two different isoforms have been found, ER alpha (ERα) and beta (ERβ) cloned in 1986 (Green *et al*., 1986) and 1996 (Kuiper *et al*., 1996), respectively. Although ERα and ERβ are encoded by two different genes, ESR1 and ESR2 (DeLisle *et al*., 2001), and the codified proteins have different sizes (595 and 530 amino acids), these have high overall sequence homology in the ligand binding domain (59%) and in the DNA binding domain (97%) (Kuiper *et al*., 1996). The ERα and ERβ genes encode 66 kDa and 59 kDa proteins, respectively (Kumar *et al*., 1987; Kumar *et al*., 1986). ERα is expressed exclusively in the cells of the luminal breast epithelium (15-30 %), which invariably also express PgR (Clarke *et al*., 1997; Petersen *et al*., 1987). On the other hand, ERβ is expressed in both luminal and myoepithelial mammary cells as well as in fibroblasts and other stromal cells (Speirs *et al*., 2002). In fact, the two receptors have similar, but distinct tissue distribution patterns (Lu *et al*., 1998). ERα is expressed in brain, bone, cardiovascular system, uterus, liver and breast cells. Tissues with predominant expression of ERβ are apparent in the lower urogenital tract, the gastrointestinal tract and some brain areas (Gustafsson, 1999).

The biological effects of estrogen are primarily mediated by these both estrogen receptors. In estrogen signalling, the binding of estrogen to the ER causes receptor dimerisation and binding to estrogen responsive elements (EREs) in the promoter and/or enhancer regions of estrogen-responsive genes. Estrogen binding alters the three-dimensional structure of ER to facilitate the recruitment of coactivator complexes, thereby activating the transcription of genes that induce estrogen production (Ao *et al*., 2011; Kocanova *et al*., 2010). Potentially, the proliferation of HR negative cells, which cannot respond directly to hormonal signals, is “mediated by a paracrine signal released from HR positive cells to which they are often adjacent” (Brisken *et al*., 1998). Mice with targeted removal of one or both ER genes have determined that ERα is the key regulator of mammary gland development. It has been reported that an ERα homozygous knockout (-/-) mouse model showed no development of the mammary gland beyond the formation of the rudimentary ductal tree formed during embryogenesis. However, when the ERα -/- cells were mixed with wild type steroid receptor positive cells, before being

engrafted into the cleared fat pad of a recipient mouse, they were able to proliferate and contribute to the normal mammary development (Mallepell *et al*., 2006). These conclusions support the theory that a paracrine signal is released from the non-dividing HR positive cells, in response to hormonal signalling, causing proliferation of the HR negative cells.

1.3.2. Estrogens, Estrogen Receptor and Breast Cancer

Estrogens play a crucial role in the development of the mammary gland and are central to the aetiology of breast cancer (McDonnell & Norris, 2002). This hormone can act as a "mitogen" by stimulating breast tissue proliferation and increasing cell divisions (mitosis) this can result in cancer due to DNA errors acquired during replication (gene mutation). Moreover, certain estrogen metabolites can act as carcinogens or genotoxins, by directly inducing DNA damage, facilitating cancer cells to form (Yager and Davidson, 2006). The resultant transcriptional changes induced by estrogen promote: cell proliferation, survival, angiogenesis, and tumour metastasis (Ao *et al*., 2011; Kocanova *et al*., 2010).

ERα is a key transcriptional regulator in breast cancer and is responsible for many effects of estrogen on cancerous breast tissue. Mutations within the ER gene are observed in roughly 1% of primary breast tumours yet it is unclear how these contribute to the regulation of ER expression (Fuqua *et al*.,2000, Herynk and Fuqua, 2004; Roodi *et al*., 1995). The majority of breast cancers are ERα-positive (75%) and depend on estrogen for growth (Ao *et al*., 2011).

In contrast to the increased ERα-positivity in the transition from normal to malignant tissue, ERβ expression was shown to be downregulated in tumours such as atypical ductal hyperplasia and DCIS (Roger *et al*., 2001). ERβ synthesis was also correlated with lower proliferation and grade. The ratio of ERα to ERβ synthesis increase with increasing proliferation and risk of breast cancer in premalignant lesions (Roger *et al*., 2001). Thus, it has been suggested that ERβ might negatively regulate ERα signalling and may play a role in suppression of tumour progression (Kocanova *et al*.,

2010). Importantly, patients whose tumours express ERα tend to have a better prognosis, that is longer periods without recurrence and overall survival rates, than those with tumours that lack ERα expression (Knight *et al*., 1980).

1.3.3. Endocrine Therapy Resistance

The fact that ERα expression (ER expression) is associated with tumour formation has led to the development of anti-hormone therapies that could suppress the estrogen signalling. Thus, ER positive breast tumours are treated with targeted anti-estrogen therapy, including selective estrogen receptor modulators (SERMs), such as tamoxifen and raloxifene (Herynk & Fuqua, 2007; Osborne *et al*., 2000), and selective estrogen receptor down-regulators (SERDs), such as fulvestrant (Faslodex, ICI 182,780) (Osborne *et al*., 2004; Vesuna *et al*., 2012; Ao *et al*., 2011). Furthermore, synthetic compounds that either act as estrogen-antagonists or block the function of aromatase (the enzyme that catalyses the last step of estrogen biosynthesis), have been also produced – aromatase inhibitors (Kocanova *et al*., 2010).

However, ER positive breast tumours frequently become hormone resistant through various molecular mechanisms and patients usually relapse within five years after the diagnosis (Herynk & Fuqua, 2007). Endocrine resistance can compromise the effective treatment and the potential cure of up to 25% of all of breast cancers, therefore finding the mechanisms of endocrine resistance has been a major research focus (Sutherland, 2011) (Figure 1.4). A study revealed that 33% of the women treated with tamoxifen for 5 years have recurrence after 15 years and die from their breast cancer disease (Figure 1.4). This poor result after tamoxifen treatment shows that is imperative to improve anti-endocrine therapies in breast cancer patients (Early Breast Cancer Trialists' Collaborative Group (EBCTCG), Lancet, 2011).

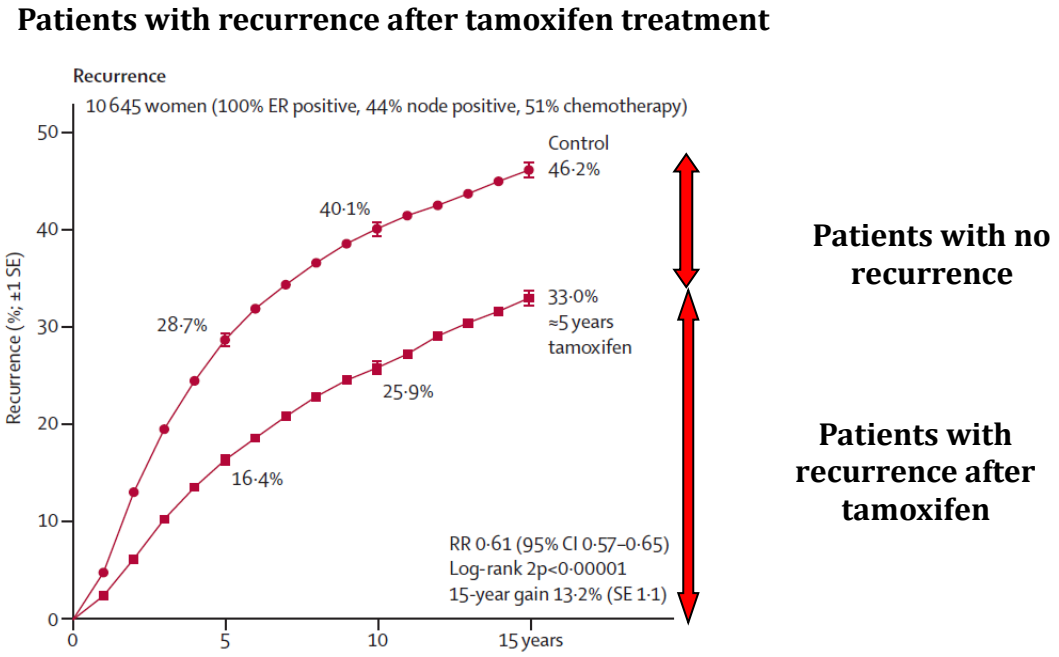

Figure 1.4. Breast cancer recurrence after treatment with tamoxifen (*adapted* from Early Breast Cancer Trialists' Collaborative Group (EBCTCG), Lancet, 2011).

Activation of classical signalling pathways, including the ones induced by HER2 and Epidermal Growth Factor Receptor (EGFR) (Herynk and Fuqua, 2007), MAPK (Oh *et al*., 2001), and PI3K/AKT (Campbell *et al*., 2001) have already been implicated in hormone resistance. Additionally, the absence or low expression of ER in breast cancer stem cells (bCSCs) might be relevant to understand endocrine resistance. These cells are likely to be endocrine resistant and respond to treatment only by virtue of paracrine influences of neighbouring, differentiated ER +ve tumour cells (O'Brien *et al*., 2009). Exposure of breast cancer cells to estrogen was shown to cause expansion of the bCSCs compartment, presumably in response to a paracrine signal released from the ER positive tumour cells to the ER -ve bCSCs. This was shown to occur through a combination of pathways including, but possibly not limited to, EGFR and Notch (Harrison *et al*., 2013). There is evidence for an ER -ve/low status of bCSCs in ER +ve cell lines and in patient derived samples. CSC amount and activity increases in response to estrogen stimulation and, as in the normal breast, this outcome is partly mediated by EGFR signalling pathway (Harrison *et al*., 2013).

A better understanding of the molecular changes associated with the endocrine resistant growth is urgently needed in order to find targeted therapies for resistant tumour cells, or treatments that can inhibit or delay the emergence of resistance (Frogne *et al*., 2008).

1.3.3.1. Tamoxifen

Tamoxifen is a tripheyllenthylene and needs to be metabolised into 4-hydroxytamoxifen (4-OHT) to bind to ER and hence block breast cancer cell growth, by stopping ER +ve cancer cells in cell cycle G1 (Kocanova *et al*., 2010). In 1977, tamoxifen was approved by the Food and Drug Administration (FDA) for breast cancer treatment and in 1985, as a therapy in conjunction with chemotherapy in postmenopausal women showing node-positive breast cancer. In 1998, tamoxifen administration in pre- and postmenopausal healthy women at high risk of developing the disease was also approved by the FDA (United States).

It has been shown an effect of anti-estrogens on expression and/or intracellular distribution of factors that control cell cycle progression. However, the administration of tamoxifen in postmenopausal women has several side effects such as increased risk of both thromboembolic disease and endometrial cancer (Fisher *et al*., 1998).

Tamoxifen competitively inhibits the binding of estrogen to its target ER resulting in a receptor conformational change blocking AF-2 function. This inhibits proliferation of ER +ve breast cancer cells, being effective in ~60% of ER +ve patients (Gee *et al*., 2005). *De novo* resistance to tamoxifen in ER +ve tumours has been described. *In vitro* experiments have shown different genetic alterations that confer a constitutive activation of ER and a loss of response to tamoxifen, such as duplication of exons 6 and 7 (Pink *et al*., 1997) and a tyrosine-to asparagine substitution at residue 537 (Y537N) (Zhang *et al*., 1997). ER mutations can affect hormone therapy response, but this is estimated to be present in only 1% of breast tumours (Roodi *et al*., 1995). Although downregulation of ERα expression can contribute to *de novo* anti-estrogen resistance, loss of the receptor during the acquisition of tamoxifen

resistance is not commonly observed in clinical samples (Clarke *et al*., 2001). However, breast tumours that respond to hormones constantly develop resistance to tamoxifen, despite the continued expression of wild-type ER in most cases (Encarnacion *et al*., 1993). Various signalling networks that control cell proliferation or survival have been implicated in acquired resistance to tamoxifen. *In vivo* studies reported that during the development of tamoxifen resistance, tumours may become able to grow in a tamoxifen-stimulated manner (Gottardis and Jordan, 1988). Studies have demonstrated the capacity of tamoxifen to function as an agonist or antagonist dependent on whether it recruits co-activators or co-repressors to the ERα transcription complex. One of these co-regulators is the AIB1 protein and its over-expression is correlated with agonistic activity of tamoxifen, especially in the presence of HER2 (Osbourne *et al*., 2003). In addition to HER2 signalling, the growth factor receptor (IGFR1) and fibroblast growth factor receptor 1 (FGFR1) can activate MAPK and PI3K pathways, which are unresponsive to treatment in breast cancer (Zhang *et al*., 2011). Differences in ER concentration also leads to tamoxifen resistance. Hypermethylation of DNA sequences containing CpG islands and histone deacetylase activity in the ESR1 promoter are similar to genomic deletion of ER because these can inactivate gene expression, therefore associated with a lower expression of ER (Sharma *et al*., 2005). Resistance to tamoxifen may also be associated to a dysregulated metabolism of the drug. Cytochrome P450 enzymes, which converts tamoxifen into metabolites, which are associated with a worse clinical prognosis after tamoxifen treatment (Desta *et al*., 2004).

Agents targeting EGFR/HER2 pathways in tamoxifen-resistant breast cancers are in clinical trials. The acquisition of enhanced EGFR/HER2 pathway signalling in ER+ breast cancer with tamoxifen resistance potentially results from selection of cells with a more stem-like phenotype. Expression of EGFR has already been demonstrated in stem cells of the normal mammary gland in both mice and humans (Asselin-Labat *et al*., 2000). In tamoxifen resistant tumours that overexpress HER2, anti-apoptotic molecules, such as Bcl-2 and Bcl-xL are upregulated (Kumar *et al*., 1996) and EGFR can promote cell survival by acting together with c-Src and Cas proteins (Riggins *et al*., 2006). Furthermore,

in tamoxifen resistant cells, the binding of tamoxifen to cytoplasmic ER can activate EGFR and HER2 signalling pathways leading to ER and ER co-factors phosphorylation (Shou *et al*., 2004). Overexpression of constitutively active AKT in breast cancer cell lines can induce estrogen independence and resistance to tamoxifen (Campbell *et al*., 2001; Faridi *et al*., 2003).

Despite this growing understanding of the molecular mechanisms underlying both *de novo* and acquired tamoxifen resistance, there is no approved targeted therapy to improve outcomes of tamoxifen- resistant breast cancers (Lee *et al*., 2012).

1.3.3.2. Fulvestrant

Since it is believed that the transcription of ER has an important role in acquired resistance process, second-line endocrine therapies, have been developed to alternatively inhibit ER (McDonnell, 2006). One of these, the pure steroidal antiestrogen fulvestrant (Faslodex, ICI 182,780, Astra Zeneca Corp., London, UK), entirely represses ER activity, inactivating both ERα-mediated genomic and non-genomic signalling. It was recently used in postmenopausal women who showed no improvement after antiestrogen therapy (tamoxifen or aromatase inhibitors). Fulvestrant binds to ER with a higher affinity, suppresses ER regulated genes more powerfully and is stronger than tamoxifen in inhibiting cell growth mediated by ER (Frogne *et al*., 2009). However, despite its potent anti-tumour effects, fulvestrant does not avoid the development of anti-endocrine resistance. Acquired resistance to fulvestrant is an ER-independent mechanism, associated with constitutive activation of autocrine-regulated growth-stimulatory pathways, ultimately dissociating breast cancer cells from growth controlled by ER. However, the mechanism(s) of upregulation of these mitogenic pathways are not clear (Rao *et al*., 2011). Experiments in MCF-7 cells demonstrated that the obstruction of cell growth with fulvestrant was correlated with a lower expression of ER protein resulting in decreased transcriptional activity, demonstrated by lower PgR mRNA and cyclin D1 protein expression levels.

These findings show fulvestrant as a powerful agent anti-ER activity (Hutcheson *et al*., 2011). It is crucial to study fulvestrant treatment and elucidade ER-ve state. Lack of ER expression is an important clinical feature in breast cancer, consisting of 30% of tumours on presentation and in some ER-ve tumours when relapse to tamoxifen occurs (Gee *et al*. 2005). In the clinic lack of ER expression is associated with poor prognosis, impeding response to all types of anti-hormones. These ER -ve tumours are more aggressive and have a higher proliferative rate, featuring fulvestrant-resistant cells (Nicholson *et al*., 2004).

1.3.3.3. Aromatase Inhibitors

The aromatase inhibitors (AIs), suppress estrogen synthesis through the aromatase pathway, blocking the synthesis of estrogen from androgens in the peripheral tissues, such as adipose tissue and muscle (Miller, 2003). AIs decrease systemic estrogen levels and therefore avoid growth of estrogen-dependent ERα positive tumours. In MCF-7 human breast cancer cells, estradiol stimulates proliferation and growth through the induction of G1- to S-phase transition (Lewis-Wambi and Jordan, 2009), protective cells against apoptosis (Song and Santen, 2003). Accordingly, estrogen deprivation inhibits cell proliferation and induces apoptosis in this breast cancer model (Kyprianou *et al*., 1991). The AIs, letrozole and anastrozole, inhibit proliferation of breast cancer cells by inducing cell cycle arrest in G0/G1 phase and cell death by apoptosis (Sasano *et al*., 1999; Thiantanawat *et al*., 2003; Itoh *et al*., 2005).

Cross-talk between the PI3K, the most frequently mutated pathway in breast cancer, and ER has been reported to be involved in endocrine resistance to anti-estrogen therapies (Musgrove and Sutherland, 2009). Experimental and clinical studies suggest that hyperactivation of the PI3K pathway leads to resistance to anti-estrogen drugs. In breast cancer cells, PI3K is usually activated by growth factor receptor (tyrosine kinases) and G-protein-coupled receptors in the breast cancer cells. A requirement for PI3K overexpression in the estrogen-independent growth of long-term estrogen-

deprived ER +ve breast cancer cells seems to mirror the clinical resistance to AIs (Sabnis *et al*., 2007; Crowder *et al*., 2009; Miller *et al*., 2010; Fox *et al*., 2012).

Additionally, high-dose of fulvestrant provides a longer period to cancer progression compared to the AI anastrozole as first-line treatment for advanced breast cancer (Robertson *et al*., 2009). In other studies, ~35% of patients who progressed on an AI responded to second-line fulvestrant treatment (Ingle *et al*., 2006; Perey *et al*., 2007). Therefore, in some clinical conditions, downregulation of ER could be higher to aromatase inhibitor therapy (Robertson *et al*., 2009). ER holds transcriptional activity in estrogen deprived cells and primary human breast tumours (following AI therapy), driving their estrogen-independent growth (Miller *et al*., 2011, Fox *et al*., 2012). Thus, it is reasonable to hypothesise that estrogen (ligand)-independent ER activity potentially promotes resistance to AI therapy. Having similar side effects, AI treatment increases the risk of bone fractures and joint disorders more so than fulvestrant (Howell *et al*., 2002; Howell and Sapunar, 2011).

Some studies have recently shown that the use of AIs (letrozole) in breast cancer therapy can increase the proportion of cells with CSCs features. Protein and gene expression of markers of the mesenchymal phenotype are increased within tumours after chemotherapy and endocrine therapy (Creighton *et al*., 2009). Therefore, the future challenge will be to combine conventional therapies with therapies that target cells with CSC/mesenchymal features to overcome any intrinsic resistance to therapy.

1.4. Breast Cancer Stem Cells

In 1994, the first cancer stem cell (CSC), the leukaemia stem cell, was identified in samples from patients with acute myeloid leukaemia and it was proposed that blocked proliferation was responsible for CSC differentiation and tumour growth (Lapidot, 1994). As well as being able to differentiate, these cells manifested self-renewal capacity, since the disease could be transferred into recipient mice (Bonnet & Dick, 1997).

The concept of CSCs is consistent with observations made by scientists over many years that there exists a robust similarity between normal development and the development of cancer (Al-Hajj *et al*., 2003). In tumours, the CSC model proposes a cellular hierarchy in which CSCs are the only cells capable of unlimited cell divisions and, as a consequence of their ability to propagate differentiated progeny by asymmetric division, generate the full heterogeneity inherent within all tumours (Reya *et al*., 2001). These CSCs or 'cancer-initiating cells' divide slowly and asymmetrically, whereas the resulting progenitor cells divide rapidly, progressively lose proliferative potential and undergo limited differentiation to form the heterogeneous populations of cells within the tumours. The verification of the existence of CSCs remains controversial but experimental evidence has gained prominence in the past 10 years and has contributed much to our understanding of tumour biology and the clinical relevance of this tumour subpopulation. The first report of the presence of CSCs in a solid tumour was in breast cancer by Al-Hajj *et al.,* (2003) where it was identified as a CD24/low/CD44þ population, with a higher capacity to initiate tumour growth when transplanted into immunocompromised mice. It has been reported other markers, such as aldehyde dehydrogenase 1 (ALDH1), CD133, Sox2, CK5, alpha-6 integrin/CD49f, beta-1 integrin/CD29 or lack of ER. Cells exhibiting these phenotypes are also present in breast cancer cell lines and may mark cells with higher tumour initiation capability (Ginestier *et al.*, 2007; Fillmore and Kuperwasser, 2008; Wright *et al.*, 2008; Charafe-Jauffret *et al.*, 2009; Lawson *et al.*, 2009). Moreover, distinct mesenchymal-like bCSCs are characterised by the CD44high /CD24low phenotype, and the epithelial-like bCSCs are characterised by the ALDH1 +ve phenotype (Mani *et al*., 2008). The mesenchymal-like bCSCs are primarily quiescent and frequently localised at the tumours invasive margins whereas the epithelial-like bCSCs are proliferative and positioned more centrally within the tumour (Mani *et al*., 2008). A study has shown that fractionating stem-like CD44high/CD24low cells by FACS from human mammary epithelial cells shows that the mesenchymal-like bCSCs exhibit phenotypes similar to cells that have undergone an EMT (Mani *et al*., 2008).

Advances in cell culture techniques have been important in the identification and study of both murine MaCSCs and human bCSCs (Dontu *et al*., 2003). The *in vitro* study of MaSCs was developed from a methodology in the neuronal field in which a cell culture assay, known as the neurosphere assay, was used to identify neural stem cells (Dontu *et al*., 2003; Ponti *et al*., 2005). Plating normal human mammary epithelial cells in non-adherent, serum-free conditions with a specific set of growth factors resulted in the formation of spherical colonies termed mammospheres (Dontu *et al*., 2003). These culture conditions mimic those which cells must survive *in vivo* to metastasise and these mammosphere colonies were shown to be enriched for cells that have functional characteristics of stem/progenitor cells, such as multipotency and self-renewal and tumour initiation (Dontu *et al*., 2004; Tao *et al*., 2011). Currently, the mammosphere-forming assay is routinely used to identify key features of stem cell behaviour and maintenance *in vitro* (Shaw *et al*., 2012).

Investigation of known bCSCs markers demonstrated that individual markers are not always expressed in an individual cancer, or co-expressed in the same cells. Currently, it is not possible to identify specific CSC sub-populations in all cell lines (Liu *et al*., 2014). Some commonly used bCSCs markers correlate with certain clinical and biological characteristics. For example, CD44- +ve/CD24-ve breast cancer cells, which are enriched for stem cells, have a higher ability to form mammospheres and/or tumours when injected into immunocompromised mice than CD44-ve/CD24-ve cells (Farnie *et al.*, 2007). Moreover, only a small percentage of primary tumours and two-thirds of breast cancer cell lines have any ALDH1+ cells, and a distinct sub-population is seen in only 25% of breast cancer cell lines (Christgen *et al.*, 2007; Tan *et al.*, 2013). A recent study summarised that none of the markers employed can be considered as a universal marker applicable to the identification of a CSC population in breast cancer cell lines or metastatic breast cancer (Liu *et al.,* 2014).

Low survival rates, therapeutic resistance and premature recurrence are associated with residual breast cancer stem cells at the time of surgery after chemotherapy. Second-line therapies are not able to improve prognosis of breast cancer patients and little research exists related to which

pathways should be targeted in patients with residual disease (Visvader *et al.,* 2012; Mitra *et al.*, 2015; Singh and Settleman, 2010). However, while invasive bCSCs are established drivers of metastasis and recurrence, targeting bCSCs may only be effective at eliminating pre-existing bCSCs, failing to prevent non-CSCs from acquiring CSC-like features in response to the tumour microenvironment and therapy (*reviewed* in Doherti *et al*., 2016).

1.4.1. Breast Cancer Stem Cells and Therapy Resistance

The role of bCSCs in therapy resistance has had minimal study but some evidence does exist that these cells have a decreased sensitivity to treatment therefore being therapy resistant (Reya *et al.,* 2001). Therapy-resistant CSCs are able to survive after current therapies as they are able to regenerate recurrent disease through their tumour-initiation properties. In order to overcome therapy resistance, CSCs should be targeted in combination with standard treatments (Reya *et al.,* 2001). Importantly, using chemotherapy to eliminate CSCs drives quiescent CSCs into activity to stimulate tumour development (Moore and Lyle S., 2010). Furthermore, the quiescent CSCs may acquire several DNA repair mechanisms, which gives protection against treatment. Therefore, both active and quiescent CSC populations should be targeted but quiescent cells are problematic to identify, isolate and study. Ffrench et al., proposed that an alternative for future treatments is a 'Proliferate to Kill' strategy, which proposes to stimulate the quiescent CSCs, making them re-enter the cell cycle causing vulnerability to standard therapeutics (Ffrench *et al.*, 2014). Overall, CSC therapy-resistance mechanisms involve five components: Quiescence; Detoxification/Multi-Drug Resistance (MDR); Repair of damaged DNA; Survival and Adaptation (*reviewed* in Gasch *et al*., 2017).

CSCs have MDR mechanisms that function to detoxify the cell in response to chemotherapy. MDR refers to the efflux mechanisms that allow chemotherapy drugs to be pumped out of the cell before DNA damage can occur (Shen *et al*., 2012). The most well-known MDR proteins are the members of the 'ABC (ATP-Binding Cassette) transporter' family, found in bacterial antibiotic

resistance (Michalet and Dijoux-Franca, 2009). ABC transporters have been described to be related with chemo-resistance of CSCs in several cancer subtypes, including ovarian, breast, colon, and non-small cell lung cancers (Zhang *et al.,* 2015; Sun *et al*., 2015; To *et al.,* 2015; Hashida *et al.,* 2015). Therefore, MDR is considered the second CSC therapy-resistance mechanism. To date, efforts to create clinical-targeting of MDR mechanisms have not been successful (Yu *et al.,* 2013), as targeting specific ABC transporters results in activation of redundant ABC transports to continue the MDR mechanism (McGrogan *et al*., 2008).

Another mechanism by which CSCs resist therapy is by detecting and repairing DNA damage, allowing them to survive by resistance to DNA damage, induced by cancer therapies. Chemotherapies using platinum consist by forcing the formation of intra- and inter-strand DNA crosslinks upon the rapidly-dividing cancer cell. These cross-links break chromatin structure, and a resultant stall of the replication fork and activation of several DNA damage response (DDR) pathways. In sensitive cells, multiple cross-link formations are more than cells can repair. As a result, unrepaired DNA lesions cause cell-cycle arrest through apoptosis, either directly, or following DNA replication during the S phase of the cell cycle (Jung and Lippard, 2007). Pathways that have been shown to be involved in platinum-induced DNA damage include the Nuclear Excision Repair (recognition and excision of single-strand DNA damage) and the FA/BRCA pathway (repair of DNA crosslinks, UV-induced dimers, and double-strand breaks). There are similar DDR mechanisms that cause resistance to DNA-damage induced by radiotherapy. In contrast, taxane-based chemotherapies (for example Paclitaxel and Docetaxel) target microtubule dynamics during mitosis. Cells cannot repair these targeted microtubules, which results in apoptosis through the G2/M checkpoint. Taxane-resistance is due to mutations in the tubulin sub-units that contain microtubules rather than therapy-resistance mechanisms (McGrogan *et al*., 2008).

The accumulation of significant DNA damage drives the activation of apoptotic mechanisms, which must be targeted to kill therapy-resistant cells. Anti-apoptotic mechanisms aid therapy-resistance; directly by inhibiting cell death, and indirectly by creating delays so enhanced DDR

mechanisms can repair therapy-induced DNA damage. These anti-apoptotic strategies comprise the extrinsic and intrinsic pathways, and the tumour suppressor protein p53. The extrinsic apoptotic pathway involves the detection of death signals by 'Death Receptors', which belong to the superfamily of tumour necrosis factor receptors (TNF-R) that are activated by TNF family ligands. Cancer cells have developed several mechanisms to resist drug-induced cell death via the extrinsic pathway (discussed in Section 1.5) (Safa *et al*., 2008; Piggott *et al*., 2011; *review*ed in Gasch *et al*., 2017)

The intrinsic apoptotic pathway drives apoptosis by interfering with mitochondrial permeability, leading to the release of cytochrome C to activate caspases. This pathway is mainly regulated by members of the BCL-2 family (Fulda *et al*., 2013). This family includes the pro-survival protein BCL-2, which binds to the pro-apoptotic BCL2-associated-X-protein (BAX) and BCL-2 homologous antagonist killer (BAK), which decreases release of cytochrome C from the mitochondria. BCL-2 family members are overexpressed in many solid tumours and have been linked to cancer development, cell survival and chemo-resistance (Kirkin *et al*., 2007). An experiment has shown that BCL-2 overexpression is also related to CSC chemoresistance. For example, Madjd *et al*. (2009) showed that CD44+/CD24-/low breast CSCs express very high levels of BCL-2. To date, this mechanism is uncertain but it is proposed that these proteins can affect chemo-resistance through induction, by other signalling pathways required for CSC survival. For example, Ma *et al*. (2008) demonstrated that BCL-2 induction by AKT1 may be a mechanism by which CSCs can mediate chemo-resistance.

Moreover, Liu *et al.,* (2014) performed repeated treatments on cell lines to enrich for a therapy-resistant sub-population (Phillips *et al*., 2006; Kabos *et al*., 2011). They found that the two cell lines investigated display distinctive changes in CSC marker expression according to the precise therapy. The only consistent finding across therapeutic agents was an expansion of ER -ve cells after exposure of the luminal cancer cell line, supporting previous findings that a lack of ER in individual cells within ER +ve breast cancer is a marker of a therapy-resistant population of CSCs (Kabos *et al*., 2011) and could account for the recurrence of ER -ve phenotypes observed in clinical practice

(Thompson *et al*., 2010; Moussa *et al*., 2012). Additionally, it has been established that cells positive for the CSC marker ALDH isolated from lung cancer cells lines, demonstrated a high resistance to multiple chemotherapeutic agents (Cisplatin, Gemcitabine, Vinorelbine, Docetaxel, Doxorubicin and Daunorubicin) when compared to ALDH -ve cells (Jiang *et al.* 2009). This data indicates that tumours have some CSCs that are resistant, or sensitive to therapies. After first treatments, sensitive CSCs are eliminated, resulting in a recurrent tumour and 'CSC hierarchy with increased levels of therapy-resistant CSCs'. Also, surgical resection of the tumour may awake quiescent CSCs to synergistically increase the production of the therapy-resistant recurrent malignancy. This may clarify why initial pre-clinical experiments are successful but such success have not largely translated to the clinic (reviewed in Gasch *et al*., 2017). It is therefore crucial to identify, study and target the specific CSCs that are responsible for specific types of resistance to treatments within specific cancers.

SCs and CSCs function is regulated by several signalling pathways such as: Wnt, Notch, Hedgehog and the mTOR signalling hub, which are frequently dysregulated in therapy-resistant CSCs (Ffrench *et al*., 2014). SCs and CSCs belonging to the same type of tissue share some self-renewal and differentiation regulatory mechanisms, which challenges to target CSCs without harming normal cells (Pardal *et al.,* 2005). For example, the blockage of the Wnt signalling pathway to treat cancer had detrimental effects on normal development that is regulates by the Wnt signalling in pre-and clinical studies (patients with bone-side effects). The primary side effects in targeting the Wnt/β-catenin pathway in anti-cancer treatments are myelo- and gastro-intestinal suppression, this is due to the side-effects effects of anti-Wnt treatments on proliferation of hematopoetic and intestinal stem cells, and also due to progenitor cells in other organs. However, it is important to find the right tool by designing specific agents to target the Wnt/FZD sub-pathways activated in certain cancer, rather than blocking the Wnt/β-catenin signalling altogether which prevents damage to normal tissue (*reviewed* in Blagodatski *et al*., 2014).

Thus, it is reasonable to say that these stemness signalling pathways may simplify coordinated CSC therapy-resistance mechanisms such as quiescence, detoxification (MDR), repair (DDR), survival (anti-apoptosis) and adaptation (*reviewed* in Gasch *et al*., 2015).

Additionally, extracellular vesicles (EVs) are believed to have an important role in breast cancer growth and metastasis and could be potential anti-cancer therapies. Cancer cells secrete high volumes of EVs, including exosomes and microvesiculess, into the local microenvironment and premetastatic niche. These EVs released by tumour cells deliver procancerous transcripts and proteins, to both other cancer cells and nontransformed cells (reviewed in Green *et al.,* 2015). Suetsugu et al., was able to visualise the transfer of exosomes from cancer cells and colonisation of these into lung cells. This study also demonstrates that breast cancer EVs can transfer nucleic acids and proteins to autologous and heterologous cells within the tumour microenvironment, culminating in the acquisition of the cancer phenotypes, tumour progression, immune evasion, and metastasis (Suetsugu *et al.,* 2013). Furthermore, many mechanisms have been described for breast cancer EV-mediated transfer of drug resistance to promote tumour growth and progression. One such mechanism includes the transfer of the P-glyoprotein (P-gp), which is linked to resistance. For example, one study showed that doxorubicin- or docetaxel-resistant breast cancer cells produce MVs into target endothelial or drug-sensitive cancer cells. Additionally, EVs act as tumour modulators within the tumour niche and are capable to succeed in the acidic, hypoxic environments common to tumours in order to confer prometastatic phenotypes such as inflammation, migration, and invasion. Cancer cells can use several methods to avoid immune system recognition through EVs, such as secretion of immunosuppressive proteins, inhibition of NK cell proliferation, or a decrease in $CD8^+$ T-cell cytotoxicity. Importantly, it is possible to take advantage of the drug delivery capabilities of exosomes for breast cancer therapy. One study has shown that Doxorubicin, fused into exosomes from immature dendritic cells and taken up by both MDA-MB-231 and MCF-7 cells, led to an impairement of cell proliferation *in vitro* and tumour growth *in vivo.* Several proteins have been

recognised within breast cancer EVs that can be used as prognostic marker and could be used in combination with other analytical methods. Currently, some targeted breast cancer therapies have been studied using exosomes as a vehicle for drug delivery, but due to the complex nature of EV-cell interactions, more studies are needed to EVs be used as a therapeutic strategy (reviewed in Green *et al.,* 2015).

1.4.2. Breast Cancer Stem Cells and Metastasis

Metastasis is the main cause of death leading to >90% of mortality from cancer (Gupta and Massagué, 2006; Steeg, 2006). Tumour removal by surgery and adjuvant therapy can treat well-confined primary tumours. However, metastatic disease is incurable because of its systemic nature and the resistance of disseminated tumour cells to current treatments. Moreover, the ability to treat cancer efficiently is mainly dependent on the capacity to inhibit or to reverse the process of metastasis. The metastasis generated by carcinomas are formed following the completion of a complex succession of cell-biological events – collectively termed the invasion-metastasis cascade – whereby epithelial cells in primary tumours (1) invade locally through surrounding extracellular matrix (ECM) and stromal cell layers, (2) intravasate into the lumina of blood vessels, (3) survive the hurdles of transport through the vasculature, (4) arrest at distant organ sites, (5) extravasate into the parenchyma of distant tissues, (6) initially survive in these foreign microenvironments in order to form micrometastases, and (7) re-initiate their proliferative programs at metastatic sites, thereby generating macroscopic, clinically detectable neoplastic growths (termed “metastatic colonisation”) (Fidler, 2003) (Figure 1.5). Many of these complex cell-biological events are coordinated by cell-intrinsic molecular pathways within cancer cells. Additionally, non-autonomous cell interactions between cancer cells and normal stromal cells have crucial roles throughout the invasion during the metastasis cascade. Deregulation of these intrinsic and extrinsic signalling cascades, allow metastatic breast cancer cells to generate high-grade malignancies (*reviewed* in Valastyan and Weinberg, 2011).

A number of cellular properties required for metastasis to occur are shared by CSCs. One such cell-intrinsic property is EMT.

1.4.3. Epithelial-Mesenchymal Transition (EMT)

During the EMT process, the epithelial cells lose their epithelial characteristics and acquire more mesenchymal properties by cytoskeleton rearrangements and alterations in adhesion, cellular structure and morphology. In fact, cell surface proteins, such as E-cadherin (CDH1) or integrins are replaced by mesenchymal markers, such as N-cadherin, vimentin or fibronectin. As a result, epithelial cells are detached from the basal membrane and are therefore more capable of migrating to other sites or becoming more invasive and entering the blood and lymphatic systems (Britton *et al*., 2011). Thus, EMT-like changes correlate with a more aggressive phenotype. High levels of Matrix Metalloproteinases (MMPs) in the tumour microenvironment can directly induce EMT in epithelial cells. During EMT, cells can then produce more MMPs facilitating cell invasion and EMT can generate activated stromal-like cells that cause cancer progression via further MMP production (Kadisky and Kadisky 2010). The molecular mechanisms involved in metastasis are not clearly understood, but it has been suggested that there is deregulation of the signalling pathways that control normal EMT. One of the most prominent EMT molecules is E-cadherin, whose expression is increased in more than 50% of metastatic tissues in breast ductal carcinoma (Chao *et al*., 2012).

A recent study attempted to characterize an EMT signature in circulating tumour cells from breast cancer patients (Yu *et al*., 2013). They investigated seven pooled epithelial transcripts (cytokeratins 5, 7, 8, 18, and 19; EpCAM [epithelial cellular adhesion molecule] and E-cadherin) and three mesenchymal transcripts (fibronectin, N-cadherin, and SERPINE1/PAI1 [serpin peptidase inhibitor, clade E]) in 11 human breast cancer samples. They found it was rare to find cells expressing both mesenchymal and epithelial markers but mesenchymal markers were enriched in these circulating tumour cells. Interestingly, they demonstrated that expression of the mesenchymal

markers was more likely to be associated with clusters of circulating tumour cells rather than a single set of migratory cells. These experiments provide evidence that a single cell may be undergoing EMT into cluster cells, or a pre-existing cluster undergo mesenchymal transformation in the bloodstream which would demonstrate evidence of EMT occurring in relation to blood-borne dissemination of human breast cancer (Yu *et al*., 2013). Additionally, circulating tumour cells from patients with advanced prostate and breast cancer expressed both epithelial and mesenchymal markers, indicating a possible switch or transition was happening between those states. Similar studies also detected EMT markers such as pan-cytokeratin, Twist, and Vimentin in circulating tumour cells from early and metastatic breast cancer patients (Papadaki *et al*., 2014).

Elucidating the molecular mechanisms responsible for EMT-mediated drug resistance and tumour metastasis is crucial to discovering strategies to prevent EMT, and restore the sensitivity of cancer cells to therapeutic treatment. It has been shown that the transcriptional factors Snail, Slug, Twist and zinc-figure E-box-binding homeobox (ZEB1 and ZEB2) are classified as EMT inducers. These can induce EMT via different cell signalling pathways. TGF-β, Wnt (wingless-type MMTV [mouse mammary tumour virus])/β-catenin, and Notch (a family of transmembrane proteins) pathways have been highly associated in inducing EMT in breast cancer epithelial cells.

Interestingly all of these signalling pathways are implicated in CSC biology, and consequently there have been numerous studies describing an association between CSCs and EMT (Mani *et al*., 2008; Morel *et al*., 2008; Scheel *et al*., 2011; Yang *et al*., 2012; Wang *et al*., 2014). The effects of TGF-β are not restricted to embryogenesis, but are also observed during cancer progression and has tumour promoting effects in almost all types of cancer. In addition, TGF-β has a direct effect on EMT by down-regulating epithelial markers and by up-regulating mesenchymal markers. TGF-β can induce the CSC phenotype and can cause EMT *in vitro* by up-regulation of Oct-4, Nanog, N-cadherin, Vimentin, Slug and Snail, and down-regulation of E-cadherin and Ck18 (Wang *et al*., 2014). Knock-down of Oct-4 and Nanog inhibited the TGF-β-induced EMT (Micalizzi *et al*., 2010, Wang *et al*., 2014).

TGF-β can also regulate EMT via the activation of additional molecules, such as MAPK, PI3K or GTPases belonging to the Rho family of proteins (Moustakas *et al*., 2007).

Additionally, ERK2 activity results in nuclear accumulation of Snail1 with no cytosolic proteasomal degradation. This mechanism, which increases in tumour fibrosis, can prolong activation of CAFs to endure tumour fibrosis and to promote tumour metastasis through the regulation of Snail1 protein level and activity (Zhang *et al*., 2016). Twist-induced EMT in breast cancer cells was followed by increased cell invasion, migration and CSC-like properties under hypoxic conditions. Twist activated PAR1 and PAR3 gene expressions, which are G-protein-coupled receptors that are "high-gain sensors" of extracellular protease concentrations, permiting cells to respond to a proteolytic microenvironmet (Wang *et al.,* 2016).

BCSCs can shift between epithelial-like and mesenchymal-like states (Gupta *et al*., 2011; Yang *et al.*, 2012; Liu *et al*., 2014). It is becoming more important to understand how cellular plasticity modifies tumour biology and affects therapeutic response. In addition, the plasticity of bCSCs that allows them to undergo these reversible transitions regulated by the tumour, may be necessary for successful metastatic colonisation (Liu *et al*., 2014). An additional subtype of breast cancer, termed basal B/claudin-low, has recently been highlighted and found to display EMT- and CSC-associated gene signatures. However, it is important to know whether claudin-low tumours reflect altered myoepithelial differentiation or, rather, de-differentiation. Is has been shown that EMT induction in an immunocompromised-mouse-derived epithelial cell line leads to a claudin-low gene expression profile with acquisition of several stem-like features, including the ability to form mammospheres, an increased tumourigenic potential, and activation of signalling pathways previously associated with cancer stem cells (for example TGFβ, Notch, Wnt and Hedgehog signalling pathways) (Asiedu, *et al*., 2011; Takebe *et al*., 2011). This further supports the hypothesis of EMT-promoted cell de-differentiation rather than altered myoepithelial differentiation. Corroborating this definition of plasticity, transgenic mouse models that combined expression of RAS and of the EMT inducer TWIST1

in luminal-committed cells induced the development of claudin-low breast tumours *in vivo* (Morel *et al*., 2012).

Therapy-resistance has been associated with EMT in a study that has found up- regulation of P-glycoprotein 1 or multidrug resistance protein 1 (MDR1) in MCF-7 cells after Adriamicyin treatment (Li *et al*., 2009). These cells displayed enhanced invasion, and ablation of Twist1 expression in these cells, blocked EMT and partially reversed drug resistance, suggesting that EMT contributes to resistance to this drug (Li *et al.,* 2013). Several studies have shown an EMT- resistance phenotype after paclitaxel/docetaxel and 5-fluorouracil treatments and after treatments targeting hormone and epidermal growth factor receptors. MCF-7 cells become tamoxifen-resistant when they acquire an EMT-like morphology—growing as dispersedly grouped colonies with loss of cell-cell junctions and altered morphology. These cells also express increased mRNA levels of Snail, Vimentin, and N-cadherin and decreased levels of E-cadherin, which are considered hallmark EMT characteristics (Hiscox *et al*., 2006; Britton *et al*., 2011) (Table 1).

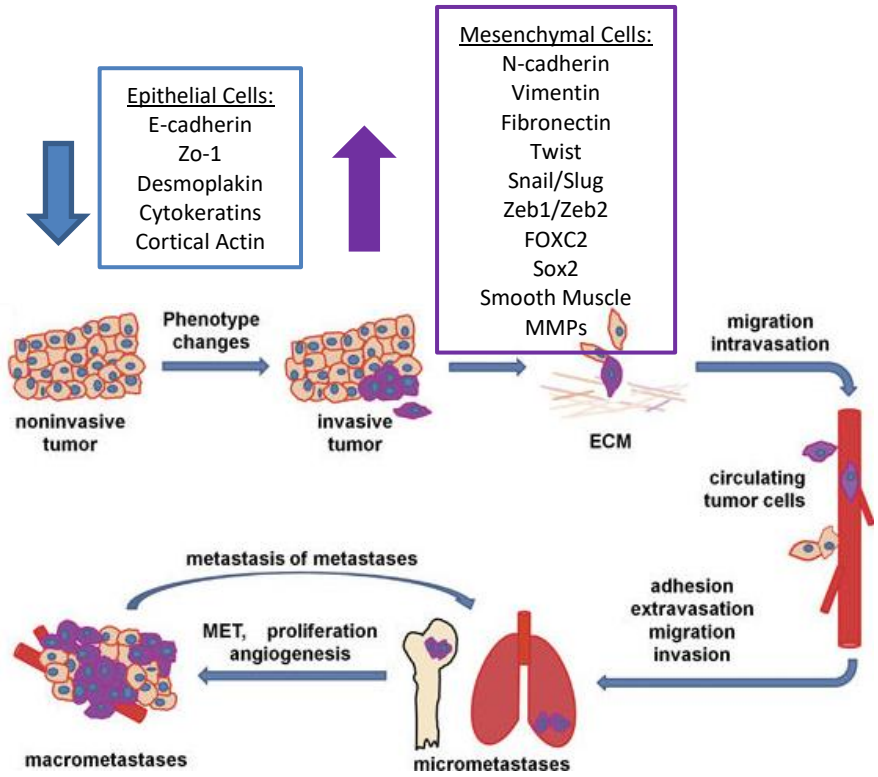

Figure 1.5 Process involved in the formation of metastases. Sequential steps of the breast cancer metastatic cascade (*adapted from* Wang and Wang, 2011 and Chang *et al*., 2014).

Table 1.2. Plasticity Cell features involved in EMT during metastasis and drug resistance. EMT results in a transformation and transition of polarised epithelial cells toward mobile mesenchymal cells. The E-cadherin to N-cadherin switch indicates epithelial cells are progressing through EMT (*reviewed in* Wu *et al*., 2016).

Epithelial-Mesenchymal Transition (EMT)	
Features	Loss of cell polarity Cell migration Cell invasion
Up-regulation	N-cadherin Vimentin Fibronectin Twist Snail Slug P-glycoprotein 1/MDR1 Zeb1/Zeb2 FOXC2
Down-regulation	E-cadherin EpCAM Ck18
Signalling Pathways	TGF-β (activates PIK3K/MAPK) Notch Wnt/β-catenin

1.5. Breast Cancer and TRAIL / c-FLIP

Therapeutic resistance and relapse are strongly associated with metastatic disease in breast cancer patients. Almost 30% of early breast cancer patients eventually develop metastatic disease and in 90% of these, a therapeutic resistance occurs and patients end-up dying from the disease (Grupta and Massangue, 2006). Functional studies in a number of malignancies suggested that CSCs may lie at the heart of this therapy resistance in metastatic disease. Tumours are treated with drugs based on their capability to cause regression of advanced tumours. These drugs are then given with adjuvant therapies after the primary tumour is removal. The CSC model, questions this strategy since regression of advanced tumours drastically affects the bulk tumour populations while growth of metastasis may be driven by CSCs. Only CSCs hold sufficient self-renewal ability to form metastases and since CSC and bulk tumour cells may be driven by different pathways, it will be crucial to use drugs that target the CSC regulatory pathways in the adjuvant setting (Korkaya and Wicha, 2013). Given the complexity of the disease, new treatments for breast cancer need to be targeted at individual patient subgroups to ensure improved efficiency either as monotherapy treatments or in combination with standard of care (Mallini *et al*., 2013). A common feature of therapy resistance in metastatic disease is the inability to respond to pro-apoptotic stimuli. Cancer cells have developed several mechanisms to resist apoptosis induced using the extrinsic pathway. For example, therapy resistant ovarian tumours have been found with absent or downregulation of surface death receptors including platinum-resistant cancer and upregulation of FAS has been shown to reverse this platinum-resistance (Fan *et al*., 2015). FAS have a pro-apoptotic role in SCs but may drive survival in CSCs. Additionally, upregulation of the adaptor-protein FADD has been shown to sensitise ovarian cancer cells to platinum treatment. CSC chemoresistance by evasion of apoptosis is not clarified but studies suggest that CSCs resist apoptosis via the extrinsic pathway. In mammalian cells, induction of apoptosis results into a perturbation of the mitochondria resulting in release of cytochrome C or factors that directly stimulate members of the

death receptor family (*reviewed* in Gasch *et al.,* 2017). Therefore, there has been much interest in finding ways to re-sensitise cancer cells to pro-apoptotic stimuli.

1.5.1. TNF-related Apoptosis Inducing Ligand (TRAIL)

The tumour necrosis factor (TNF) superfamily of cytokines are key extracellular mediators of apoptosis (Ashkenazi, 2002). This family includes TNFα, FAS and TRAIL signalling pathways. Targeting TRAIL has become a good candidate for cancer therapy due to its well-recognised ability to induce apoptosis in cancer cells with limited toxicity to normal cells *in vitro* (Ashkenazi *et al*., 1999). Tumour necrosis factor-related apoptosis inducing ligand (TRAIL) or Apoptosis 2 ligand (APO-2L) was first identified due to its sequence homology to the extracellular domain of CD95 ligand (FasL) and tumour necrosis factor (Pitti *et al*., 1996; Wiley *et al*., 1995). The primary, but not exclusive, function of human TRAIL ligand is the induction of extrinsic apoptosis in target cells. It performs this function by binding to its cognitive receptors on the cell surface. TRAIL interacts with membrane-bound TRAIL receptors (TRAIL-R1/DR4 and/or TRAIL-R2/DR5) leading to receptor clustering and trimerisation. Intracellular adaptor protein FADD is recruited to the death domain of the TRAIL receptor. In the appropriate cellular context, the initiator caspase-8 is recruited to the complex, collectively known as the death-inducing signalling complex (DISC) and interacts with FADD through its death effector domains. DISC activation of caspase-8 leads to caspase cascade activation where caspase-8 can either directly activate caspase-3 to induce apoptotic cell death (extrinsic pathway), or it can cleave the protein BID, leading to release of cytochrome-c from the mitochondria with subsequent apoptosome formation and activation of the caspase-9 (intrinsic pathway). Within the apoptosome caspase-9 is activated and cleaves caspase-3 to induce apoptotic cell death (Figure 1.6) (Crowder and Deiry, 2012). Activation of caspase-8 is inhibited by the intrinsic caspase-8 inhibitor, c-FLIP (Siegelin and Siegelin, 2011). C-FLIP plays an important role in moderating alternative downstream responses to TRAIL-inducing survival and proliferative activity. Endogenous TRAIL is expressed on natural killer cells, macrophages, T-cells

and dendritic cells and is believed to have an immune defence function destroying virus-infected and malignant cells (Duiker *et al*., 2006). Furthermore, the use of antibodies against the TRAIL receptor have been used to good effect in preclinical studies. For example, the TRAIL-R2 agonist lexatumumab is more effective than the TRAIL-R1 agonist mapatumumab at (1) initiating apoptosis in several metastatic, triple-negative cancer cell lines and (2) reducing lymph node and lung metastases in an orthotopic model of triple-negative breast cancer. These findings provide robust preclinical evidence for targeting TRAIL-R2 in metastatic breast cancer. However, it also provides fundamental knowledge of the different TRAIL receptors' roles in each breast cancer subtype (Malin *et al*., 2011). Moreover, a subset of triple-negative breast cancer, those with mesenchymal features, may be the most likely to benefit from TRAIL targeted therapy (Rahman *et al*., 2009). In regards to clinical trials, compounds such as: soluble rhTRAIL (dulanermin), the TRAIL-R1 mAb agonist mapatumumab and TRAIL-R2 mAb agonists tigatuzumab, lexatumumab and Apomab have demonstrated low toxicity. However, their anti-cancer activity was poor with the majority of patients showing no improvement. To date, the most promising monotherapy has been mapatumumab which entered a phase II clinical trial in patients with non-Hodgkin lymphoma with almost one-third of patients responding and one showing complete recovery (Hayes and Lewis-Wambi, 2015).

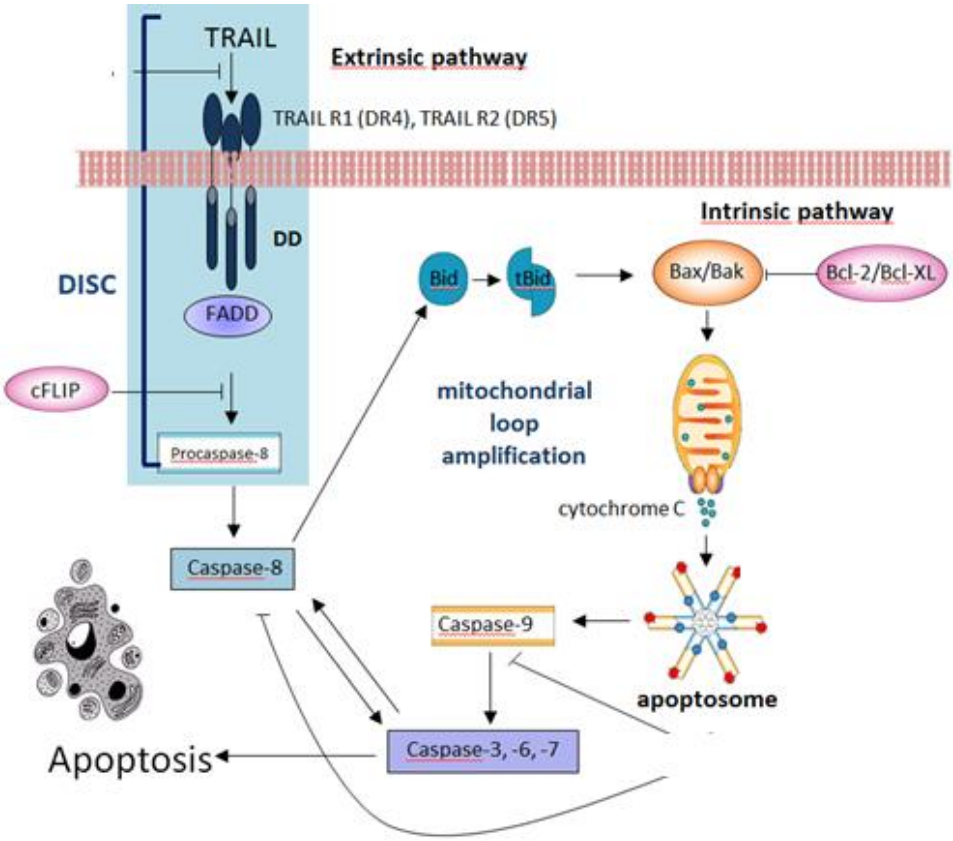

Figure 1.6. Extrinsic and intrinsic TRAIL signalling pathways. TRAIL ligation to a pro-apoptotic TRAIL receptor causes receptor trimerization and activation of initiator caspase-8 and effector caspase-3, leading to cell death. Alternatively, caspase-8 can cleave Bid. Truncated Bid triggers the release of cytochrome c and formation of the apoptosome. The apoptosome activates caspase-9 resulting in activation of caspase-3 and cell death (Goncharenko-Khaider *et al*., 2013)

1.5.2. Cellular FLICE-Like Inhibitory Protein (c-FLIP)

1.5.2.1. c-FLIP Structure and Function

Cellular FLICE-Like Inhibitory Protein (c-FLIP) was first identified in 1997, as a cellular homologue to viral FLIPs (Thome *et al*., 1997; Irmler *et al*., 1997; Hu *et al*., 1997). A number of c-FLIP mRNA splice variants exist but at present only three proteins have been isolated, c-FLIP short (c-FLIPS), long (c-FLIPL) and Raji (c-FLIPR). C-FLIPS is a truncated version of procaspase-8, containing tandem DEDs only, whereas c-FLIPL closely resembles full-length procaspase-8 but lacks the active site catalytic cysteine residue and proteolytic activity. C-FLIPS inhibits DR-mediated apoptosis by blocking caspase-8 activation at the DISC (Krueger *et al*., 2001b and Scaffidi *et al*., 1999) (Figure 1.7).

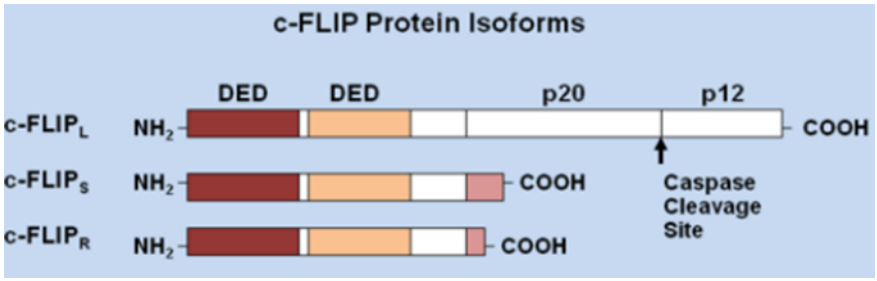

Figure 1.7. c-FLIP isoforms. Three c-FLIP isoforms, c-FLIPL, c-FLIPs, and c-FLIPR, contain two death effector domains (DEDs) at their N-termini. In addition to two DEDs, c-FLIPL contains a large (p20) and a small (p12) caspase-like domain without catalytic activity. c-FLIPS and c-FLIPR consist of two DEDs and a small C-terminus (Safa and Pollok, 2011)

C-FLIPS might act purely as an antagonist of caspase-8 activity but c-FLIPL has a more controversial role, being either an activator or inhibitor of procaspase-8 (*reviewed* in Oztürk *et al*., 2012). Both c-FLIPL and c-FLIPS have been implicated as regulating a number of signalling pathways involved in cell survival and apoptosis, whereas the functional role of the c-FLIPR isoform is not so well known. The c-FLIPL and c-FLIPS isoforms have been shown to be overexpressed in a number of cancer cells and their downregulation using siRNA or non-specific compounds can successfully render previously resistant tumours sensitive to treatment with apoptotic cytokines and chemotherapy. Numerous transcription factors transcriptionally regulate the c-FLIP gene such as: NF-κB, p53 tumour suppressor protein, p63, E2F1, c-myc, IRF5, c-Fos, nuclear factor of activated T cells (NFAT), heterogeneous nuclear ribonucleoprotein K (hnRNP k), the forkhead transcription factor FOXO3a, early growth response-1(EGR1), androgen receptor (AR), E2F, AP-1, and SP1 (Safa *et al*, 2008, Shirley *et al.*, 2010). While NF-kB, p63, NFATc2, EGR1, hnRNP K, AR and SP1 are known to induce c-FLIP expression, c-myc, Foxo3a, c-Fos, IRF5, and SP3 suppress c-FLIP transcription (Safa *et al.*, 2008, Shirley and Micheau, 2010). The c-FLIP isoforms, especially c-FLIPL, conform structurally to the pro-apoptotic caspases -8 and -10 and are also found in close proximity on the genome suggesting they may have evolved from gene duplication. C-FLIPL is a 55kDa protein made up of two death effector domains (DEDs) and a c-terminal caspase-like domain. The caspase-like domain is catalytically inactive as a

result of various amino acid substitutions, especially the critical cysteine residue found in the catalytic domain which has been substituted by a tyrosine residue. All three isoforms are capable of interacting with the adaptor protein FADD through their DED at the DISC. Although c-FLIP has been implicated in development, cell proliferation and drug resistance, the primary function of the c-FLIP protein is as an apoptosis regulator. The precise mechanism by which c- FLIP regulates apoptosis still remains unknown yet it is reasonable to say that regulatory roles differ between the distinct isoforms)Figure 1.7). For example, it has been demonstrated that c-FLIP directly inhibits TRAIL-induced DISC formation by interaction with the adaptor molecule FADD preventing the activation of caspase-8 (Kataoka *et al*. 2000; Safa *et al*. 2008; Shirley and Micheau, 2010; Safa and Pollok, 2011). Thus, the variable ways in which c-FLIP isoforms regulate apoptosis in different cell types suggests that its' apoptosis regulatory mechanism is cell dependent. However, a clarification as to how c-FLIP modulates procaspase-8 activation/activity to produce diverse signalling outcomes has been elucidated by a recent study. A study conducted by Hughes *et al*. (2016) has revealed that c-FLIP L/S isoforms are recruited to the DISC and differentially regulate caspase-8 activation to control cell fate. In their model, using structure-guided DED mutants of full-length FADD, procaspase-8, and c-FLIP L/S, it was shown that contrary to what is known, c-FLIP isoforms do not directly compete with procaspase-8 by binding to FADD. When procaspase-8 is recruited to FADD it recruits and heterodimerises with c-FLIP L/S via a co-operative and hierarchical binding process. The composition of this procaspase-8:c-FLIP heterodimer then constitutes the important decision step, which determines procaspase-8 activation and further cell fate. Heterodimer composition is critically regulated by the ratio of unbound c-FLIP L/S to procaspoase-8. Therefore, at physiological concentrations, the procaspase-8:c-FLIPL heterodimer forms the first active protease at the DISC, exhibits localised activity, and is an activator that promotes procaspase-8 oligomer assembly cell death. In contrast, high levels of c-FLIP preclude procaspase-8 oligomer assembly, restricting caspase-8:c-FLIPL heterodimer activity inhibiting cell death. C-FLIPS does not readily form DED oligomers; thus, high levels of c-FLIP disrupt procaspase-8 oligomer

assembly resulting in a catalytically inactive pro-caspase-8:c-FLIPS heterodimer and inhibition of cell death (Figure 1.8). Significantly, this alternative mechanism for c-FLIP L/S recruitment to the DISC and regulation of DED:DED interactions critically determines procaspase-8 function. This then explains the dual function of c-FLIP where the ratio of c-FLIP isoforms to procaspase-8 differentially control cell survival or apoptosis. Additionally, c-FLIP regulation of caspase-8 is required in T cells where different concentrations of c-FLIP isoforms control cell fate during development of the immune response (Hughes *et al*., 2006).

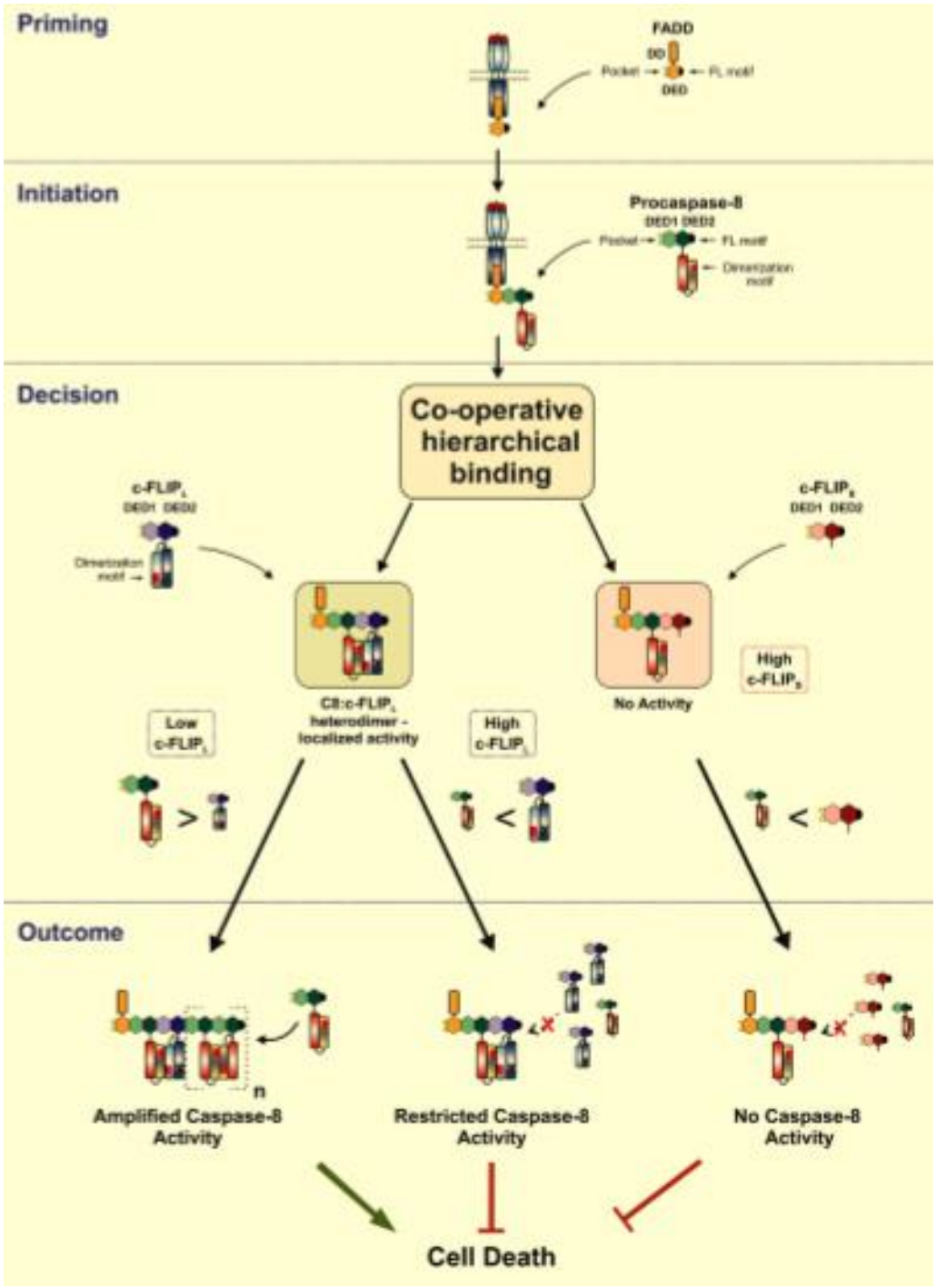

Figure 1.8. c-FLIP mechanisms in controlling apoptosis. The composition of this procaspase-8:c-FLIP heterodimer constitutes a key decision step, which determines procaspase-8 activation and further cell fate. Heterodimer composition is critically regulated by the ratio of unbound c-FLIP L/S to procaspoase-8. Therefore, at physiological concentrations, procaspase-8:c-FLIPL heterodimer forms the first active protease at the DISC, acts as an activator, promoting procaspase-8 oligomer assembly cell death. In contrast, high levels of c-FLIP preclude procaspoase-8 oligomer assembly, restricting caspase-8:c-FLIPL heterodimer activity and inhibiting cell death. C-FLIPS does not readily form DED oligomers; thus, high levels of c-FLIP disrupt procaspase-8 oligomer assembly resulting in a caticaticaly inactive pro-caspase-8:c-FLIPS heterodimer and inhibition of cell death (Hudghes *et al*., 2016).

1.5.2.2. c-FLIP and Cancer

Several *in vitro* studies have demonstrated the importance of the role of c-FLIP in resistance to apoptosis induced by death receptors and chemotherapy (Safa *et al*., 2008; Kruyt, 2008; Yang, 2008; Piggott *et al*., 2011). Increased expression of c-FLIP is identified in many malignant cancers such as: breast, pancreatic, colorectal, bladder urothelial, cervical, gastric, hepatocellular, Burkitt's lymphoma, non-Hodgkin's lymphoma, head and neck squamous cell carcinoma. It also plays an important role in lymph node metastasis, which ultimately contributes to tumour progression (reviewed in Safa, 2011). Importantly c-FLIP expression and is highly associated with a poor prognosis (Safa *et al*., 2008). C-FLIP has therefore been proposed a potential therapeutic target to overcome this drug resistance, by lowering the threshold of cancer cell apoptosis (Safa, 2008). Interestingly, reduction of c-FLIP has been demonstrated to induce cell death without the need of extra therapy. Specifically, it was found that siRNA knockdown of c-FLIP induced a DR5, FADD, caspase-8 and caspase-9 dependant cell death in MCF-7 cells (Day *et al*., 2008). *In vivo* results corroborated with these results demonstrating that injection of liposomal c-FLIP-specific siRNA into MCF-7 xenografts destroyed neoplastic cells with no effect on the normal stromal and fibroblastic cells (Day *et al*., 2009). The *in vivo* results seen from these RNAi-based therapeutic interventions of c-FLIP are crucial to further preclinical development. However, siRNA design, delivery and stability are still difficulties that must be overcome before RNAi-based therapies are truly feasible as a clinical intervention. Besides inhibiting c-FLIP gene expression directly, alternative methods, including degradation and transcriptional regulation of c-FLIP, may also have potential for c-FLIP intervention. For example, a small molecule inhibitor of c-FLIP, 4-(4-Chloro-2-methylphenoxy)-N-hydroxybutanamide (CMH) or droxinostat has been identified, which downregulates c-FLIPL and c-FLIPS mRNA and protein levels, decreases cell survival and induces apoptosis (Safa and Pollok, 2011). Furthermore, cancer cell pre-treatment with chemotherapy has proven to be a successful method of sensitisation to extrinsic cell death ligands. It has been demonstrated that the HDAC inhibitors, suberoylanilide hydroxamic acid (SAHA, vorinostat) inhibit

transcription/translation of a large variety of gene targets, including c-FLIP (Bijangi-Vishehsaraei *et al*. 2010; Shankar *et al*. 2009; Yerbes and Lopez-Rivas 2010). Despite being clinically approved, vorinostat exhibits some side effects in patients and limited efficacy as a monotherapy for breast cancer (Luu *et al*., 2008). However, studies in transgenic mouse models indicate that targeted loss of c-FLIP activity in mammary tissues is not detrimental to normal mammary development (Piggott *et al*., 2011) and c-FLIP remains an attractive therapeutic target (Kruyt, 2008; Yang, 2008; Piggott *et al*., 2011). It has also been found that c-FLIPL is a potential target in TRAIL treatment in HER2 +ve breast cancer because it has been found to be upregulated in these types of tumours. Moreover, cell studies have shown that downregulation of c-FLIPL sensitised a HER2+ cells line (SKBR3) to TRAIL-induced apoptosis, in a dose- and time-dependent manner. Furthermore, c-FLIPL inhibition enhanced cleavage and activation of caspase-8 and caspase-3, which may cause an attenuation to TRAIL resistance in HER2+ breast cancer (Zang *et al*., 2014).

A previous study from our laboratory showed that CSC-like activity was selectively abrogated following c-FLIP inhibition and TRAIL treatment, while the *in vivo* tumour-forming ability of these cells following treatment was reduced by more than 95% (Piggott *et al*., 2011). It has also been shown that c-FLIP upregulates Wnt signalling pathway (one of the pathways associated with cancer stem cells proliferation and survival) (Katayama *et al*., 2010) and affects Gsk3β activity, p27 and caspase-3 levels (Quintavalle *et al*., 2010). These findings highlight cFLIP as a promising target to improve prognosis in breast cancer but as these studies were exclusively performed in cell lines this efficiency still has to be establish in primary breast cancer tissues.

1.6. Breast Cancer and the Tumour Microenviromnent

The tumour-stroma communication has been reported as a hallmark of cancer. The tumour microenvironment is composed of local fibroblasts, endothelial cells, pericytes, leukocytes, and an

extra-cellular matrix. It is well known that the tumour stroma plays an important role in cancer initiation, growth and progression (Pietras and Ostman, 2010). Importantly, the quantity of tumour stroma has been reported as an independent prognostic factor in the clinic. Higher proportion of stroma within the tumour has been correlated with three times increased for risk of recurrence (Kruijf *et al*., 2011).

Cancer associated fibroblasts (CAFs) form an integral component of the tumour microenvironment, and are one of the major components of breast tumours (Orimo *et al*., 2006). These cells have been shown to originate from a variety of sources such as bone-marrow mesenchymal stem cells, local fibroblasts and from cancer cells that have undergone an EMT process (Spaeth *et al*., 2013).

CAFs can either control normal or cancer development. Fibroblasts can hamper neoplastic growth in normal tissues, but can also potentiate invasion and tumour growth in cancer progression (Kuperwasser *et al*., 2004; Schauer *et al*.,2011). The origin of CAFs is uncertain but a previous study recognised two potential pathways: local fibroblasts may be converted into CAFs through stimulation by cytokines, including transforming growth factor-beta (TGF-β) and stromal cell-derived factor-1 (SDF-1). Alternatively, epithelial or endothelial cells may transform into CAFs via epithelial-mesenchymal transition (EMT) and endothelial-to-mesenchymal transition (EndMT), which are also mediated by cytokines, including fibroblast growth factor (FGF), osteopontin (9), TGF-β and SDF-1 (Schauer *et al*., 2011).

Genetic alterations of tumour suppressors in cancer stroma or cross-signalling that upregulates key paracrine pathways (which stimulate cell growth) successful for tumour initiation probably depend on proximal stroma activation (Schauer *et al*.,2011). Other studies have shown that fibroblasts directly modulate tumour growth by secreting factors with oncogenic and mitogenic functions capable of increasing tumour cell proliferation and protecting from apoptosis (Pietras and Ostman, 2010). Additionally, CAFs are able to, indirectly, secrete chemotactic factors to recruit other stromal cell types

into the tumour compartment and also secrete pro-angiogenic molecules resulting in increased angiogenesis. In fact, CAFs release large levels of pro-angiogenic factors including VEGF, CXCL12, FGF, IL-8/CXCL8 and PDGF-C in the ECM to recruit other stromal cell types, such as endothelial cells and their precursors, in order to stimulate tumour angiogenesis and vasculogenesis (Schauer *et al*., 2011). Moreover, co-culture of fibroblasts/CAFs increased the proliferation of lung, pancreas and breast cancer cells. Additionally, co-cultures induced expression of different soluble factors dependent of the cancer type. EGF was mainly secreted by co-cultures of pancreatic and breast cancer cells, HGF was highly secreted by lung cancer cells and fibroblasts, and IL-6 was mainly secreted by the breast cancer co-cultures indicating a cancer-specific pattern in cytokine secretion. Therapies with blocking antibodies against some factors or their receptors inhibited the cancer cell proliferation in the co-cultures. Specifically, blocking IL-6 led to a significant decrease in the survival of BT20 cells that were co-cultured with fibroblasts, demonstrating that the increase in cell proliferation was mediated by IL-6 (Majety *et al*., 2015). Furthermore, PI3K/Akt and MAPK/Erk pathways may be the common key pathways by which both normal and cancer fibroblasts regulate cancer cell proliferation. High secretion of one or more cytokines by CAFs (IL-6, IL-8, VEGF, CCL2 (RANTES) and CCL5 (MCP-1)) may potentially mediate the activation of these pathways to induce cancer cell proliferation (Subramaniam *et al*., 2013). In addition, co-culturing the MDA-MB-231 breast cancer cell line with human CAFs, *in vitro*, resulted in an increased proliferation rate, with a great proportion of tumour cells in S phase compared to tumour cells co-cultured with normal fibroblasts (Peng *et al*., 2013).

CAFs can also promote EMT, invasion and metastasis (Bhowmick *et al*., 2004, Straussman *et al*., 2012). The mesenchymal-like state is associated with the expression of mesenchymal markers, relative quiescence, and high invasive capacity, whereas the epithelial-like state is associated with expression of epithelial markers, establishment of cell polarity, and extensive proliferation (Moreno-Bueno *et al*., 2008, Liu *et al*., 2014). IL-8, a known EMT marker is able reduce the expression of epithelial E-cadherin and increased fibronectin expression in MCF-7 and T47D luminal breast cancer cells (Palena *et al*.,

2012). In addition, activation of EMT could induce the generation of the CSC population (Wellner *et al*., 2009). In prostate cancer, CAFs can stimulate EMT and increase the stemness properties of cancer cells through the secretion of MMPs (Giannoni at al., 2010). Furthermore, CAFs can promote EMT in breast cancer cells through the secretion of stromal-derived factor 1 (SDF-1) and TGF-β1 providing additional support, suggesting that CAFs may promote cancer stemness (Soon *et al*., 2013). Several genes expressed in the cell population defined as stem-like (for example ZEB1, VIM, and DCN) have been shown previously to contribute to the EMT signature. The deregulated balance of these EMT markers might therefore reflect the reversibility of EMT and the influence of microenvironmental changes (Taube *et al*., 2010). In order to accommodate the potential plasticity of these tumour-microenvironmental changes, a combination approach targeting the CSC and non-CSC like populations may present the best strategy for therapy to treat aggressive breast cancers. Accordingly, a number of CSC-targeting agents are now entering clinical trials (Pinto *et al*., 2014).

1.7. Experimental Models of Breast Cancer

1.7.1. Breast Cancer Cell lines and Primary Culture

In general, cell lines mirror both the genomic heterogeneity and the recurrent genome copy number abnormalities found in primary tumours with high fidelity. The evolution of a normal somatic epithelial cell into an immortalised, metastatic cell requires deregulation of multiple cellular processes including genome stability, proliferation, apoptosis, motility, and angiogenesis (Albertson *et al*., 2003; Hanahan and Weinberg, 2000). Considering the fact that many of the cell lines have been cultured for long periods of time, this indicates that they have not accumulated substantial new recurrent aberrations during extended culture and is supported that stable genomic and expression patterns in the cell lines are kept over multiple passages. Important genome mutations like the high-level amplifications associated with poor prognosis in primary tumours are well represented. Furthermore, cell lines also group into basal-like and luminal expression subsets in a similar manner to primary

tumours and show heterogeneous responses to targeted therapeutics mirroring observations in the clinic (Neve *et al*., 2006). Clearly there are distinct advantages for the use of cell lines. However, their relevance in disease is questionable due to the lack of a surrounding microenvironment (for example stroma and vasculature) that, as discussed above, plays a major role in the development and progression of human disease notwithstanding any additional acquired mutations during the transformation process (Place *et al*., 2011). In addition, another disadvantage in using established cell lines is the fact that most breast cancer cell lines are derived from metastatic lesions such as pleural effusions, and may not reflect important features of the biology of the primary tumour (Drews-Elger *et al*., 2014). Thus, the primary tumour heterogeneity and consequently the early stages of breast tumourigenesis are more appropriately modelled by patient-derived primary, short-term cultures from dissociation of specimens from breast tumours. These *ex vivo* models, therefore better mirror the characteristics features of primary breast cancer. Knowledge of breast cancer subtypes, correlation with clinico-pathological features and response to current treatments by means of genomic studies and profiling have significantly increased our understanding of the relevant properties of primary breast cancer cultures (Perou *et al*., 2000; Prat *et al*., 2010). Studies have shown that the tumourigenic primary cultures retain important markers in breast cancer biology (EGFR and HER2) in both the *in vitro* and *in vivo* settings, and shows significant gene expression similarities to their correspondent primary tumour.

Moreover, it is becoming increasingly clear that cells from the tumour microenvironment including immune cells, pericytes, cancer-associated fibroblasts (CAFs), adipocytes, and endothelial cells play a vital role in tumour progression and metastasis (Mueler *et al*., 2004; Hanahan and Weinberg, 2011). Therefore, using cellular models of CAFs in the context of breast cancer biology may lead to the better understanding of crucial interactions within primary breast tumours. In addition, it has been shown that primary cultures consist of two groups of cellular models; one comprising tumourigenic and metastatic breast cancer cells and another group formed by CAFs. These primaries

cultures provide important models for the study of breast cancer pathogenesis including metastatic disease, *in vivo* assessment of drug sensitivities, and discovery of new therapeutics (Drews-Elger *et al*., 2014).

Recently, primary 3D organoid culture of tumours has become a promising strategy for studies of solid, epithelial tumours. Organoids comprise all components of the original tissue, including cancer epithelial cells, endothelial cells, leukocytes, and fibroblasts. 3D organoid cultures recapitulate *in vivo* tissue structural organisation, functional differentiation, chemical and mechanical signals, and therefore, may be more physiologically relevant than 2D cultures of primary or immortalised cells (reviewed in Walsh *et al*. 2016).

Hans Clevers and colleagues developed 3D culture conditions where single epithelial stem cells grow to form the physiological architecture of the organ. They have seen that single Lgr5 positive stem cells were able to form organoids with the appropriate crypt-villus structure with all of the component cell types, including stem cells, goblet cells, transiently amplifying cells, and villus cells. Because these 3D epithelial structures repeat the histology and differentiation of the intestinal epithelium *in vivo*, they were named “organoids”. Organoid has been defined as containing several cell types that develop from stem cells or progenitors and self-organise through cell sorting and spatially-restricted lineage commitment, which occurs *in vivo* (Clevers, 2016). Organoid conditions that allow propagation of multiple benign or cancer epithelial lineages can be used as an *in vitro* patient-derived cancer model. In regards to the mammary epithelium, Sokol and collegues generated an hydrogel scaffold that contained both the protein (collagen, laminins, and fibronectin) and carbohydrate components (hyaluronan) of human breast tissue. Primary mammary epithelial cells isolated from patient breast tissues were cultured into these hydrogels and were able to self-organise, expand, and differentiate to form mature mammary tissues. They found stem cells at the TEBs (Sox9 and slug staining) and it is consistent with findings in the human breast. Culture of hormone-responsive human breast tissues in hydrogels with defined components will allow deeper

investigations of the human mammary gland development and biology, giving a btter knowledge of breast cancer biology (Sokol *et al.,* 2016). Moreover, one disadvantage of organoid protocols involve immediate processing of fresh tissue into organoids, however, it has been recently shown that organoids can be grown and are viable when generated from flash-frozen and DMSO-frozen tissues. Importantly, the drug responses of organoids derived from frozen tissues correlates with that of organoids derived from fresh tissue (Walsh *et al.,* 2016). Additionally, Clevers group has created a living biobank comprising over one hundred breast cancer organoids where they mimic the breast cancer histology: ductal tumours generate solid organoids and lobular generate discohesive organoids. These breast cancer organoids have the advantage of allowing extraction of genetic data from pure tumour epithelium. The lack of contamination with normal cells generates a cleaner DNA profiles and easier detection of somatic mutations. Organoids should be created from breast cancer biopsies and treated in parallel to the respective patients in defined clinical trial and could help to identify possible treatment strategies and resistances for individual patients (Sachs *et al.,* 2018).

1.7.2. Mouse Models of Breast Cancer - Patient-derived Xenografts

Mouse models can provide an excellent resource to study human disease and the development of cancer mouse models has provided important insight into the development of breast cancer. However, it is essential to ensure the chosen models accurately replicate genetic alterations and overall phenotypes observed in human tumours. Moreover, these models serve as preclinical platforms to verify efficacy of potential drug therapies. In some of the early models, mammary lesions were induced by external factors such as the mouse mammary tumour virus (MMTV) and chemical carcinogens. Progress in transgenic technology had provided the development of a new generation of models where tumour suppressors can be knocked out, or oncogenes overexpressed, genetically (Allred and Medina, 2008). In addition to making clear the role of specific genes in breast carcinogenesis or progression, these models have also been useful in elucidating molecular pathways.

Despite advances in controlling transgene expression specifically in the mammary compartment, there are still limitations to constitutively active promoters especially when a transgene of interest has no desirable effects throughout development. This problem has been addressed with the use of inducible transgenic systems, such as the tetracycline-controlled system. This has also proved useful in revealing mechanisms such as oncogene addiction. This is feasible with conditional systems because gene expression can be switched on or off in the presence or absence of its inducer (Allred and Medina, 2008). Another approach to mouse modelling breast cancer has been the use of xeno-transplantation where human cancer cells are transplanted into immunocompromised mice (Vargo-Gogola and Rosen 2007). It has been hypothesised that tumour xenografts produce tumours that are more closely related to breast cancers observed in humans in the clinic. However, the use of immunocompromised mice to establish xenografts lacks the contribution of certain components of the immune system to tumour progression. In general, using established transformed cancer cell lines for transplantation omits certain aspects related to tumour initiation. Therefore, hetero-transplantation of primary tumour biopsies from patients into immune-deficient mice – patient derived xenografts (PDXs) - has many advantages over xenografts using cancer cell lines, for example they also carry human stroma. The hetero-transplant tumours can be directly compared to the original patient tumour biopsies, and to annotated information on patient features, family history, patient outcome, etc. (Marsden *et al*., 2012). With the improvement of mouse clinical trials, it is possible to achieve and to predict important clinical treatments and to optimise new therapeutics more rapidly. However, the individual PDX created based on similarity between patient and PDX responses is challenged by low engraftment rates, time (several months) required to establish a PDX model and high costs in animal maintenance (Whittle *et al*. 2015). Given the current clinical challenge of eliminating metastatic disease, there is an emerging need for models that better predict metastatic behaviour (Whittle *et al*., 2015). It was shown that in studies using a large cohort of breast cancer subtypes: (i) grafts maintain key features of the original tumours, including histopathology, clinical markers, gene expression profiles, copy number

variants and estrogen dependence and/or responsiveness; (ii) the grafts spontaneously metastasise to many of the same organs that were affected in the subjects that were studied; and (iv) tumour engraftment is a prognostic factor for survival time, even in individuals with newly diagnosed breast cancer without known metastatic disease. Not only does this suggest a potential functional assay for assessing tumour aggressiveness, but it also supports the notion that tumour grafts accurately model the cancers from which they are derived (DeRose *et al*., 2012).

1.8. Aims and Objectives

Several compounds targeting TRAIL receptors have shown to be efficient at targeting selected tumour subtypes in preclinical studies but have failed to translate similar potency in clinical trials (*reviewed* in De Miguel *et al*., 2016). These compounds were intended to be used as a monotherapy and to date have largely been undertaken on patients with advanced solid tumours. These compounds demonstrated a low toxicity, however, their anti-cancer activity was poor with the majority of patients showing no improvement (*reviewed* in Hayes and Lewis-Wambi, 2015). Therefore, there is a contradiction between TRAIL efficiency in preclinical studies compared to clinical trials. It is important to note that none of these trials pre-selected patients on the basis of degree of TRAIL sensitivity nor correlated with tumour molecular/histological subtype. Based on *in vitro* evidence of TRAIL sensitivity in mesenchymal-like breast cancer cell lines, we hypothesised that stratification of breast cancers may reveal sub-types that preferentially respond to TRAIL treatment besides mesenchymal cell lines (Rhaman *et al*., 2009). Additionally, acquirement of tamoxifen resistance has been associated with a mesenchymal phenotype, which led us to hypothetise that these endocrine resistant cells might be sensitive to TRAIL. Moreover, there are several studies demonstrating the effect of c-FLIP suppression at sensitising bCSCs to the apoptotic mechanisms of TRAIL (Kruyt, 2008; Yang, 2008; Piggott *et al.,* 2011). Therefore, we hypothetise that Tamoxifen-resistant cells will be sensitive to TRAIL and suppression of c-FLIP will sensitise resistant breast cancer cells to the apoptotic mecanisms of TRAIL.

As there is no work testing this hypothesis in primary breast tissues, TRAIL and c-FLIP suppression will be tested in primary breast tissue directly from patients.

Thus, this part of the project had three key objectives:

(1) To perform TRAIL treatment as a monotherapy in primary breast tissues to identify a particular cohort of patients that might benefit most from TRAIL therapy. Cells will be treated with TRAIL in adherent and non-adhrent conditions.

(2) To combine TRAIL and c-FLIP-inhibition in primary breast tissues to investigate whether c-FLIP suppression can sensitise TRAIL-resistant tumours to TRAIL. c-FLIP would be ideally suppressed by viral transduction of primary cells with lentiviral shRNA targeting c-FLIP. As an alternative c-FLIP would be suppressed via a transient knockdown using siRNA. In addition, c-FLIP would be suppressed using OH14, a compound developed in our laboratory that is a competitive inhibitor of c-FLIP. OH14 binds to the c-FLIP DED domains not allowing c-FLIP binding to the DISC.

(3) To combine TRAIL and c-FLIP-inhibition in human mammary epithelial primary cells (HMECs) to evaluate any toxicity to normal cells.

The tumour microenvironment has been suggested to promote metastatic disease and the maintenance of a cancer stem-like cell phenotype. We hypothesise therefore that cancer associated fibroblasts, may sensitise tumour cells to TRAIL by promoting a more mesenchymal/stem cell-like phenotype. Furthermore, identification of the types of cancer associated fibroblasts that can confer this sensitisation to TRAIL, could be applied as a biomarker for TRAIL sensitivity. For this purpose, we tested:

(4) TRAIL treatment of a human breast cancer cell line and primary breast cancer lines in co-culture with a panel of CAFs or treated with CAF-conditioned medium.

CHAPTER 2

Materials and Methods

2. Materials and Methods

2.1. Cell Lines and Cell Culture

2.1.1. MCF-7 Cell Line

The human immortalised MCF-7 breast cancer cell line was a gift from Dr. Julia Gee, Cardiff University These cells originate from invasive breast ductal carcinoma and are estrogen and progesterone receptor positive but do not over-express HER2 receptor (Neve *et al.*, 2006). Cells were cultured in RPMI 1690 medium (Invitrogen) supplemented with L-glutamine mix (Invitrogen); 10% foetal bovine serum (FBS) (Gibco) and Penicillin (100 U/ml)/Streptomycin (100 U/ml) (Invitrogen). Cells were cultured in T25 (25 cm^2) or T75 (75 cm^2) cell culture flask (Nunc, Fisher) and maintained at 37° C in 5% CO_2.

Cells were split when 80-100% confluent every 3-4 days. The medium was removed from the tissue culture flask and replaced with trypsin-EDTA (Invitrogen) and incubated at 37° C for 5 minutes. Cell detachment was confirmed by microscopy. Trypsin was inactivated by the addition of cell culture medium containing FBS (Invitrogen). Cells were split at a ratio of 1:10 and the remaining cells were used for cell-based assays.

2.1.2. Primary Patient-derived Samples

2.1.2.1. Human Mammary Epithelial Cells

Human primary mammary epithelial cells (HMECs) were purchased from Lonza (Walkersville, MD, USA). Single-cell suspensions of HMECs were obtained by mechanical and enzymatic dissociation from reduction mammoplasties. Cells arrived to the host laboratory in single cells suspensions in a T75 (75 cm^2) at passage 7 and were maintained under culture for a maximum of 15 passages. After centrifugation, cells were cultured in MEBM media (Lonza) supplemented with SingleQuots™ Kit: Gentamicin; Hydrocortisone; Bovine Pituitary Extract; Insulin and Epidermal growth factor (Lonza).

Cells were split at 60-80% of confluency. Medium was aspirated and replaced by 5 ml of room temperature HEPES-BSS (Lonza) prior to trypsin-EDTA because the medium contains complex proteins and calcium that neutralise the trypsin. HEPES-BSS was then removed and replaced with 2ml of trypsin for 6 minutes until 90% of cells were rounded up. After cell detachment, the trypsin was neutralised with 4 ml of trypsin neutralising solution (TNS) (Lonza). The mix was collected into a 15 ml falcon and centrifuged at 200 x g for 5 minutes to pellet cells. Cells were cultured in a T25 (25 cm^2) or T75 (75 cm^2) cell culture flask (Corning, Costar) and maintained at 37° C in 5% CO_2.

2.1.2.2. Primary Culture of Breast Metastatic Samples (n=9)

Primary culture breast metastatic samples were a gift from Dr Robert Clarke, at the University of Manchester. Cells from nine different pleural effusion ascites were collected from patients at The Christie NHS Foundation Trust. All patients were fully informed and gave their consent in accordance with local research ethics committee guidelines (study numbers: 05/Q1402/25 and 05/Q1403/159). Clinico-pathological details and treatments of the samples are summarised in Table 2.1. Single cells were extracted by Clarke's laboratory. Cells were centrifuged at 1,000 × g for 10 min at 4°C. The cell pellets were diluted in PBS. Erythrocytes and leucocytes were removed using Lymphoprep (Axis-Shield) and CD45-negative magnetic sorting (Miltenyi Biotec), respectively. Single cells Cells were cultured in adherence for 7–9 days in DMEM/F-12 medium, GlutaMAX (GIBCO) with 10% fetal bovine serum (FBS; GIBCO), 10 µg/ml insulin (Sigma-Aldrich), 10 µg/ml hydrocortisone (Sigma-Aldrich), and 5 ng/ml epidermal growth factor (EGF; Sigma-Aldrich). Cells were then trypsined and single cells were frozen – 80° C. Vials were shipped to our laboratory and cells were thawed and cultured using the same media. Cells were split at 80-100 % confluence every 3 days. Medium was removed from the tissue culture flask and replaced with trypsin-EDTA (Invitrogen) and incubated at 37° C for 5-10 minutes. Cell detachment was confirmed by microscopy. Trypsin was inactivated by addition of cell culture medium containing FBS (Invitrogen). The mix was collected into a 15 ml falcon and centrifuged

at 200 x g for 5 minutes to pellet cells. Cells were cultured in T25 (25 cm^2) or T75 (75 cm^2) cell culture flask (Nunc, Fisher) and maintained at 37° C in 5% CO_2, 5% O_2.

Table 2.1. Characteristics of nine metastatic endocrine therapy-treated, and patient-derived tumours. IDC: invasive ductal carcinoma; ILC: invasive lobular carcinoma: #: unknown; 5-FU:%-Fluoroucil; FEC: 5-FU, Epirubicin and Cyclophosphamide; ECF: Epirubicin, Cisplatin, 5-FU; EOX: Epirubicin, Oxaliplatin, Capecitabine.

Sample name	Type	Grade	ER	PgR	HER2	Chemotherapy	Hormonal Therapy	Target Therapy
BB3RC29	IDC	2	+	+	-	FEC Paclitaxel Epirubicin	Anastrazole, Exemestane Fulvestrant, Letrozole	-
BB3RC59	ILC	2	+	+	-	EOX Capecitabine Paclitaxel	Letrozole, Tamoxifen, Exemestane, Fulvestrant,	-
BB3RC68	IDC	2	+	#	-	EFC	Tamoxifen, Letrozole, Anastrozole, Fulvestrant,	-
BB3RC71	IDC	3	+	+	+	FEC Capecitabine Vinorelbine Docetaxel	Tamoxifen, Anastrozole, Fulvestrant, Exemestane	Herceptin Lapatinib
BB3RC79	IDC	3	-	-	-	FEC Capecitabine Docetaxel Epirubicin Gemcitabine Carboplatin	-	-
BB3RC81	IDC	2	+	+	-	FEC	Tamoxifen, Anastrazole	
BB3RC90	#	#	+	+	-	-	-	-
BB3RC94	#	#	+	+	-	-	-	-
BB3RC96	#	#	-	-	+	FEC Paclitaxel Trastuzumab Capecitabine	-	Lapitinib

2.1.2.3. Breast Diagnostic Biopsies and Surgical Samples

Primary human breast diagnostic biopsies (n=149; 145 females and 2 males) and post-surgical core biopsies (n=90; 89 females and 1 male) were obtained following consent from the Cardiff and

Vale Breast Cancer Centre at Llandough Hospital under NISCHR ethical approval (12/WA/0252). Clinico-pathological details of the samples used to generate data for the drug treatment result chapters are summarised in Table 2.2.

Cells were processed, maintained and stored according to the Human Tissue Act, 2004 with local (Cardiff University) research ethics approval. Samples were collected in storage solution (Miltenyi Biotec) and washed in RPMI (Gibco). These samples were placed onto white discs and chopped using a McIlwain Chopper. When an homogeneous mash was visible, the aggregates were transferred into a 15 ml falcon containing RPMI with no additives and an enzyme mix from the Human Tumour Dissociation Kit (Miltenyi Biotec): 200 µl of enzyme 1; 100 µl of enzyme 2 and 25 µl of enzyme 3. The 15 ml falcon tube was then placed on the Gentle MACS Dissociator (Miltenyi Biotec) using the program "h_tumour_01" (36 seconds). Samples were then incubated for minutes at 37 °C under continuous rotation using the MACSmix Tube Rotator (Miltenyi Biotec). The previous two steps were repeated twice before the digested tissue was filtered through 70 µm cell strainers and then centrifuged at 1200 rpm for 7 minutes. Cells were cultured in non-adherence conditions in DMEM/F12 media containing 1× B-27 serum-free supplement (Invitrogen), 0.4% bovine serum albumin (BSA)(Sigma), 20 ng/ml epidermal growth factor (EGF) (Sigma), 10 ng/ml basic fibroblast growth factor (bFGF) (Sigma), 4 µg/ml insulin, human recombinant (Sigma) and Penicillin (100 U/ml)/Streptomycin (100 U/ml). Primary cells were maintained in 5% CO2, 5% O2 at 37°C and were cultured in low-attachment plates for 10-14 days to allow tumoursphere formation.

Table 2.2. Characteristics of biopsies and surgical samples and their therapies. IDC: invasive ductal carcinoma; ILC: invasive lobular carcinoma: DCIS – Ductal carcinoma *in situ*; #: unknown. B – core diagnostic breast biopsy; SS – Surgical sample – post-surgical core breast biopsy; PDX – Patient-derived xenografts - tumour obtained after engrafment of a core biopsy or surgical sample.

Sample number		Type	Grade	ER	HER2	Chemotherapy	Hormonal Therapy	Target Therapy
194	SS	IDC	2	+	+	-	-	-
149	B	IDC	3	+	-	-	-	-
61	PDX	ILC	2	+	-	-	-	-
209	SS	IDC + DCIS+ ILCS	3	+	-	-	-	-
202	SS	IDC + High Grade DCIS	2	+	+	-	-	-
195	B	IDC	3	-	+	-	-	-
180	SS	IDC + Mucinous	3	+	-	-	-	-
123	B	IDC + High Grade DCIS	3	+	-	-	-	-
165	SS	IDC	3	+	-	-	-	-
220		Papillary proliferation	2	+	-	-	-	-
72	PDX	IDC	3	-	-	-	-	-
236	SS	IDC + DCIS	2	+	-	-	-	-
229	SS	IDC + DCIS	2	+	-	-	-	-
206	SS	ILC	2	+	-	-	-	-
215	SS	IDC + ILC	2	+	-	-	-	-
164	SS	IDC	3	+	+	-	-	-
217	SS	IDC + DCIS	2	+	-	-	-	-
207	SS	IDC + DCIS	3	+	-	-	-	-
188	SS	IDC + DCIS	3	-	+	FEC Docetaxel	Tamoxifen	-
139	SS	IDC	3	+	+	-	-	-
127	B	IDC	3	+	-	-	Tamoxifen	-
120	B	High grade comedo DCIS	3	-	#	-	-	-
253	SS	IDC + DCIS	2	+	+	FEC	Tamoxifen Letrozole	
77	B	IDC + DCIS	2	+	-	-	-	-
261	SS	IDC + DCIS	3	-	+			
248	SS	IDC + Mucinous	2	+	+	Vinorelbine	-	Rituximab
242	SS	IDC + DCIS	2	+	+	-	-	-
243	SS	IDC + DCIS	3	+	-	-	-	-
218	B	IDC	2	+	-	-	-	-
170	SS	IDC	3	-	-	-	-	-

2.1.3. Fibroblasts Isolation and Culture

After breast samples dissociation (either breast diagnostic biopsies or surgical samples), cells were resuspended in 1ml of DMEM-F12 with 10% FBS and cultured in a 12 well-plate. Fibroblasts are fast growing cells and will rapidly adhere to the surface of the plate. One hour after culture, fibroblasts have already adhered to the plate and then the supernatant was collected and fresh media was added to the top of the fibroblast monolayer. Fibroblast monolayer purity was confirmed using a microscope. These primary fibroblasts were maintained under culture in 5% CO2, 5% O2 at 37°C until passage number 10. Cell morphology was analysed under the microscope to confirm the purity of the fibroblasts cultures.

2.1.4. Co-culture of Fibroblasts with MCF-7 and Fibroblasts Conditioned Medium

On day 1, 160000 cancer-associated fibroblasts (CAFs) from five surgical samples (148, 168, 207, 209 and 253) were plated in 6 well-plates. On day 4, the medium was removed and wells were washed with PBS. Then, 80000 or 160000 of MCF-7 cells expressing GFP were seeded on top of the confluent monolayer of fibroblasts. Co-cultures were fed with 1 ml of medium to mimic the experiments with conditioned medium. After 24 hours, cells were treated with 20 ng/ml of TRAIL for 18 hours. To quantify the percentage of MCF-7 cells expressing GFP, cells were analysed by flow cytometry using BD Accuri. Results were analysed using FlowJo software.

Fibroblasts from either normal breast samples (98) benign breast conditions (213 and 214) or breast cancer (isolated from the diagnostic samples and surgical samples; 61, 89, 105, 148, 153, 168, 206, 207, 209 and 253) were used to generate conditioned medium. Confluent fibroblasts (90 - 100%) were incubated with fresh medium for 24 hours to generate fibroblasts-conditioned medium (CM). After 24 hours, medium was filtered through a 70 µM strainer and either used directly fresh the CM experiments or frozen at - 80°C. For the CM experiments, the immortalised breast cancer cell line

MCF-7 and the metastatic breast cancer cells from pleural effusions BB3RC29, BB3RC81 and BB3RC90 were incubated with 100 µl of 100% CM during 24 hours when at 60-70% of confluency in a 96 well-plate.

2.2. Cell Seeding and Long-term Storage of Cell Lines

MCF-7, HMECs and cells from pleural effusions of patients with advanced breast cancer were detached with trypsin and cells were collected in a 15 ml falcon tube (see previous section for individual protocols used for each sample). Cells were centrifuged at 1200 rpm. Medium containing trypsin was removed and the cells were diluted in medium. Cells were counted using Fast Read Slides (Immune Systems, UK). Cells were then seeded at optimal concentrations into appropriate culture plates (Costar, Sigma, UK), depending on the assay being performed and number of days left for culture (Table 2.3). When all the primary cells used for this study were no longer needed for culture, cells were frozen and cryo-stored in liquid nitrogen at the lowest passage possible. Cells were resuspended in a solution containing 10% v/v dimethyl sulfoxide (DMSO) and 90% FBS and 1ml aliquots were placed in 1.5 ml cryo-tubes (Nunc, Leics, UK). These aliquots were then placed in isopropanol for a slower freezing process at - 80°C in a freezer. On the next day, cells were moved to liquid nitrogen at -180°C. To defrost cells, cells were quickly thawed in a 37°C waterbath and re-suspended in 10 ml of complete media, centrifuged for 5 minutes at 1200 rpm, the supernatant was then removed and the pellet re-suspended in 7 ml of complete media in a T25 flask.

Table 2.3. Plates surface area, media volume and number of cells used for cell culture.

Plate	Surface Area (cm^2)	Volume (ml)	Number of cells
96-well	0.2	0.1	5000 - 15000
24-well	1	0.5	50000
12-well	205	1	100000

2.3. Animal Experiments - Patient-derived Xenografts

All animal xenograft procedures were performed in accordance with the Animals (Scientific Procedures) Act 1986 and approved by the UK Home Office (PPL 30/2849). Samples (see Table 3.3) were transplanted into 8-10 week old NOD/SCID/IL-2γ-receptor null (NSG) mice, commercially obtained from Charles River Laboratories (Wilmington, US). Mice were maintained in individually ventilated cages (Allentown Inc, US) in the Animal House, at the Heath Hospital, Cardiff. Mice were fed with Teklad global 19% protein extruded rodent diet (Harlan Laboratories) and water. Before transplantation tumour/cells were washed with RPMI 1640 medium with no additives. Several methods of sample transplantation were tested such as: chunks, tumourspheres, single cells and aggregates. Chunck refers to a approximately 2 mm segment of the core biopsy or surgical samples. Aggregates refer to the homogeneous mash generated after mechanical disaggregation with the McIlwain Chopper. Single cells refer to the last step of the mechanical and enzymatic digestion of the samples and tumourspheres are obtained 10 days after single cell culture into non-adherent conditions. Chunk and aggregates from biopsies were transplanted directly into the abdominal mammary fat pad of anaesthetised animals in the presence and absence of 100 µl of Matrigel (BD Biosystems) depending on the experiment. Tumourspheres and single cells (either from the diagnostic biopsies or MCF-7 expressing GFP) were diluted with 50% of Matrigel. Mice were supplemented with estrogen and palpated weekly to check possible tumour growth.

2.3.1. TRAIL Treatment *in vivo* and Tumour monitoring

Mice were treated with four daily doses of vehicle or with 16 mg/kg of TRAIL via intraperitoneal injection. Mice were monitored at least twice per week via palpation and measurements were taken with digital calipers (Fisher Scientific, UK). The size of tumours was calculated as volume in mm^3 using the formula: Volume = (Length x ($Width^2$))/2.

2.4. c-FLIP Genetic Suppression using Small Interfering RNA

Small interfering RNA (siRNA) targeting c-FLIP, or a non-specific scrambled control were both custom designed and used in either fast-reverse transfection (ON-target plus SMART pool GE Dharmacon, L-003772-00-0005, UK) or reverse transfections (Stealth siRNA, Invitrogen Life Technologies Ltd, UK). Two different constructs of siRNA for c-FLIP were used: (A) targets long and short form of c-FLIP and (B) is a smartpool siRNA that targets four siRNA duplexes all designed to target distinct sites within the specific gene of interest which target both long and short forms of c-FLIP (Table 2.5).

Cells were transfected using lipofectamine RNAimax (Invitrogen) according to manufacturer's instructions. Mastermixes were prepared by diluting siRNA to a final concentration of 10 or 20 nM in serum-free OptiMEM (Invitrogen) containing lipofectamine as these molarities have proven to be efficient at transfecting cells.

For the reverse transfection, cells were plated and the transfection performed on the same day. Mastermixes were incubated in wells of culture plate at room temperature for 20 minutes prior to cell seeding. Then, 5000 to 10000 cells were trypsinised and seeded into 96 well-plates containing 20 µl of 10 nM siRNA in serum free OptiMEM in a volume of 100 µl per well, together with 0.3 µl of Lipofectamine.

For the fast-forward transfection, cells were plated 24 hours prior to transfection. 20 nM of siRNA was prepared in 10 µl serum-free OptiMEM (Invitrogen) before the addition of 0.1 µl of lipofectamine. This solution was mixed and kept at room temperature for 5min before 10 µl being added to cells in the 96 well-plates containing 90 µl of medium (Table 2.4). Cells were cultured in the presence of siRNA for 48 or 72 hours prior to subsequent assay.

Table 2.4. Volumes and concentrations for siRNA transfections.

96-well Culture Plates	Volume of plating media (µl)	Volume of OptiMEM medium (µl)	Volume Lipofectamine RNAiMAX (µl)	Final siRNA concentration (nM)
Fast-forward Transfection	80	20	0.3	10
Reverse Transfection	90	10	0.1	20

Table 2.5. siRNA sequences for fast and reverse transfection.

Target	Sequence
c-FLIP 1	Sense: GGAUAAAUCUGAUGUGUCCUCAUUA Anti-sense: UAAUGAGGACACAUCAGAUUUAUCC)
c-FLIP 2 (smartpool)	Sense: GUGCCGGGAUGUUGCUAUACAAGCAGUCUGUUCAAGGA Anti-sense: CAUGGUAUAUCCCAGAUUCCCUAGGAAUCUGCCUGAUA
Scrambled	Sense: GGACUAAUAGUUGUGCUCCAAUUUA Anti-sense: UAAAUUGGAGCACAACUAUUAGUCC

2.5. Drug Treatments

2.5.1. TRAIL and Caspase Inhibitor Treatments

TRAIL was obtained from Enzo technologies (Human SuperKillerTRAIL trade), diluted 1:4 in TRAIL buffer and stored at -80°C. Cells were treated with 20 -100 ng/ml of TRAIL for 18 hours. Prior to TRAIL treatment cells were cultured with the caspase inhibitor Z-VAD-FMK (R&D Systems) for 1 hour at a concentration of 20 ng/ml.

2.5.2. OH14 Treatment

OH14 was developed by the Clarkson group, Cardiff University (Figure 2.1). OH14 is a small molecule compound selected as part of an *in silico* screen on the surface of c-FLIP DED1 for compounds which interfere with the interaction between c-FLIP DED1 and DED of FADD in order to prevent its competitive inhibition of caspase-8 activity. OH14 was diluted from DMSO stock at 100 mM and then diluted in medium to give concentrations of 100 µM and 10 µM of OH14. Cells were treated with 100 µM/10 µM of OH14 and 0.1% and 0.01% of DMSO in the control wells 1 hour before TRAIL treatment.

For assays using OH14, caspase inhibitor and TRAIL, cells were first treated with OH14 before, then 45 minutes between caspase inhibitor and TRAIL.

2.6. Stem Cell Culture and Sphere Assay

The sphere assay is an assay designed to isolate normal stem cells (mammosphere assay) and cancer stem cells (tumoursphere assay) by their ability to survive in anoikis conditions (Dontu *et al.,* 2003). A very low concentration of cells is plated into ultralow attachment plates (Corning). These plates are covered with a covanlently bound hydrophilic, non-ionic, neutrally charged hydrogel, which induce anoikis in the bulk population meaning only stem cells are able to survive and form spheroids.

MCF-7 cells were plated at a density of 5000 cells/ml in serum-free epithelial growth medium (MEBM, Lonza), supplemented with growth supplement B27 (Invitrogen), 20 ng/ml EGF (Sigma), Insulin (Sigma), and hydrocortisone (Sigma).

Metastatic cells were plated at a density of 20,000 viable cells/ml in primary culture (exception for BB3RC29, which was at a density of 10000 cell/ml). Diagnostic biopsies and post-surgical samples were plated using the entire number of single cells harvested after tumour dissociation. These cells were seeded in DMEM/F-12 medium, GlutaMAX (Gibco) supplemented with B27 and 0.4% bovine serum albumin, 4 µg/ml insulin (Sigma), 20 ng/ml EGF (Sigma), 10 ng/ml bFGF (BD Biosciences), and Penicillin (100 U/ml)/Streptomycin (100 U/ml). Alternatively, these cells were cultured in MammoCult™ medium with supplements commercially bought from STEMCELL Technologies in ultra-low attachment plates (Costar, Corning).

HMECs were seeded at a density of 20000 cells/ml and grown in a serum-free mammary epithelial growth medium (MEGM, Lonza), supplemented with B27 (Invitrogen), 20 ng/mL EGF and 20 ng/mL basic fibroblast growth factor (bFGF) (BD Biosciences), and 4 µg/mL heparin (Sigma). Bovine pituitary extract was excluded.

For a second passage to test self-renewal, spheres were collected by gentle centrifugation (800 rpm) after 7–10 days and dissociated enzymatically (10 min in 0.05% trypsin-0.25% EDTA, Invitrogen) and mechanically, using a 200 µl pipette. The cells obtained from dissociation were analysed microscopically for single-cellularity. Cells were counted under the microscope and it was only considered spheroids bigger than 50 µM of diameter.

2.7. Lentiviral Transduction

MCF-7 cells were transduced using a lentivirus carrying GFP as a fluorescent marker to investigate how transduction efficiency could be recapitulated into tumoursphere cultured. The lentivirus carrying GFP was a gift from Dr Matt Smalley's group and it was ready to use. 75000 single cells were resuspended in 100 µl of lentivirus and plated under adherent conditions with antibiotic-free media and 6 – 10 µl of Polybrene (neutralises charge repulsions between the virus and the cells and greatly enhances transduction efficiency). The medium was changed after 72 hours and GFP positive cells were analysed when cells were confluent.

To test the efficiency of lentiral transduction *in vivo,* 80 GFP positive MCF-7 spehres resuspended in 100 µl of PBS and 100 µl of Matrigel and then transplanted into the mammary fatpad of an immunocompromised mouse, which generated primary tumours over a 7 week period. Palpable tumours were excised and viewed under fluorescence microscope along with excised lungs. Primary tumours were dissociated using the same protocol used for the patient-derived samples.

To investigate the transduction efficiency of MCF-7 cells versus primary cells, the metastatic cell line BB3RC81 was transduced using the same protocol.

Additionally, an inducible lentivirus carrying shRNA for c-FLIP was tested in MCF-7 cells. This ready-to-use lentivirus expressing GFP and RFP was commercially purchased from AMSBIO (AMS Biotechnology Europe Ltd, UK). The shRNA sequences (Table 2.6) were cloned into a lentiviral shRNA expression vector that also contains a marker GFP-Puromycin under Rsv promotor. The target is driven

by a tetracycline CMV promoter. For inducible expression, a tetracycline protein must be present in advanced to inhibit the expression.

35000 MCF-7 cells were cultured in a 24 well-plate and 24 hours later at 50% confluence, cells were transduced with the tetracycline repressor (TetR) particles (AMSBIO) marked with blastomycin. The expression could be induced after the addition of tetracycline which removes TetR from the promoter. After 72 hours, medium was replaced with complete medium containing 10 µg/ml of Blastomycin to select the stably transduced cells. When cells reach confluency, cells were trypsinised and the number of RFP positive cells was assessed. RFP positive cells were sorted and plated into 24 well-plated.

MCF-7 cells were also transduced with the expression particles to test single transduction efficiencies. Cells were transduced at 50% confluency with the inducible expression particles. Medium was replaced 72h after with medium containing 10 µg/ml of puromycin.

All cells were sorted using the BD Accuri and data was analysed using FlowJo software.

Table 2.6. shRNA sequences for lentiviral transduction.

shRNA	Sense	Anti-sense	Titer (IFU/ml)
Negative Control	GTCTCCACGCGCAGTACATTT	AAATGTACTCGCGTGGAGAC	1.33 x10^7 IFU/ml
Sequence #2	AGATTGGTGAGGATTTGGATA	TATCCAAATCCTCACCAATCT	1.02 x10^7 IFU/ml
Sequence #3	GTGGTTGAGTTGGAGAAACTA	TAGTTTCTCCAACTCAACCAC	1.15 x10^7 IFU/ml

2.8. Gene Expression Analysis Using Quantitative Real-Time PCR

2.8.1. RNA Analysis and Extraction

Prior to working with RNA, all equipment and work surfaces were cleaned using RNAseZAP (Ambion) to prevent contamination from RNAses. Then total RNA was extracted using the RNeasy Plus Mini Kit (QIAGEN, 74104). The RNeasy procedure is a methodology for RNA isolation that combines

the selective binding properties of a silica-gel based membrane with the speed of microspin technology. Biological samples are lysed and homogeneised in the presence of a highly denaturing guianidine isothiocyanate containing buffer, which immediately inactivates RNases. Ethanol is added to provide appropriate binding conditions, and the samples are then applied to an RNeasy mini column where the total RNA binds to the membrane, contaminants are washed away, and RNA is eluted in RNase-free water.

RNA extraction and analysis were performed for HMECs, MCF-7 cells or Metastatic breast samples. Culture medium was removed from well-plates, washed with PBS and replaced with 350 µl RLT buffer for 5min. After cell lysis cells were mixed 1:1 with 70% ethanol and RNA extraction was performed using the RNeasy Plus Mini Kit. After addition of 70% ethanol (350 µl), each samples was applied to an RNeasy minicolumn placed in a 2 ml collection tube and centrifuged for 15 seconds at 8000 xg. The flow-through was discarded and 700 µl of washing RW1 buffer was added to the columns and centrifuged for 15 seconds at 8000 x g. The columns were then washed using 500 µl of RPE buffer and centrifuged for 15 seconds at 8000 x g and flow-through was discarded. The columns were washed again with RPE buffer at the same centrifugation speed but for 2 minutes. To dry the silica-gel membrane, columns were centrifuged again for 1 minute at 13200 x g. Finally, the RNA was diluted by adding 30 µl pf RNase-free water directly onto the silic-gel membrane and centrifuging the columns for 1 minute at 13200 xg. The concentration and purity of RNA preparations were determined by the spectrophotometric measurement of the absorvances of the samples at 260 nm and 280 nm using the Nanodrop 3000 spectrophotometer (Thermo Scientific). RNA samples were stored at -80°C.

2.8.2. c-DNA Synthesis

Reverse transcription of 100 ng of RNA was performed with the High-Capacity c-DNA Reverse Transcription Kit (ThermoFisher, 4368814). Samples were treated with a mastermix containing: 2µ 10X RT Buffer; 0.8 µl 10X dNTP Mix (100 nm); 2 µl 10X RT Random Primers, 1 µl MultiScribe™ Reverse

Transcriptase and 4.2 µl of Nuclase-free water giving a total volume of 10 µl. Then, the RNA was added giving a final volume of 20 µl reaction. Samples were incubated on a thermal cycler (BioRad) for 10 minutes at 25°C, 120 minutes at 37°C and 5 minutes at 85°C. c-DNA was stored at -20°C until future use.

2.8.3. qRT-PCR Analysis

2.8.3.1. Primer Design

All primers were commercially bought from ThermoFisher Scientific. Each primer was designed to express a FAM-reporter dye with the exception of β-actin controls (ACTB) which was designed to carry a VIC-reporter dye so multiplex PCR reactions could be performed (Table 2.7).

Table 2.7. qPCR primers.

Target	Assay ID (Taqman probes)
β-Actin	Hs99999903_m1
c-FLIP	Hs.00390736_m1
E-cadherin	Hs01023894_m1
N-cadherin	Hs00983056_m1
Vimentin	Hs00958111_m1
Snail	Hs00161904_m1
Slug	Hs00161904_m1
IL-6	Hs00985639_m1
IL-8	Hs00174103_m1

2.8.3.2. qRT-PCR Reaction and Analysis

Quantitative real-time PCR reactions were designed to include primers targeting the gene of interest and the house-keeping control gene β-actin (ACTB) together in the same well. This method gives a more accurate reading of gene expression because it is possible to normalise target

amplification specific to the amount of cDNA in each sample. Experiments were set up in triplicate for each biological triplicate. 96 well-plates or 384-well plates and performed on the QuantStudio 7 Flex PCR machine (Applied Biosystems) using TaqMan® Universal PCR Master Mix (Applied Biosystems). 1 µl of c-DNA was added to the well and then 9 µl of a mastermix containing: 5 µl TaqMan Universal Master Mix II; 0.5 µl of target primer; 0.5 µl of ACTB primer and 3 µl of RNAse free water.

The plate was sealed with Micro AMP optical adhesive films (Applied Biosystems) and shortly centrifuged to remove any drops from the lid. Plates were then run on a QuantStudio 7 Real-Time PCR machine (Applied Biosystems). Conditions used for amplification of cDNA fragments were as follows: 95°C for 10 minutes, 40 cycles of amplification at 95^{o}C for 15 seconds (denaturation), 60^{o}C for 1 minute (annealing/elongation).

The expression levels were calculated using the ΔΔCt method and normalised to the housekeeping gene β-actin in Excel Office 2013. In these calculations, Ct values were subtracted from ACTB control Ct values for individual wells to create a ΔCt, which was then averaged from triplicate wells for each sample. To calculate difference in gene expression between samples, ΔCt of treated samples was subtracted the to the ΔCt of the untreated control resulting in a ΔΔCt value. This value was then calculated as -2 ΔΔCt to give the relative fold change, which was then transformed on a log10 scale.

2.9. Cell Viability Assay

Cell viability was assessed by CellTiter blue assay (Promega, UK). This assay measures cell viability by measuring their ability to convert the blue dye reasurin into the fluorescent product resofurin. Non-viable cells do not have the metabolic capacity to convert this subtract and do not produce a fluorescent signal. Cells were washed with PBS and fresh medium was added to the plates. Then the appropriate amount of cell titre blue reagent (kept at -20°C and thawed at room temperature) was added to the medium (eg. 20 µl of reagent in 100 µl of media). Plates were

incubated for 1-4 hours at 37 °C 5% CO_2 5% O_2. Fluorescence was assessed using a ClarioStar plate reader (BMG Labtech).

2.10. Live/dead Assay

Live/Dead Assay (Invitrogen) was performed to access the number of dead cells using a the far-red fluorescent reactive label. Cells were trypsined and washed in PBS. Red dye was diluted in PBS at a ratio 1:20. Cells were centrifuged and resuspended in 10 µl of dye/PBS. Samples were incubated at 4C for 15 minutes and then resuspended in 100 µl PBS. Flow cytometry was performed using Accuri Flow Cytometer (BD Biosciences) for analysed using FlowJo software.

2.11. Aldefluor Assay

Identification of stem cells with high activity of aldehyde dehydrogenase (ALDH) was assessed usng the Aldefluor assay (Stemcell Technologies). The amount of fluorescence released by the product is directly proportional to the ALDH activity in cells. Dissociated single cells were suspended in Aldefluor assay buffer containing an ALDH substrate, bodipyaminoacetaldehyde (BAAA) at 1.5 mM, and incubated for 45 minutes at 37ºC. To distinguish between ALDH-positive and -negative cells, cells were incubated under identical conditions in the presence of a 2-fold molar excess of the ALDH inhibitor, diethylaminobenzaldehyde (DEAB) previous the incubation. Cells were centrifuged at 12000 rpm and resuspended in 100 µl of PBS. Data was acquired on a flow cytometer, Accuri Flow Cytometer (BD Biosciences) and analysed using the FlowJo™ software.

2.12. Immunofluorescense of Fixed Cells

MCF-7 cells were seeded onto sterile glass coverslips previously place into 24 well-plates at a density of 10000 cells/ml. On the day of analysis, cells were rinsed with PBS to remove any dead cells. Cells were fixed with 4% formalin for 15 minutes followed by 3 x 5minute washes in PBS. Non-specific epitopes were then blocked with 10% normal goat serum (Dako) in PBS with 0.5% triton-X (Sigma) for

1 hour. Cells were incubated with primary antibody overnight at 4°C (Table 2.8). A negative control without primary antibody was used for every sample. After another 3 x 5 minute wash with PBS, cells were incubated in fluorescence-conjugated secondary antibodies (Invitrogen) diluted in 10% normal goat serum (Dako) and containing DAPI nuclear stain at a ratio of 1:1000 (Invitrogen) for 1 hour. Cells were then washed for 3 x 5 minute in PBS and mounted in Mowiol solution (Sigma). Cells were visualised on a confocal microscope from Leica.

Table 2.8. Antibodies used for immunofluorescence.

Primary Antibody (Dilution)	Secondary Antibody (Dilution)	Species	Company
E-cadherin (1:100)	Goat Anti- Mouse (1:200)	Mouse	Abcam

2.13. Statistical Analysis

Independent experiments were performed in triplicate and data are represented as mean +/- standard deviation (SD) or standard of mean (SEM) as stated in respective legends. Statistical analysis was used using Graphpad Prism version 6.0. Unpaired paired data set were parametrically tested using Student's t test. A value of probability (p) equal or inferior to 0.05 was considered to be statiscally significant.

Pearson's correlation coefficient (r) was calculated to statiscally investigate whether two sets of groups were linearly associated. The correlation coefficient 'r' was calculated using Excel 2016 software. Results were considered significant if the calculated value of r was greater than or equal to the tabulated value at the 5% significance level for n – 2 degrees of freedom.

The waterfall plots were used to help and visualisation and interpretation of the TRAIL treatment on all the samples used in this study. Graphs were ploted from the sample with the least response to the sample that had the best response to TRAIL treatment.

2.14. Workflow Chart

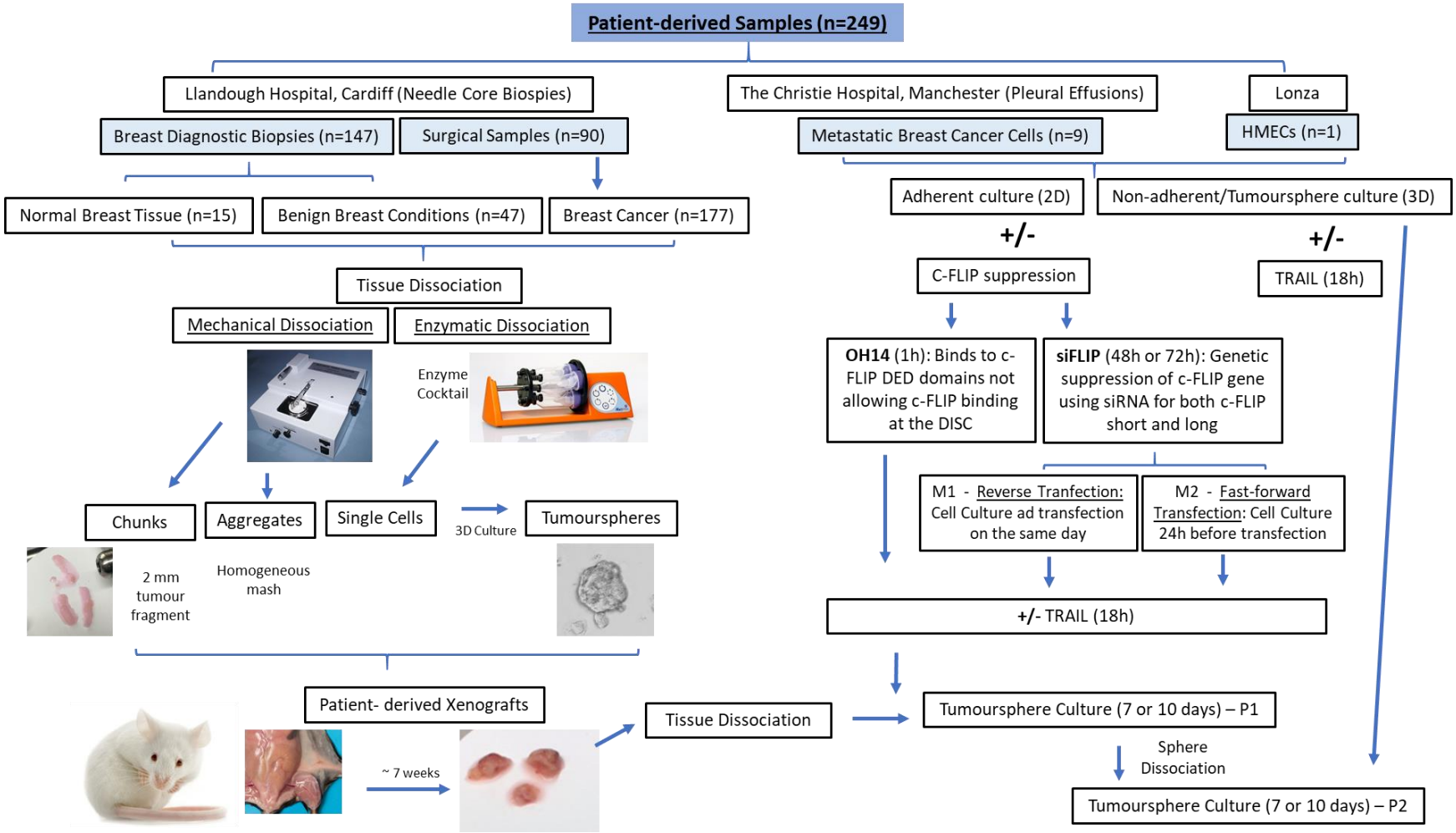

CHAPTER 3

Optimising Cell Culture Conditions and Lentiviral Transduction for Primary Human Breast Biopsies

3. Optimising Cell Culture Conditions and Lentiviral Transduction for Primary Human Breast Biopsies

3.1. Introduction

Primary tumour heterogeneity and early stages of breast tumourigenesis are more appropriately modelled by cultures from dissociated primary breast tumours than by established transformed cell lines. These *ex vivo* models, better mimic the characteristic features of primary breast cancer (Perou *et al*., 2000). Assays utilising primary cultures provide important models for the study of breast cancer pathogenesis including metastatic disease, *in vivo* assessment of drug sensitivities and discovery of new therapeutics (Drews-Elger *et al*., 2014). Furthermore, hetero-transplantation of primary tumour biopsies from patients into immune-deficient mice, patient-derived xenografts (PDXs), has many advantages over xenografts using cancer cell lines. Histologically, PDX models are able to retain the architecture and stromal components of the original tumour potentially representing the complex biochemical and physical interactions between the cancer cells and their microenvironment, not observed in cell lines (Tentler *et al*., 2012). At the cellular level, PDXs preserve the inter-tumoural and intra-tumoural heterogeneity, as well as the phenotypic and molecular characteristics of the original tumour, including chromosomal copy number variants, single-nucleotide polymorphisms and gene expression profiles (*reviewed by* Choi *et al*., 2014.) Thus, the tumours from these transplants can be more directly compared to the original patient tumour biopsies (Marsden *et al*., 2012). Moreover, given the current clinical challenge of eradicating metastatic disease, there is a pressing need for models that better predict metastatic behaviour.

There is robust evidence supporting a potent effect of c-FLIP suppression and TRAIL treatment on bCSCs in cell lines (Piggott *et al*., 2011). As these studies have so far only been performed on breast cancer cell lines, the key question still remains whether these findings have direct clinical relevance for breast cancer patients. As such, this study will test the hypothesis that c-FLIP suppression

combined with TRAIL reduces cell viability of primary breast cancer cells (bCSCs) including bCSCs *ex vivo*. To achieve this aim, breast cancer samples were collected from the clinic and maintained in different culture conditions supporting bCSC growth. These cells were then to be used to investigate breast cancer cell response to TRAIL alone and in combination with c-FLIP suppression. A range of tumour types were tested to determine if this strategy is most effective in a specific cohort of patients or if this approach may be effective across a broad spectrum of breast cancer subtypes as demonstrated in cells lines (Piggott *et al*., 2011). Moreover, we wished to investigate as to whether serial passaging of patient-derived xenografts altered their phenotype or morphology in order to determine the translational relevance of these models.

3.2. Results

3.2.1. Different tumour samples have different sphere forming efficiency

During the course of this three year study, 239 samples have been processed and cultured *ex vivo*. Due to the different parameters that affects quality and quantity of the samples, such as: differing proportions of tumour versus normal tissue; heterogeneity of relative epithelial, adipose, connective tissue, haematopoeitic cells and non-tumour content within tumours; and the variability associated with mechanical and enzymatic digestion of bulk tissues; the efficiency of recovery of epithelial cells from primary biopsies were subject to substantial variation. Of the 239 tumour samples collected: 6.3% (n=15) were subsequently characterised as normal breast samples including microcalcifications and cysts that naturally occur within the breast due to the aging process; 18.8% (n=47; female + male) were benign breast conditions such as: fibroadenomas; sclerotic tissue and hyperplasia; and 74.0% (n=177; diagnostic biopsies + surgical samples; female + male) were found to contain bone fide tumour. In regards to grade: 8.0% (n=14) of the tumour samples were grade 1; 43.0% (n=76; female + male) were grade 2 and 36.9% (n=65) were grade 3 (Table 3.1). Additionally, 37.9% were pre-menopausal; 64.8% post-menopausal and 2.1% were peri-menopausal.

Table 3.1. Statistical analysis of the samples received.

Samples (n=239)		
Characteristics	**Female (n=236)**	**Male (n=4)**
Age (Range)	22-95	45-85
Normal breast samples	15 (6.3%)	0
Benign condition samples	45 (18.8%)	2 (0.8%)
Diagnostic biopsy tumour samples	87 (36.4%)	0
Surgical biopsy samples	89 (37.2%)	1 (0.4%)
Family history	5 (2.8%)	-
Grade		
Grade 1	14 (8.0%)	0
Grade 2	75 (42.6%)	1 (0.4%)
Grade 3	65 (36.9%)	0
Previous therapies		
Chemotherapy	7 (4.0%)	-
Radiotherapy	5 (2.8%)	-
Endocrine	13 (7.4%)	-
Surgery	3 (1.7%)	-

The initial proportion of viable samples growing under culture was very low and to overcome this issue the protocol to process these samples has been optimised. Firstly, we adopted a method used by Marsden *et al*., 2012: a mechanical dissociation with a scalpel and enzymatic dissociation with collagenase and hyaluronidase. 15 samples were dissociated using this method and only 3 samples have grown spheres under culture (20%). Further optimisation was introduced to improve enzymatic dissociation of samples. For enzymatic dissociation, a collagenase and trypsin mix was replaced by the Miltenyi Biotec "tumour dissociation kit" which was introduced to alleviate undue stress on the cells imparted during long enzymatic digestion, thus increasing cell viability. To improve mechanical dissociation of samples a scalpel was also replaced by a McIlwain mechanical chopper. This was consistent with a study conducted by Turin *et al*. 2014, where two different approaches to obtain viable cells from surgical samples were performed: the use of mechanical disaggregation with a cell scraper and a Gentle MACS Dissociator. Here, it was shown that primary culture was considered effective if they met the following requisites: presence of a pure line of tumour cells confirmed by morphological and immunological experiments; sufficient cell number to perform the previous experiments and cell survival when cells are frozen and subsequently thawed. They found that the disaggregation using the GentleMACS improved the capacity to establish the tumour cell lines with a successful rate of 50% and resulted in 100% efficiency when generating primary cultures from pleural effusions (Turin *et al*., 2014).

After dissociation, cells were originally washed with RPMI and passed through a 40 µM strainer, however, cells were found to be retained in the strainer due the presence of the adipose and connective tissue resulting in a reduced cell recovery. Thus, a 70 µM strainer was found to be more suitable for the protocol, increasing the number of cells collected for plating and substantially decreasing the probably of cell-clogging whilst still providing single cell isolates. Furthermore, before cell culture, the number of cells counted and the number of cells extracted did not correlate nor predict the sphere forming efficiency. This might be explained by the heterogeneity of the tissue

processed. Within the isolated cells, red blood cells, adipose cells, fibroblasts, etc., are also present with the tumour cells. Consequently, prior to culture, a red blood cells lysis buffer was used to eliminate red blood cells. To increase the purity of epithelial cells, cells were incubated in adherent conditions for 1 hour in DMEM to allow the fibroblasts to attach to the plate surface leaving a suspension of purer epithelial cell population that could be collected (Smalley *et al.,* 2007).

After fibroblast removal, the medium was removed and cells were centrifuged and resuspended in tumoursphere medium. Initially, cells were cultured in the tumoursphere medium optimised for use in cell lines. To increase the sphere forming efficiency, the cell line tumoursphere media was replaced by medium detailed in the Marsden *et al*. 2012 protocol, which includes the addition of fresh growth factors (EGF and bFGF) prior to every tumoursphere culture. However, as the number of spheres did not substantially increase with these medium changes, another tumoursphere medium, Mammocult™ (Stem Cell Technologies, Canada), was used in attempt to further improve the sphere forming efficiency. Mammocult™ significantly increased the number of spheres in four out of seven samples. However, the increase was relatively small. Despite of existing a trend towards the Mammocult medium, this increase in the number of spheres was not much higher than the other medium (Figure 3.1 A).

Analysing all the samples, were able to calculate: the percentage of viable samples (samples that formed any number of spheres under culture) and successcul samples (samples that formed more than 20 spheres in three wells used for control). Therefore, within normal or breast benign conditions, 48.8% (n=29) of the samples were viable, while out of all the diagnostic biopsies, only 36.7% were able to grow spheres under culture (Table 3.2). In regards to the percentage of successful samples within the viable samples: 75% (n=32) of the normal and benign conditions and 28.9% (n=39) of the diagnostic samples were able to successfully form more than 20 spheres (Table 3.2).

Spheres formed from biopsies may not be derived purely from tumour cells as, despite the isolation step, it is possible that benign (or normal) stem/progenitors could be plated among the

tumour cells. To overcome this problem, core tumour tissues have been extracted from surgically resected tumour samples where nearly the entire sample processed is tumour tissue. However, despite this enrichment for tumour cells, the total number of cells extracted did not increased compared to diagnostic biopsies (Figure 3.1 B) and the percetange of viable samples only increased 8%. However, the efficiency of these tumour-rich samples to successfully form spheres increased by 47.6% (Table 3.2). This leads us to believe that the efficiency of successfully growing spheres is not related to the number of cells extracted but rather to the type (number of tumour cells) and proportion of stem-like progenitors within the samples and that cell number cannot predict the number of spheres that can be generated in culture.

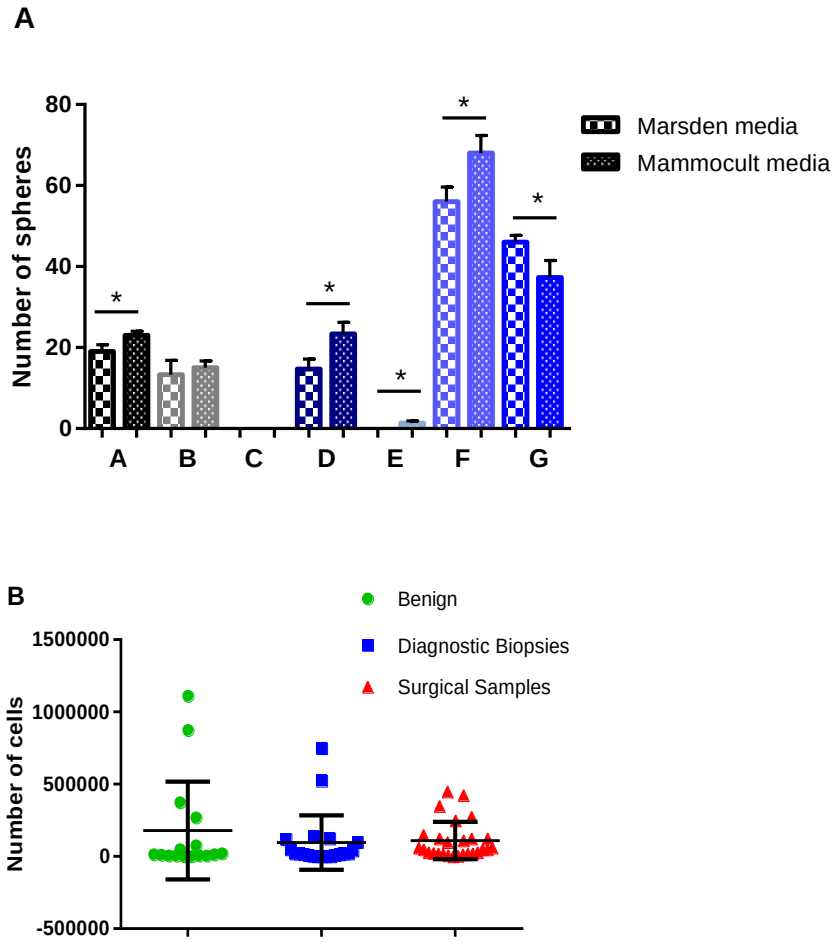

Figure 3.1 Number of cells and of spheres in breast samples| | **A.** Number of spheres in 7 samples (A-G) cultured with Marsden and Mammocult™ media. | **B.** Number of cells extracted from benign, diagnostic and surgical breast samples. | Bars represent mean +/- SD; *(p) < 0.05; t-test.

Table 3.2. Statistical analysis of cell number and spheres formed under culture of the breast samples received from the clinic. "Viable" samples refers to samples that have formed any number of spheres under culture. "Successful" refers to the samples within the viable samples that formed more than 20 spheres.

Breast samples (n=239)			
	Normal + Benign samples	**Diagnostic biopsy tumour samples**	**Surgical samples**
Number of processed samples (total %)	62 (25.9%)	87 (36.4%)	90 (37.7%)
Total number of cells extracted (Mean)	375000 (178869)	525000 (95571)	425000 (109704)
Average number of spheres	51	37	57
% "Viable" Samples	48.8%	36.7%	44.5%
% "Sucessful" Samples	75.0%	28.9%	76.5%

The short-term survival of primary cells under adherent conditions and poor propagation during passages unable to achieve our objective of subjecting cells to shRNA and siRNA for c-FLIP, prior to tumoursphere culture, as although a mean of 500,000 cells would be sufficient for knockdown protocols. Also, attempts to increase cell number by passaging the spheres in non-adherent culture were unsuccessful since the cell numbers remained stable over several passages and ultimately declined. However, we were able to test the effect of TRAIL treatment alone, through administration of the peptide to the culture medium. Furthermore, we adopted a pharmacological inhibitor of c-FLIP, OH14, for use in sphere conditions.

Using these small molecules we set out to correlate histological and molecular subtypes of the samples with tumoursphere forming capacity, and ultimately (Chapter 5) their susceptibility to TRAIL stimulation and/or c-FLIP suppression.

The most common histological subtype was Ductal (50% of the tumour samples), including Invasive Ductal and/or DCIS with the lobular subtype being the second most common (8%). We have received additional histological subtypes such as: high grade comedo; Invasive Mucinous; Phylloides; Pappilary; Micropapillary and Cribiform DCIS. However, very few of these samples could be cultured in sphere conditions such that no statistically robust data could be generated. The Invasive Ductolobular subtype had the highest sphere forming capacity, with an average of 78 spheres although only two samples of this kind were collected. The Ductal subtype had an average of 73 spheres and Lobular 18 (Figure 3.2. D) demonstrating that ductal subtype might have a higher capacity than lobular at generating spheres. In addition, to histological grade and molecular subtype comparisons, receptor expression was believed to be another potential predictive marker of sphere forming capacity. Estrogen Receptor (ER) – positive (+ve) samples and ER- negative (-ve) samples generated an average of 58 and 53 spheres, respectively (Figure 3.2. E). The molecular subtype luminal B (ER +ve and HER2 +ve) generated an average of 64 spheres; luminal A (ER +ve HER2-ve) an average of 59 spheres; HER2 (ER -ve HER2 +ve) generated 30 spheres and the triple negative, basal-like (ER -

ve HER2 -ve) counted with 54 spheres (Figure 3.2 F). This may suggest that HER2 may possibly play an important role in stem cell survival in mammosphere conditions. This is consistent with previous reports of the role of HER2 in CSC-like activity *in vitro* (Farnie *et al*., 2007; Korkaya *et al*., 2008).

Hitherto, 14 samples of grade 1 have been collected, however, none were capable of generating spheres. Grade 2 samples and grade 3 samples generated an average of 62 and 79 spheres, respectively (Figure 3.2 C), highlighting the importance in grade for sphere forming capacity.

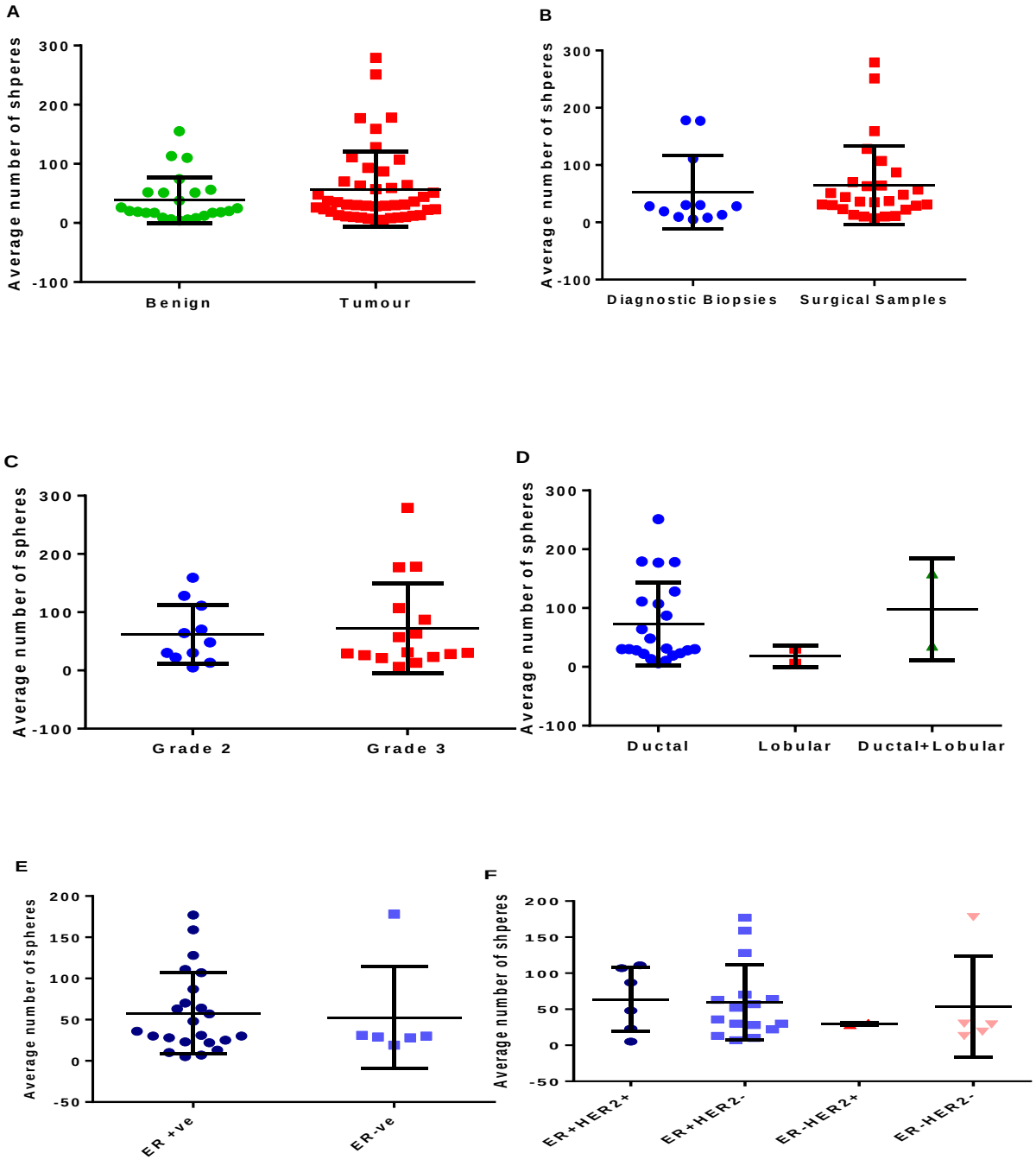

Figure 3.2 Sphere forming efficiency of the breast samples. Y axes represents number os spheres formed from normal/benign brest condtions, diagnoastic biopsies and surgical samples. | **A.** Number of spheres in benign and tumour samples. | **B.** Number of spheres in diagnostic and surgical samples | **C**. Number of spheres in grade 2 and grade 3. | **D.** Number of spheres in ductal, lobular and ductolobular breast samples | **E**. Number of spheres in estrogen receptor positive and estrogen receptor negative tumours. | **F.** Number of spheres for ER and HER2 receptors: luminal B (ER +ve HER2 +) luminal A (ER +ve HER2 -ve); and triple negative (ER -ve and HER2 -ve). | Bars represent mean +/- SD.

3.2.2. Patient-derived xenografts increase the number of cells for *in vitro* studies

Due to the number of cells not being sufficient to successfully address the aforementioned aims, we investigated another methodology using patient-derived xenografts (PDXs) to address this. The rationale for this was that PDX tumours would provide a larger, more homogeneous tumour tissue sample for processing. For this purpose, chunks, aggregates, single cells and spheres from the biopsies/surgical samples were orthotopically xenografted into immune-compromised NOD.Cg-Prkdc^{scid}Il2rg^{tm1Wjl}/SzJ (NSG) mice. These are immunodeficient mice, which lack B- and T-cell function but retain innate cellular immunity (including natural killer cells, macrophages).

Overall, ER negative tumours achieved a more successful engraftment rate than ER-positive tumours (45% and 7%, respectively; Table 3.3). The efficiency of transplanting aggregates and single cells was 0% (Table 3.3). Transplanting 30 spheres generated from *ex vivo* culture samples 120 and 123 were able to generate metastases in the lungs but no primary tumour, whereas 10 spheres from sample 7, and 89 spheres from the surgical sample 202 were not able to form tumours in the primary site or metastasise. Interestingly, transplantation of 244 spheres from a tumour harvested from the PDX 151 model (this PDX was previously established by transplanting a 2mm chunk) was able to generate a primary tumour and lung metastases (Table 3.3). Transplantation of tumour chunks proved to be the most successful mechanism for establishing tumours in NSG mice where transplanting 2 mm tumour chunks prepared directly from the biopsy resulted in approximately 29% of xenografts generating primary tumours and metastases (Table 3.3). Additionally, ER -ve tumours (2/4 – 50%) have a higher engraftment rate than ER +ve tumours (2/10 – 20%), however, this did not correlate with histological subtype (Table 3.3).

Table 3.3. Patient-derived xenogratfs characteristics vs Transplantation Methods and Primary tumour Metastasis forming efficiency. (1) – unknown (2) Sample is still growing *in vivo*.

Transplantation Method	Sample characteristics					Primary tumour	Metastasis
	No	Type	Grade	ER	HER2		
Chunk	11	Invasive Ductal	2	+	-	✗	✗
	12	Invasive Ductal	1	+	(1)	✗	✗
	61	Invasive Lobular	2	+	+	✓	✗
	72	Invasive Ductal	3	-	-	✓	(1)
	110	Invasive Ductal	2	+	-	✗	✗
	151	Invasive Ductal	3	-	-	✓	**Lung**
	160	Invasive Ductal	3	+	-	✗	✗
	188	Invasive Ductal + DCIS	3	-	+	✗	✗
	190	Lobular pleomorphic	3	+	-	✗	**Kidney**
	191	Invasive Ductal + DCIS + LCIS	3	+	-	✗	**Lung**
	204	Invasive Ductal	3	+	-	✗	**Lung**
	218	Invasive Ductal	2	+	-	✗	✗
	227	Invasive Ductal	3	-	-	✗	✗
	231	Invasive Ductal	3	+	+	✓	(2)
	232	Invasive Ductal	3	-	-	✗	✗
	253	Invasive Ductal + DCIS	2	+	+	✗	✗
	255	Invasive Ductal + DCIS	(1)	+	-	(2)	(2)
	262	Invasive adenocarcinoma	3	-	-	✓	(1)
	262	Invasive adenocarcinoma	3	-	-	✓	(1)
Single Cell	60	Invasive Carcinoma	(1)	-	-	✗	✗
Aggregates	62	Invasive Ductal	2	+	-	✗	✗
Spheres	7	DCIS	(1)	(1)	(1)	✗	✗
	120	High grade comedo + cribiform DCIS	(1)	-	(1)	✗	**Lung**
	123	Invasive Ductal + High grade DCIS	3	+	+	✗	**Lung**
	151	Invasive Ductal	3	-	-	✓	**Lung**
	202	Invasive Ductal + High grade DCIS	2	+	+	✗	✗

Moreover, the number of cells extracted from PDXs was significantly higher than from biopsies and surgical samples (Figure 3.3 A). The number of spheres generated from the tumour harvested from the PDX was higher than the original biopsies A, B and C. Samples A, B and C tissues were cut into 2 mm chunk for orthotopic transplantation into mammary fat pad and processed for *in vivo* studies and the rest of the tissue for *in vitro* culture. The tissues plated in sphere conditions generated a low number of spheres (Table 3.4). However, 7 weeks after xenograft a primary tumour in the mammary gland was palpable and the tumours were dissected and dissociated using the same protocol used for biopsies. The single cells were plated under non-adherent conditions and samples A, B and C generated 61, 49 and 357 spheres, respectively indicating xenografts may be a suitable model to increase cell number and culture efficiency (% of viable and successful samples). This higher number of cells and spheres was probably due to the much larger tumour size that could be acquired from PDX tumours compared to biopsies (Figure 3.3 D and E). For example, a 2 mm chunk of the sample A was able to generate an 8mm diameter tumour after 8 weeks *in vivo* (data not shown) which could be successfully dissociated to generate a high number of spheres.

Furthermore, serial passaging of established PDX models was investigated to determine whether the key characteristics (ER and HER2 status) remained stable through further tumour generations. To date, PDX 151 has been passaged 4 times and has maintained a stable phenotype with identical ER and HER2 status throughout passages. This phenotype was analysed by Dr Fauad Alchami, a histopathologist at The Heath Hospital in Cardiff and receptor status was analysed using immunohistochemistry by Dr. Julia Gee in School of Pharmacy, Cardiff University (data not shown).

Table 3.4. Number of cells extracted and tumouspheres formed from original tumours vs PDXs. Number of cells and spheres formed from three original tumour (A, B and C) and respective PDXs. PDXs were generated by transplanting 2mm chunks into mice and a palpable primary tumour was grown in 7 weeks.

Sample	Original tumour		PDX	
	No. cells extracted	**No. spheres formed**	**No. cells extracted**	**No. spheres formed**
A Invasive Lobular G2 ER+ HER2+	Undetermined	**0**	30000	**61**
B Invasive Ductal G3 ER- HER2+	Undetermined	**3**	Undetermined	**49**
C Invasive Ductal G3 ER- HER2+	2500	**19**	1250000	**357**

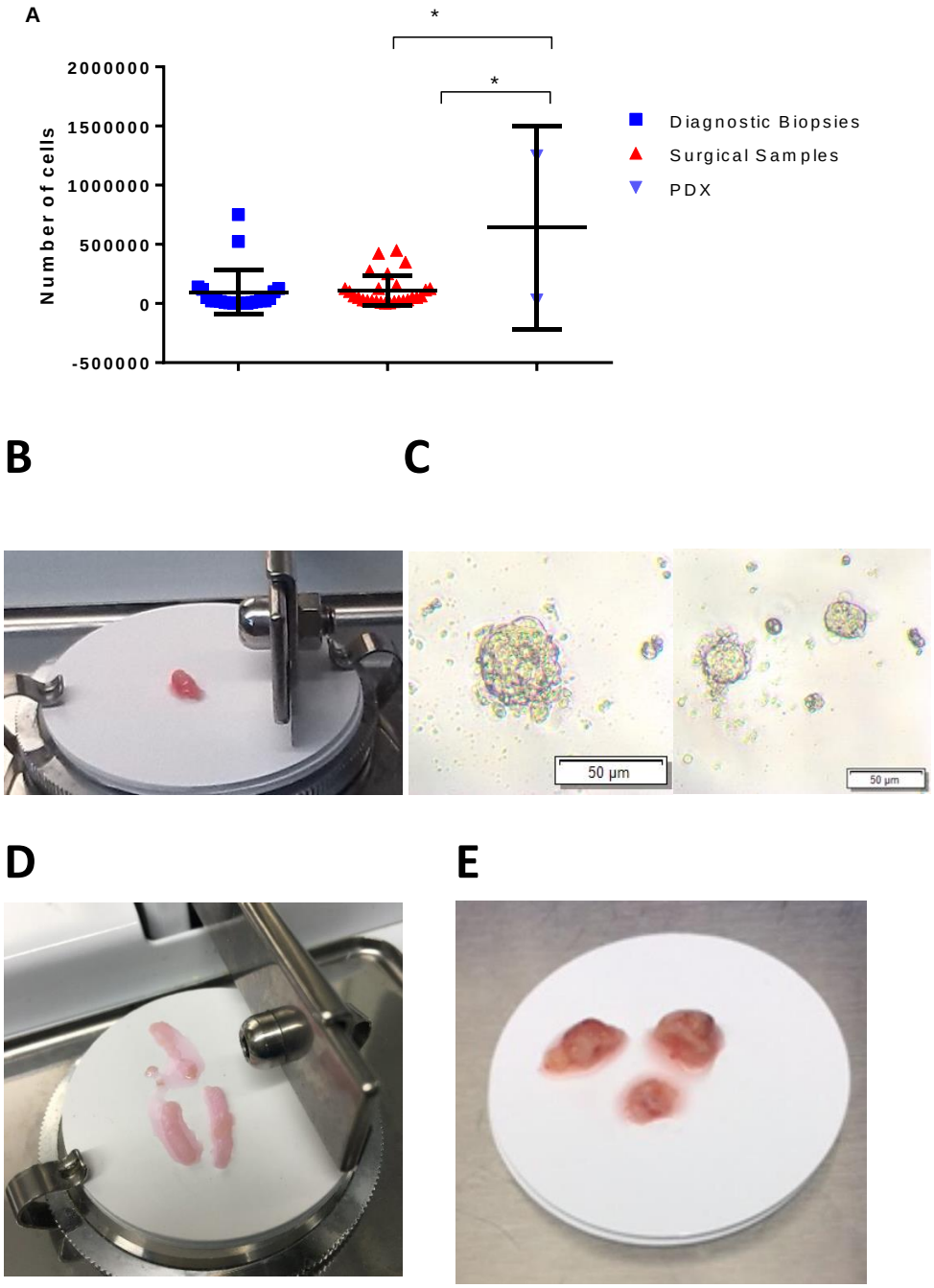

Figure 3.3 A. PDX tumours. | **A.** Number of cells extracted from diagnostic biopsies, surgical samples and PDXs Bars stood for mean +/- SD. *(p)<0.05; t-test. | **B.** A 2mm chuck from an Invasive Ductal G3 ER- HER+ biopsy was transplanted into the mammary fat pad (PDX B). 7 weeks after, the primary tumour was dissected and dissociated into single cells. | **C.** Tumourspheres formed after 5 days under non-adherent culture from the PDX B. | **D.** Surgical samples ready to be mechanically dissociated. | **E.** Primary tumours generated from a PDX.

3.2.3. MCF-7 cells are efficiently transduced with a lentivirus carrying GFP compared to primary cells

Luminal-like breast tumour cell lines, which represent 60-70% of the breast cancer population are resistant to TRAIL killing but can be sensitised to TRAIL through suppression of c-FLIP (Safa *et al*., 2008; Piggott *et al.,* 2011). In order to determine if this is also true for primary tumours, we proposed to suppress c-FLIP in primary breast cancers using: 1) an inducible lentivirus carrying shRNA to inhibit c-FLIP gene expression and 2) OH14, a pharmacological compound that binds to c-FLIP DED domain inhibiting c-FLIP binding to FADD in the disc complex.

Since the aim was to use an inducible lentivirus for tumoursphere culture of breast primary tissues, it was important to optimise conditions first in an immortalised breast cancer cell line with known tumoursphere characteristics. Therefore, transduction efficiency of a constitutive lentiviral vector carrying GFP into MCF-7 cells was investigated and how this efficiency could be recapitulated into tumoursphere culture. These cells were transduced under adherent conditions and GFP positive cells was assessed by flow cytometry, which showed 87.9% of MCF-7 cells expressing GFP (Figure 3.4 B). Cells were sorted and 100% GFP positive cells were plated into non-adherent conditions to propagate tumourspheres (Figure 3.4 C). On second passage, tumourspheres were dissociated and cells were analysed by flow cytometry which showed 99% of the MCF-7 population expressing GFP (Figure 3.4 D). Thus, MCF-7 CSCs can be transduced in adherent culture and with high efficiency by lentivirus to stably express GFP in subsequent progenitor cells. Furthermore, 80 GFP positive MCF-7 spheres were transplanted into the mammary fatpads of recipient immunocompromised mice, which generated primary tumours over a 7 week period. Palpable tumours were excised and viewed under fluorescence microscope along with excised lungs. Primary tumour exhibited strong fluorescence, indicating that a high proportion of cells retained GFP expression while small foci of fluorescence were seen within the lung tissue, indicating the presence of metastatic tumours (Figure 3.4 E). Primary tumour was dissociated and single cells were plated in sphere conditions. Seven days later, spheres

were dissociated and single cells from these cultures were assessed by FACS. Cell analysis showed that 94.5% of the cells were expressing GFP (Figure 3.4 F). These data confirm the stable expression of GFP in stem/progenitors and their progeny.

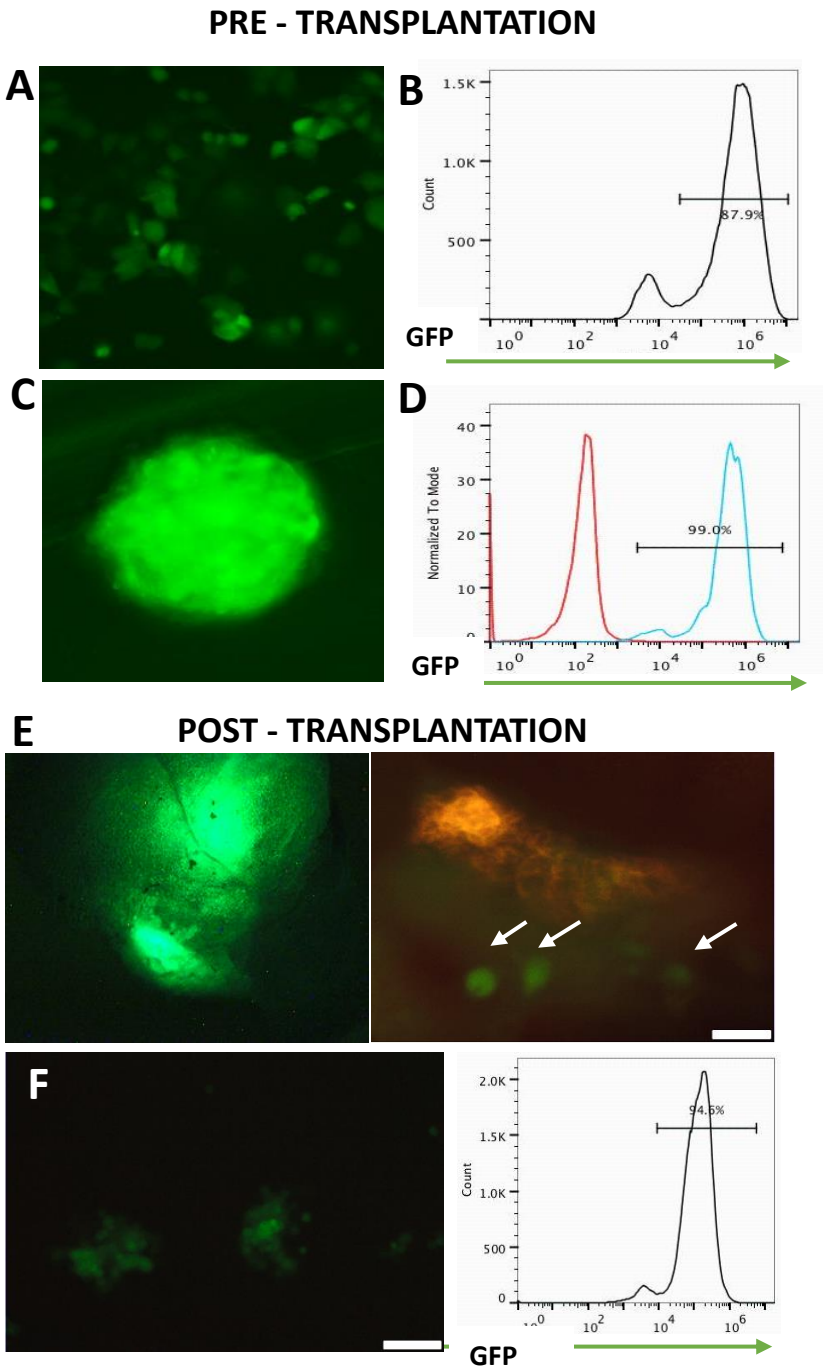

Figure 3.4. MCF-7 expressing GFP. | Pre- transplantation. A. Adherent culture 7 days post-infection with a lentivirus carrying GFP.| **B.** MCF-7 GFP +ve cells were analysed by flow cytometry which showed 87.9% GFP +ve cells. | **C.** Cells were sorted and plated under sphere condition. | **D.** After second passage, spheres were dissociated and 99% were expressing GFP (FACS plot showing representative percentage of MCF-7 expressing GFP (blue) compared to the control after GFP-cell sorting (red). | **Post-transplantation**. **E.** 80 GFP positive MCF-7 spheres were transplanted into the mammary fatpads of recipient immunocompromised mice, which generated primary tumours after 7 weeks. Then, primary tumour (left side) and lungs (right side) were harvested and observed through a fluorescent microscope. White arrows show lung metastases. | **F.** Three primary tumours were harvested (5.1 mm; 4.4 mm and 3.1 mm) and one of the primary tumours was dissociated and cells were plated under sphere conditions (left side). One week after, spheres were disaggregated and cells were analysed by FACS. 94.5% of the MCF-7 cells were GFP +ve (right side). | Scale bars represent 200 µm.

Parallel to this transduction, we tested an inducible lentivirus acquired from AMSBIO (AMS Biotechnology Europe Ltd, UK), which expressed GFP and RFP (RFP for the lentiviral particles expressing the tetracycline regulator (TetR) and GFP for the lentivirus expressing short hairpin RNA (shRNA) to target c-FLIP expression). The efficiency and stability of the shRNA lentiviral construct was tested initially in MCF-7 cells.

MCF-7 cells were transduced with different concentrations of TetR particles and different concentrations of two different shFLIP constructs (seq#2 and seq#3, Table 3.5). Cells were treated with different concentrations of puromycin to select cells that were tranduced with TetR particles and blastomycin to select cells with shFLIP. A lentivirus lacking a sequence to target c-FLIP was used as a negative control. To enhance transduction efficiency, cells were treated with 8-12 µg/ml of polybrene. Cells were transduced according to the manufactures protocol (Section 2.7) where cells are firstly transduced with the TetR particles and transduced with the shFLIP construct 24 hours later. The ultimate objective was to work with an inducible dual transduction lentivirus but first the efficiency of single transductions was tested. Transduction with TetR particles was very low, only 19% of the cells expressed RFP using the highest titration of the virus (Table 3.5) Moreover, using different concentrations of the shFLIP vectors for sequence 2 (seq#2) and sequence 3 (seq#3) resulted in an equally low percentage of GFP positive cells, with the negative control giving the highest transduction efficiency (Table 3.6). Cells were sorted and 100% of GFP +ve cells were plated into adherent conditions to collect RNA for c-FLIP gene analysis by qPCR. qPCR analysis of c-FLIP gene expression showed that seq#3 was effective at knocking down c-FLIP gene by 80% using the lowest concentration of virus (#3_15) (Figure 3.5). However, after a few passages the number of GFP +ve cells was significantly lower showing that the lentivirus transduction was unstable (perhaps due to GFP silencing) and subsequent progenitor cells were not expressing GFP. Using the dual transduction, TetR particles plus shFLIP for the seq#3 showed an efficiency of 0.5% when cells were analysed by flow cytometry (data not shown).

Table 3.5. Efficiency of a lentivirus carrying RFP in MCF-7 cells. 35000 MCF-7 cells were plated in 24 well-plates and 24h after cells were transfected at 50% confluency. Cells were treated with blastomycin for antibiotic selection and 8 µg/ml of polybrene. After cell growth, cells were analysed by flow cytometry to measure the percentage of cells expressing RFP.

TetR (µl) (Titer- $5x10^7$ IFU/ml)	% RFP+ cells
10	3
20	4.1
30	5.5
50	19

Table 3.6. Efficiency of a lentivirus carrying shFLIP and GFP in MCF-7 cells. 35000 MCF-7 cells were plated in 24 well-plates and 24 after cells were transfected at 50% confluency. Cells were treated with puromycin for antibiotic selection and 8 g/ml of polybrene. After cell growth, cells were analysed by flow cytometry to measure the percentage of cells expressing GFP.

shFLIP (µl)	% GFP+ cells
cneg (10 µl, $121x10^3$ IFU)	40
#2 (30 µl-$306x10^3$ IFU)	2
#2 (50 µl- $510x10^3$ IFU)	7
#3 (15µl - $173x10^3$ IFU)	4
#3 (30 µl - $345x10^3$ IFU)	5.5
#3 (50 µl - $575x10^3$ IFU)	4.5

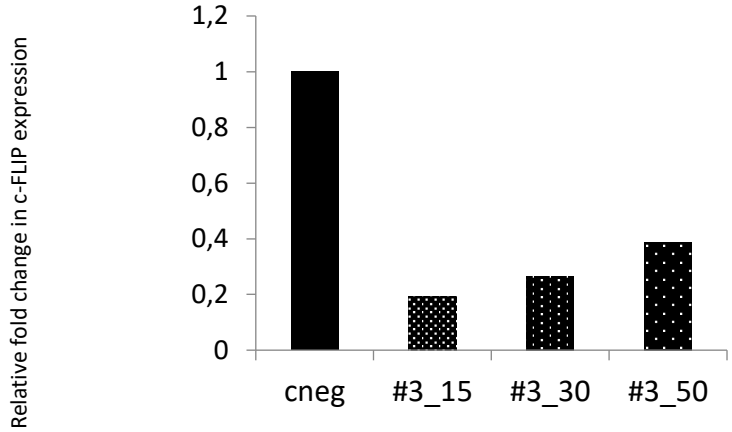

Figure 3.5. c-FLIP expression after transduction with a lentivirus carrying shRNA for c-FLIP. Relative fold change in c-FLIP gene expression. Cells were transduced using three different concentrations of the sequence 3 (#3) as seen in table 5.2 and 15 days after RNA was extracted and c-FLIP expression was analysed using qPCR.

Subsequently, lentivirial transduction in primary cells was investigated. A simple lentiviral vector carrying only GFP was used to determine the efficiency of lentiviral transduction in primary cells. The lentivirus efficiency was investigated using metastatic primary cells obtained from a pleural effusion (BB3RC81). Using the same protocol as for the MCF-7 cells, the efficiency was very low; only 4% of the total population was expressing GFP (Table 3.7). To improve this efficiency, the protocol was optimised by centrifuging the cells with the virus to increase the number of viral particles entering into the cells. In addition, cells were plated with 50% of concentrated virus plus 50% of media. However, this efficiency only improved to 14% of the total population expressing GFP (Table 3.8). During this optimisation, it was determined that the optimal number of cells (for the BB3RC81) for lentiviral transduction was 10,000 cells, below this number, cells did not form more than 10 spheres and higher numbers of cells (50000 and 100000) appeared to decrease the transduction efficiency (Table 3.6). Thus, the efficiency on transducing primary cells was very low compared to the 89.7% efficiency observed with the transformed MCF-7 cell line.

Moreover, the lentiviral vector targeting c-FLIP was not stable in MCF-7 cells and it is reasonable to suggest that this efficiency would be even lower in primary cells. Yet, another primary cell line or another vector from another company could be optimised to extend the voracity of these results. Having no strategy to inhibit c-FLIP in a long and inducible manner, we opted to suppress c-FLIP using a transient knockdown (siFLIP) and using the in house made c-FLIP “inhibitor”, OH14.

Table 3.7. Lentiviral transduction efficiency in the surviving population in tumoursphere assay using primary cells. Primary cells were transduced with a lentivirus carrying GFP. Cells were resuspended in the virus and plated for 72h. Media was changed after 72h. Spheres were counted after 7 days, dissociated to single cells and sorted for cells expressing GFP. After sorting cells GFP +ve cells were plated under non-adherent conditions.

BB3RC81	Number of spheres	GFP+ cells	
Number of cells		% GFP+ cells	Number GFP+ cells
Control (4000)	11	0	0
500	0	0	0
4000	0	0	0
10000	N/A	4	43

Table 3.8. Lentiviral transduction efficiency in the surviving population in tumoursphere assay using primary cells. Primary cells were transduced with a lentivirus carrying GFP. Cells were resuspended in the virus, centrifuged and plated with a ratio 1:1 with media:virus. Media was changed after 72h. Spheres were counted after 7 days, dissociated to single cells and sorted for cells expressing GFP. After sorting cells GFP +ve cells were plated under non-adherent conditions.

BB3RC81	Number of spheres	GFP+ cells	
Number of cells		% GFP+ cells	Number GFP+ cells
Control (4000)	15	0	0
500	1	0	0
4000	8	0.5	0
10000	N/A	14	110
50000	N/A	3.5	-
100000	N/A	0	0

3.3. Discussion

The aims for this project were straight forward: to generate a sufficient number of tumour cells from primary culture to enable shRNA transfection prior to propagation of tumourspheres. There were a number of key technical hurdles to overcome related to tumour heterogeneity and cell viability *in vitro*. After biopsy collection, the core tumours were dissociated and primary cells cultured under non-adherent conditions. Due to the nature of some samples, the obstacle to culturing these cells was determined to be having a sufficient number of cells after harvest that will allow enough replicates to perform a statistically robust experiment. Moreover, due to the large variety of breast tumour sub-types it proved difficult to obtain sufficient sample numbers to reach statistical power when correlating the response to treatment with tumour subtype. Furthermore, among the several biopsies that we received, we observed that in most cases it was the quality (high proportion of adipose tissue; red blood cells and non-tumour tissue) of the original tumour that determined yield and not the amount of the tissue. The efficacy in establishing and maintaining tumour cells in culture depends on the characteristics of the original sample, which in most cases could be rich in connective and adipose tissue, in some cases small fragments were obtained at the completion of the dissociation protocol and it was not possible to count the number of cells that were cultured. One study tried to establish primary cultures from surgical breast samples using mechanical and enzymatic dissociation and culture with feeder cells (Janik *et al*., 2016). This feeder layer has been associated with numerous technical issues, including incomplete inactivation of fibroblasts leading to overgrowth of feeder cells, and there is a risk that feeder cells will not be able to provide epithelial cancer cells with adequate support (Pourreyron *et al*., 2011). Janik *et al.,* 2016 found that using Geltrex coating had a similar efficiency to feeder layer, while being substantially less complicated and easier to validate. Also, commercial primary cell media demonstrated lower efficiency than tissue-specific ones. This strategy

using feeder cells could be adopted for optimisation of our protocol in the future to improve primary cell growth in adherent conditions.

During the 3 year project, 239 breast samples were processed from the clinic with two thirds being characterised as carcinomas, half derived from diagnostic biopsies and half from surgical resections.

In our study, the majority being tumour samples, the non-cancer samples (normal and benign breast conditions) had a slightly higher percentage of viable cells than diagnostic biopsies and surgical samples (49%; 37% and 45%, respectively) (Table 3.2).

Furthermore, the surgical samples had a higher rate of viable samples compared to the diagnostic samples, 44.5% and 36.7%, respectively. Additionally, surgical samples had a higher rate of successful samples compared to the diagnostic samples, 76.5% and 28.9%, respectively (Table 3.2). The size of the surgical resection material was similar to the diagnostic biopsies which may explain why the number of cells extracted and number of spheres were similar between those samples (Figure 3.1 B and 3.2 B). However, as surgical samples were more enriched with tumour cells, which explain the higher rate of successful samples compared to diagnostic biopsies.

Moreover, tumourspheres generated from grade 3 breast cancers were found to form a greater number of spheres compared to grade 1 which is consistent with previous studies (Allan, 2011). Previous studies have also detailed that grade 3 tumour samples generate a greater number of spheres when compared to the grade 2, suggesting that more aggressive samples have a higher sphere forming capacity (Farnie *et al.,* 2007). However, in the data presented here, the number of spheres from grade 3 was not significantly higher than grade 2 (Figure 3.2 C). In conjunction with this hypothesis we would also expect the typically more aggressive ER -ve samples to also grow a higher number of spheres. However, Farnie *et al*. 2007 showed that ER-positive samples have a higher sphere forming efficiency (growing higher number of spheres) than ER-negative. In our study, the average number between the two groups was very similar although for the purpose of comparison only six

samples that were ER-negative were propagated (Figure 3.2 E). This might be explained once again by the quality of the samples and we might have received better (more tumour-rich) samples from grade 2 and ER +ve specimens. The majority of the samples collected were luminal A, ER +ve HER2 -ve. This is not surprising since 50 – 60 % of the breast cancer cases belong to this subtype (Carey, 2010). We hypothesised that tumour samples that express HER2 would have a better capacity to generate spheres as previous studies have shown HER2 plays an important role in regulating the CSC population in luminal breast cancers, increasing the frequency of spheres formation (Farnie *et al*., 2007; Korkaya *et al*., 2008). In this study, luminal B (ER +ve and HER 2 +ve) subtype had slightly higher sphere forming capacity than Luminal A, this might be because this subtype is more aggressive than luminal A and expresses HER2 (Creighton *et al*., 2012). In regards to HER2 and ER -ve samples, we have had only received two ER -ve and HER2 +ve samples and so we are not able to provide any significant conclusion (Figure 3.2 F).

PDXs generated from fresh tumour recapitulate the heterogeneity of the disease and reflect histopathology, tumour behaviour, and the metastatic properties of the original tumour (Whittle *et al*., 2015). Improvement has been made in xenografts engraftment: implantation into the orthotopic site, estrogen supplementation, the use of more highly immunosuppressed mice; the addition of mesenchymal stem cells and/or Matrigel have all improved the successful establishment of PDX models (Whittle *et al*., 2015).

We have demonstrated that sphere cultures can be enhanced if propagated from PDX samples rather than the primary tissue. To bulk up the number of cells for future studies, tumour samples are currently being xenografted into immunocompromised mice, with estrogen supplementation in the presence or absence Matrigel. Thus far, our results suggest that Matrigel does not have an impact in the engraftment rate which is consistent with other studies establishing breast cancer PDX models (Zhang and Lewis, 2013). Several methods of sample transplantation were tested such as: chunks, tumourspheres, single cells and aggregates. To date, transplanting chunks from biopsies seems to be

the best method to propagate a primary tumour formation when transplanted into the mammary fat pad (Table 3.3). This higher transplantation efficiency might be because in chunks the cell contacts are maintained, may contain blood vessels, stroma, immune cells and extracellular matrix.

Furthermore, when three biopsy samples were plated directly *in vitro* these did grow a low number of spheres but the dissociation of the tumour from the matched PDX tumour generated enough spheres for our experiments with TRAIL and OH14 *ex vivo* (Table 3.4; see Chapter 5). The use of these PDXs seems promising as a method to increase the number of spheres in order to perform larger more statistically robust studies *ex vivo*. Moreover, in order for PDXs to be translated to the clinic at the level of the individual patient and to incorporate drug efficiency, the engraftment rate (particularly of ER +ve and HER2 +ve) needs to be drastically increased, and the time required for engraftment needs to be reduced, without compromising biological fidelity relative to the original tumour. Early biopsy and engraftment of samples might enable determination of important changes in the tumour at the time when tumour resistance becomes clinically apparent (Whittle *et al*., 2015).

It was our intention to use a lentivirus that could genetically suppress c-FLIP in an inducible and long-term manner (TetR particles that express RFP and shRNA for c-FLIP that expresses GFP). As the aim was to use the inducible lentivirus for tumoursphere culture it was important to test this method first in a cell line with known tumoursphere characteristics. Firstly, the lentivirus was tested in a breast cancer cell line prior to its use in primary cells to fully evaluate the lentiviral shRNA system. Secondly, it was tested in a primary cell line prior to the biopsies. In addition, lentiviral transduction efficiency could also be compromised on transducing tumourspheres because the lentivirus may not reach the cells in centre of the spheres. For the reasons outlined, a series of optimisation steps were used to address issues associated with handling small cell numbers and the nature of primary cells to transduce.

As a tumoursphere is the result of clonal expansion of a single CSC into a heterogeneous collection of cells, the fact that almost 100% of the cells in tumoursphere conditions were GFP positive indicates that: (1) all the viable CSCs in the cell population were transduced; (2) all progeny of the CSC was also positive suggesting stable GFP expression by the lentivirus. MCF-7 was infected with a lentivirus carrying GFP and after the second passage the efficiency still remained with 99% of the stem cell/stem progenitor tumoursphere cells expressing GFP (Figure 3.4 D). Additionally, the spheres generated from the PDX tumours kept 94.5% of GFP positivity, which means that GFP positivity is stable *in vivo* (Figure 3.4 F).

Transduction efficiency in primary cells with the TetR particles was very low (Table 3.5). The optimal number for the metastatic cell line used for this experiment was 4000 cells. However, experiments were also run with 500 cells, to mimic the low number of cells extracted from the biopsies. Moreover, 10000, 50000 and 100000 primary cells were also transduced but such numbers are not suitable for a sphere assay due the generation of aggregates. However, even using a high number of cells, the transduction efficiency remains very low. These results, where a single transduction was used, lead to the conclusion that transducing the biopsy cells might not be feasible by this method. Parallelly to this, the efficiency of the shRNA construct used in the lentiviral transduction adequately supressed c-FLIP in MCF-7 cells with 80% of knockdown, yet, when cells were transduced with the TetR particles these efficiency was equally low, cells started to die and transduction was not stably maintained after passages (data not shown). This low efficiency could be: GFP and RFP silencing after passages or the promoter used was not suitable for the cells used in this study.

The primary objective was to transduce the biopsies with an inducible lentivirus that required a double transduction. Since the experiments using a single vector had failed, it seems reasonable to conclude that using a double transduction would not be at all feasible in primary cells. Since a

transduction with shRNA for c-FLIP was not possible with these samples, it was thought that cells could be treated with siRNA and OH14 to suppress c-FLIP in the short term.

CHAPTER 4

Investigating TRAIL Treatment and c-FLIP Suppression in Human Primary Breast Cells

4. Investigating TRAIL Treatment and c-FLIP Supression in Human Primary Breast Cells

4.1. Introduction

TRAIL has become a strong candidate for cancer therapy due to its well-recognised ability to induce apoptosis in cancer cells, with almost no toxicity to normal cells (Ashkenazi *et al*. 1999; Zhang *et al*., 2005). One study investigated TRAIL-mediated cytotoxicity in sixteen breast cell lines, including; six primary human mammary epithelial cells (HMECs), two immortalized non-tumourigenic breast epithelial cell lines (including MCF-10A), and eight breast cancer cell lines (Keane *et al*., 1999). This study demonstrated that MCF-10As and one breast cancer cell line were significantly sensitive to TRAIL-induced apoptosis. Additionally, the HMEC lines were relatively resistant to TRAIL-induced apoptosis, with 65–100% viability following treatment at 25 μg/ml and even 10-fold higher concentrations of TRAIL failed to induce a greater degree of apoptosis (Keane *et al*., 1999).

There is currently no experimental data on the effects of c-FLIP suppression and TRAIL treatment on normal primary breast cells. This is key to determining the potential *in situ* toxicity of c-FLIP inhibitors. Here, we set out to establish the cytotoxicity of c-FLIP inhibition (with and without TRAIL stimulation) in primary breast epithelial cells *ex vivo*.

Our laboratory has seen that using siRNA against both isoforms of c-FLIP (for siFLIPL and siFLIPS) with and without TRAIL does not affect bulk and stem cell viability in the non-tumourgenic breast cell line, MCF-10As (Piggott *et al*., 2011). This was confirmed using the novel c-FLIP inhibitor OH14 developed in our laboratory. Up to 100 μM OH14 failed to affect bulk cell or stem-like cell viability in the MCF-10A cell line (L. Piggott, unpublished data). In contrast, another study has shown that using siRNA against both forms of c-FLIP, with or without TRAIL increased the percentage of apoptotic cells in MCF-10A cells (Yerbes *et al*., 2011). These two contradictory outcomes may reflect differences in the specificity of the siRNA sequences for c-FLIP isoforms used in these experiments.

However, the relevance of the MCF-10A cell line has recently been challenged. Liu *et al.*, showed that MCF-10A cells exhibit a unique differentiated phenotype in 3D culture which may not exist or be rare in normal human breast tissue (Qu *et al*., 2014). This study questioned whether this immortalised cell line appropriately represented normal mammary cell biology.

To overcome these limitations, we proposed to inhibit c-FLIP with pan-isoform siRNA and a pharmacological inhibitor in primary breast tissues. Thus, cytotoxicity assays were performed on bulk and stem cell cultures of HMECs and non-tumourigenic tissues from the clinic.

4.2. Results

4.2.1. TRAIL treatment has no effect on HMECs viability in adherent conditions

Prior to combining c-FLIP suppression and TRAIL, we investigated the effect of TRAIL alone in HMECs. These normal primary breast cells were sourced from a commercial supplier (Lonza, Switzerland) and maintained under culture up to a maximum of 15 passages. HMECs were treated with different concentrations of TRAIL to investigate the optimal concentration where viability was not affected by TRAIL but still induced apoptosis in cancer cells. HMECs were treated with 20-100 ng/ml of TRAIL in adherent conditions, a dose range in which TRAIL-sensitive breast cancer cell lines have previously been shown to significantly respond (Piggott *et al*., 2011). After 18 hours, cell viability was assessed by the cell titre blue and Live/Dead assays. TRAIL treatment at 20 ng/ml, 60 ng/ml and 100 ng/ml slightly decreased (2%; 5% and 7%, respectively) the viability of the cells compared to the untreated controls (Figure 4.1. A). Despite a statisticaly significant decrease of 7% for HMECs viability at 100 ng/ml TRAIL, 7% was a small percentage to be considered overly detrimental.

An analysis of the number of dead cells after treatment (Figure 4.1. B), demonstrated a non-significant 2% increase in cell death using 20 ng/ml of TRAIL, correlating with cell-titre blue viability data. These results show that TRAIL has no significant effect on HMECs viability.

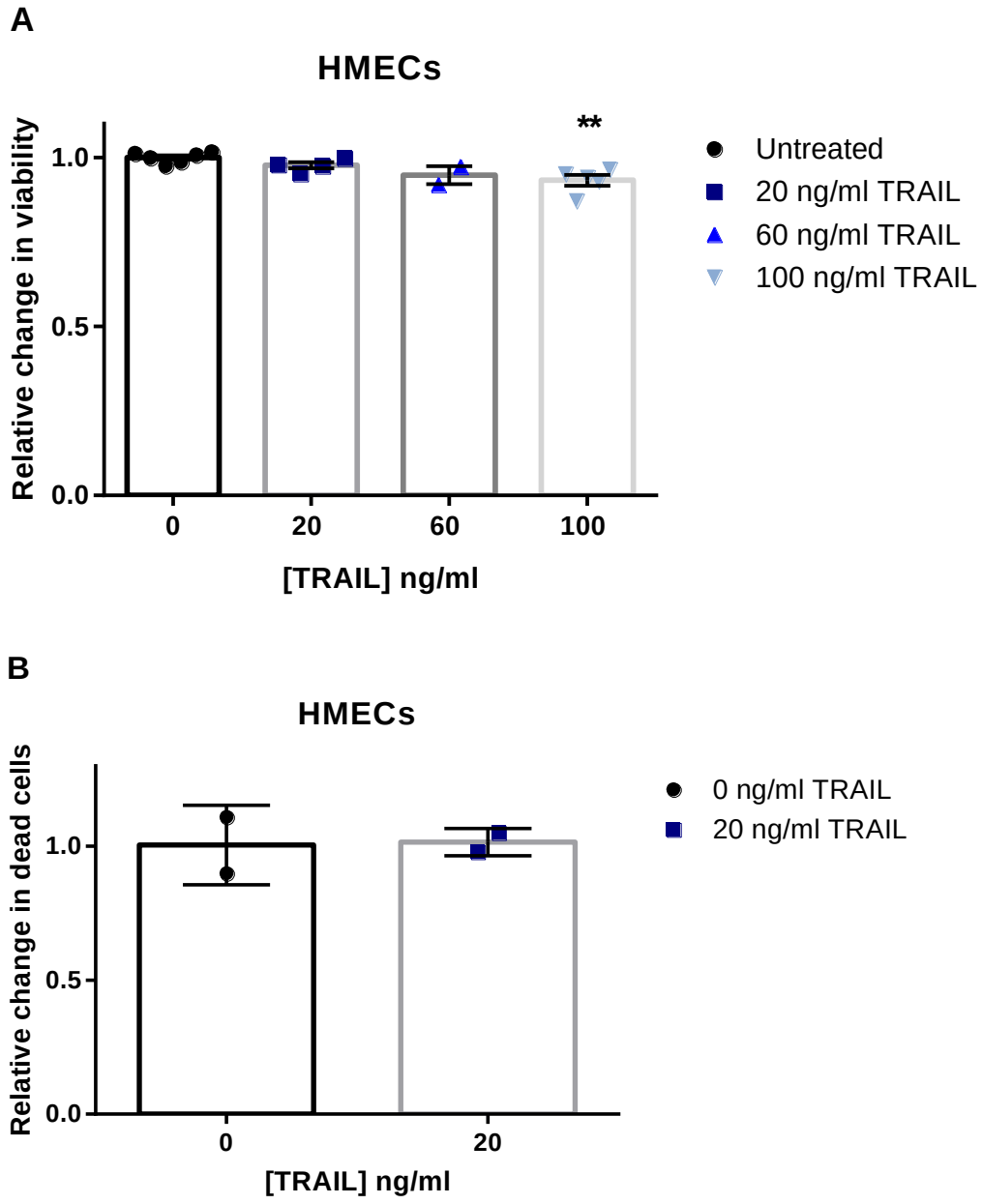

Figure 4.1. TRAIL treatment has no effect on HMECs viability in adherent conditions. | A. HMECs viability was assessed by fluorescence (cell titre blue assay) after +/- 20 ng/ml (n=4), 60 ng/ml (n=2) and 100 ng/ ml (n=5) of TRAIL treatment normalised to untreated control. Each biological replicate was performed with 3 internal replicates. Bars represent mean +/- SEM. | **B.** HMECs were incubated with +/- 20 ng/ml TRAIL and assessed by FACS for live/dead cells using Live/Dead assay. Treatment was normalised to the control. Two independent experiments with 3 internal replicates. Bars represent mean +/- SD. ** (p) significant vs untreated control <0.005; t-test.

4.2.2. TRAIL does not affect mammary stem cells originating from HMECs or tissues from benign conditions

The effect of TRAIL on normal mammary stem cells (MaSCs) was investigated using two methods: (1) by treating single cells, directly, when plated in non-adherent mammosphere conditions (3D); and (2) by pre-treating cells in adherent (2D) before plating in 3D for the mammosphere assay. These different treatment designs aimed to represent the effect of the drug in the whole tumour (bulk – adherent culture) and when breast cancer stem cells are circulating as a single cell in the blood stream (single cell in non-adherent culture). While, the 3D treatment method was recognised to be limited for MaSCs, as these are unlikely to be circulating in the blood stream as a single cell *in vivo*, this method was used here *in lieu* of future analysis of 3D cancer stem cell assays (tumoursphere assays) using primary breast cancer tissues.

Cells were treated using a range of different concentrations from 0 to 100 ng/ml of TRAIL. Pre-treating HMECs in adherent conditions with 20 ng/ml of TRAIL did not affect the number of spheres but 100 ng/ml decreased by 38% the mammosphere forming units (MFUs)(Figure 4.2 A, left side). To confirm the presence of stem cells, spheres were dissociated into single cell for a second passage, where only stem cells are able to self-renew and form new spheres. In passage 2 (P2), 100 ng/ml of TRAIL decreased 20% of the spheres, which was not statistically significant suggesting that TRAIL was primarily targeting the anchorage dependent transit-amplifying cell population and not self-renewing stem cells (Figure 4.2 A, right side).

Treating cells directly when plated in non-adherent conditions up to a concentration of 60 ng/ml with TRAIL does not affect the number of spheres (Figure 4.2 B). Concentrations of 20 ng/ml and 40 ng/ml slightly increased the number of spheres (4.81% and 4.05%, respectively) although not statistically significant. However, at concentrations of 70; 80 and 100 ng/ml of TRAIL the number of spheres decreased significantly by 44%; 53% and 72%, respectively (Figure 4.2. B and C).

Some biopsies collected from the clinic were histopathologically characterised as benign conditions, such as: fibroadenomas (solid benign tumours); cystic hyperplasia of the breast (fluid-filled sacs with overgrowth due to proliferation of cells) and sclerotic adenosis (extra growth of tissue within the breast lobules). These were treated with either 20 ng/ml or 100 ng/ml of TRAIL and did not, significantly, compromise sphere number in any of the samples tested (Figure 4.3 B).

Overall, with six fibroadenomas tested with 20 ng/ml of TRAIL and five fibroadenomas tested with 100 ng/ml, there was a slightly decreased in the number of spheres by 13% and 12%, respectively, but not significantly (Figure 4.3 B). Therefore, 20-100 ng/ml TRAIL does not affect MaSCs in breast benign conditions.

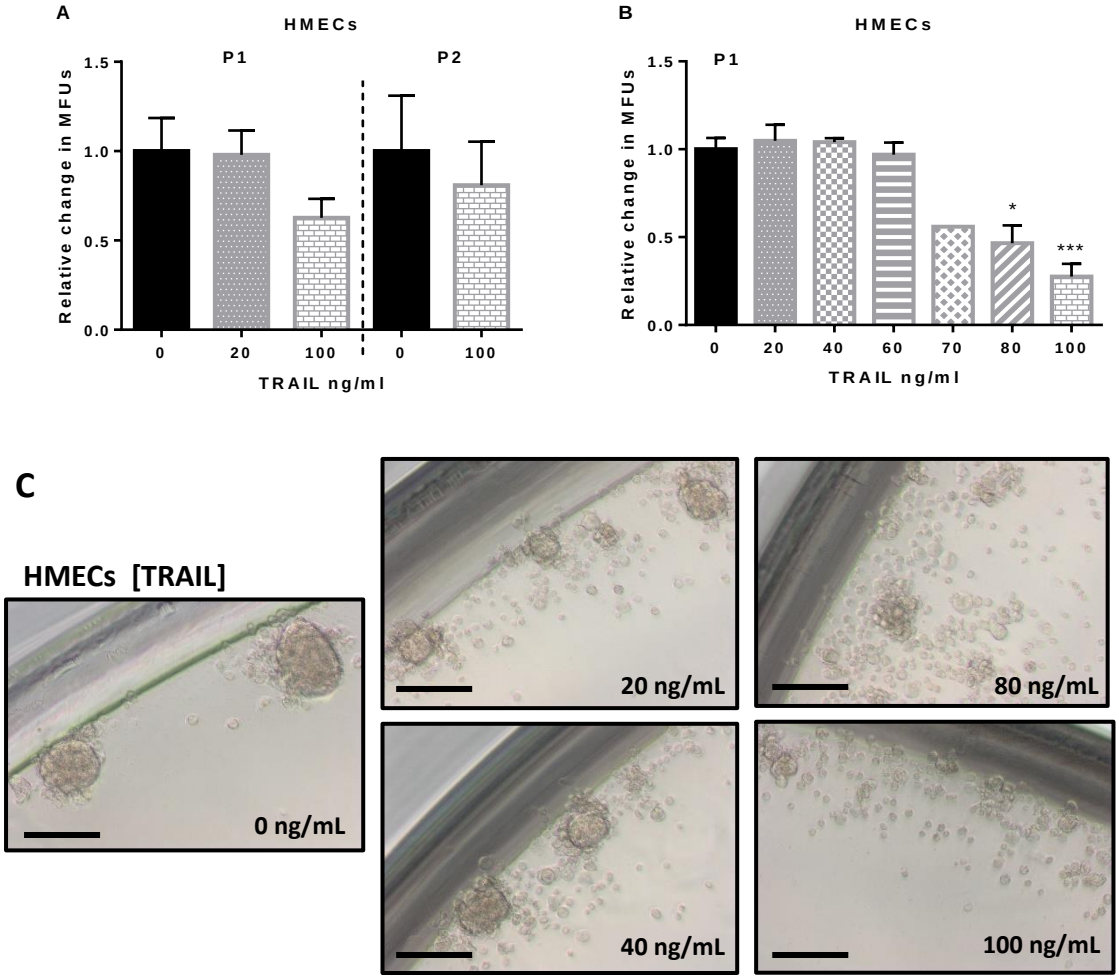

Figure 4.2. High doses of TRAIL affect HMECs mammosphere forming units (MFU) in 3D. Mammosphere assay: Cells were either pre-treated with TRAIL (2D) and then passaged into spheres or cells were directly treated with TRAIL into non-adhrent conditions (3D). Cells were treated with 20-100 ng/ml TRAIL for 18h. TRAIL was not removed from the cultures. The number of spheres were counted after 10 days of culture. To confirm stem cell self-renewal, spheres were dissociated and then plated again under 3D for passage 2 (P2). |**A.** Relative change in MFUs after 20 ng/ml and 100 ng/ml of TRAIL after treatment in 2D. Treatments were normalised to the untreated control. P1: Bars stood for mean +/-SEM. n=3 independent experiments with 5 internal replicates. P2: Bars stood for mean +/- SD represents one single experiment with 5 internal replicates. | **B.** Relative change in MFUs after 20 ng/ml- 100 ng/ml of TRAIL treatment in 3D. Bars represent mean +/-SEM. n=3 independent experiments, except for 70 ng/ml, which is a single experiment. All with 5 internal replicates. | **C.** Light microscope images representing HMECS spheres after treatment in **B** (40x magnification). Scale bar = 200 µM. *(p)<0.05; **(p)<0.005; t-test.

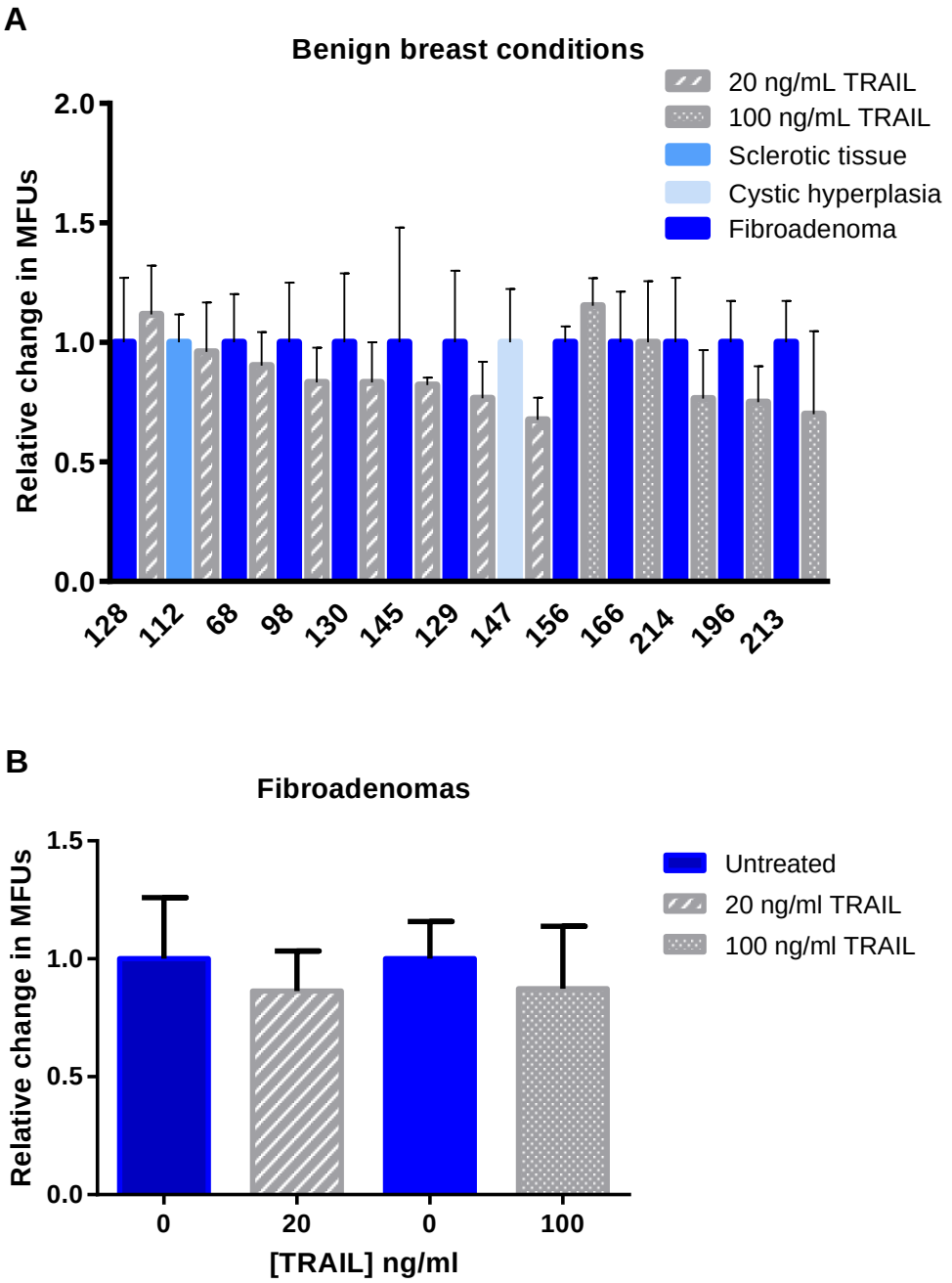

Figure 4.3. 20- and 100 ng/ml of TRAIL does not affect mammosphere forming units (MFUs) in breast tissue from benign conditions such as fibroadenomas; cyst hyperplasia and sclerotic breast tissues. | 13 breast samples were dissociated into single cells and plated under non-adherent conditions. Cell suspensions were treated with 20 ng/ml or 100 ng/ml TRAIL for 18 hours. Number of spheres were counted after 10 days. | **A.** TRAIL treatment in 13 samples represented in a waterfall plot based on TRAIL sensitivity at 20 ng/ml and 100 ng/ml normalised to each untreated control. | **B.** Representation of the three breast benign conditions grouped together for 20 ng/ml (8 samples) and 100 ng/ml of TRAIL (5 samples). | Bars represent mean +/- SD. n=1 for each sample performed in triplicate.

4.2.3. siFLIP and TRAIL decreases HMECs viability

It was shown that TRAIL treatment has a minimal effect on bulk HMECs viability (Figure 4.1A and 4.1B). To explore the effects of c-FLIP suppression on normal mammary cells, HMECs were treated with a scrambled control (SC) and siRNA targeting both long and short form of c-FLIP (siFLIP). c-FLIP knockdown was confirmed by qPCR that showed 76% efficiency in the gene suppression (Figure 4.4 B). To further investigate the specificity of the knockdown for TRAIL mediated killing, cells were treated with a pan caspase inhibitor (iCAS), Z-VAD-FMK, at pre- and post-transfection. Cells were treated with SC and siFLIP, 10 ng/mL of iCAS for 48h and fresh iCAS added 1h prior 100 ng/ml of TRAIL. 18h later the viability of the cells was checked by cell titre blue.

siFLIP treatment alone decreased viability of HMECs by 24% (although this was not statistically significant) and the combined treatment siFLIP/TRAIL reduced viability by 48%. The overall sensitivity of the combined treatment was 30% (Figure 4.4 A, red asterisk). This provides evidence of sensitisation by c-FLIP inhibition for TRAIL mediated killing, as the loss of viability in combination was significantly more than the cumulative reduction in viability of either treatment alone. The caspase inhibitor was able to rescue the cell death caused by c-FLIP suppression demonstrating the participation of caspases in this process (Figure 4.4 A).

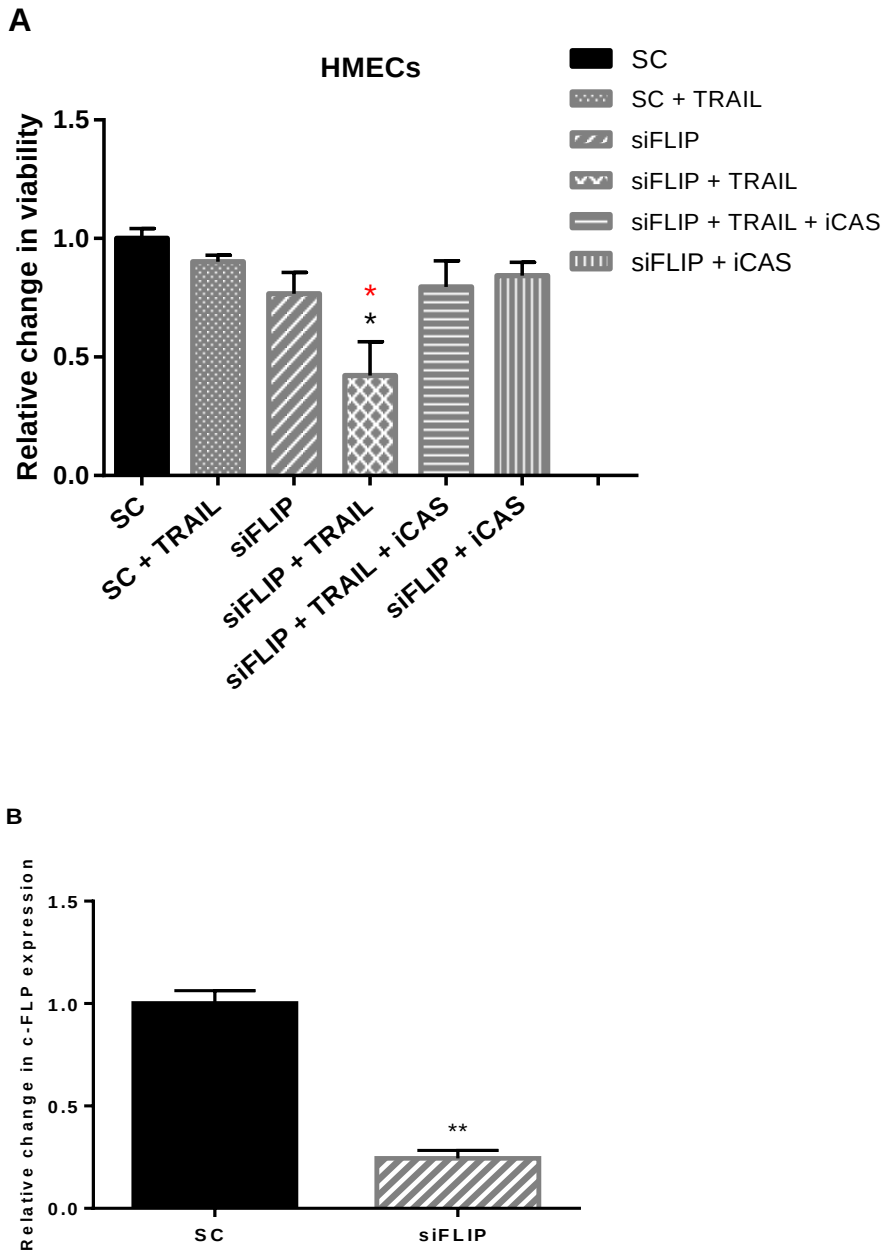

Figure 4.4. siFLIP and TRAIL decrease HMECs viability. Cells were treated with SC (scrambled control), siFLIP (transient knockdown using siRNA), 20 ng/mL of iCAS (pan caspase inhibitor, Z-VAD.FMK) for 48 hours and fresh iCAS added 1 hour prior 100 ng/ml of TRAIL. 18 hours later the viability of the cells was assessed by cell titre blue. | **A.** Representation of the HMECs viability after treatments normalised to scrambled untreated control (*p=0.0179; t-test). * - red asterisks highlight combination treatments (siFLIP + TRAIL) that are more than the sum of the respective individual treatments. Data represents 3 independent experiments with at least 3 internal replicates. | **B.** c-FLIP gene knockdown confirmed by qPCR after treatment in **A.** (**p=0.0031; t-test). | Bars represent mean +/- SEM.

4.2.4. OH14 and TRAIL decreases HMECs viability

After demonstrating that c-FLIP suppression +/- TRAIL affects HMECs viability in the bulk population, we want to investigate whether OH14 had a similar effect. To test drug specificity of inhibiting c-FLIP for sensitising to TRAIL, a pan caspase inhibitor (iCAS) was used before TRAIL treatment. Cell viability was assessed by cell titre blue after 18 hours of 100 ng/ml of TRAIL treatment. Concentrations of 0.1% and 0.01% DMSO, the vehicle for OH14, had no significant effect on viability in HMECs (Figure 4.5 A). To test OH14 in HMECs, 100 µM and 10 µM of OH14 were used because our group have seen that these concentrations display cytotoxicity to breast cancer cells without harming MCF10-As cells (unpublished data). 100 µM of OH14 in 0.1% DMSO showed the most significant effect on cell viability by reducing cell viability by 42%, with 10 µM OH14 resulting in a reduction of 18%. This compared to a 24% reduction in cell viability following c-FLIP siRNA knockdown (Figure 4.4 A).

The combination of OH14 and TRAIL led to a 59% and 30% reduction in viability at 100 µM and 10 µM, respectively, which was partially rescued by the addition of the caspase inhibitor (Figure 4.5 A) confirming that at least some of the loss in cell viability was mediated by caspases (Figure 4.5 A). This rescue by caspase inhibition was relatively more pronounced when cells were treated with 10 µM OH14 compared to 100 µM. While inconclusive, one explanation for this was that an undefined non-specific toxicity of OH14 was more pronounced at the higher concentration of OH14/TRAIL.

Combined use of OH14 represented a 14% sensitisation to TRAIL at 100 µM OH14 and 10% sensitisation at 10 µM OH14, thus the primary cytotoxicity of OH14 occurred in the absence of TRAIL.

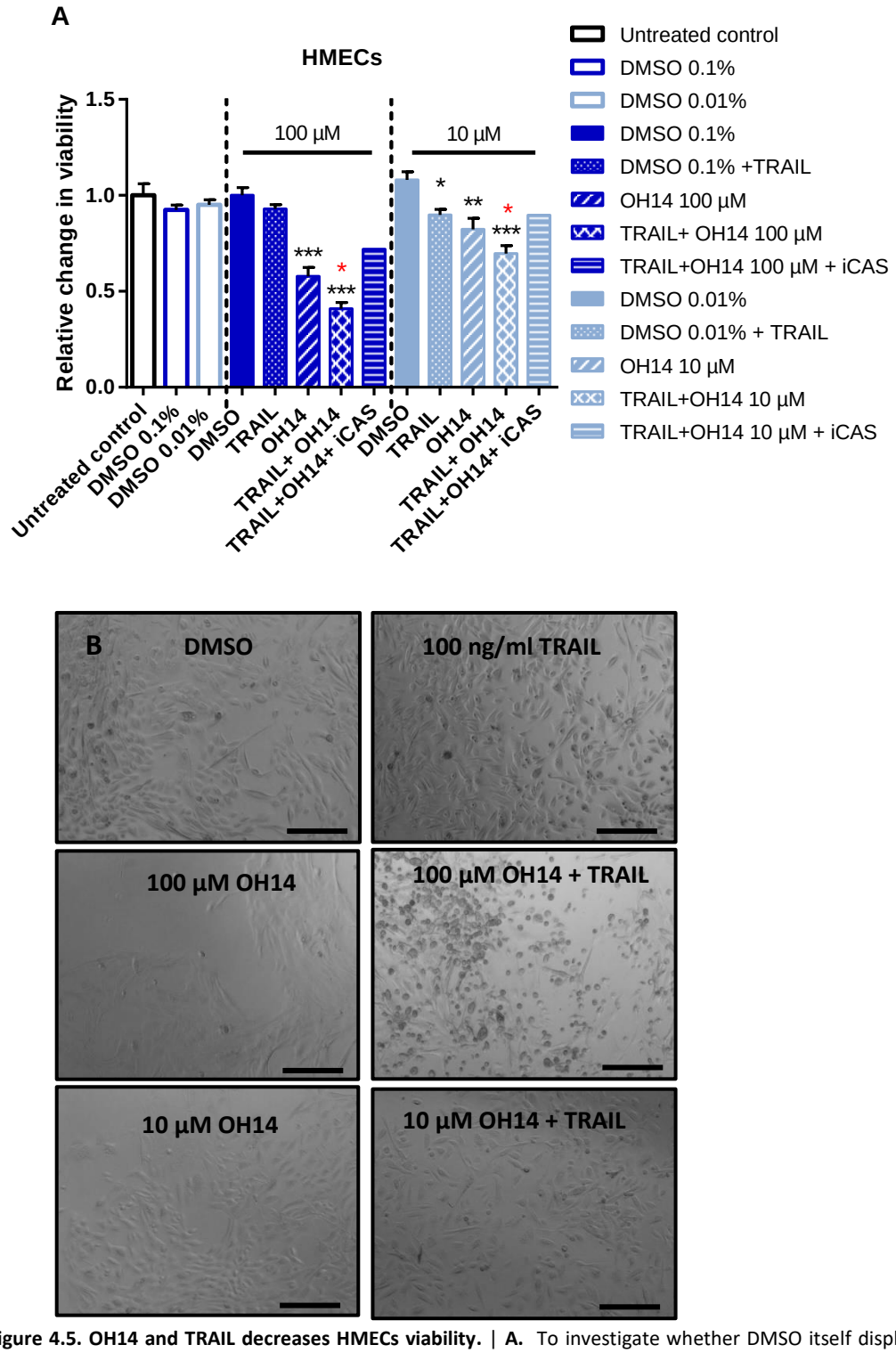

Figure 4.5. OH14 and TRAIL decreases HMECs viability. | **A.** To investigate whether DMSO itself displays any toxicity to normal cells, these were treated with 0.1% and 0.01% of DMSO, which mirrors the same concentration of DMSO present in 100 µM and 10 µM of OH14, respectively. Graph represents HMECs viability (cell titre blue assay) following TRAIL +/- 100 µM and 10 µM of OH14 treatment normalised to the control treated with DMSO. HMECs were treated with OH14 1h prior to 100 ng/ml of TRAIL treatment for 18h. * - red asterisks highlight combination treatments (OH14 + TRAIL) that are more than the sum of the respective individual treatments. Data represents 3 independent experiments with at least 3 internal replicates. Bars represent mean +/- SEM. **(p)<0.005 and *** (p)<0.0005; t-test.| **B.** Light microscope images representing HMECS spheres after treatment in **A** (40x magnification). Scale bar =100µM.

4.2.5. OH14 sensitises mammary stem cells to TRAIL

We have demonstrated that OH14 reduced HMECs viability in a dose-dependent manner. We also wished to address whether the pharmacological suppression of c-FLIP also affected MaSCs viability, and whether this led to a sensitisation of otherwise resistant CSCs to TRAIL. HMECs were pre-treated in adherent conditions with OH14 and/or TRAIL (2D assay) and, also, treated directly in sphere conditions (3D assay). To avoid potential non-specific toxicity at higher concentrations of OH14, thus limiting toxicity in normal tissues, these experiments were performed at 10 μM OH14, with or without 100 ng/ml of TRAIL.

In pre-treated cells, under 2D conditions, TRAIL and OH14 alone did not significantly decrease the number of spheres, with a 13% reduction seen in both treatments. Combined treatment, however, reduced the number of spheres by 54% compared to the DMSO control. Therefore, OH14 resulted in an overall sensitisation of tumoursphere forming cells to TRAIL by 28%. The second passage after the treatment in 2D showed a similar result to the first passage. TRAIL plus OH14 decreased the number of spheres and OH14 sensitised cells to TRAIL (Figure 4.6 C).

In cells treated in 3D, a different pattern of responses was observed. TRAIL decreased the number of sphere by 44%, OH14 by 25% and OH14 with TRAIL by 44%. Therefore, OH14 did not sensitise the non-adherent sphere forming cells to TRAIL, with the major sensitivity being to TRAIL alone.

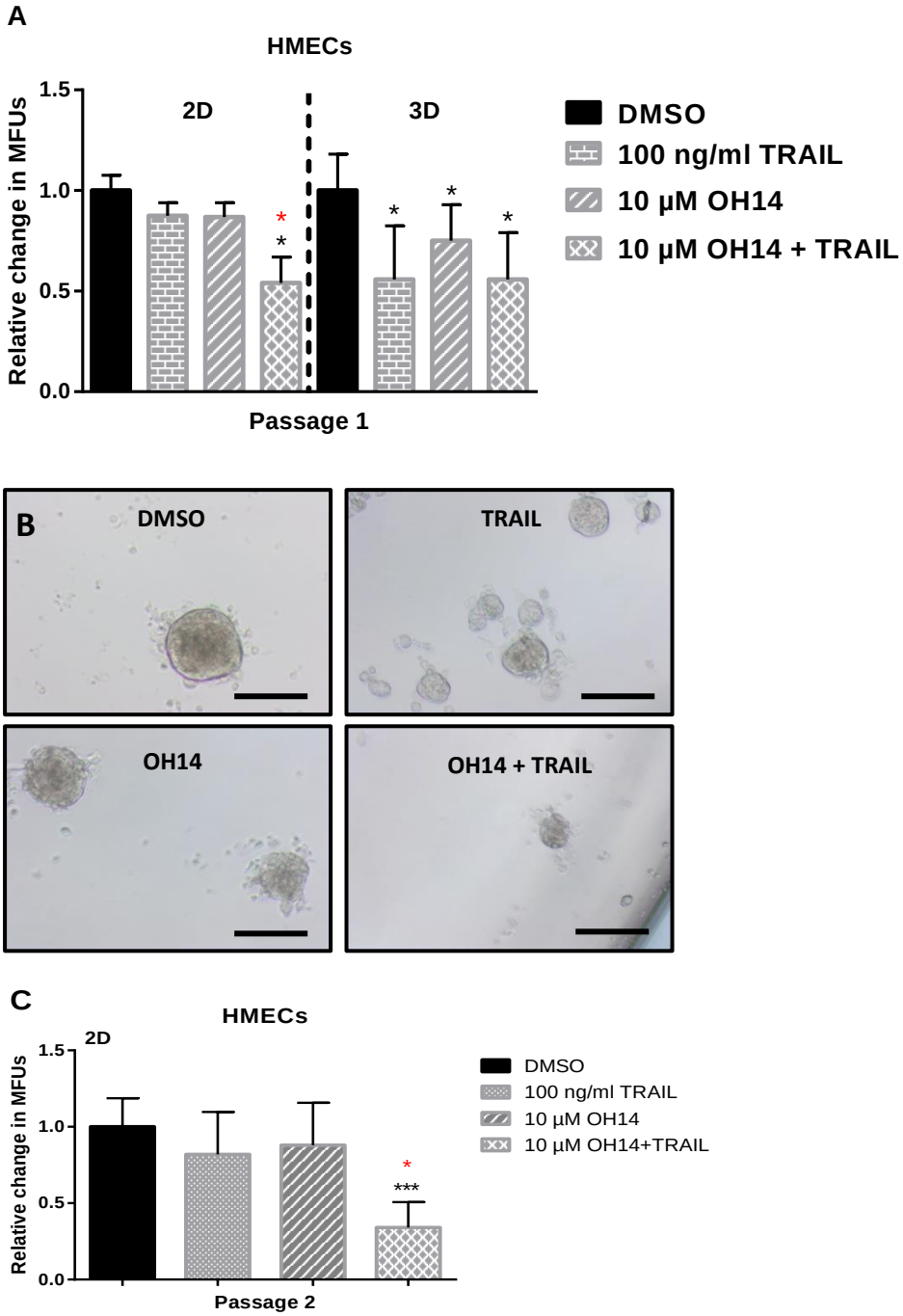

Figure 4.6. **OH14 sensitises mammary stem cells (MFUs) to TRAIL**. Y axis represents Mammosphere Forming Units (MFUs) after TRAIL, OH14 and TRAIL/OH14 treatments normalised to the DMSO control. Mammosphere assay: Cells were treated with 10 µM of OH14 for 1hour prior a 18 hour treatment of 100 ng/ml of TRAIL. Number of spheres were counted 10 days after passage 1 and after passage 2. | **A**. **Left side:** Cells were pre-treated in adherent conditions (2D) and then cultured under non-adherent conditions (n= 5). Bars represent mean +/- SEM. **Right side:** Cells were treated directly into non-adherent conditions (3D) (n=1). Bars represent mean +/- SD. | **B.** HMECs spheres after the treatments in 3D represented in A. | **C.** Passage 2 after the treatment in A in 2D. Bars represent mean +/-SD (n=1). | *(p) <0.05; t-test. * - red asterisks highlight combination treatments (OH14 + TRAIL) that are more than the sum of the respective individual treatments. Scale bar = 200µM.

4.3. Discussion

Following *in vitro* studies using cell lines, we and others have proposed that c-FLIP mediated sensitisation of breast cancer cells and breast cancer stem cells to TRAIL, may be an effective targeting therapy. In order to substantiate this, it is crucial not only to demonstrate the efficacy of this approach in primary tumours, but also to investigate the cytotoxicity of TRAIL and c-FLIP inhibitors in normal primary breast cells. This will then help to establish the effective therapeutic window – the difference between the effective therapeutic dose for the cancer cells and the dose at which normal cells are compromised. It is known that TRAIL preferentially induces apoptosis in cancer cells over normal cells, however, this has not been demonstrated for c-FLIP inhibition (LeBlanc and Ashkenazi, 2003; Daniels *et al*., 2005). TRAIL is expressed in several tissues and activates apoptosis through the death receptors DR4, DR5, DcR1 and DcR2. DcR1 and DcR2 receptors have an incomplete death domain and do not trigger apoptosis (Daniels *et al*., 2005). Therefore, these receptors function as 'decoys', competing for TRAIL's binding with the pro-apoptotic molecules, DR4 and DR5. Increased expression of these decoy receptors on normal cells explains why these cells have increased protection from TRAIL-induced apoptosis (LeBlanc and Ashkenazi, 2003; Daniels *et al*., 2005). It also has been reported that TRAIL does not induce toxicity in several animal models such as mice, cynomolgus monkeys, and chimpanzees (*reviewed* in Rahman *et al.,* 2013)

To test TRAIL cytotoxicity, HMECs were treated with increasing concentrations of TRAIL in adherent and sphere conditions. In agreement with previous findings, we found TRAIL to have a minimal effect on bulk HMECs even at a concentration of 100 ng/ml (Figure 4.1 A and B). This minimal cell death response was demonstrated in a study by Keane *et al*., which investigated TRAIL-mediated cytotoxicity in six primary HMECs and two immortalised non-transformed breast epithelial cell lines (including MCF-10A). They observed that HMEC lines were relatively resistant to TRAIL-induced apoptosis (65–100% viability compared with control cells) with the MCF-10A cell line showing the highest sensitivity to TRAIL (Keane *et al*., 1999). However, subsequent studies have questioned

whether the MCF-10A cell line is a suitable model for human mammary cell studies (Qu *et al*., 2014). Ideally, TRAIL should be tested in normal tissues taken directly from patients.

It is known that mammospheres are enriched in progenitor cells, capable of differentiation along multiple lineages and 0.4% of the bulk population are stem cells (Dontu *et al*., 2003). To investigate whether TRAIL displays any cytotoxicity in normal mammary stem cells (MaSCs), we have used two methods: (1) pre-treating cells in adherent conditions (2D) and then passaging cells into non-adherent conditions (3D); (2) treating cells directly into 3D at the moment cells are plated in single cells. These models crudely recapitulate when drugs target the whole tumour (2D) and cancer stem cells circulating in the blood stream (3D). However, this effect is not a very representative assay for MaSCs as they are unlikely to ever be under these stresses. The purpose of these assays therefore was two-fold: to be able to compare a normal cell response with subsequent cancer cell assays in order to estimate a therapeutic window; and to compare the responses of bulk cells and MaSCs at the appropriate drug concentrations to establish if normal stem cells are protected from killing.

In the first method, pre-treating HMECs in 2D with 20 ng/ml of TRAIL did not affect the number of spheres but 100 ng/ml of TRAIL decreased sphere number by 38% (Figure 4.2 A, left side). To confirm the presence of stem cells, spheres were dissociated into single cells for a second passage where only stem cells are able to self-renew and form new spheres. In passage 2, 100 ng/ml of TRAIL decreased the spheres but not significantly (Figure 4.2 A, right side) demonstrating that this concentration is only affecting the cells undergoing anoikis and not stem cells. In the second method, using up to a concentration of 60 ng/ml of TRAIL did not affect the number of spheres but 70, 80 and 100 ng/ml of TRAIL drastically decreased the number of spheres (Figure 4.2. B). In addition, increasing TRAIL dose, the spheres become smaller (using 20 ng- 60 ng/ml TRAIL), until the sphere forming efficiency becomes compromised (70 ng/ml - 100 ng/ml TRAIL) (Figure 4.2 C). These differences on TRAIL-mediated cytotoxicity in 2D and 3D, could be explained by the susceptibility or stress caused by the anoikis inducing conditions that single cells suffer during 3D conditions. An alternate explanation

is that higher concentrations of TRAIL are non-specifically toxic to the proliferative/progenitor stem cell compartment. A passage 2 for the 3D conditions would help to test these two hypotheses. Also, an experiment where TRAIL would be either removed from cultures or added every 18h would answer whether the toxicity is mediated by TRAIL or anoikis resistance. If the anoikis-resistant population dies after TRAIL treatment, this would be a drug-mediated killing.

Additionally, 20 ng/ml and 100 ng/ml of TRAIL did not have a significant effect on spheres in fibroadenomas, cystic hyperplasia or in sclerotic breast tissue (Figure 4.3), which is an indication that HMECs are more susceptible to higher concentrations of TRAIL than benign breast conditions. Although the HMCs are closer to normal breast cells, the freshly harvested benign breast samples are a more relevant model of primary tissues. Additionally, one limitation of this experiment was not testing 20 ng/ml and 100 ng/ml of TRAIL on the same. Each sample should have been tested with the two concentrations but it was not possible as the number of cells was very low to allow enough technical replicates.

It is well known that some breast cancer cells show resistance to TRAIL due to c-FLIP expression (Safa *et al*., 2008; Yerbes *et al*., 2010; Piggott *et al*., 2011). c-FLIP plays an important role in T cell proliferation and heart development (Zhang *et al*., 2008). Yet it is of note that abnormal c-FLIP expression has been found in various diseases such as cancer, multiple sclerosis, Alzheimer's disease, diabetes mellitus, and rheumatoid arthritis (Safa *et al*., 2011). In regards to apoptosis, c-FLIP is an important caspase-8 regulator: c-FLIP short is anti-apoptotic being able to inhibit caspase 8 and c-FLIP long can either inhibit or activate apoptosis depending on its expression levels and location in the cell (French *et al*., 2014, Hughes *et al*., 2016).

Having demonstrated that TRAIL displayed a minimal non-significant cytotoxicity in pre-treated MaSCs, we aimed to investigate whether c-FLIP suppression was detrimental to these cells. c-FLIP was inhibited using two methods: (1) knocking-down c-FLIP gene expression using siRNA for both long and short form of c-FLIP (siFLIP) over 48 hours and (2) using OH14, a pharmacological compound

developed by our lab, that is a competitive inhibitor of caspase-8 mediated apoptosis. To investigate the specific effects of the inhibition, cells were treated with a pan caspase inhibitor. Using the first method, siFLIP treatment alone resulted in a non-significant decrease of viability by 24% and it sensitised cells to TRAIL by 30% (Figure 4.4 A). Importantly, the caspase inhibitor was able to almost completely rescue the cell death caused by the c-FLIP suppression confirming a caspase-mediated apoptosis (Figure 4.4 A). Our findings partially agree with Yerbes *et al*. 2010, where they showed that using siRNA targeting c-FLIP with different constructs resulted in a drastic increase in cell death with 100 ng/ml of TRAIL. However, c-FLIP suppression using siRNA or preferably, shRNA still remains to be tested on MaSCs in HMECs or any other normal primary breast tissue.

Using the second method, 100 µM OH14 reduced viability by 42% while 10 µM OH14 only reduced it by 18%. Additionally, OH14 also resulted in a minimal sensitisation of HMECS to TRAIL since the overall sensitivity at 100 µM and 10 µM was 14% and 10%, respectively (Figure 4.5 B). Thus, siRNA and 10 µM OH14 exhibited similar effects on HMECs viability while 100 µM OH14 showed significantly higher toxicity in HMECs. Despite both methods inhibiting the role of c-FLIP, the first method was able to inhibit c-FLIP genetically whereas OH14 only inhibits c-FLIP binding in the DISC. After OH14 treatment, c-FLIP is still active inside the cell and can still interfere with other signalling pathways. Our lab has seen no increase in c-FLIP levels after OH14 treatment in cancer cells (unpublished data). These data suggest that OH14 may exhibit non-specific toxicity. To test this, c-FLIP could be supressed genetically in a long and inducible manner using shRNA in samples taken directly from patients. This could test whether is c-FLIP suppression itself or c-FLIP is interfering with other pathways that is causing the decrease in viability. Future studies could involve investigations of c-FLIP effects after OH14 treatments, in both normal and cancerous tissues. Additionally, investigation of the caspase inhibitor effects only with OH14 would be important to check whether the apoptosis is mediated by caspases.

Yerbes *et al.,* in 2010 demonstrated that, in MCF-10As, knockdown of c-FLIP long form (siFLIPL) up-regulates the expression of the TRAIL receptor DR5 and activates caspase-8 in the absence to TRAIL induction (exogenous TRAIL). Endogenous TRAIL is required for the activation of spontaneous apoptosis by siFLIPL and increased DR5 expression by siFLIPL could result in the formation of a DISC that contains endogenous TRAIL, DR5, FADD and procaspase-8 activation. Furthermore, they suggest that c-FLIP levels are up-regulated following detachment from the extracellular matrix and during morphogenesis. This up-regulation of c-FLIP could be due to preventing cells from undergoing anoikis in 3D (Mawji *et al*., 2007). This presumption could explain the differences in response of 2D and 3D generated spheres to c-FLIP/TRAIL. Using OH14 resulted in a sensitisation of MaSCs to TRAIL in 2D but not in 3D after passage 1. Passage 2 of 2D suggested a similar sensitisation to TRAIL but this experiment was only performed once. Future experiments could involve: more repeats of passage 2; passage 2 assays for the 3D conditions; OH14 treatment in breast tissues from mastectomies or breast reductions and an investigation of c-FLIP levels after treatments. Additionally, more stem cell assays could be performed such as FACS analysis for stem cell markers and transplantation of MaSC in cleared fat pads.

Overall, 20-100 ng/ml of TRAIL does not affect the bulk population of HMECS nor MaSCs when pre-treated in 2D. However, concentrations of 70-100 ng/ml affect cells in non-adherent culture (3D) likely because TRAIL more easily targets cells undergoing anoikis rather than targeting stem cells. Additionally, 20 ng/ml and 100 ng/ml of TRAIL does not affect MaSCs in primary biopsies from patients with benign breast conditions. Suppressing c-FLIP using siRNA sensitises the bulk population to TRAIL, while OH14 significantly reduced bulk and stem cell viability alone and sensitised to TRAIL.

Therefore, this data suggests that pharmacological suppression of c-FLIP may reduce normal mammary epithelial cell and stem/progenitor cell viability.

CHAPTER 5

Investigating TRAIL and c-FLIP Suppression in Breast Tumour Tissues *ex vivo*

5. Investigating TRAIL and c-FLIP Suppression in Breast Tumour Tissues *ex vivo*

5.1. Introduction

It is well known that TRAIL has failed numerous clinical trials with patients showing no improvement (Hayes and Lewis-Wambi, 2015; De Miguel *et al.,* 2016). Reasons for failure have been attributed to lack of potency of agents but also a lack of stratification. These trials were driven based on the potent effects *in vitro*, however, none of these trials have stratified patients within each histological or molecular subtype or based on previous cancer treatments. We hypothesise that there is sub-group of patients that could benefit from TRAIL as a monotherapy.

Additionally, there is robust evidence supporting a potent effect of c-FLIP suppression using siRNA in combination with TRAIL (siFLIP/TRAIL) on bCSCs in cell lines. It has been shown that this treatment efficiently eliminated CSC-like (tumoursphere forming and surrogate marker) activity from breast cancer cell lines (Safa *et al*., 2009; Piggott *et al*., 2011). Moreover, intravenous injection of MDA-MB-231 cells pre-treated with siFLIP/TRAIL into immunocompromised mice led to a 98% reduction in metastatic tumour burden (Piggott *et al*., 2011). As these studies have so far only been performed on breast cancer cell lines, the key question still remains whether these findings have direct clinical relevance for breast cancer patients. Taking this into account, the study tested the hypothesis that c-FLIP suppression combined with TRAIL reduces cell viability of primary bCSCs *ex vivo*.

To achieve these aims, primary diagnostic breast biopsies, surgical resection samples and pleural effusions from breast cancer patients were cultured under conditions supporting and conditions that enriched for bCSCs and then subjected to TRAIL +/- c-FLIP suppression. C-FLIP was inhibited using siRNA (siFLIP) or a pharmacological inhibitor of c-FLIP (OH14), that had previously been developed in the host laboratory. A range of tumour types were tested to determine if there was a cohort of patients that this strategy may prove most effective against.

5.2. Results

5.2.1. TRAIL sensitivity correlates with acquired resistance in bCSCs to endocrine treatments

Firstly, we aimed to find a particular subtype of breast cancer that could benefit most from TRAIL treatment alone as a monotherapy, without c-FLIP suppression. For this purpose, several breast tumours from diagnostic biopsies, surgical and metastatic pleural effusion samples were treated with 100 ng/ml of TRAIL. We chose a range of TRAIL concentrations that we had previously determined did not affect normal mammary epithelial cell viability (Chapter 4), but were effective in breast cancer cell lines (Piggott *et al*., 2011).

Despite having received and processed 176 breast biopsies/surgical samples, only 30 samples generated a satisfactory number of spheres (>20 spheres in the three control wells) to enable statistically robust data to be generated. TRAIL treatment did not have any effect in 26 of the 30 samples, a reduction of tumoursphere-forming cells (tumoursphere-forming units-TFUs) was observed in the remaining 4 samples (Figure 5.1. A). However, overall an average, TRAIL significantly reduced the number of spheres by 21% (Figure 5.1 B).

Samples were divided by tumour histological and molecular subtype to investigate any possible correlation with TRAIL sensitivity. Within the 30 samples, 10 were Invasive Ductal; 12 were Invasive Ductal + DCIS; 2 were Invasive Lobular; 1 was Invasive Ductal + DCIS + LCIS; 1 was Invasive Ductal + Lobular; 2 were Invasive Ductal + Mucinous; 1 was Papillary Proliferation and 1 was High grade comedo DCIS. Overall, the data indicated that TRAIL had no significant effect in any particular subtype (Figure 5.2 A). To investigate whether there was a correlation between TRAIL treatment and Ductal or Lobular histological subtype, these samples were grouped by Ductal, Lobular and Ductal + Lobular. A significant result was found in the Ductal subtype, however, while the fold decrease in tumourspheres was lowest in this sub-group, the significance of this decrease was likely due to a higher number of samples in this group than in the other subtypes (25 out of 30) (Figure 5.2 B).

We also tried to correlate TRAIL sensitivity with molecular subtype to investigate whether the treatment correlated with the ER or HER2 status. Six samples were ER -ve and 24 samples were ER +ve (Figure 5.3 A). Both groups responded similarly to TRAIL (Figure 5.3. B). Furthermore, TRAIL did not correlate with HER2 receptor status (Figure 5.4). Similarly, when samples were further stratified on the basis of both HER2 and ER status, no significant differences were observed (Figure 5.5).

Some of these samples were derived from patients with recurrent breast cancer, which had acquired resistance to endocrine treatments such as tamoxifen and/or aromatase inhibitors. Within the 4 samples that were TRAIL-sensitive, 2 were tamoxifen resistant (TAMR) and 2 were aromatase inhibitor resistant (AIR). TRAIL decreased the number of spheres in 2 out of 2 TAMR samples and 1 out of 2 AIR samples (Figure 5.6 A). Overall, endocrine- resistant samples were significantly more sensitive to TRAIL than their naïve counterparts, with endocrine-resistant samples exhibiting a significant 50% reduction in sphere forming activity compared to untreated controls. Additionally, endocrine-resistant samples have responded 35% less than the other endocrine-naïve samples (Figure 5.6 B).

Moreover, TRAIL treatment was tested in primary samples from patients with metastatic breast cancer. These samples were removed from the pleural cavity and processed in order to obtain the epithelial population for *ex vivo* culture purposes. As there were larger populations of cells available from these *ex vivo* cultures, these cells were treated with 20 ng/ml and 100 ng/ml of TRAIL in adherent conditions (2D) and then passaged into sphere conditions (3D) or treated directly in 3D. To assess cell self-renewal, spheres were disaggregated and plated in the same conditions for a second passage. Analysing 3D treatments that recapitulates the treatments performed for the biopsies/surgical samples, TRAIL significantly decreased the number of spheres in 5 out of 7 samples (Figure 5.7 A) and in 2D, TRAIL decreased TFUs in 4 out of 6 samples (Figure 5.7 B). Furthermore, TRAIL correlated with ER status decreasing sphere number in 2 out of 2 ER -ve samples but there is no correlation with HER2 expression (Figure 5.8 and 5.9). Similarly, when samples were further stratified on the basis of both HER2 and ER status, no significant differences were observed (Figure 5.10).

Importantly, TRAIL decreased sphere number in 3 out of 4 endocrine resistant samples with no effect in AE-naïve samples. All of the metastatic pleural effusion samples had received endocrine treatments, except for BB3RC90 and BB3RC94. Additionally, 2 out of 2 TNBC samples were significantly sensitive to TRAIL regardless of their treatment history (Figure 5. 11 A). Comparing all endocrine-naïve and endocrine-resistant metastatic samples, there is a sensitivity in endocrine-resistant samples but it is not statistically significant due to the limited number of endocrine naïve samples assessed (Figure 5.11 C).

Overall, 9 of 11 samples (82%) from all clinical groups (solid tumours and pleural effusions) that had replaced following endocrine treatment responded to TRAIL *ex vivo*, compared to the samples that had not previously seen endocrine therapy (Figure 5.12 A). Additionally, grouping all samples together, endocrine-resistant tumours benefit from TRAIL treatment alone compared to the naïve samples with a 30% decrease in tumourspheres (Figure 5.12 B). Taken together, the findings from these *ex vivo* models provide pre-clinical evidence that TRAIL may be valuable in controlling endocrine-resistant breast cancers and potentially provide long-term benefits by targeting the bCSC subset.

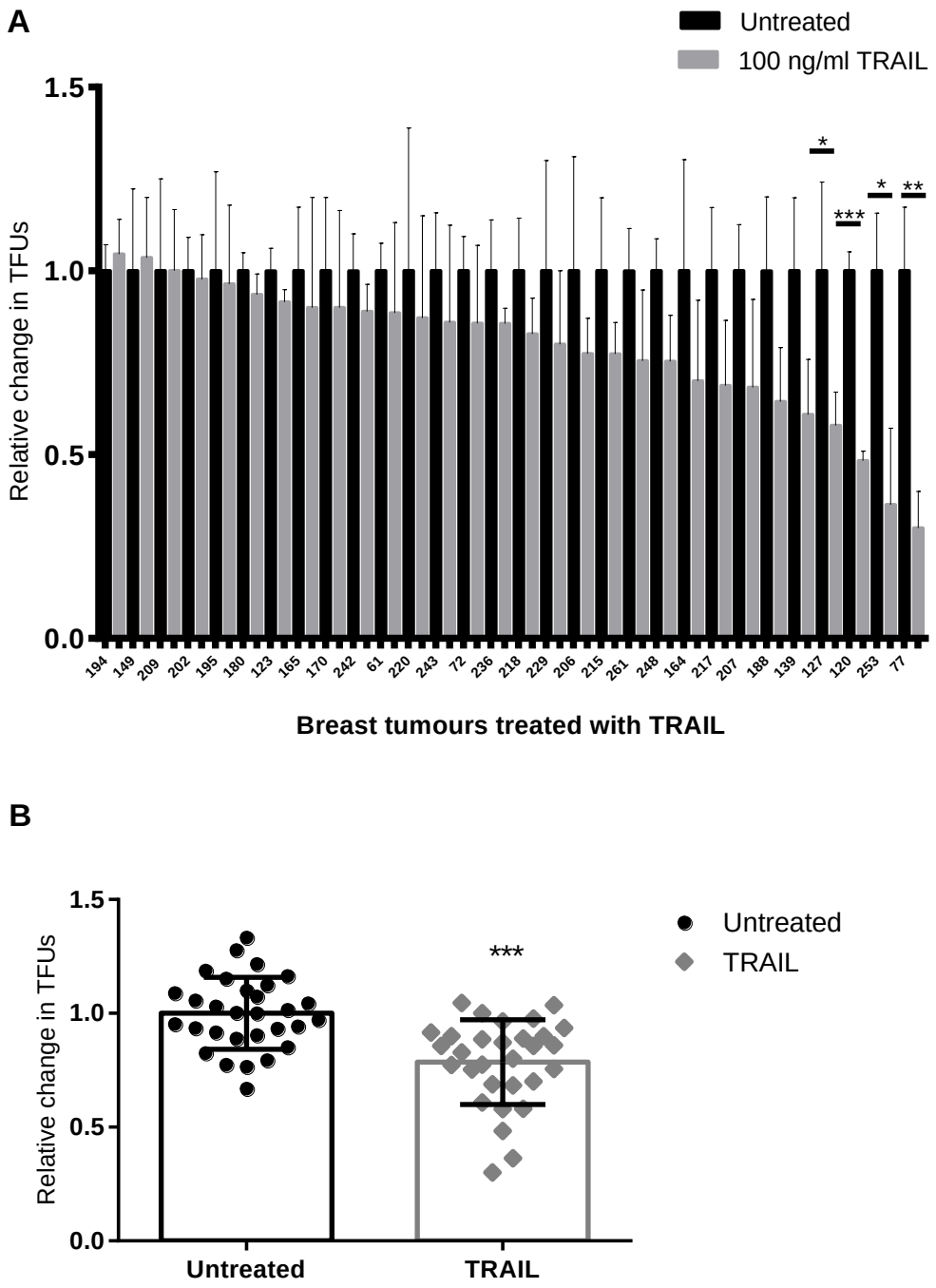

Figure 5.1. TRAIL decreases bCSCs (TFUs) in breast tumour samples. Y axes represents relative change of Tumoursphere Forming Units (TFUs) relative to the untreated control. 30 breast tumours were dissociated into single cells, plated into non-adherent conditions (tumoursphere assay) and treated with 100 ng/ml of TRAIL. | **A.** TRAIL treatment in 30 samples represented in a waterfall plot by TRAIL sensitivity normalised to the untreated control. | **B.** Overall relative change in TFUs after TRAIL treatment was calculated in the 30 samples. For the untreated control group, each sample was normalised to the mean of all untreated samples. | Bars represent mean +/- SD of one single experiment for each sample with three internal replicates. (*- significant vs untreated control *p<0.05; **p<0.005; ***p<0.0005; t-test).

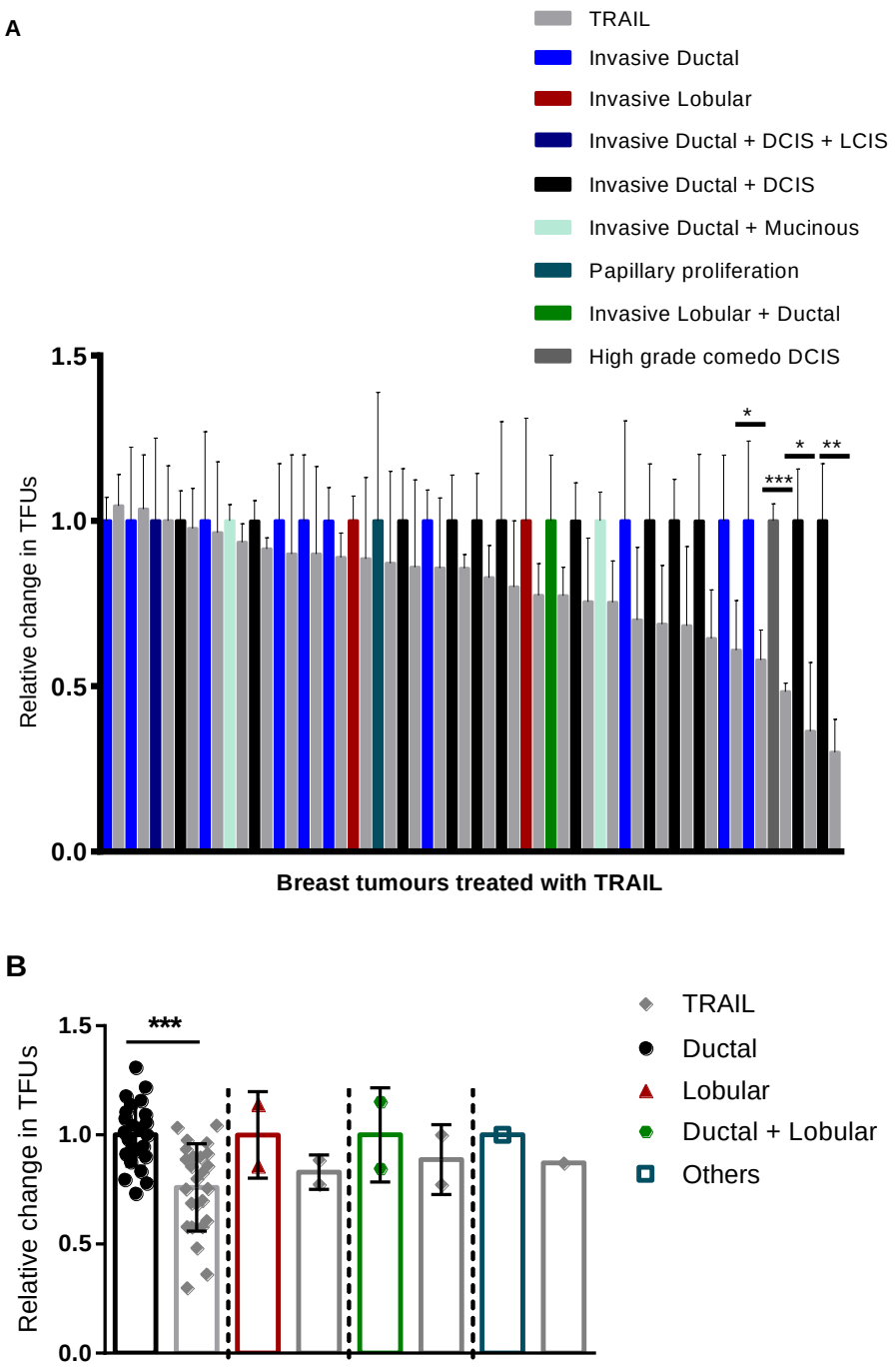

Figure 5.2. TRAIL treatment does not correlate with tumour histological subtype. 30 breast tumours were dissociated and plated as single cells in non-adherent conditions (tumoursphere assay) and treated with TRAIL. Y axes represents relative change of Tumoursphere Forming Units (TFUs) relative to the untreated control. | **A.** Waterfall plot representing TRAIL treatment in 30 samples in the same order as **5.1**. Different colours based on different histological subtype of each sample. | **B.** Overall TRAIL sensitivity for in Ductal, Lobular, Ductal + Lobular and other samples. Graph represents relative change in TFUs normalised to the untreated control for each group. Within each untreated group, each sample was normalised to the mean of untreated samples. | Bars represent mean +/- SD of one single experiment for each sample with three internal replicates. (*- significant vs untreated control *p < 0.05; **p<0.005; ***p<0.0005; t-test).

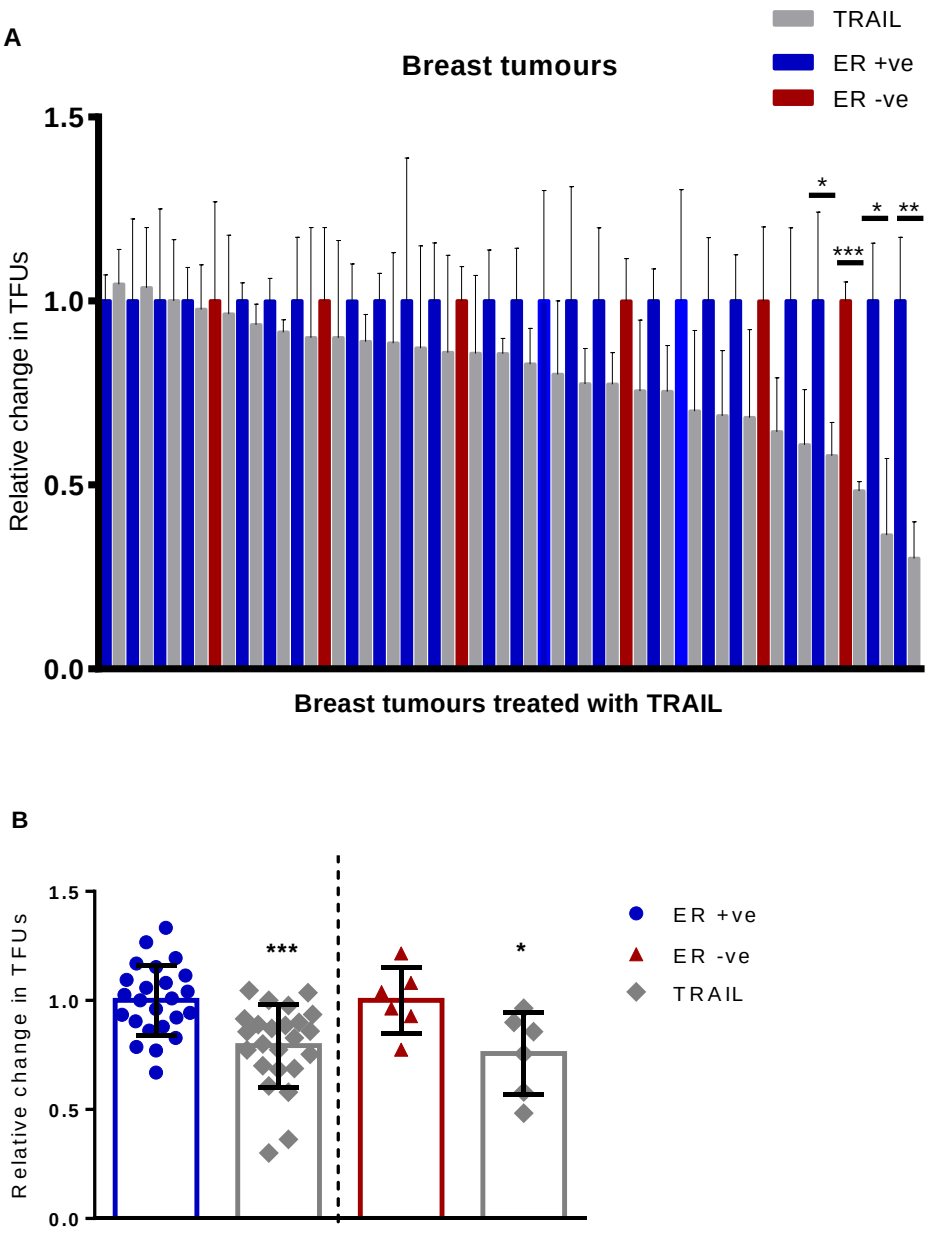

Figure 5.3. TRAIL treatment does not correlate with tumour estrogen receptor status. 30 breast tumours were dissociated and plated as single cells in non-adherent conditions (tumoursphere assay) and treated with TRAIL. Y axes represents relative change of Tumoursphere Forming Units (TFUs) to the untreated control. | **A.** Waterfall plot representing TRAIL treatment in 30 samples in the same order as **5.1**. Different colours based on ER status for each sample. | **B.** Overall sensitivity for ER +ve and ER -ve samples. For each untreated group, each sample was normalised to the mean of untreated samples. | Bars represent mean +/- SD of one single experiment for each sample with three internal replicates. (*- significant vs untreated control *p < 0.05; **p<0.005; ***p<0.0005; t-test).

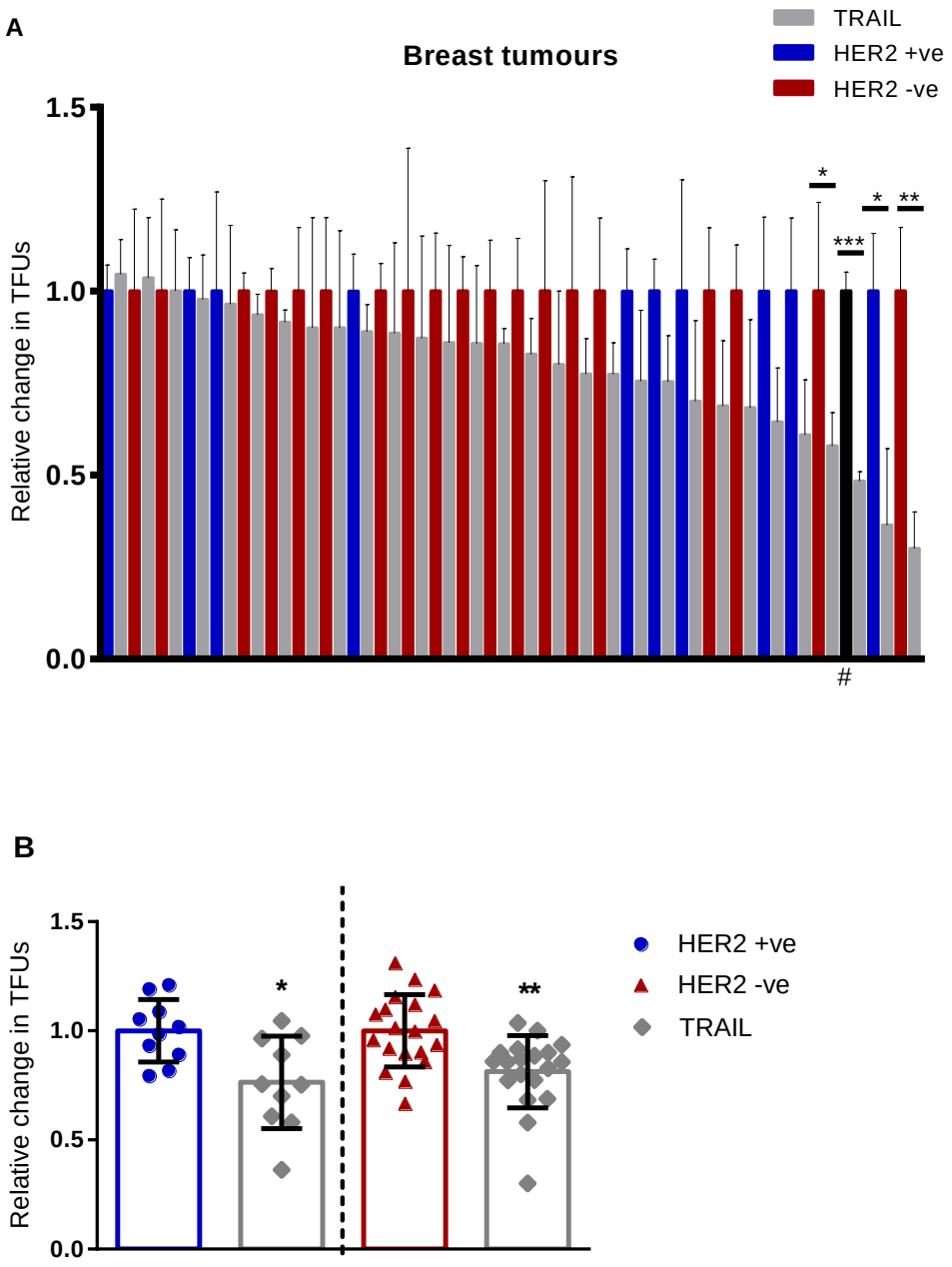

Figure 5.4. TRAIL treatment does not correlate with tumour HER2 receptor status. 30 breast tumours were dissociated and plated as single cells in non-adherent conditions (tumoursphere assay) and treated with TRAIL. Y axes represents relative change of Tumoursphere Forming Units (TFUs) to the untreated control. | **A.** Waterfall plot representing TRAIL treatment in 30 samples in the same order as **5.1**. Different colours based on HER2 status for each sample. | **B.** Overall sensitivity for HER2 +ve and HER2-ve samples. For each untreated group, each sample was normalised to the mean of untreated samples. | Bars represent mean +/- SD of ne single experiment for each sample with three internal replicates. (*- significant vs untreated control *p < 0.05; **p<0.005; ***p<0.0005; t-test). # - HER2 status is unknown.

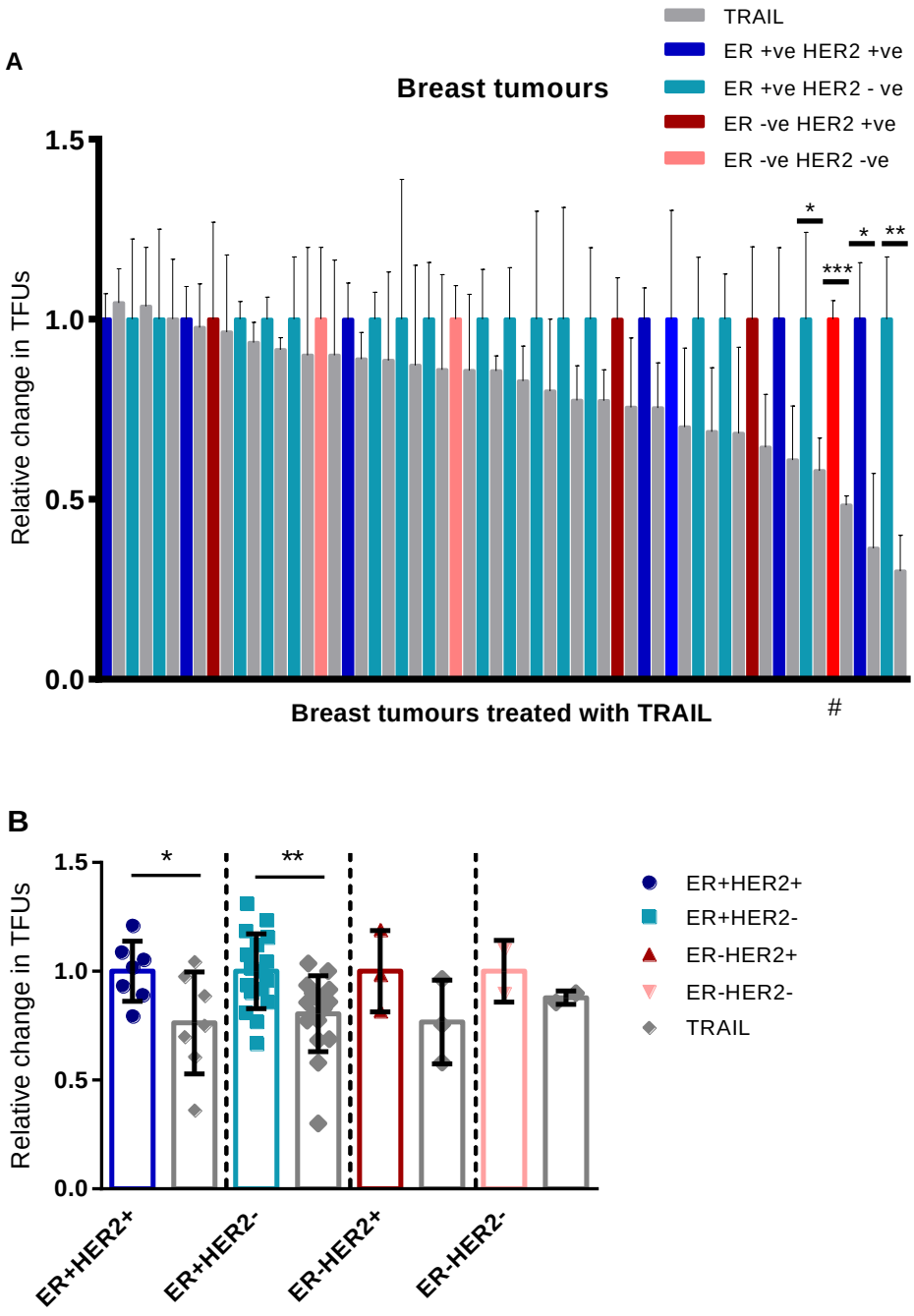

Figure 5.5. TRAIL treatment does not correlate with tumour molecular subtype. 30 breast tumours were dissociated and plated as single cells in non-adherent conditions (tumoursphere assay) and treated with TRAIL. Y axess represents relative change of Tumoursphere Forming Units (TFUs) to the untreated control. | **A.** Waterfall plot representing TRAIL treatment in 30 samples in the same order as **5.1**. Different colours based on ER and HER2 status for each sample. | **B.** Overall relative change in TFUs was calculated for each group. For each untreated group, each sample was normalised to the mean of untreated samples. | Bars represent mean +/- SD of one single experiment for each sample with three internal replicates. (*- significant vs untreated control *p < 0.05; **p<0.005; ***p<0.0005; t-test). # - HER2 status is unknown.

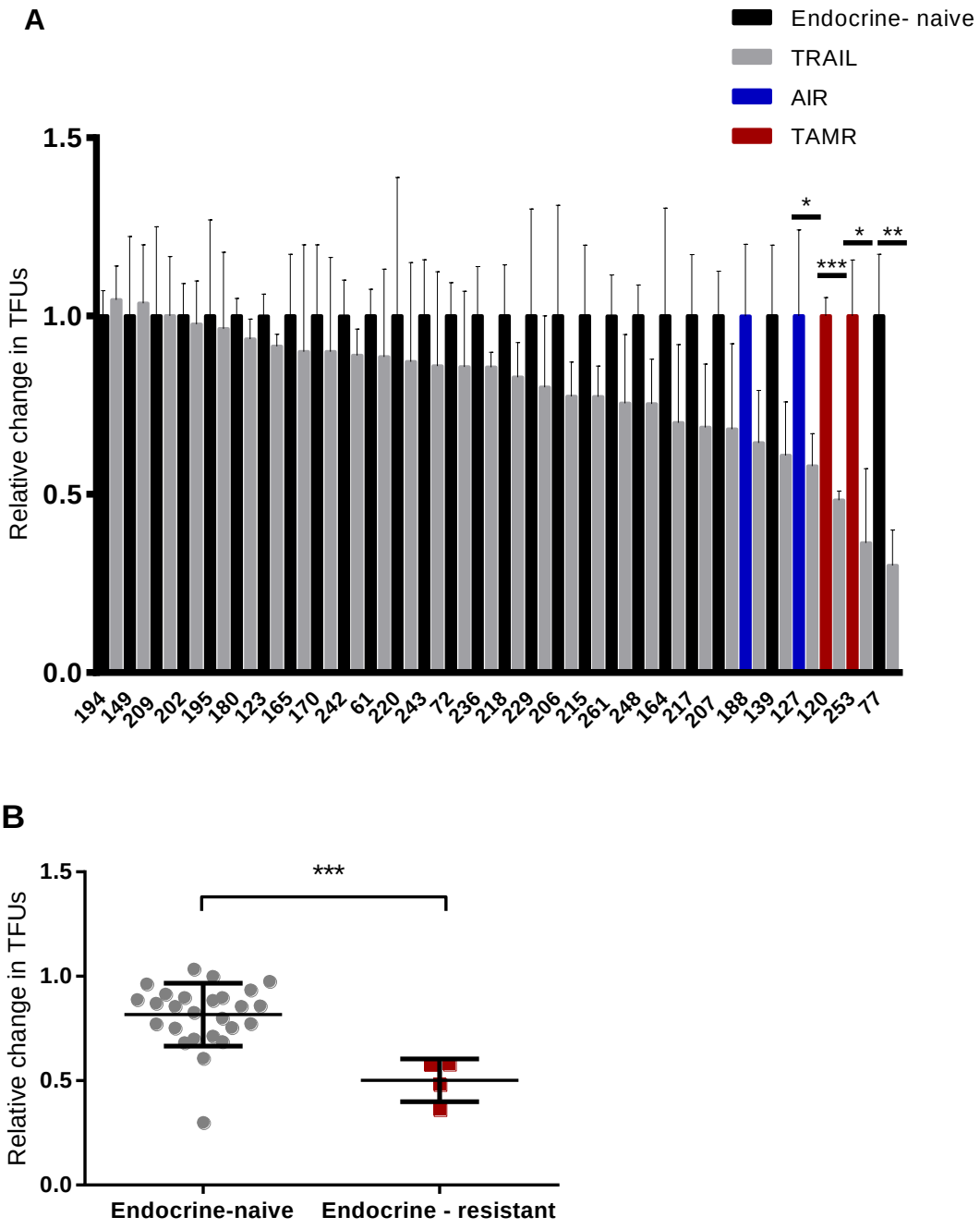

Figure 5.6. TRAIL reduces bCSCs in endocrine-resistant tumours. | TRAIL treatment of tumour samples in tumoursphere culture after 100ng/ml of TRAIL. Y axes represents relative change of Tumoursphere Forming Units (TFUs) relative to the untreated control. | **A.** Waterfall plot representing TRAIL treatment in 30 samples in the same order as 5.1. Different colours based in the ressitance to endocrine treatments (anastrozole or tamoxifen) | **B.** Overall relative changes in TFUs after TRAIL treatment based on endocrine resistance. TRAIL responses in endocrine-naïve samples vs TRAIL responses in endocrine-ressitant samples.| Bars represent mean +/- SD of one single experiment for each sample with three internal replicates. (*- significant vs untreated control *p < 0.05; **p<0.005; ***p<0.0005; t-test).

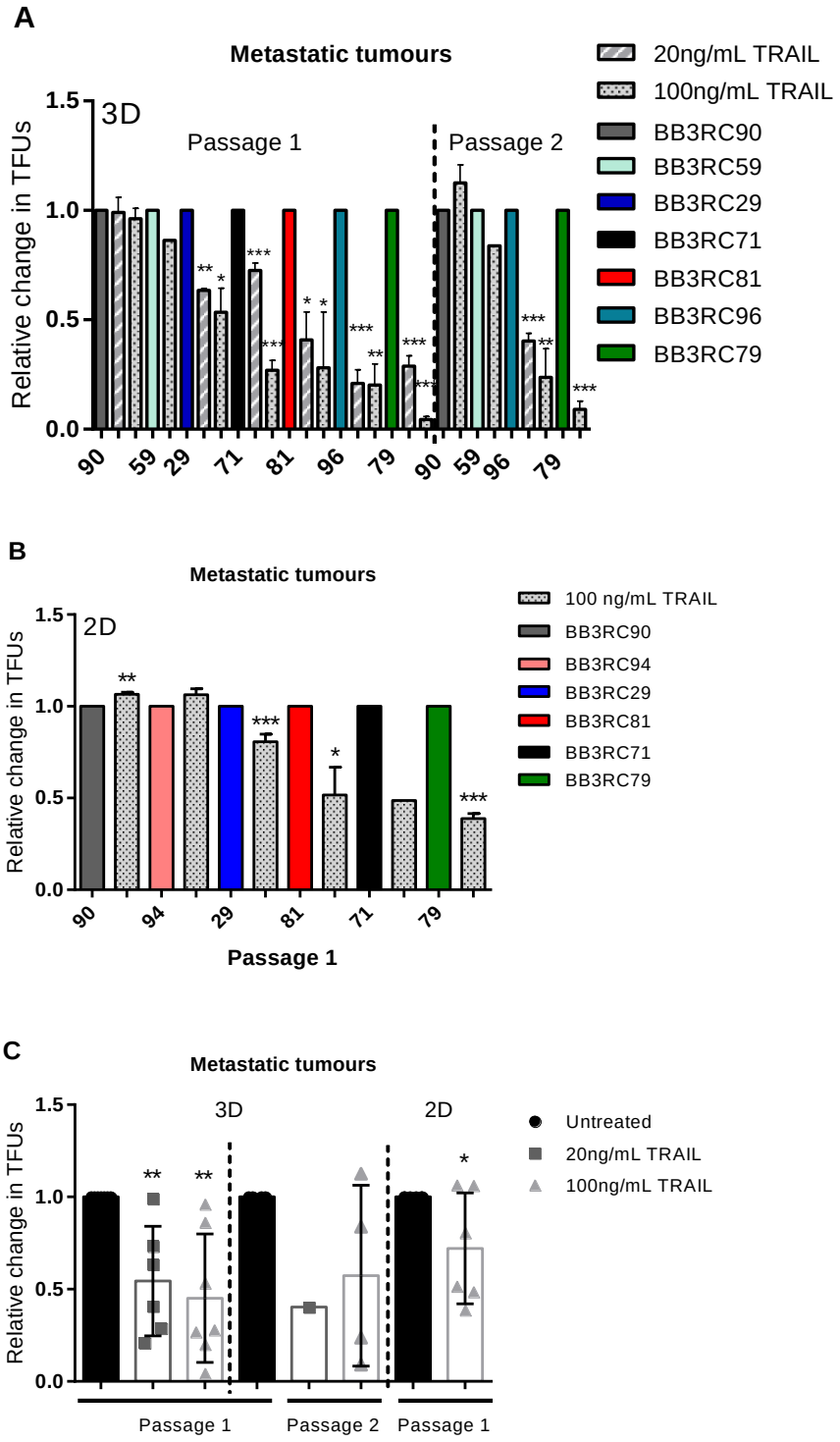

Figure 5.7. TRAIL reduces bCSCs (TFUs) in metastatic tumours from pleural effusions (n=9). Y axes represents relative change of Tumoursphere Forming Units (TFUs) relative to the untreated control. Spheres were counted after 7-10 days in culture for Passage 1. For passage 2 spheres were dissociated using trypsin and plated in the same conditions for self-renewal | **A.** Tumoursphere culture after 20 ng/ml (bars with stripes) and 100 ng/ml (bars with dots) of TRAIL treatment directly into non-adherent conditions (3D). Waterfall plot representing relative change in TFUs after TRAIL treatment in 7 samples. | **B.** Cells were pre-treated with TRAIL in adherent culture (2D) and then passaged into 3D. | **C.** Overall sensitivity to TRAIL in 2D (P1) and 3D in (P1 and P2) normalised to the untreated control. |Bars represent mean +/- SD of three single experiments for each sample with three internal replicates. (*- significant vs untreated control *p < 0.05; **p<0.005; ***p<0.0005; t-test).

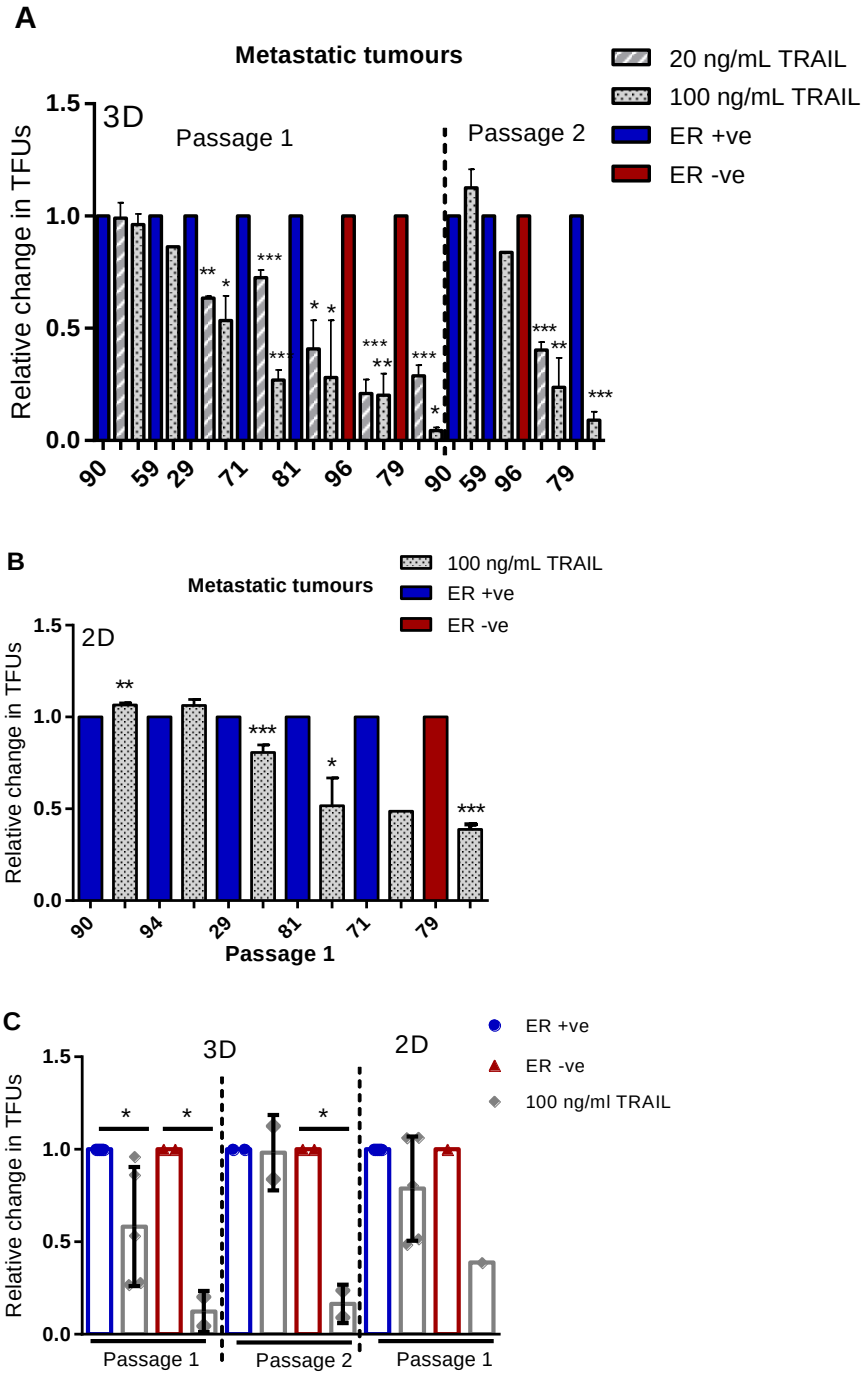

Figure 5.8. TRAIL treatment does not correlate with ER receptor status in metastatic tumours. Y axes represents relative change of Tumoursphere Forming Units (TFUs) relative to the untreated control. Spheres were counted after 7-10 days in culture for Passage 1. For passage 2 spheres were dissociated using trypsin and plated in the same conditions for self-renewal | **A.** Tumoursphere culture after 20 ng/ml (bars with stripes) and 100 ng/ml (bars with dots) of TRAIL treatment directly into non-adherent conditions (3D). Waterfall plot representing relative change in TFUs after TRAIL treatment in 7 samples. Colours bases in ER status. | **B.** Cells were pre-treated with TRAIL in adherent culture (2D) and then passaged into 3D. | **C.** Overall sensitivity to TRAIL in 2D (P1) and 3D in (P1 and P2) based on ER status normalised to the untreated control. |Bars represent mean +/- SD of three single experiments for each sample with three internal replicates. (*)- significant vs untreated control *p < 0.05; **p<0.005; ***p<0.0005; t-test).

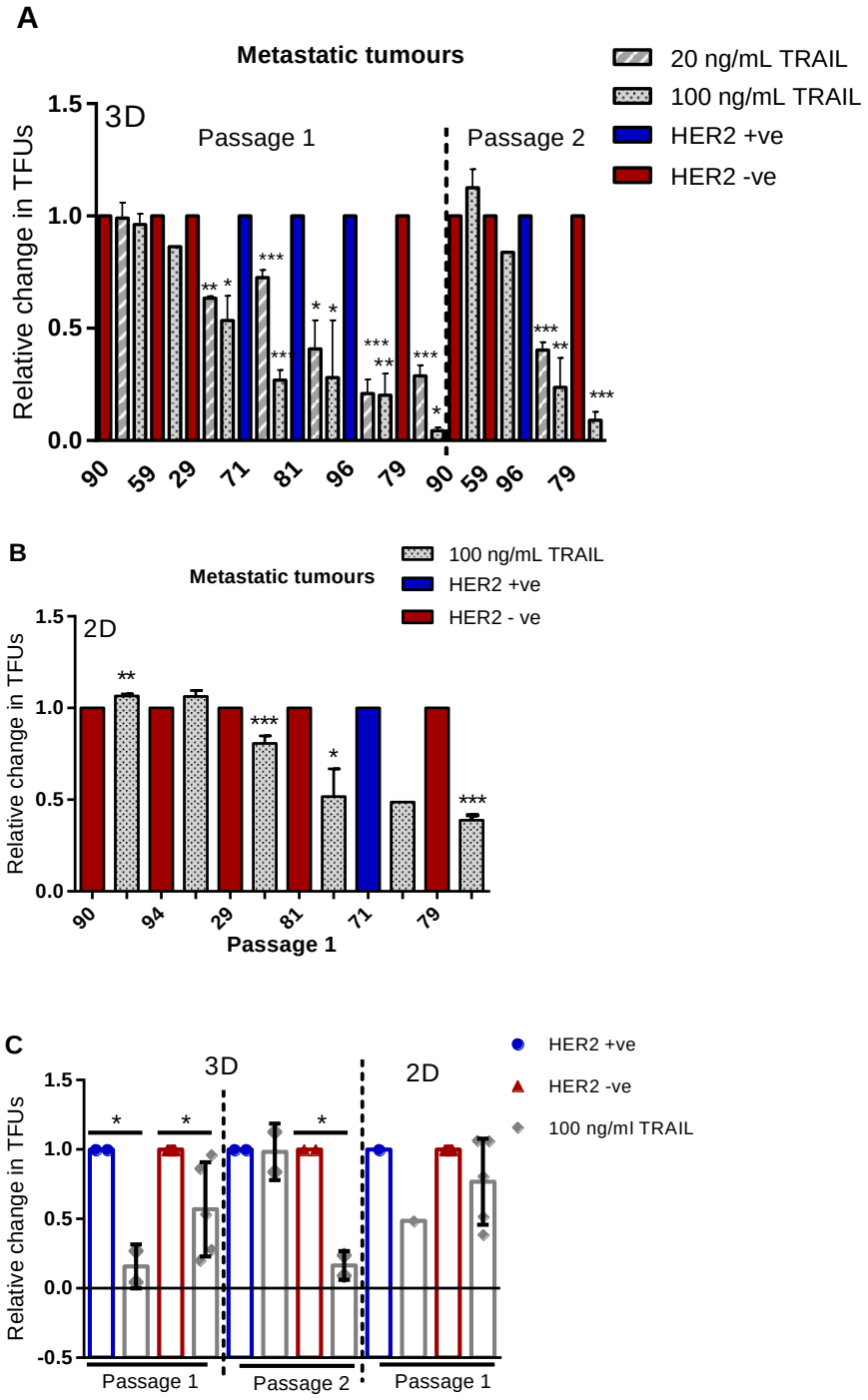

Figure 5.9. TRAIL treatment does not correlate with HER2 receptor status in metastatic tumours. | Y axes represent relative change of Tumoursphere Forming Units (TFUs) relative to the untreated control. Spheres were counted after 7-10 days in culture for Passage 1. For passage 2 spheres were dissociated using trypsin and plated in the same conditions for self-renewal | **A.** Tumoursphere culture after 20 ng/ml (bars with stripes) and 100 ng/ml (bars with dots) of TRAIL treatment directly into non-adherent conditions (3D). Waterfall plot representing relative change in TFUs after TRAIL treatment in 7 samples. Different colours based on HER2 status for each sample. | **B.** Cells were pre-treated with TRAIL in adherent conditions (2D) and then passaged in to non-adherent conditions. | **C.** Overall sensitivity to TRAIL in 2D (P1) and 3D in (P1 and P2) based on HER2 status normalised to the untreated control. | Bars represent mean +/- SD of three single experiments for each sample with three internal replicates. (*- significant vs untreated control *p < 0.05; **p<0.005; ***p<0.0005; t-test).

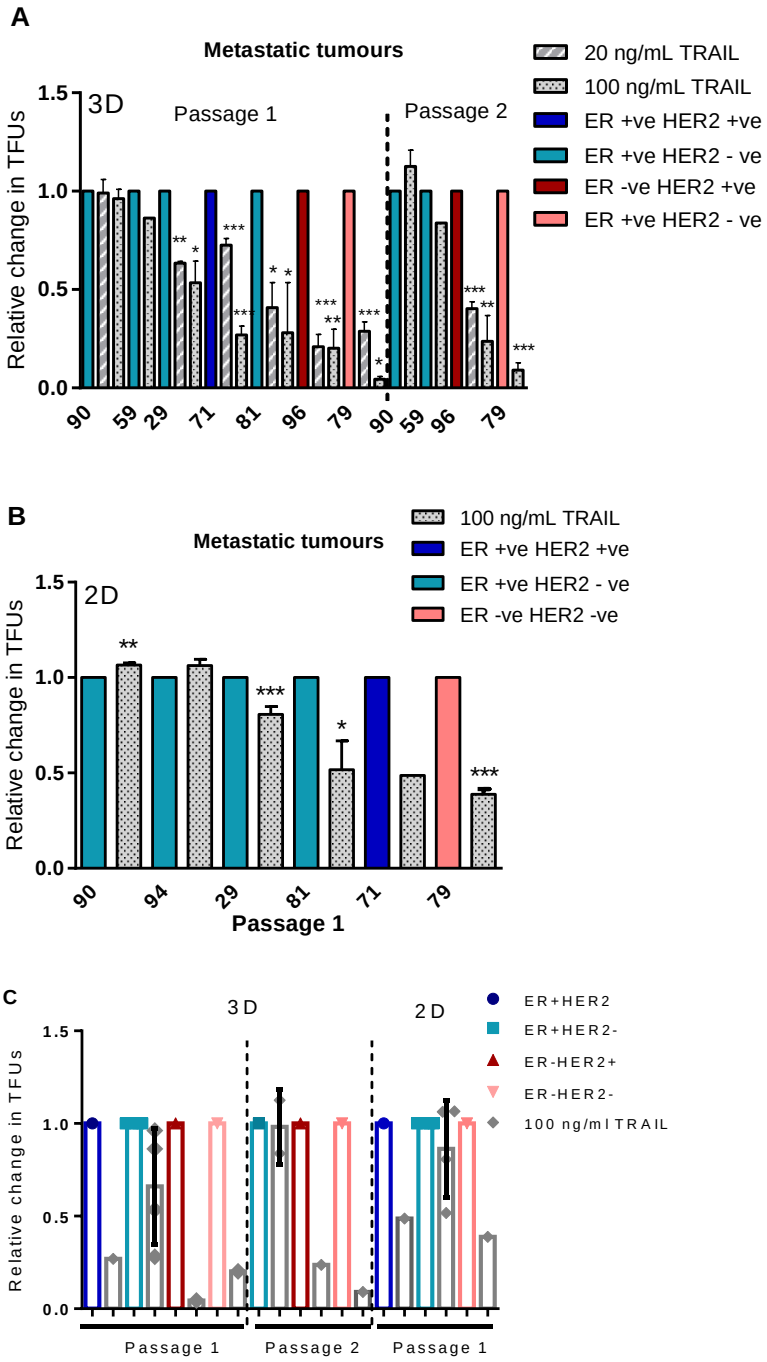

Figure 5.10. TRAIL treatment does not correlate with molecular subtype in metastatic tumours. | Y axes represent relative change of Tumoursphere Forming Units (TFUs) relative to the untreated control. Spheres were counted after 7-10 days in culture for Passage 1. For passage 2 spheres were dissociated using trypsin and plated in the same conditions for self-renewal | **A.** Tumoursphere culture after 20 ng/ml (bars with stripes) and 100 ng/ml (bars with dots) of TRAIL treatment directly into non-adherent conditions (3D). Waterfall plot representing relative change in TFUs after TRAIL treatment in 7 samples. Different colours based on ER/HER2 status for each sample. | **B.** Cells were pre-treated in adherent culture (2D) with TRAIL and then passaged in to non-adherent culture. | **C.** Overall sensitivity to TRAIL based on ER/HER2 status in 2D (P1) and 3D in (P1 and P2) normalised to the untreated control. |Bars represent mean +/- SD. Three single experiments for each sample with three internal replicates. (*- significant vs untreated control *p < 0.05; **p<0.005; ***p<0.0005; t-test).

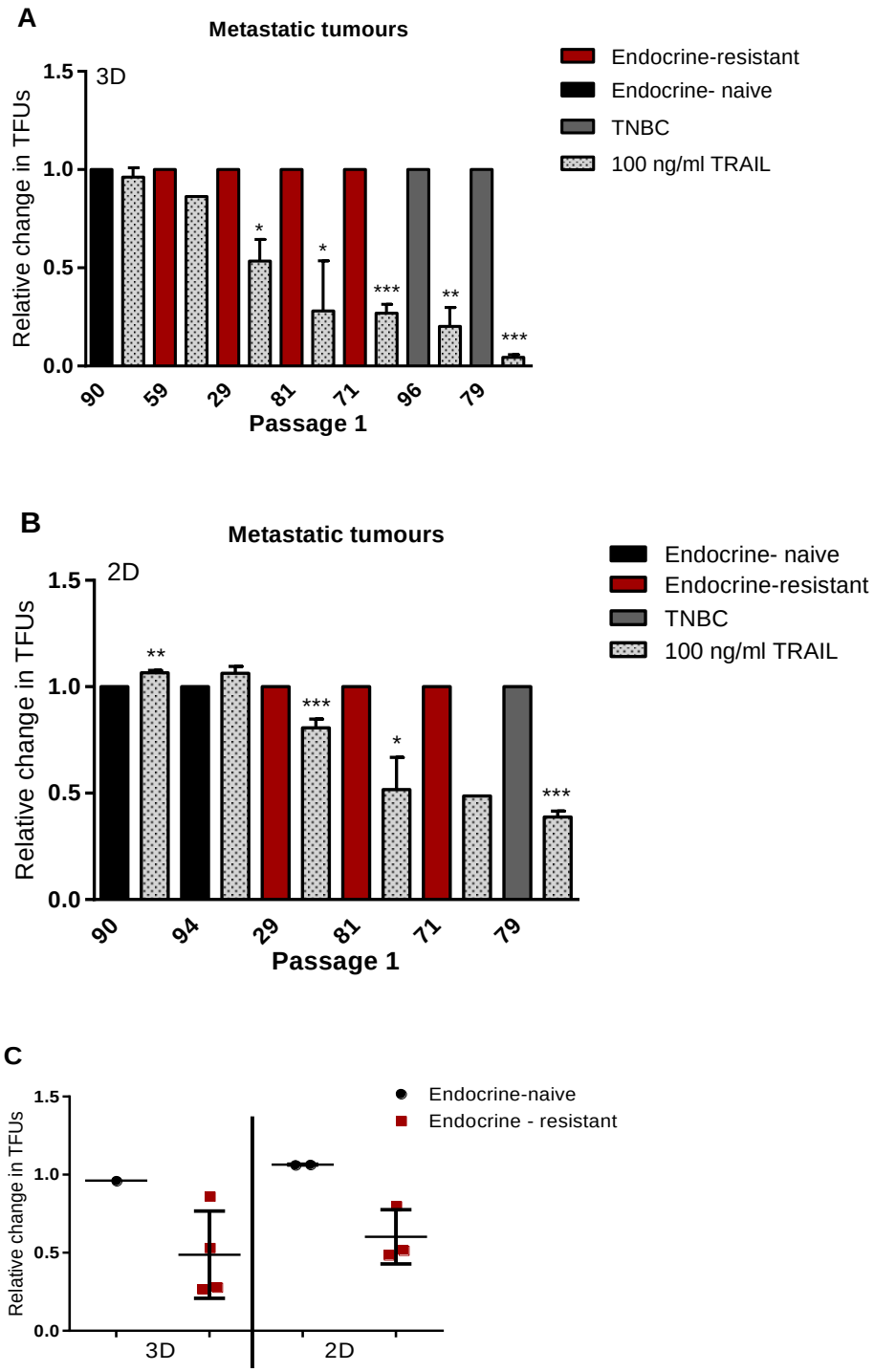

Figure 5.11. TRAIL reduces bCSCs (TFUs) in endocrine resistant metastatic tumours from pleural effusions. | Y axes represent relative change of Tumoursphere Forming Units (TFUs) relative to the untreated control. Spheres were counted after 7-10 days in culture for Passage 1.| **A.** Tumoursphere culture after 100 ng/ml of TRAIL treatment directly into non-adherent conditions (3D). Waterfall plot representing relative change in TFUs after TRAIL treatment in 7 samples. Different colours based on endocrine resistance for each sample and TNBC. | **B.** Cells were pre-treated with TRAIL and then passaged in to non-adherent conditions adherent culture (2D). | **C.** Overall sensitivity to TRAIL in 3D and 2D. TRAIL response in endocrine naïve vs. TRAIL response in endocrine-resistant samples. |Bars represent mean +/- SD of three single experiments for each sample (except BB3RC59) with three internal replicates. (*- significant vs untreated control *p < 0.05; **p<0.005; ***p<0.0005; t-test).

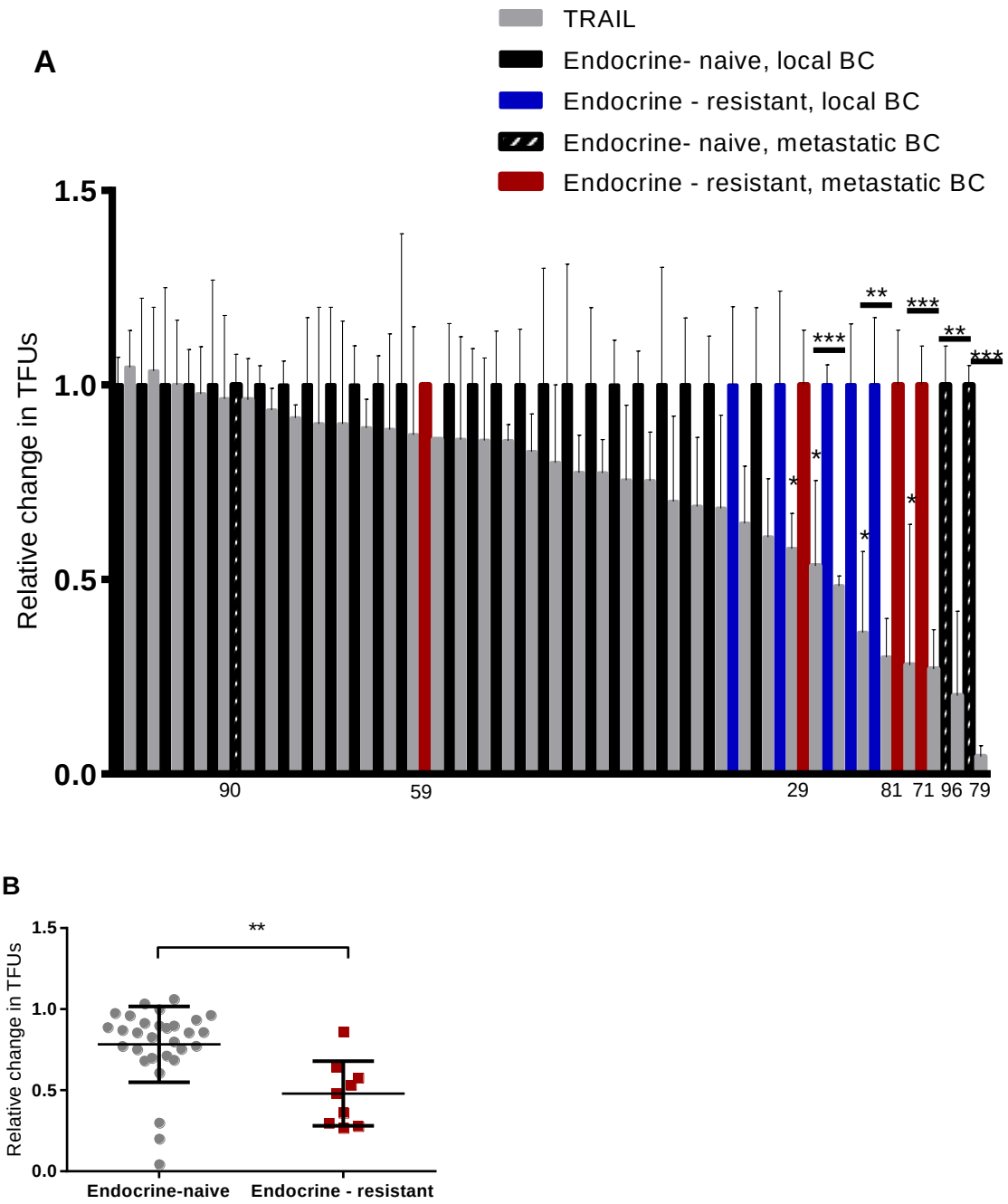

Figure 5.12. TRAIL reduces bCSCs (TFUs) in endocrine-resistant tumours from core biopsies/surgical samples and pleural effusions. Y axes represent relative change of Tumoursphere Forming Units (TFUs) for each sample normalised to its own untreated control. Numbers represent the metastatic samples only. All other samples (biopsies/surgical samples) are in the same order as Figure 5.1. Cells were treated with 100 ng/ml of TRAIL directly into non-adhrent conditions. | **A.** Waterfall plot representing relative change in TFUs after TRAIL treatment in 37 samples | **B.** Overall relative changes in TFUs after TRAIL treatment based on endocrine resistance. TRAIL responses in endocrine-naïve samples vs TRAIL responses in endocrine-resistant samples.| Bars represent mean +/- SD of one single experiment for each sample with three internal replicates. (*- significant vs untreated control *p < 0.05; **p<0.005; ***p<0.0005; t-test).

5.2.2. *In vivo* PDX models of endocrine-resistant breast cancer demonstrate sensitivity to TRAIL treatment

It was demonstrated that tumours that have acquired resistance to endocrine treatments are particularly sensitive to TRAIL. Therefore, this finding establishes the value of TRAIL treatment in this cohort of patients that are endocrine-resistant. To further evaluate this finding, TRAIL was tested *in vivo* using two patient-derived xenograft (PDX) models.

In the first PDX experimental model, performed by our collaborators (I. Fichtner and M. Becker – EPO Berlin-bush, Berlin), a primary ER +ve tumour was kept orthotopically by serially passaging in immunocompromised mice receiving either estradiol (MaCa 3366) or tamoxifen (MaCa 3366 TAMR) for up to 3 years, generating estradiol dependant and tamoxifen-resistant models, respectively, from the same parental tumour tissue (Naundorf *et al.,* 2000). Mice were subjected to systemic administration of 8 intraperitoneal (IP) injections of TRAIL over 2 weeks (treatment windows highlighted in pink, Figure 5.13 A and B). Tumour growth kinetics were monitored from the beginning of treatment by measuring tumours. In the tamoxifen-naive estrogen-dependent control tumours, systemic *in vivo* TRAIL treatment did not have an effect at inhibiting tumour growth compared to the vehicle control (Figure 5.13 A). In contrast, a transient (10 day) significant suppression of MaCa 3366 TAMR tumour growth was observed following TRAIL treatment resulting in a significant reduction of tumour size (Figure 13 B) evident after 4 weeks post-treatment.

Tumours from the MaCa 3366 study were shipped to our laboratory whereupon we dissociated the tissue into single cells (confirmed using microscope) and plated in non-adherent conditions to investigate stem cell activity. TRAIL treated, *in vivo*, tumours showed a 2-fold increase in percentage of spheres compared to the control (Passage 1 and 2) demonstrating that *in vivo* treatment of MaCa 3366 tamoxifen-naive tumours significantly increased the proportion of bCSCs within the tumours (Figure 5.13 C and D). However, this increase was not significant, possibly due to the intra-tumour biological variability of the tumours. Tumours from MaCa 3366 TAMR mice, both untreated

vehicle and TRAIL treated, were also shipped, dissociated and plated in tumoursphere culture. TRAIL treated, *in vivo*, tumours showed a 40% reduction in spheres compared to the vehicle (Passage 1 and 2) demonstrating that *in vivo* treatment of MaCa 3366 TAMR tumours significantly reduced the bCSCs within the tumours (Figure 5.9 E and F). In addition, the MaCa 3366-TAMR vehicle tumours were treated with TRAIL *ex vivo* and the treatment led to a 35% reduction in the number of spheres in Passage 1 and Passage 2, showing similar sensitivity as the endocrine-resistant breast tumours in section 5.2.1 (Figure 5.12).

For the second PDX model (Biopsy and PDX 151), a biopsy obtained from a locally ER -ve relapsed tumour from an ER +ve (prior to endocrine treatment) breast cancer patient who had relapsed on the aromatase inhibitor (AI) anastrazole. This biopsy was transplanted in recipient immunocompromised mice to model AI-resistant breast cancer. In order to determine AI-resistant breast cancer sensitivity to TRAIL, mice transplanted with biopsy 151 tumours (PDX 151) were administered 8 intraperitoneal injections of TRAIL over 2 weeks. This resulted in a significant reduction in AI-resistant tumour growth compared to vehicle control (Figure 5.14 B). *Ex vivo* vehicle PDX 151 tumour cells also demonstrated significant sensitivity of bCSCs to *ex vivo* treatment with TRAIL (Figure 5.14 B). Furthermore, the sensitivity of PDX 151 bCSCs *ex vivo* was consistent with the sensitivity of the primary tumour (Biopsy 151) treated *ex vivo* prior to transplantation (original biopsy straight from the patient) (Figure 5.14 C). This was paralleled by a drastic reduction in both the number and size of spontaneous lung metastases *in vivo* (Figure 5.14 D and E) confirming TRAIL sensitivity of AI-resistant tumours, bCSCs reduction after treatment and decreased ability to metastasise in other organs.

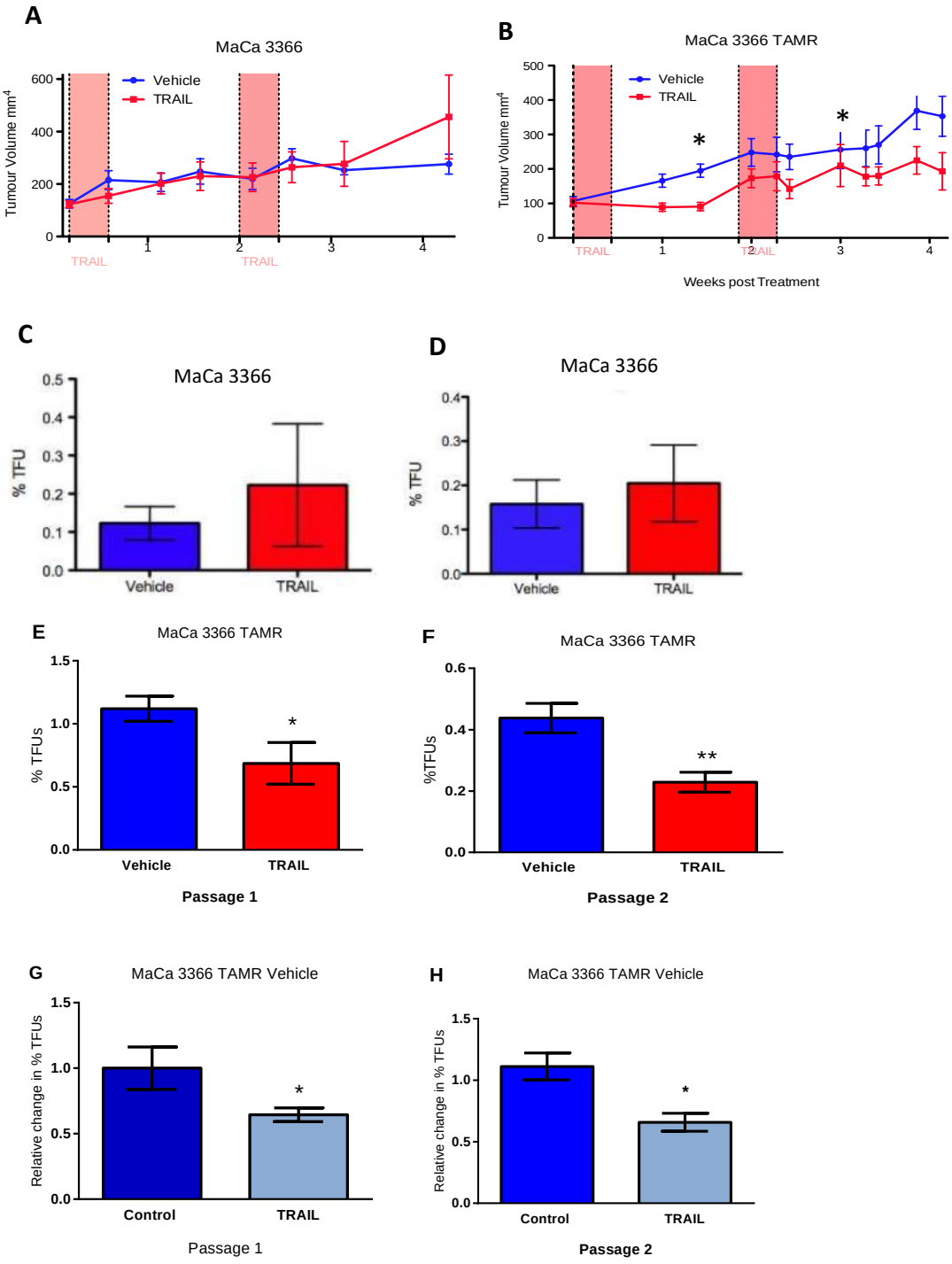

Figure 5.13. Endocrine-resistant PDX models demonstrate sensitivity to TRAIL. | Y-axes represent relative % change of Tumoursphere forming Units (TFUs)| **A**. Change in tumour volume: Established Tamoxifen-sensitive and **B.** Acquired Tamoxifen-resistant MaCa 3366 PDX tumours (n=8 each) were treated 8 times in 2 weeks with 16 mg/kg of TRAIL I.P (pink = 4 x daily treatment windows) and growth kinetics monitored weekly by caliper measurement compared with vehicle control. | **C.** Tumours from A. Vehicle and TRAIL-treated tumours harvested 24 hours following the final TRAIL administration were dissociated and tumoursphere forming capacity assessed (P1) | **D.** Tumourspheres from C. were then disaggregated and passaged to assess self-renewal capacity (P2). | **E.** Tumours from B. Vehicle and TRAIL-treated tamoxifen resistant tumours harvested 24 hours following the final TRAIL administration were dissociated and TFUs assessed (P1) | **F.** Tumoursphers from **E.** into P2. | **G**. Vehicle tumours from B. were treated with TRAIL *ex vivo* for a P1 and **H**. Tumourspheres from G. into a P2 | Bars represent mean +/- SEM of 3 independent experiments with at least 3 internal replicates. * - significant vs vehicle (p) < 0.05, ** (p) < 0.005; t-test.

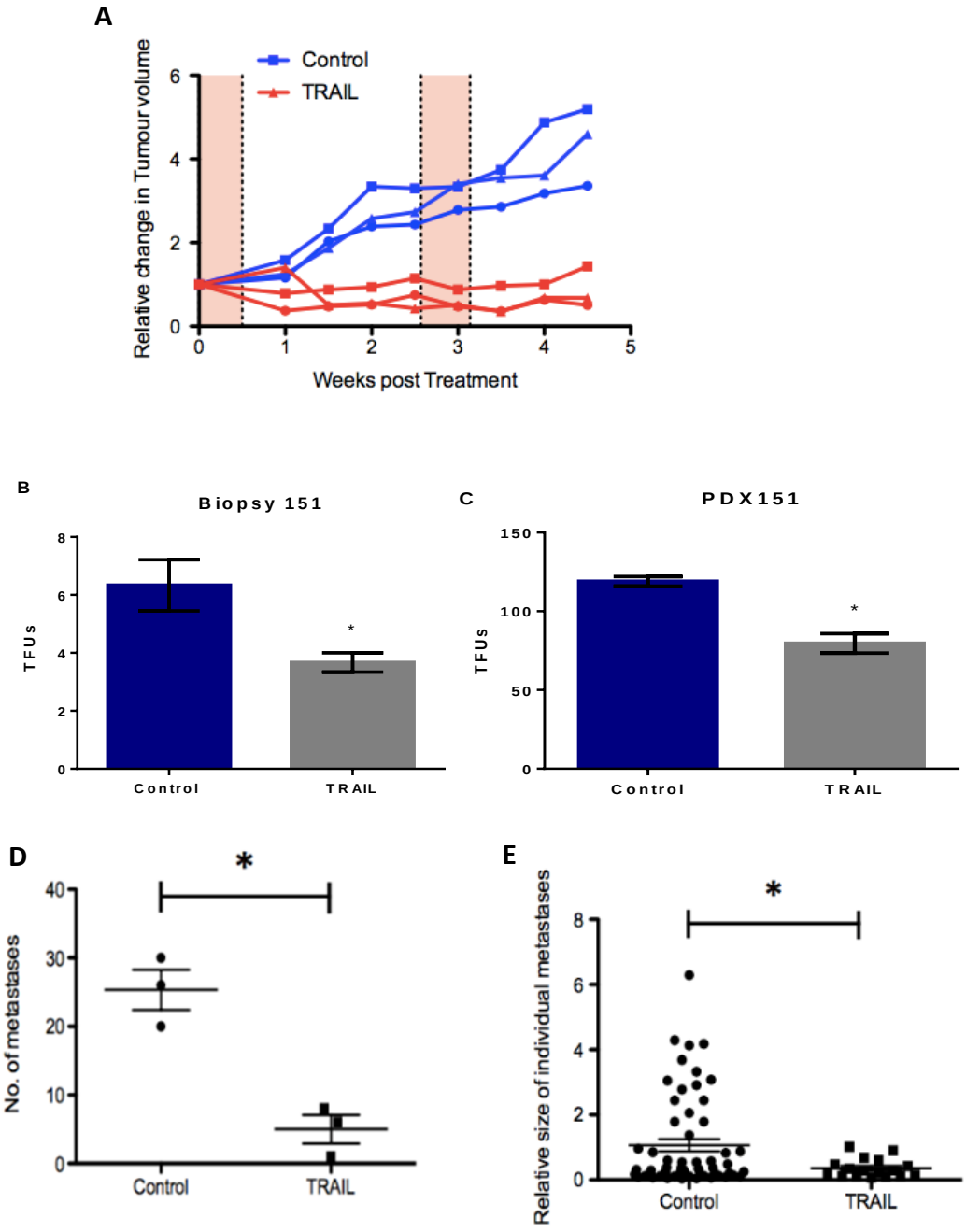

Figure 5.14. TRAIL reduces tumour growth of endocrine-resistant tumours *in vivo* and tumourspheres pre- and post-transplantation of the same sample. | **A**. An anastrozole resistant (AR) tumour was used to generate an aromatase Inhibitor (AI)-resistant PDX model (biopsy and PDX 151). Mice were treated 8 times in 2 weeks with 16 mg/kg of TRAIL IP (pink = 4 x daily treatment windows) and growth kinetics monitored weekly by caliper measurement compared with vehicle control (n=3). |**B.** AR tumour (biopsy 151) was tested *ex vivo* with 100 ng/ml of TRAIL prior transplantation for stem cell activity by tumoursphere assay. Graph represents change of Tumoursphere forming Units (TFUs) |**C.** Vehicle control PDX 151 - AI-resistant tumours were excised, dissociated and TFU assessed following treatment with 100 ng/ml TRAIL for 18 hours *ex vivo* (n=3 performed in triplicate). |**D.** Assessment of lung metastatic burden (mean number of six metastasis +/- SEM) in H+E serial sections from vehicle control and TRAIL treated PDX151 tumours 2 weeks following last TRAIL treatment. | **E.** Relative size of the individual metastases after treatment in A. |* - significant vs control (p) < 0.05, ** (p) < 0.005, t-test.

5.2.3. siFLIP/TRAIL reduces bulk cell viability in primary metastatic cells

Since an inducible and long-term suppression of c-FLIP could not been achieved for this project (see Chapter 3), cells were treated with a transient knockdown to genetically suppress c-FLIP (siFLIP) for 48 hours or 72hours. Metastatic primary samples from pleural effusions (BB3RC29, BB3RC90, BB3RC81 and BB3RC79) were treated with siRNA targeting c-FLIP. Firstly, c-FLIP was suppressed using reverse transfection (M1) where plating and transfection of cells are performed on the same day and siRNA is diluted in culture medium without serum. Reverse transfection allows cells to be plated and transfected simultaneously saving a day in the procedure. Cells were treated with siRNA and scramble control (SC) for 48 hours or 72 hours and treated with 100 ng/ml of TRAIL for 18 hours before viability analysis by cell titre blue. Suppressing c-FLIP using a construct (A) (Table 5.5) that targets both long and short form of c-FLIP led to a reduction in viability in the presence and absence of TRAIL (Figure 5.15). In BB3RC29, 48 hours and 72 hours c-FLIP suppression lead to a reduction in viability by 21.8% and 20.1%, respectively. The addition of TRAIL led to further sensitisation in viability by 55.6% at 48 hours and 49.5% at 72 hours (Figure 5.15 A). In BB3RC90, 48 hours and 72 hours c-FLIP suppression lead to a 15.1% and 32.9%, reduction in viability respectively. The addition of TRAIL led to a sensitisation in viability of 30.6% at 48 hours and 20.1 at 72 hours (Figure 5.15 B). In BB3RC81, 48 hours and 72 hours c-FLIP suppression lead to a 15.0% and 20.6% reduction in viability, respectively. The addition of TRAIL led to a 47.3% reduction in viability at 48 hours and 60.3% at 72 hours (Figure 5.15 C). In BB3RC79, 48 hours and 72 hours c-FLIP suppression lead to a reduction in viability by 46.6% and 59.7%, respectively. Unlike the other primary samples tested, in which TRAIL and siFLIP effects were synergistic, the combination of these interventions in the triple-negative breast cancer BB3RC79 was no more than additive presumably due to the fact that these cells were already sensitive to TRAIL alone, as previously reported for TNBC cell lines (Figure 5.15 D; Rahman *et al.*, 2009). C-FLIP suppression was confirmed by qPCR (Figure 5.15 E). However, c-FLIP protein levels were only

performed for BB3RC81 (Piggott et al., 2018). In order to improve these results, a second method of transfection using siRNA was tested.

For the second method, fast-forward transfection (M2), cells were plated 24 hours prior to transfection. Using efficient, fast-forward transfection protocols, some cell lines are more effectively transfected, siRNA concentrations can often be decreased (which may reduce the chance of off-target effects). In addition, two different constructs of siRNA for c-FLIP were used: (A) the construct previously used that targets long and short form of c-FLIP and (B) a smartpool siRNA that targets four siRNA duplexes all designed to target distinct sites within the specific gene of interest which target both long of short form of c-FLIP (Table 5.5).

M1 method resulted in an overall sensitisation in BB3RC90 and BB3RC29 cells by 59.96% and 30.16%, respectively (M1A in Figure 5.16 A and B). In BB3RC90, using M2 and the construct B decreased this sensitisation to 55.02% (Figure 5.16 A). Analysing c-FLIP gene expression by qPCR showed that M1 knocked down c-FLIP by 30% and M2 by 60% explaining why using the construct B had a higher impact on viability (Figure 5.16 C). Additionally, this viability change was due to M2 causing less toxicity to the cells.

In BB3RC29, the better sensitisation of cells to TRAIL of M2 compared to M1 was primarly due to the lack of cytotoxicity alone (Figure 5.16 B). Analysing c-FLIP gene expression by qPCR showed that construct M1A and M2B resulted in a 45% and 90%, respectively, gene knockdown at 48 hours (Figure 5.16 D). In this cell line, the result suggests that partial depletion of c-FLIP (M1A, Figure 5.16 D) results in a lower viability than a more complete depletion of c-FLIP (M2B Figure 5.16 D). This counterintuitive result could be explained by the recent findings from the MacFarlane laboratory who have shown that very efficient depletion of c-FLIP levels leads to an increase in cell viability compared to partial depletion, due to c-FLIP having a stabilising effect on DISC formation at low concentrations (Hughes *et al*., 2016). However, simply differences in stress given on cells by M1 vs M2 could also contribute to this efficiency.

Therefore, in general it seems that using a reverse reaction (M1) with the construct A would be a better strategy to knockdown cells to ensure optimal sensitisation to TRAIL, by ensuring that knockdowns do not exceed 90%.

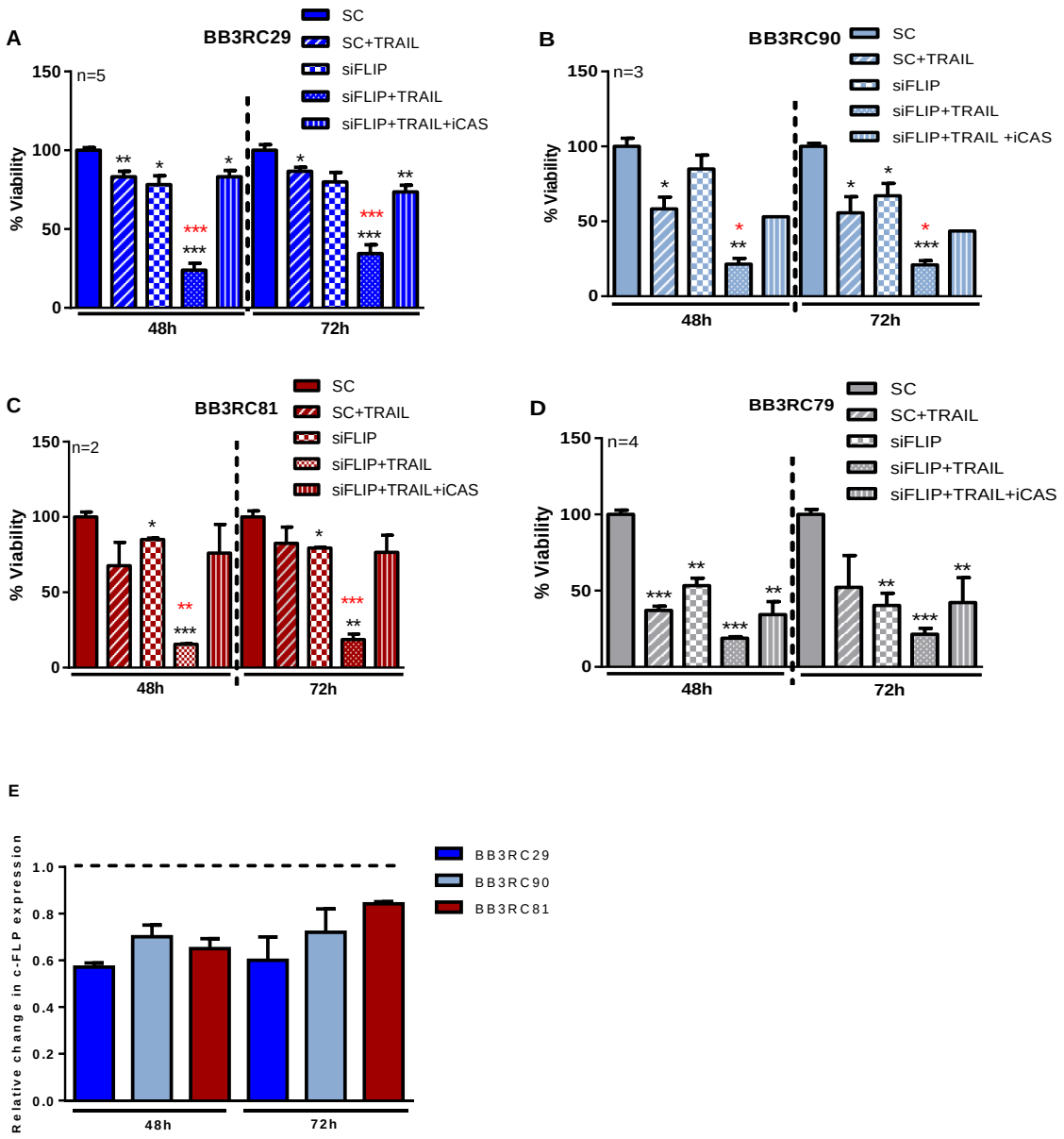

Figure 5.15. siRNA-mediated suppression of the c-FLIP gene and TRAIL treatment in pleural effusion samples. | **A-D**. BB3RC29, BB3RC90, BB3RC81 and BB3RC90 viability (cell titre blue assay) following TRAIL, siFLIP (reverse transfection, M1), iCAS (caspase inhibitor) and siFLIP/TRAIL treatment normalised to the scrambled untreated control (SC). C-FLIP was suppressed by siRNA for 48 hours and 72 hours prior to TRAIL addition. Cells were treated with 100 ng/ml TRAIL for 18 hours and with 10 ng/ml of iCAS at 0h and 10 ng/ml 1 hour prior TRAIL. | **E.** c-FLIP gene expression analysed by qPCR after siFLIP normalised to SC. | * - significant vs SC (p) < 0.05, ** (p) < 0.005; ***(p)<0.0005, t-test. * - red asterisks highlight combination treatments (siFLIP + TRAIL) that are more than the sum of the respective individual treatments. * - an additional 20-35% loss of viability; **- an additional 35-50% loss in viability; ***- an additional 50-65% loss in viability.

Table 5.1. Methods of transfection using two different c-FLIP siRNA constrcuts for c-FLIP. Cells were transfected using reverse transfection (M1) where plating and transfection of cells are performed on the same day. siRNA is diluted in culture medium without serum. On the second method, fast-forward transfection (M2), cells are plated 24 hours prior to transfection. Two different constructs of siRNA for c-FLIP were used: (A) targets long and short form of c-FLIP and (B) is a smartpool siRNA that targets four siRNA duplexes all designed to target distinct sites within the specific gene of interest which target both long of short form of c-FLIP.

Transient trasnfection			**c-FLIP siRNA construct**	
			siRNA_A	siRNA_B
Transfection Method	Reverse	M1	M1A	M1B
	Fast-forward	M2	M2A	M2B

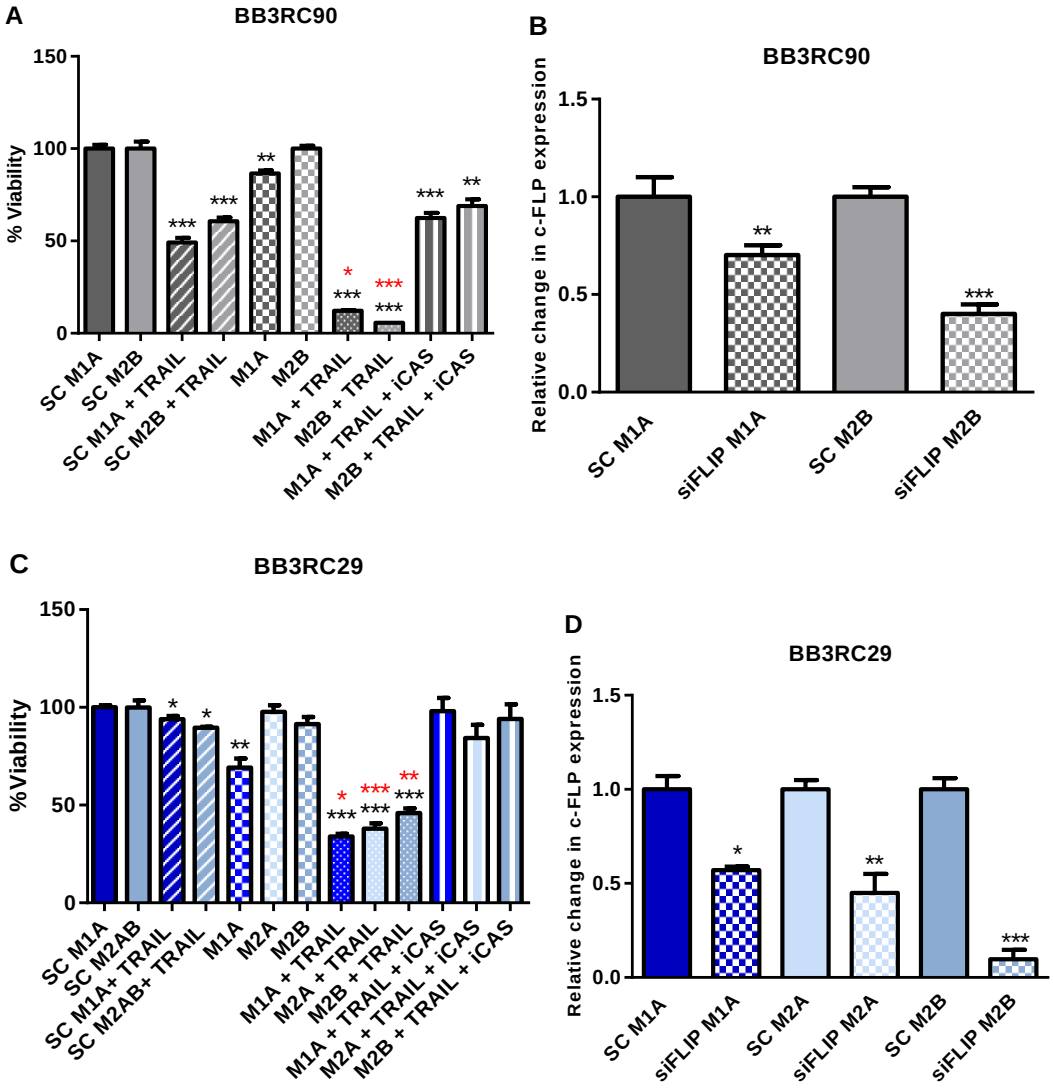

Figure 5.16. Relative efficiency of two different transfection methods and two c-FLIP siRNA constructs. BB3RC29 and BB3RC90 were transfected using the methods described in Table 5.5 and viability was assessed using cell titre blue. Cells were treated with 100 ng/ml of TRAIL and 10 ng/ml of caspase inhibitor (iCAS) at 0h and 10 ng/ml 1hour prior TRAIL. | **C**. qPCR for c-FLIP gene expression after treaments in A and B. | * - significant vs SC (p) < 0.05; ** (p) < 0.005; *** (p) < 0.0005; t-test. * - red asterisks highlight combination treatments (siFLIP + TRAIL) that are more than the sum of the respective individual treatments. * - an additional 20-35% loss of viability; **- an additional 35-50% loss in viability; ***- an additional 50-65% loss in viability.

5.2.4. siFLIP/TRAIL reduces breast cancer stem cells in primary metastatic cells

To investigate the effect of c-FLIP suppression on bCSCs, cells were plated in non-adherent conditions after the siRNA +/- TRAIL treatments detailed in section 5.2.4. In BB3RC29, TRAIL and siFLIP led to a reduction in viability of 58% in sphere number (Figure 5.17 A). In BB3RC90, inhibiting c-FLIP did significantly reduce the number of spheres, however, siFLIP significantly sensitised cells to TRAIL leading to a 98% reduction in viability (Figure 5.17 B). In BB3RC81 and BB3RC79 siFLIP led to a reduction of the spheres by 47% and 64%, respectively, and TRAIL significantly sensitised both to TRAIL eliminating all the spheres (Figure 5.17 C and D).

Overall, siFLIP sensitised bCSCs to TRAIL treatment in all the primary metastatic breast samples. The combined treatment had a synergetic effect of the individual treatments and not an additive effect of both (red asterisks in Figure 5.17).

In BB3RC29, BB3RC81 and BB3RC79 the tumoursphere assay was performed after the reverse transfection with siRNA(A) method, while BB3RC90 was after using fast-forward transfection with the smartpool. Since reverse transfection may give some toxicity to the cells it is likely that cells were more susceptible to TRAIL and maybe explain why BB3RC90 does not show any cytotoxicity after c-FLIP suppression.

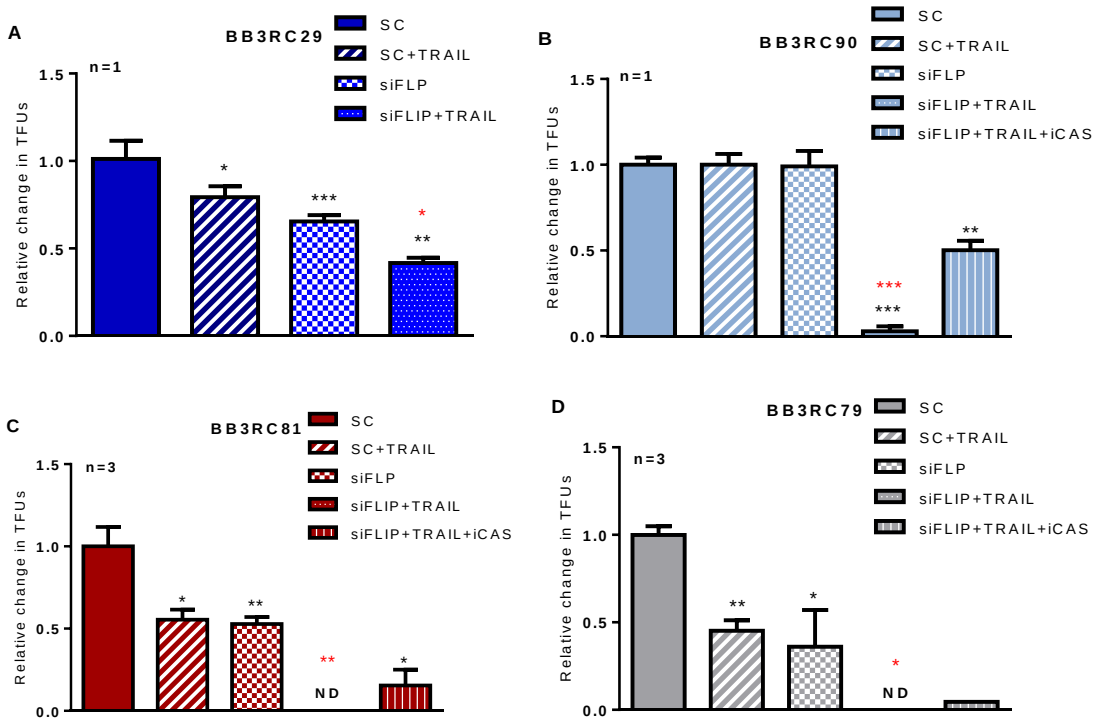

Figure 5.17. siRNA-mediated suppression of the c-FLIP gene sensitises bCSCs (Tumoursphere forming Units- TFUs) to TRAIL treatment in four metastatic cell lines. |A- D. Tumoursphere assay: Relative change in TFUs after TRAIL, siFLIP, iCAS (caspase inhibitor) and siFLIP/TRAIL pre-treatments on adherent conditions. Treatments were normalised to the scrambled untreated control. C-FLIP was suppressed by siRNA for 48 hours prior TRAIL addition. Cells were treated with 100 ng/ml TRAIL for 18 hours and with 10 ng/ml of iCAS at 0 hours and 1 hour prior TRAIL). | Bars represent mean +/- SD for n=1 experiments and mean +/- SEM for n=3 experiments. * - significant vs SC (p) < 0.05, ** (p) < 0.005; ***(p)<0.0005; t-test. * - red asterisks highlight combination treatments (siFLIP + TRAIL) that are more than the sum of the respective individual treatments - siFLIP resulted in a sensitisation of cells to TRAIL * - an additional 20-35% decrease of TFUs; **- an additional 35-50% decrease of TFUs; ***- an additional 50-65% decrease in TFUs.

5.2.5. OH14/TRAIL has a more modest effect on viability in primary metastatic cells

Having demonstrated that a transient suppression of c-FLIP sensitises breast metastatic cells to TRAIL, cells were treated with OH14 to investigate whether treatments lead to a similar result. Seven primary metastatic breast samples: BB3RC29, BB3RC90, BB3RC94, BB3RC81, BB3RC79, BB3RC96 and BB3RC68 were treated with 100 µM and 10 µM of OH14 1 hour prior to addition of 100 ng/ml of TRAIL. These concentrations were used because they were efficient at sensitising bCSCs to TRAIL treatment in cell lines. After 18 hours of TRAIL treatment, viability was assessed by cell titre blue assay. 100 µM of OH14 sensitised the bulk population to TRAIL in 5 out of 7 samples and 10 µM in 3 out of 6 samples (Figure 5.18 A-H).

BB3RC81 showed the best result for the combined therapy with a sensitisation of 19.71% at 100 µM and BB3RC96 a sensitisation of 7.38% at 10 µM (Figure 5.18 C and E).

Therefore, siFLIP is demonstrated to be more efficient at sensitising bulk population to TRAIL. This is probably because siFLIP genetically suppresses the total levels of c-FLIP levels within the cells while OH14 is a competitive inhibitor leaving some c-FLIP still active inside the cells.

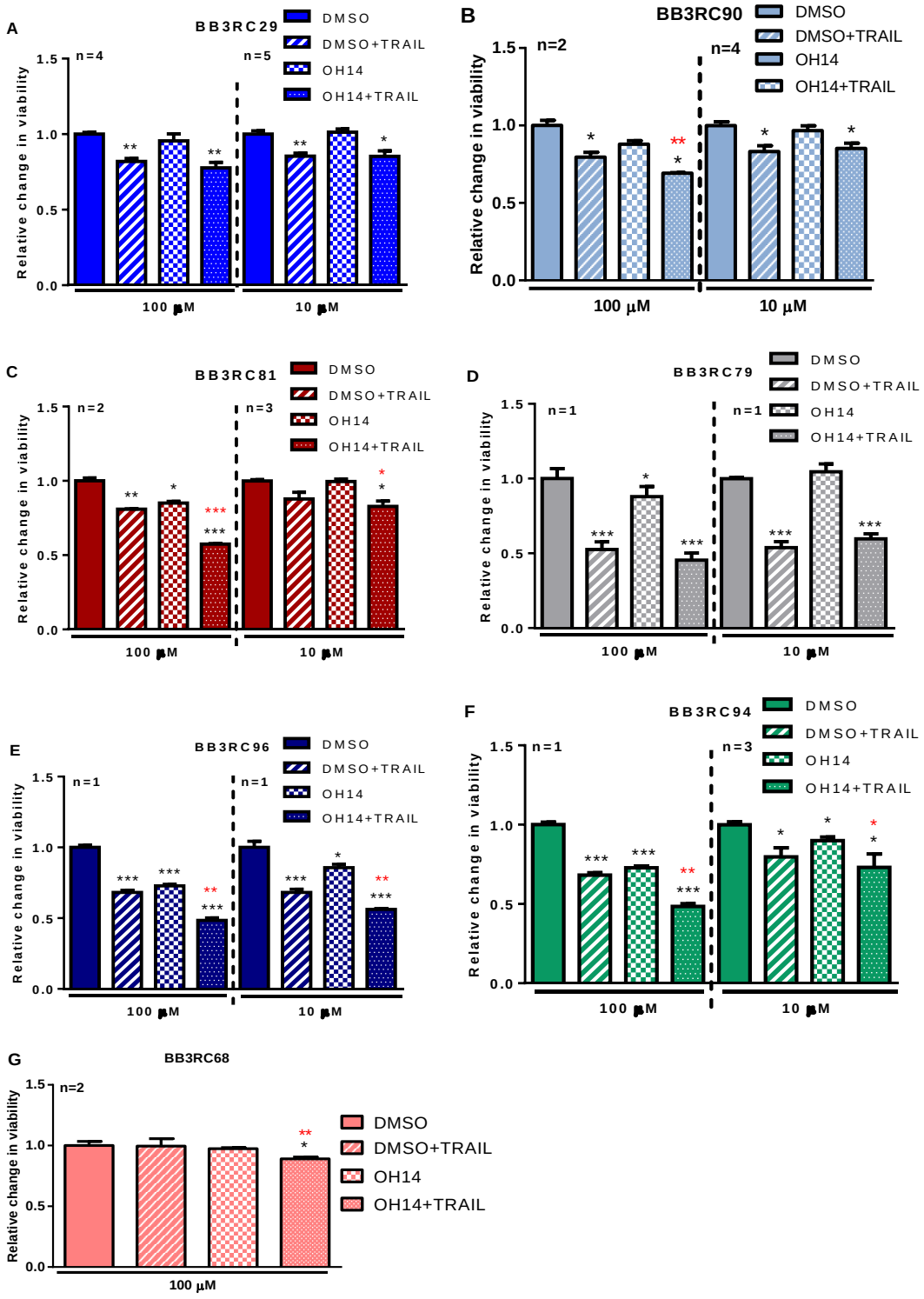

Figure 5.18. iFLIP-OH14/TRAIL does not affect the viability in primary metastatic cells. | A.- G. Viability (cell titre blue assay) following DMSO, TRAIL, OH14 and OH14/TRAIL treatment normalised to the DMSO control set as 1. Cells were treated with 100 ng/ml TRAIL for 18 hours and with 100 µM and 10 µM of OH14 1 hour prior TRAIL. | Bars represent mean +/- SD for experiments with n=1 and n=2 and +/- SEM for experiments with at least n=3. * - significant vs DMSO (p) < 0.05, ** (p) < 0.005; *** (p) < 0.005; t-test. | * - red asterisks highlight combination treatments (OH14 + TRAIL) that are more than the sum of the respective individual treatments - OH14 resulted in a sensitisation of cells to TRAIL. * -sensitisation < 5%, ** - sensitisation between 5% and 15%; *** - sensitisation between 15% and 20%.

5.2.6. OH14/TRAIL reduces bCSCs in primary metastatic cells

Suppressing c-FLIP using OH14 in combination with TRAIL treatment had a small but detectable sensitisation effect on the bulk population of primary metastatic breast cancer cells. Given that TRAIL alone decreased bCSCs in 5 out of 7 samples (Figure 5.6 A), the aim here was to either further increase this sensitivity or to sensitise the resistant cells to TRAIL with the addition of OH14. Cells were pre-treated with 100 µM and 10 µM of OH14 1h before TRAIL in adherent conditions (2D) or treated directly in non-adherent conditions (3D) and cancer stem cell activity assessed.

Pre-treating cells in 2D and using 100 µM of OH14 led to a sensitisation to TRAIL in all samples. Using 10 µM of OH14 sensitised bCSCs in 3 out of 5 samples tested: BB3R3RC94, BB3RC29 and BB3RC90 (Figure 5.17-19). However, 10 µM of OH14 is more effective than 100 µM at sensitising bCSCs to TRAIL. Therefore, OH14 and TRAIL are a good combination at eliminating bCSCs in a cohort of primary metastatic tissues.

Treating cells directly in 3D with 100 µM of OH14 sensitised cells to 20 ng/ml of TRAIL in BB3RC29, BB3RC71, BB3RC79 and BB3RC81. Additionally, using 100 ng/ml of TRAIL did not have a synergetic effect since cells were already sensitive at that concentration. Using 10 µM of OH14 only sensitised BB3RC71 and BB3RC79 cells to 20 ng/ml of TRAIL (Figure 5.20).

In conclusion, despite pre-treatment of adherent cells resulting in a comparatively higher proportion of tumour samples responding, the fact that less spheres remained after treatment in 3D suggests that, TRAIL and OH14 may be more effective at targeting bCSCs circulating in the blood stream than in the solid tumour.

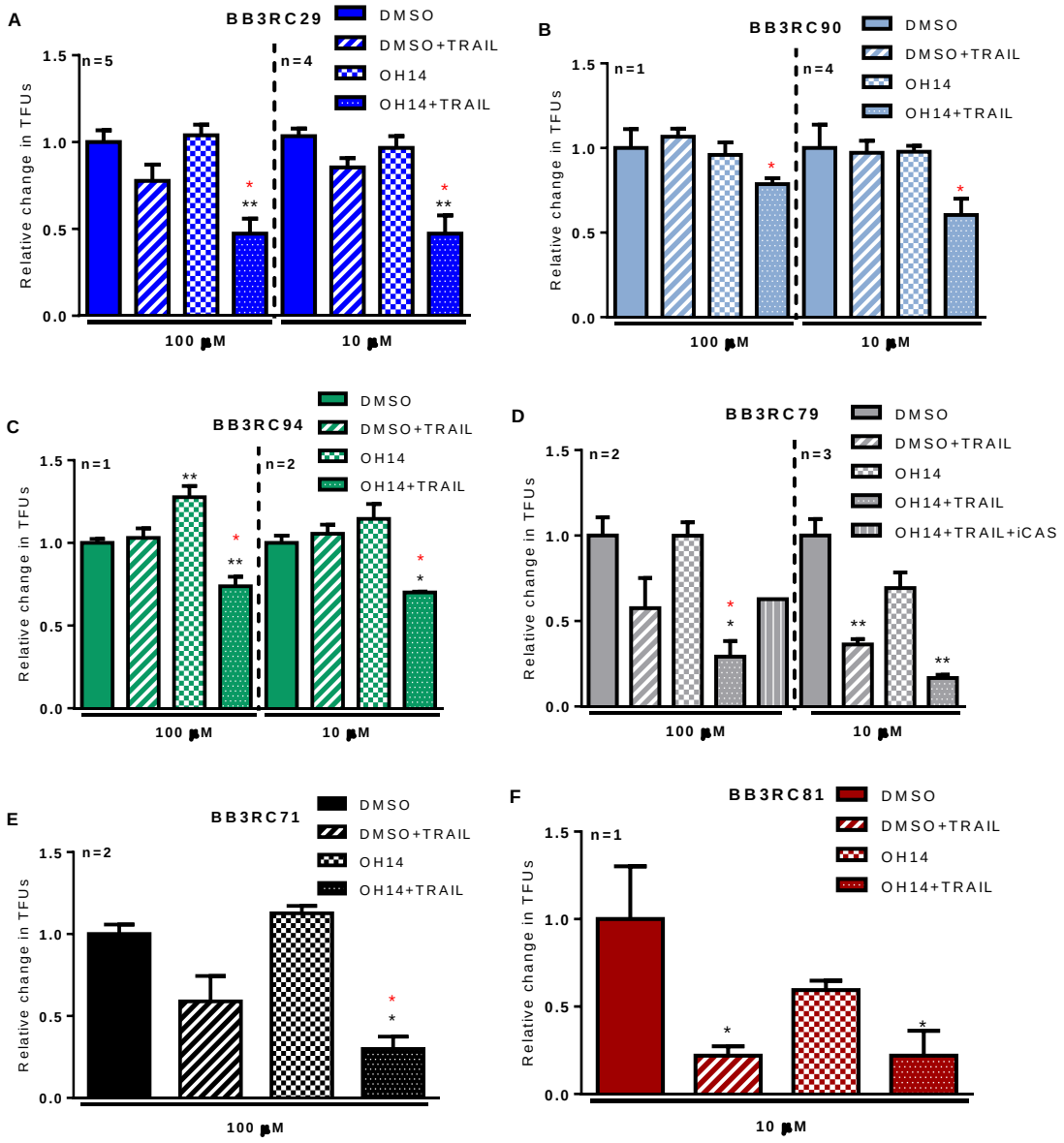

Figure 5.19. OH14 sensitises bCSCs in metastatic tumour cells from pleural effusions to TRAIL when pre-treated in adherent culture (2D). | A-F. Cells were pre-treated in 2D with TRAIL, OH14, and caspase inhibitor (iCAS, FMK-ZVAD, 20 ng/ml 1 hour prior TRAIL) and then cells were plated into non-adherent conditions for tumoursphere assay. Treatment was normalised to DMSO control. Cells were treated in adherent culture with 100 ng/ml TRAIL for 18 hours and with 100 µM or 10 µM OH14 1 hour prior TRAIL. Tumourspheres from at least three replicate wells per condition were counted following 7-10 days in culture. |Bars represent mean +/- SD for experiments with n=1 and n=2 and +/- SEM for experiments with more than n=3. | * - significant vs DMSO (p) < 0.05, ** (p) < 0.005; t-test. * - red asterisks highlight combination treatments (OH14 + TRAIL) that are more than the sum of the respective individual treatments.* - siFLIP resulted in a sensitisation of cells to TRAIL; siFLIP + TRAIL is not an additive effect of the single treatments.

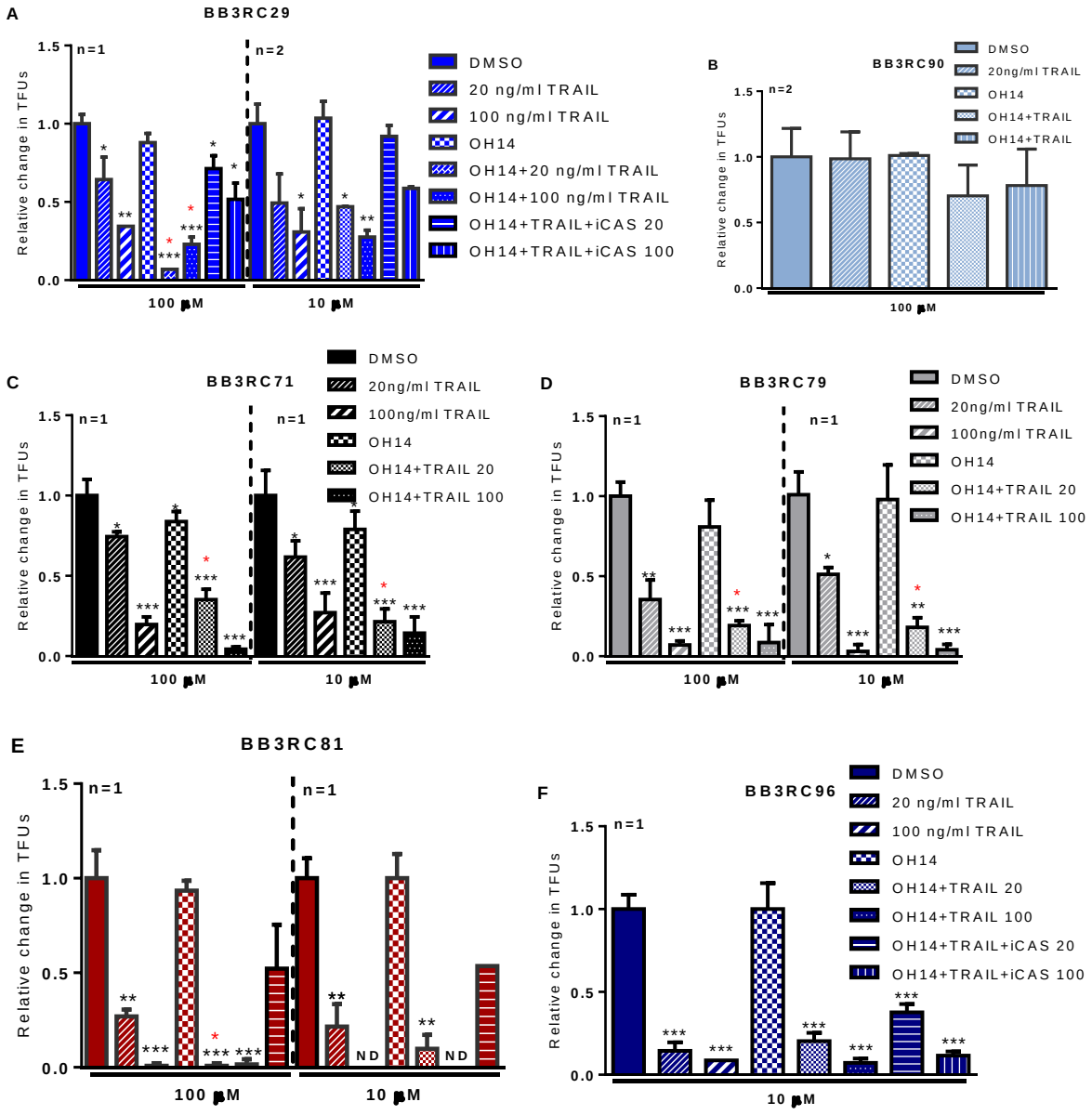

Figure 5.20. OH14 sensitises bCSCs in metastatic tumour cells from pleural effusions to TRAIL when treated in non-adherent culture (3D). | A-F. Relative change in Tumourspehre Forming Units (TFUs) after TRAIL, OH14 and caspase inhibitor (iCAS, FMK-ZVAD, 20 ng/ml 1 hour prior TRAIL). Single cells were plated into non-adhrent conditions for tumoursphere assay (Passage 1). Treatment was normalised to DMSO control. Cells were seeded at a density of 40000 cells/well and treated with 20 ng/ml and 100 ng/ml of TRAIL for 18 hours and with 100 µM or 10 µM of OH14 1 hour prior TRAIL. Tumourspheres from at least three replicate wells per condition were counted following 7-10 days of culture. | Bars represent mean +/- SEM. * - significant vs DMSO (p) < 0.05, **(p) < 0.005; ***(p) < 0.0005; t-test. * - red asterisks highlight combination treatments (siFLIP + TRAIL) that are more than the sum of the respective individual treatments.

5.2.7. OH14/TRAIL reduces the stem cell marker ALDH1 in primary metastatic cells

It was demonstrated that OH14 sensitises bCSCs to TRAIL through depletion and in some instances ablation of functional tumourspheres (Figure 5.19 and 5.20). To confirm this result, cells were stained for Aldehyde dehydrogenase (ALDH) activity after 100ng /ml of TRAIL +/- 10 μM of OH14. ALDH isozymes metabolize several different intracellular aldehydes and can therefore provide resistance to alkylating chemicals such as cyclophosphamide. High ALDH1 activities have been reported in CSCs from many cancers including those found in breast, lung, liver, colon, pancreatic, ovarian, head and neck and prostate (Luo *et al*., 2012). In breast cancer, elevated ALDH activity was mainly found in CSC of HER2 subtype and basal/epithelial breast cancer cell lines (Ricardo *et al*., 2011). In BB3RC29 and BB3RC71, both cell lines exhibited significant reductions in the relative proportion of ALDH +ve cells in the surviving populations following TRAIL. Additionally, OH14 resulted in a sensitisation of ALDH positive cell to TRAIL (Figure 5.21 B). This result corroborated the tumoursphere assay followed by the treatments in bulk population using the same conditions (Figure 5.21 A). Moreover, BB3RC71 had a higher level of ALDH positive cells (34.91%) than BB3RC29 (17.96%) probably due to the expression of HER2 (Figure 5.21 B). BB3RC71 belongs to Luminal B subtype and BB3RC29 belongs to Luminal A breast cancer.

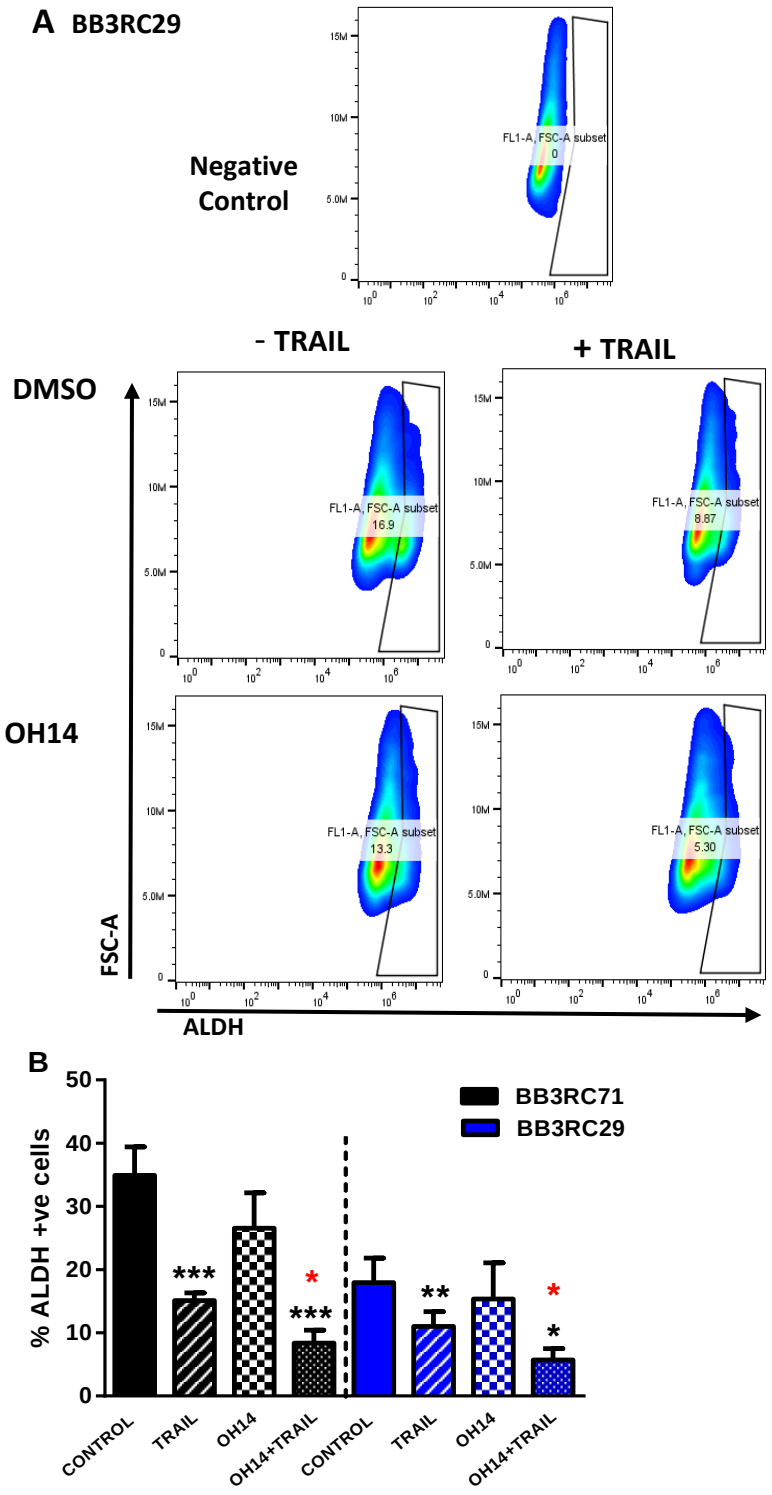

Figure 5.21. TRAIL and OH14 treatment decreases ALDH1 expression. Cells were treated with 100 ng/ml TRAIL for 18 hours and with 10 µM of OH14 1 hour prior TRAIL. | **A.** ALDH expression in cells was measured by flow cytometry in BB3RC29. Data represents one of three independent experiments. | **B.** Percentage of ALDH +ve cells in BB3RC29 and BB3RC71 cells after treatments. Data represents two independent experiments.| Bars stood for mean +/- SD. * - significant vs DMSO (p) <0.05. ** (p) <0.005; t-test. * - red asterisks highlight combination treatments (OH14 + TRAIL) that are more than the sum of the respective individual treatments - OH14 resulted in a sensitisation of bCSCs to TRAIL.

5.2.8. Investigating c-FLIP impact in cancer cells and normal cells

In chapter 4, it was demonstrated that suppressing c-FLIP affects HMECs viability and MaSCs and sensitises to TRAIL. However, it is important to compare c-FLIP suppression (siFLIP and OH14) in normal and cancer cells. Suppressing c-FLIP using siRNA (M1 and M2), M1 led to a similar toxicity in normal cells and cancer cells with 24.0% and 28.0% increase cell death, respectively. M2 also led to a similar toxicity in normal and cancer cells with 8.8% and 2.7% increase in cell death, respectively (Figure 5.22 A). As mentioned in section 5.2.3., the method of transfection M1 decreases cell viability by either partially suppressing c-FLIP or by causing off-target effects to cells. Therefore, if we only consider method M2, siFLIP has a minimal effect on normal and cancer cells (9% and 3%, respectively).

Suppressing c-FLIP using 100 µM OH14 increased death by 42.2% in normal cells and 12.1% in cancer cells. Additionally, using 10 µM increased death in normal cells and cancer cells by 17.7% and 3.7%, respectively although this effect was non-significant (Figure 5.22 A).

Thus, despite 100 µM OH14 having demonstrated a better result at sensitising cancer cells to TRAIL, this concentration should not be used due to its extensive toxicity to normal cells.

Furthermore, using 10 µM of OH14 in a mammosphere assay led to a similar decrease of MaSCs in 2D and 3D by 16.5% and 25.0%, respectively. In cancer cells 100 µM led to a decrease of spheres by 12.4% in 2D and 3.9% in 3D. Additionally, 10 µM only decreased spheres in 3D with 10.6% reduction (Figure 5.22 B). Despite OH14 having a higher effect on MaSCs than CSCs this is only in theory since MaSCs are unlikely to be circulating as a single cell in the body.

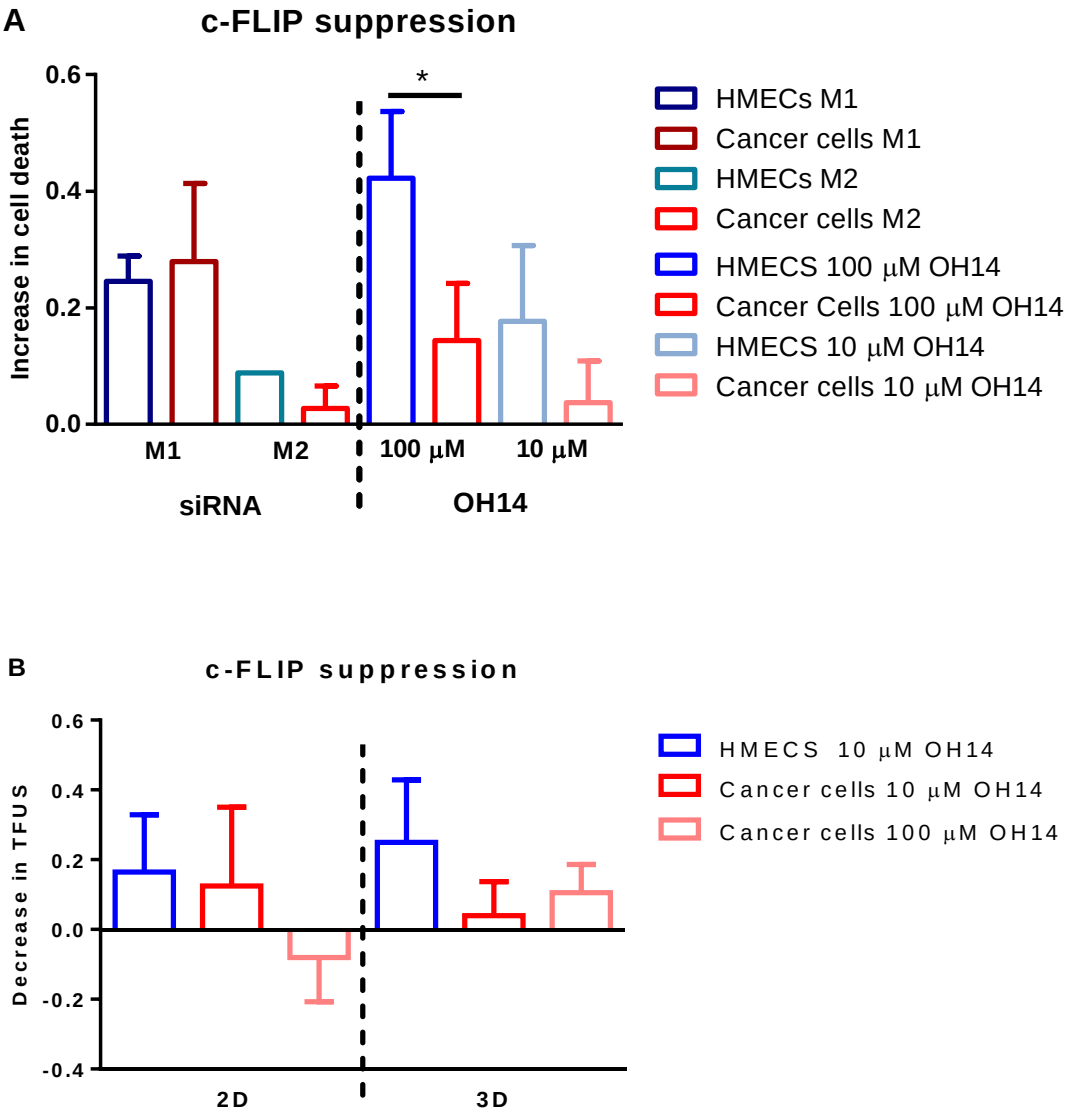

Figure 5.22. c-FLIP suppression in HMECs and metastatic cancer cells (BB3RCs). Data represents relative number of Tumousphere forming units (TFUs) normalised to untreated controls. Cells were treated with 100 ng/ml TRAIL for 18 hours and with 100 µM and 10 µM of OH14 1hour prior TRAIL. | **A.** Increase in cell death after c-FLIP suppresion in HMECs and Cancer cells in bulk population | **B.** HMECs vs cancer cells in tumoursphere culture conditions. * (p) <0.05; t-test.

5.3. Discussion

The main goal of this study was to test the effects of TRAIL treatment as a monotherapy and in conjunction with c-FLIP inhibition in primary breast cancer tissues, with a specific focus on the potential specificity for this combination for breast cancer stem cells. TRAIL had a significant effect on bCSCs on 4 out of 30 samples tested. Trying to stratify these samples by histological or molecular subtype did not result in any correlation. However, analysis based on endocrine treatments showed that 3 out of the 4 TRAIL responders have received endocrine treatments in the past (Figure 5.6). An analysis of 7 primary metastatic breast tumours, showed that TRAIL did not have any effect in any endocrine-naïve samples. Importantly, TRAIL decreased bCSCs in 3 out of 4 samples that have received endocrine treatments before (Figure 5.11 A). Overall, the bCSCs from 82% (9/11) endocrine resistant samples responded to TRAIL while only 10% (1/31) treatment naive samples significantly responded (Figure 5.12). These results demonstrate, in a cohort of patients currently with poor prognosis, the specific targeting of CSCs following acquisition of resistance supporting future clinical investigations into the use of TRAIL receptor agonists to improve the long-term survival of patients who relapse on endocrine therapy. Additionally, TRAIL has shown to be more effective in decreasing bCSCs when cells are treated in 3D compared to when treated in 2D. This could potentially mean that TRAIL is more efficient targeting bCSCs circulating tumour cells rather than bCSCs in the whole tumour or also more efficient at targeting cells undergoing anoikis resistance, which is a property of bCSCs.

To further evaluate TRAIL efficiency in endocrine-resistant tumours, PDX models were generated to investigate TRAIL efficiency *in vivo*. In the first model, the resistance to tamoxifen was acquired *in vivo* and TRAIL administration did not have an effect at inhibiting tumour growth in the estradiol-dependent control group but did lead to a significant reduction of tumour size in the tamoxifen-resistant tumours (Figure 5.13 A and B). Additionally, the tumours from the tamoxifen-naïve group were harvested and used to investigate stem cell activity *ex vivo* and TRAIL-treated samples showed a higher proportion of bCSCs (Figure 5.13 C and D). This agrees with studies that

demonstrated for endocrine therapies, such as tamoxifen and fulvestrant, in ER +ve patient samples and in early and metastatic, PDXs increases in bCSCs proportions within the tumours. This suggests that endocrine therapies do not target bCSCs, which might explain how residual endocrine-resistant cells are responsible for the relapse of ER +ve tumours (O'Brien *et al*., 2011; Simões *et al*., 2015). Tumours from the TAMR-resistant model were also harvested and TRAIL was able to compromise bCSCs ability to self-renew (Figure 5.13 E and F). To further evaluate TRAIL efficiency *in vivo,* an anastrozole-resistant sample was transplanted into mice. TRAIL caused a significant reduction in tumour volume and led to a reduction of bCSCs *ex vivo* (Figure 5.14). This finding confirmed our hypothesis since we have found a group of patients that may benefit from TRAIL as a monotherapy. It is well known that TRAIL has failed numerous clinical trials with patients showing no improvement. However, none of these clinical trials have preselected patients based on TRAIL- sensitivity in ER +ve tumours. In this study, we show evidence that patients who acquire resistance to endocrine therapies such as tamoxifen or aromatase inhibitors may benefit from TRAIL alone.

It is also of note therefore that the metastatic samples corresponding to TNBC have shown a particular susceptibility to TRAIL (Figure 5.8). These findings are in accordance with a study, which shows that bCSCs from basal-like breast cancer cell lines were sensitive to the TRAIL DR5 receptor agonist TRA8 (Londoño-Joshi *et al.,* 2012). Moreover, it has been reported that bCSCs are sensitive to TRAIL due to the reduced cytoplasmic location of c-FLIP. It is proposed that in order to inhibit the extrinsic apoptosis pathway, c-FLIP must be available in the cytoplasm in order to form a complex with DISC components and therefore determinate caspase-8 recruitment to the complex (French *et al*., 2016). It would be important to analyse c-FLIP levels in all the samples that have received TRAIL treatment. However, after testing and optimising 20 antibodies for c-FLIP in our laboratory by immunohistochemistry, none have proved to be specific for c-FLIP (data not shown). We hypothesised a correlation between TRAIL sensitivity and low levels of c-FLIP protein or RNA. The acquisition of TRAIL sensitivity by endocrine-resistant cell lines and clinical samples was attributed to a reduction in

the intra-cellular levels of the TRAIL pathway inhibitor, c-FLIP, and a concomitant increase in the Jnk-mediated phosphorylation of E3 ubiquitin ligase, ITCH (p-ITCH), previously shown to target c-FLIP for proteosomal degradation. Restoration of c-FLIP protein levels in TAMR cells through Jnk inhibition lead to the reacquisition of TRAIL resistance in TAMR cells, illustrating a dependence of TAMR TRAIL-sensitivity on Jnk-mediated degradation of c-FLIP (Piggott *et al.,* 2018). It would be interesting to determine whether the endocrine-resistant samples that have responded to TRAIL have low levels of c-FLIP and the TNBC samples have low levels of cytoplasmic c-FLIP. A clinical trial investigating TRAIL administration in patients with TNBC has failed (Forero-Torres *et al*., 2015). However, pre-selection of patients based on c-FLIP levels within this group would be crucial. Perhaps recurrent ER -ve tumours that have been previously diagnosed as ER +ve and treated with hormonal treatments could then benefit from TRAIL alone. Since we only had a few representative samples from each of these subtypes, a robust statistical analysis for TRAIL treatment was not possible.

Consistent with previous work in cell lines (Piggott *et al*., 2011) the combined treatment of siFLIP/TRAIL led to a reduction in the viability in three out of four metastatic primary breast samples (Figure 5.15). In addition, siFLIP sensitised bCSCs to TRAIL in all samples and importantly in a TRAIL-resistant and endocrine-naïve cell line, BB3RC90 (Figure 5.16 B). Additionally, siFLIP and TRAIL resulted in a complete ablation of bCSCs in a metastatic endocrine resistant breast cancer primary cell line and in a metastatic primary TNBC (Figure 5.17 C and D). It has been reported that cytoplasmic c-FLIP levels were particularly low in anoikis-resistant cells, which could clarify why c-FLIP inhibition and TRAIL treatment results in the complete ablation of bCSCs (French *et al*., 2015).

Suppressing c-FLIP using 100 µM and 10 µM of OH14 led to a reduced sensitisation of bulk cells to TRAIL compared to siFLIP (Figure 5.18 and Figure 5.15). Investigating c-FLIP levels in the cytoplasm/nucleus after treatment with OH14 in order to investigate a correlation between c-FLIP localisation and TRAIL sensitivity may help to understand the relative inefficiency of OH14 in these conditions.

Furthermore, OH14 has been shown to be more efficient at sensitising bCSCs to TRAIL compared to the bulk population (Figure 5.19 and 5.20). This concurs with the study that shows cytoplasmic c-FLIP levels were particularly low in anoikis-resistant cells explaining why the double treatment is more effective for bCSCs than the bulk population (Piggott *et al*., 2011; French *et al.,* 2015).

Additionally, our lab has seen that OH14 treatment does not change cytoplasmic levels of c-FLIP in MCF-7 cells (data not shown). A recent study proposes that the amount of the unbound c-FLIP long form available inside the cell can determine caspase-8 activity. Low levels of c-FLIP would result in cell death and high levels of c-FLIP would inhibit apoptosis (Hughes *et al.,* 2016). This achievement may explain why siFLIP is more efficient than OH14 at sensitising cells to TRAIL. In regards to OH14-mediated suppression, c-FLIP can no longer promote its apoptotic activity at the DISC complex and therefore c-FLIP is potentially available inside the cell to modulate other signalling pathways.

Finally, it is important to analyse the effects of c-FLIP suppression in normal and cancer cells. There is literature supporting that siFLIP does not display any toxicity in the MCF-10As (Piggott *et al*., 2011) but other study demonstrated that siFLIP is detrimental to the same cell line (Yerbes *et al.,* 2011). In chapter 4 and 5, we have shown that siFLIP displays a similar toxicity to normal or cancer cells using siRNA. However, 100 µM of OH14 was significantly more detrimental for normal cells rather than cancer cells (Figure 5.22). This toxicity to normal cells was hypothesised by drug off-target effects or by cytotoxicity, the caspase inhibitor was able to rescue part of the caspase-mediated killing. HMECs may not have been the best model to study drug mechanisms in normal cells since it lacks other components from the mammary gland, such as the stroma. A better model, for example breast samples from mastectomies, may be best placed to evaluate the mechanisms of c-FLIP inhibition in normal cells.

Overall, TRAIL could be used as a single agent for tumours that have acquired resistance to endocrine therapies such as tamoxifen and anastrozole. c-FLIP suppression results in a sensitisation of

epithelial and bCSCs to TRAIL, but there may be issues regarding cancer cell specificity when targeting c-FLIP.

CHAPTER 6

The Role of Tumour Microenvironment in TRAIL Response

6. The Role of Tumour Microenvironment in TRAIL Response

6.1. Introduction

Fibroblasts have a dual role in controlling normal and malignant development: fibroblasts can hamper neoplastic growth in normal tissues, whereas in cancer they can potentiate invasion and tumour growth (Kuperwasser *et al*., 2004; Schauer *et al*., 2011), EMT, invasion (Bhowmick *et al*., 2004), and metastasis (Straussman *et al*., 2012). Furthermore, cancer associated fibroblasts (CAFs) have a role in constructing the extracellular matrix and metabolic and immune reprogramming of the tumour microenvironment with an effect on adaptive resistance to drug responses (Kasani *et al*., 2015, Kalluri, 2016).

There are studies that have demonstrated a relationship between a mesenchymal-like phenotype and sensitivity to TRAIL (Rahman *et al*., 2009; Piggott *et al*., 2011; French *et al*., 2015). In addition, our laboratory has seen that soluble factors produced by MDA-MB-231-conditioned medium are capable of inducing upregulation of mesenchymal markers in MCF-7 cells and sensitise to TRAIL (Rhiannon French, unpublished data). whereas Wang and co-workers have reported an association between a resistance to TRAIL and EMT (Wang *et al*., 2014). Using a TRAIL-resistant breast cancer cell line, generated from the TRAIL-sensitive MDA-MB-231, Wang *et al*., demonstrated that TRAIL resistance induced EMT and invasiveness through deregulation of PTEN compared with the parental cell line (Wang *et al*., 2014). Additionally, reversion of EMT has been proposed as a novel strategy for TRAIL sensitisation. A study using a HDAC inhibitor led to angiogenesis, reversed EMT, attenuated metastasis, and sensitised TRAIL-resistant breast cancer MDA-MB-468 xenografts *in vivo* (Srivastava *et al*., 2010).

When epithelial cells commit to a mesenchymal phenotype, the process is designated as a complete EMT. Partial EMT can also exist, and this happens when one or more of the key characteristics of complete-EMT are not exhibited, such as loss of cell-cell contact. For example, during re-epithelialisation of cutaneous wounds, keratinocytes undergo several changes reminiscent of EMT

including loss of polarity, rearrangement of the actin cytoskeleton, alterations in cell-cell contacts, and breakdown of basement membrane; however, some intercellular junctions are kept and migrate as a cohesive cell sheet (Welch-Reardon *et al*., 2015). Recent studies in defining EMT as more of a "spectrum of phenotypes instead of a binary process" has driven an hypothesis that unlike during development, in which terminally differentiated epithelial and mesenchymal states exist, cancer cells could undergo more partial transitions to an incomplete mesenchymal phenotype. However, while several cancers may undergo only a partial transition, some cancers reflect a more complete phenotypic transition based on typical morphological and molecular features. For example, a rare population of cells expressing low levels of E-cadherin that underwent spontaneous full EMT without any exogenous induction from EMT-inducing transcription factors were converted to an epithelial state when located at the metastatic site (Jolly *et al.*, 2017).

These findings, raise intriguing questions about the complex relationship between mesenchymal phenotype/EMT and TRAIL sensitivity of breast tumours and whether an EMT induced by CAFs would result in TRAIL sensitisation or resistance. This chapter will study the role of the microenvironment on TRAIL responses, specifically, it will test whether: fibroblasts induce mesenchymal-like phenotype changes in luminal cells and whether fibroblasts might or might not sensitise the epithelial tumour population to TRAIL.

6.2. Results

6.2.1. Co-culture of cancer cells with fibroblasts sensitises to TRAIL

To explore how the microenvironment can modulate TRAIL responses, fibroblasts were separated from the epithelial population of a range of breast biopsy/surgical samples (Table 6.1). We aimed to test the direct effect of CAFs on TRAIL response. For this purpose, CAFs were co-cultured with the resistant breast cancer cell line MCF-7 (Piggott *et al.,* 2011; French *et al.,* 2015) to test whether CAFs from different tumour types can sensitise the MCF-7 to TRAIL. Five different CAF

cultures (CAF 168, 148, 209, 207 and 253) were used in co-culture experiments. Fibroblasts were cultured on 96 well-plates for four days until reaching 90-100% confluency. Pure fibroblast monolayer was confirmed using a microscope. Then, 80000 or 1600000 of MCF-7 cells expressing GFP were plated on top of the fibroblasts. Epithelial cells were in contact with fibroblasts for 24h and co-cultures were treated with 20 ng/ml of TRAIL for 18h. Cells expressing GFP were quantified using flow cytometry to efficiently separate epithelial cells from fibroblasts. GFP positivity was checked prior to the assay to confirm a homogeneous epithelial (MCF-7) population expressing GFP (98% for GFP +ve cells similar to the result in Chapter 3).

Overall, all five of the CAFs tested led to a sensitisation of the MCF-7 cells to TRAIL (Figure 6.1). Fewer MCF-7 cells in the co-culture (80000) resulted in a higher sensitivity. The fibroblast sample that led to the highest sensitisation was the CAF 253 derived from a tamoxifen-resistant sample, 253 (red bar). This experiment showed a sensitisation to TRAIL by direct contact with fibroblasts.

Table 6.1. Histological and molecular characteristics of the samples used to collect the fibroblasts. Histological features, Grade, Receptor (ER and HER2) status and respective responses to 100 ng/ml of TRAIL in tumoursphere conditions.

CAF	Histology	Grade	Receptor	Response to TRAIL %
98	Benign Intralobular Microcalcification			-
213	Fibroadenoma			-
214	Fibroadenoma			25
61	Invasive Lobular	2	ER+HER2-	-
148	Invasive Mucinous	3	ER+HER2+	-
153	Invasive Ductal	1	ER+HER2+	
168	Invasive Lobular + LCIS	2	ER+HER2-	-
206	Invasive Lobular	2	ER+	-
207	Invasive Ductal + DCIS	3	ER+HER2-	32
209	Invasive Ductal	2	ER+HER2-	0
253	Invasive Ductal + DCIS	2	ER+HER2+	64
89	Invasive Ductal + DCIS high grade	3	ER-HER2+	-
105	Invasive Ductal + DCIS high grade	2	ER+HER2-	-

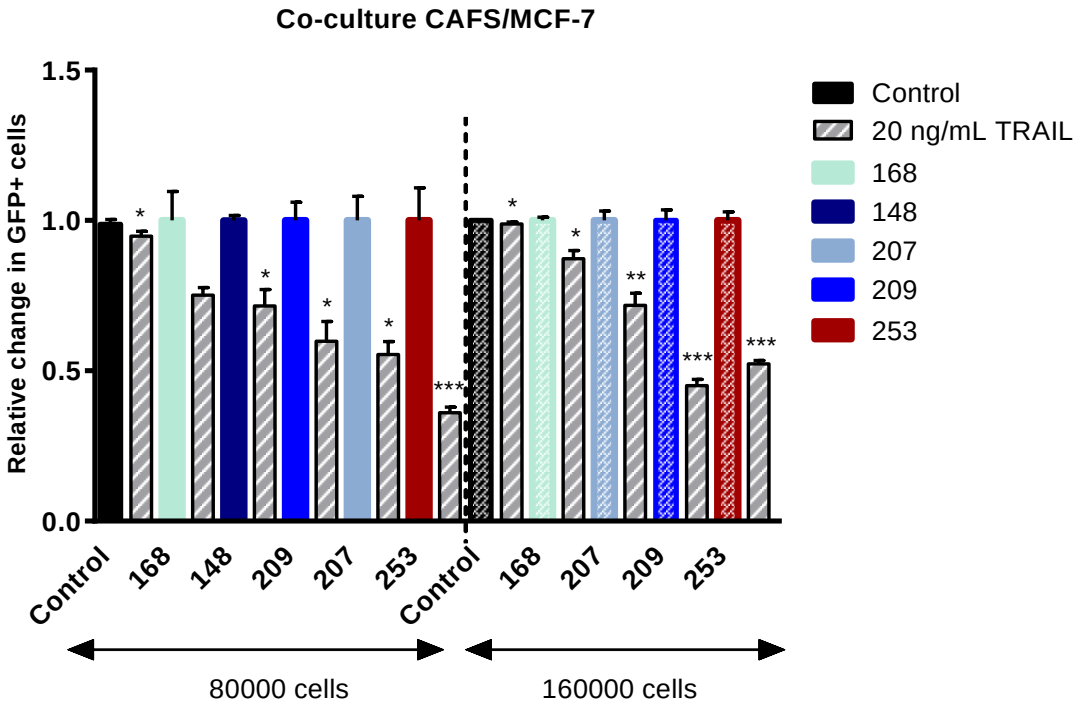

Figure 6.1. Co-culture of cancer cells with fibroblasts sensitises to TRAIL: *relative change in MCF-7 GFP +ve cells (flow cytometry) in co-culture with different CAFs following TRAIL treatment normalised to the untreated control.* On day 1, 800000 fibroblasts were plated in 6-well plates for 4 days until reaching 90%-100% of confluency. On day 4, 80000/1600000 of GFP +ve MCF-7 cells were cultured on top of the fibroblasts. Cells were left in co-culture for 24 hours prior 20 ng/mL of TRAIL treatment. After 18 hours, GFP +ve MCF-7 cells were analysed by flow cytometry. Wells with MCF-7 +/- TRAIL were used as controls to measure TRAIL response in the absence of fibroblasts. TRAIL treatments were normalised to the co-culture control (168, 148, 207, 209, 253). Bars represent mean +/- SD of two experiments with three internal replicates. and p-value (p) - significant vs untreated untreated control (calculated using t-test). *(p) <0.05; **(p)<0.005; ***(p)<0.0005; t-test.

6.2.2. Fibroblast-conditioned medium increases cell viability in primary metastatic epithelial cells

Previously, it was seen that direct contact of CAFs and MCF-7s resulted in an increase in the sensitivity of these cells to TRAIL. However, it is important to test whether this might be due to soluble factors released by fibroblasts. We wanted to investigate whether fibroblast-conditioned medium (CM) could result in a similar sensitisation as the co-cultures.

Firstly, we investigated CM treatment alone in different cell lines. Confluent fibroblasts were incubated with fresh medium for 24h to generate CM. CM was generated from three non-cancer-associated fibroblasts or normal fibroblasts (NFs): 98, 214 and 213; seven cancer-associated fibroblasts: 61, 148, 153, 168, 206, 207 and 209 and one cancer-associated fibroblast derived from a tamoxifen-resistant sample, 253. Each CM was then incubated with MCF-7 cells or three primary metastatic cell lines BB3RC90, BB3RC29 and BB3RC81 for 24 hours and viability determined by a cell titre blue assay (Figure 6.2) In MCF-7 cultures all the fibroblasts increased viability except fibroblast 214 (Figure 6.2 A). In BB3RC81, CM from fibroblasts 214, 148, 168,253, 207 and 209 increased cell viability (Figure 6.2 B). In BB3RC29, fibroblasts 148, 168, 206, 61 and 253 increased viability (Figure 6.2 C). In BB3RC90, CAF 61, 206, 253, 209 (Figure 6.2 D) were able to increase metabolic activity.

Additionally, in order to determine whether CAFs having a stronger ability of increasing cell metabolic activity/viability compared to normal fibroblasts, the combined data from CAFs and normal fibroblasts were compared, to reveal that this indeed was the case (Figure 6.2 E). Moreover, we aimed to determine if the grade of the tumour of origin for each CAF sample correlated with its effect on metabolism/viability. Thus, by scoring each fibroblast sample according to grade: (benign tissue- score 0; fibroadenoma – score 1; grade 1 – score 2; grade 2 – score 3; grade 3 – score 4) we ranked fibroblasts versus relative viability. In MCF-7 and BB3RC81 cultures, (rs=0.577), the hypothesis must be rejected because significance levels were greater than 5% (rs< rs critical). In BB3RC29 (rs=0.605)

and BB3RC90 (rs= 0.618) cultures, grade can be correlated with the ability to increase cell metabolic activity with a confidence of 95%.

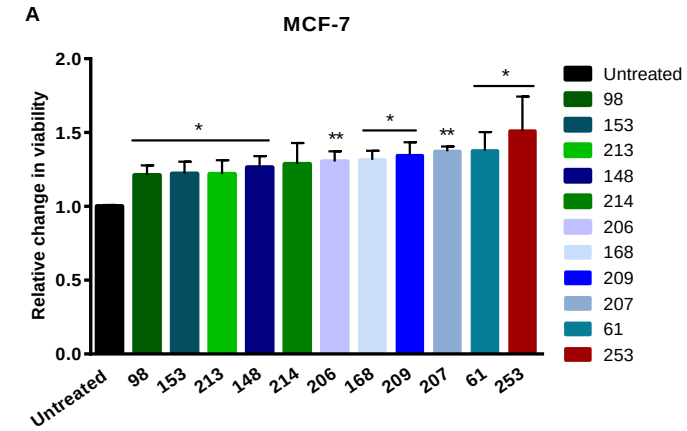
A
MCF-7
Relative change in viability
2.0
1.5
1.0
0.5
0.0
Untreated
98
153
213
148
214
206
168
209
207
61
253
*
**
*
**
*

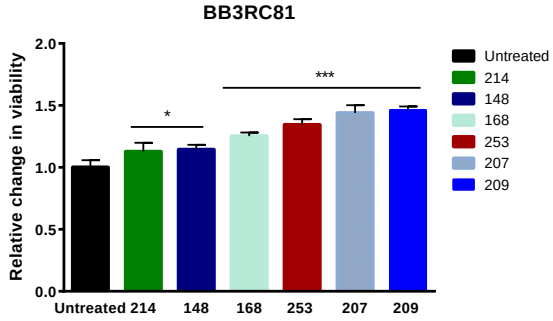
B
BB3RC81
Relative change in viability
2.0
1.5
1.0
0.5
0.0
Untreated
214
148
168
253
207
209
*
***

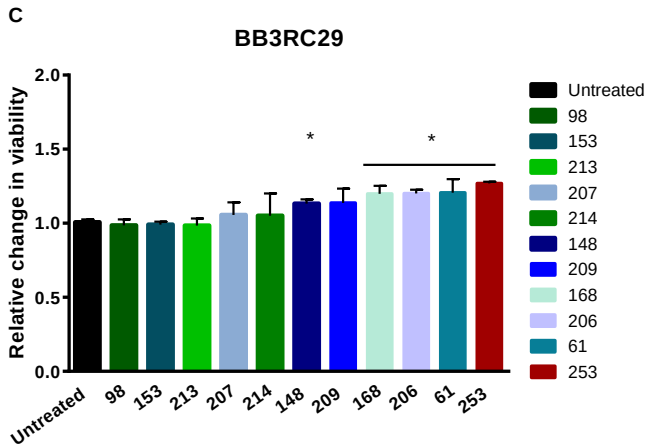
C
BB3RC29
Relative change in viability
2.0
1.5
1.0
0.5
0.0
Untreated
98
153
213
207
214
148
209
168
206
61
253
*
*

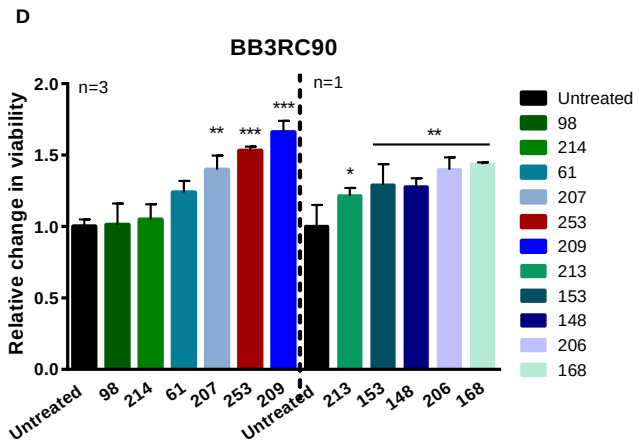
D
BB3RC90
n=3
n=1
Relative change in viability
2.0
1.5
1.0
0.5
0.0
Untreated
98
214
61
207
253
209
213
153
148
206
168
**
***
***
*
**

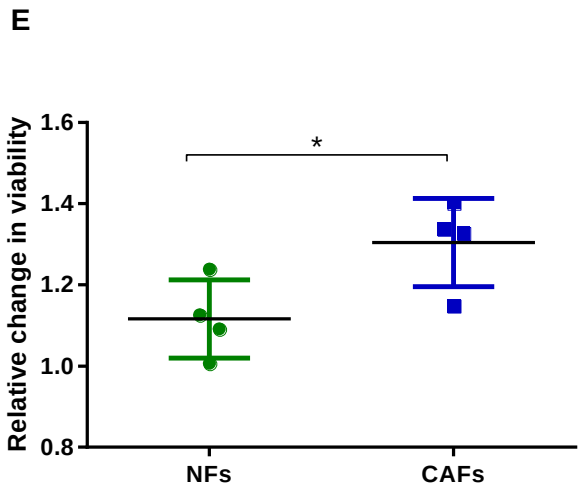

Figure 6.2. Fibroblast-conditioned medium increases cell viability in primary metastatic epithelial cells. *Relative change in viability (cell titre blue assay) following fibroblasts conditioned medium (CM) treatment normalised to the untreated control.* Confluent fibroblasts (98, 213, 153, 214, 61, 148, 168, 206, 207, 209 and 253) were incubated with fresh fibroblast medium for 24 hours to generate CM. Untreated control cells were cultured with only fibroblast medium and treated cells with CM for 24 hours. |**A. MCF-7**. Relative change in viability in MCF-7 cells after CM treatment. Graph is representative of n=3 with 4 internal replicates. | **B. BB3RC81** Relative change in viability in BB3RC81 cells after CM treatment. Graph represents n=1 with 3 internal replicates. | **C. BB3RC29** Graph represents n=2 with 3 internal replicates | **D. BB3RC90.** Left side: Relative change in viability in MCF-7 cells after CM treatment. Right side: n=1 with 3 internal replicates. | **E.** Graph shows change in viability of NFs vs CAFs of the four cell lines together. Bars represent mean +/- SD. (p)-value - significant vs untreated control. *(p) <0.05; **(p)<0.005; ***(p)<0.0005; t-test.

6.2.3. Fibroblast-conditioned medium sensitises primary epithelial cells to TRAIL

Having established that CAFs induce an increased metabolism/viability in untreated epithelial cancer cell cultures, our next step was to test whether the CM could sensitise these cell lines to TRAIL. For this purpose, cells were treated with TRAIL alone and TRAIL in the presence of conditioned medium taken 24 hours after incubation with the respective fibroblasts. After 18 hours of 20 ng/ml and 100 ng/ml TRAIL treatment, viability was assessed by cell titre blue. In this section, we show two graphs for each cell line. In the first graph, each treatment is normalised to its own CM control. The second graph is a waterfall plot which shows the change in viability after TRAIL treatment. The final graph shows the average sensitising ability of each CAF over all cell lines tested. Fibroblast-CM treatment resulted in a sensitisation to TRAIL, irrespective of the fibroblasts origin (Figure 6.3 – 6.7). Overall, CAFs 209, 207 and 253 exhibited the highest sensitisation to TRAIL, while fibroblasts 98, 213 and CAF 148 showed the least. We propose that the cell line MCF-7 showed the highest degree of sensitisation potentially because it is the cell line that is the most resistant to TRAIL.

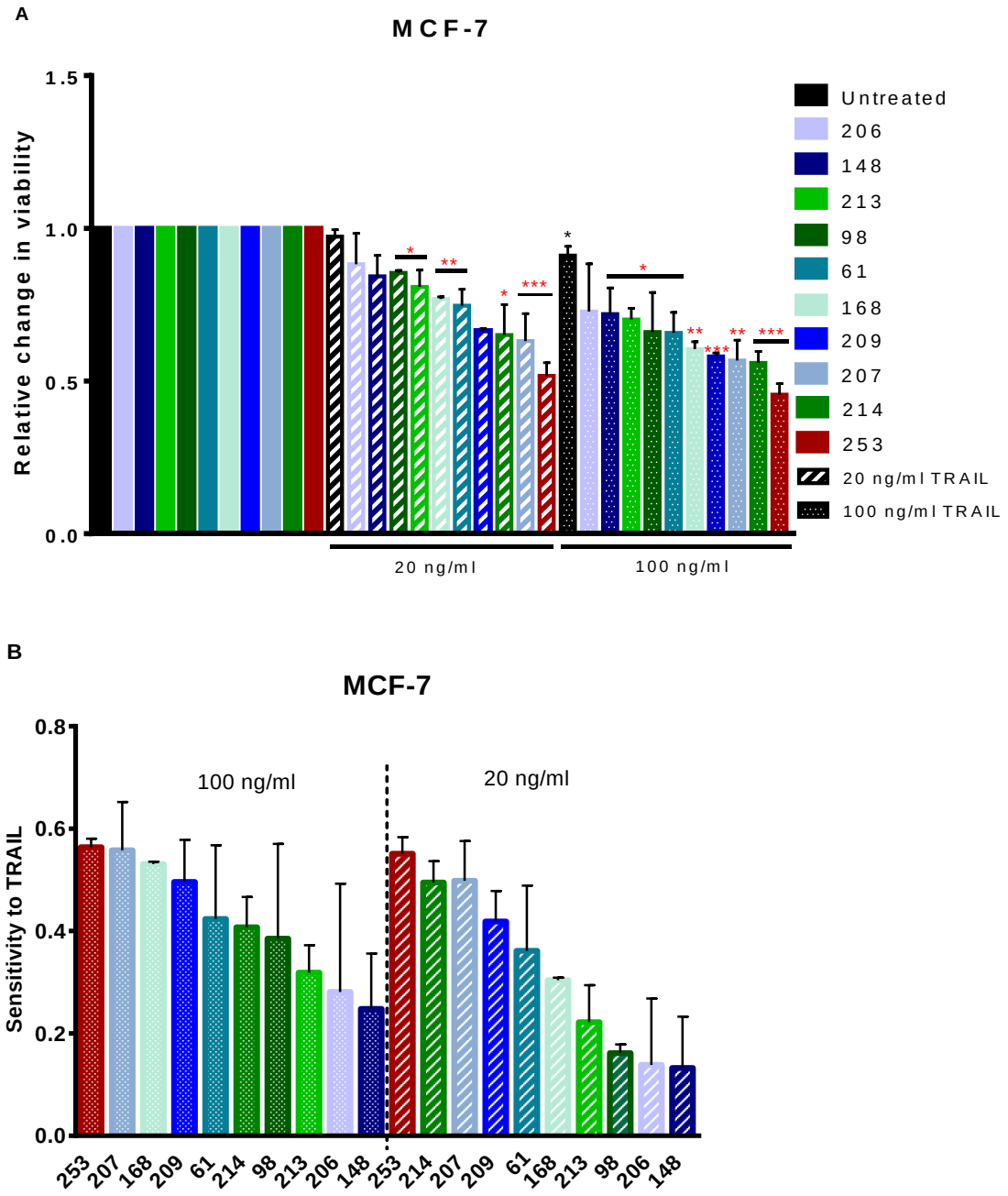

Figure 6.3. Fibroblast-conditioned medium sensitises MCF-7 cells to TRAIL. A. Relative change in viability (cell titre blue assay) following TRAIL, Fibroblasts conditioned medium (CM) and TRAIL/CM treatments. Confluent fibroblasts (98, 213, 214, 61, 148, 168, 206, 207, 209 and 253) were incubated with fresh fibroblast medium for 24 hours to generate CM. Untreated control cells were cultured with only fibroblast medium and treated cells with CM for 24 hours before 20 ng/mL and 100 ng/mL of TRAIL treatment. CM treatments were normalised to the untreated control and TRAIL treatments were normalised to the CM control.| **B**. Waterfall plot representing overall sensitivity to TRAIL. Bars represent mean +/- SD. (p)-value - significant vs untreated control. * (p)-value - significant vs TRAIL alone. *(p) <0.05; **(p)<0.005; ***(p)<0.0005; t-test.

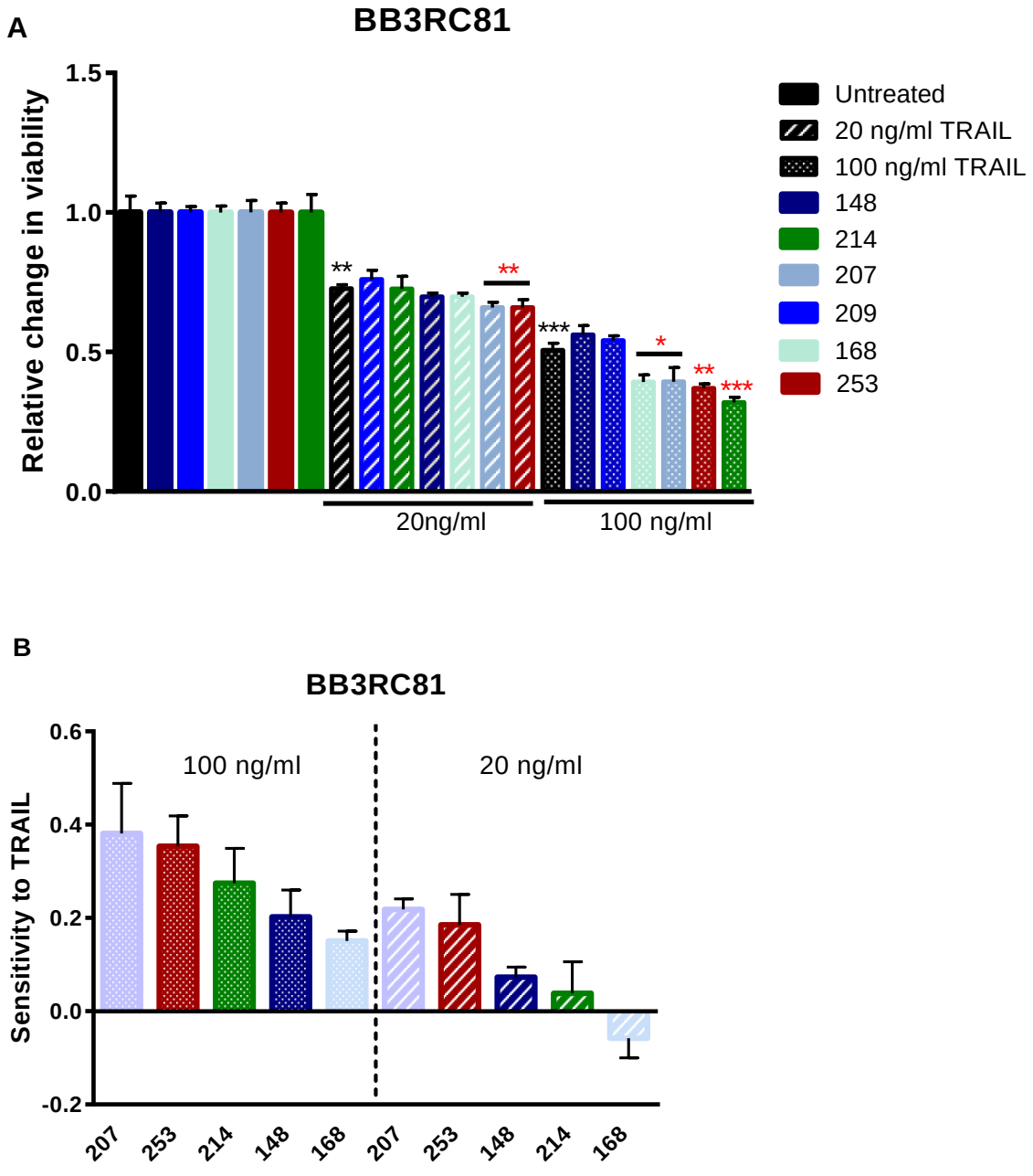

Figure 6.4. Fibroblast-conditioned medium sensitises primary epithelial cells (BB3RC81) to TRAIL. A. Relative change in viability (cell titre blue assay) following TRAIL, Fibroblasts conditioned medium (CM) and TRAIL/CM treatments. Confluent fibroblasts (214, 148, 168, 207, 209 and 253) were incubated with fresh fibroblast medium for 24 hours to generate CM. Untreated control cells were cultured with only fibroblast medium and treated cells with CM for 24 hours before 20 ng/mL and 100 ng/mL of TRAIL treatment. In the first graph of each cell line CM treatments were normalised to the untreated control and CM+TRAIL treatments were normalised to the CM control. The second graph shows overall TRAIL sensitivity. | **B.** Waterfall plot of the overall sensitivity to TRAIL. | Bars represent mean +/- SD. (p)-value - significant vs untreated control. * (p)-value - significant vs TRAIL alone. *(p) <0.05; **(p)<0.005; ***(p)<0.0005; t-test.

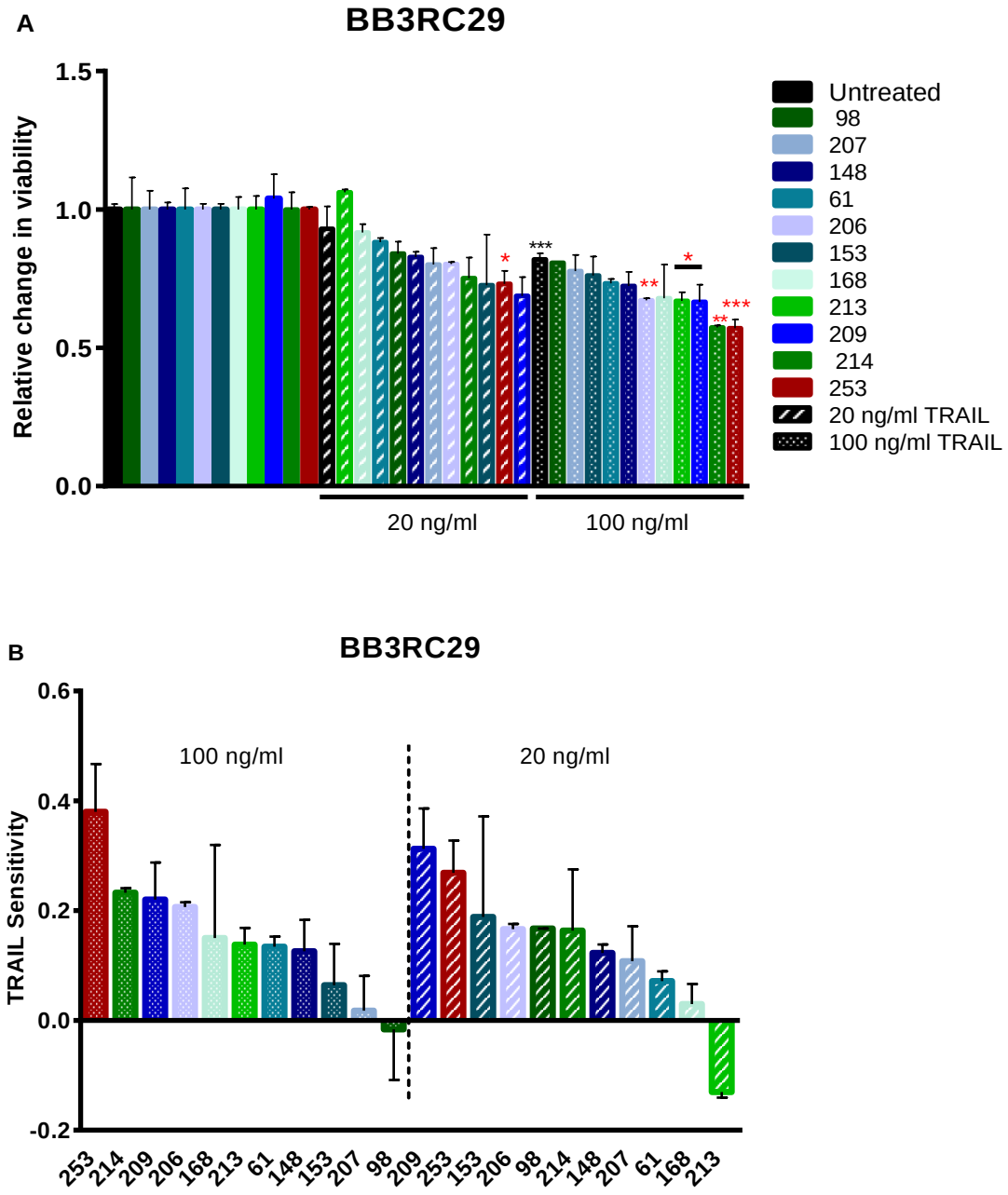

Figure 6.5. Fibroblast-conditioned medium sensitises primary epithelial cells to TRAIL. A. BB3RC29. Relative change in viability (cell titre blue assay) following TRAIL, Fibroblasts conditioned medium (CM) and TRAIL/CM treatments. Confluent fibroblasts (98, 213, 153, 214, 61, 148, 168, 206, 207, 209 and 253) were incubated with fresh fibroblast medium for 24 hours to generate CM. Untreated control cells were cultured with only fibroblast medium and treated cells with CM for 24 hours before 20 ng/mL and 100 ng/mL of TRAIL treatment. In the first graph of each cell line CM treatments were normalised to the untreated control and TRAIL treatment was normalised to the CM control. | **B.** Waterfall plot representing the overall change in TRAIL sensitivity. |Bars represent mean +/- SD. (p)-value - significant vs untreated control. *(p) <0.05; **(p)<0.005; ***(p)<0.0005; t-test. * (p)-value - significant vs TRAIL alone.

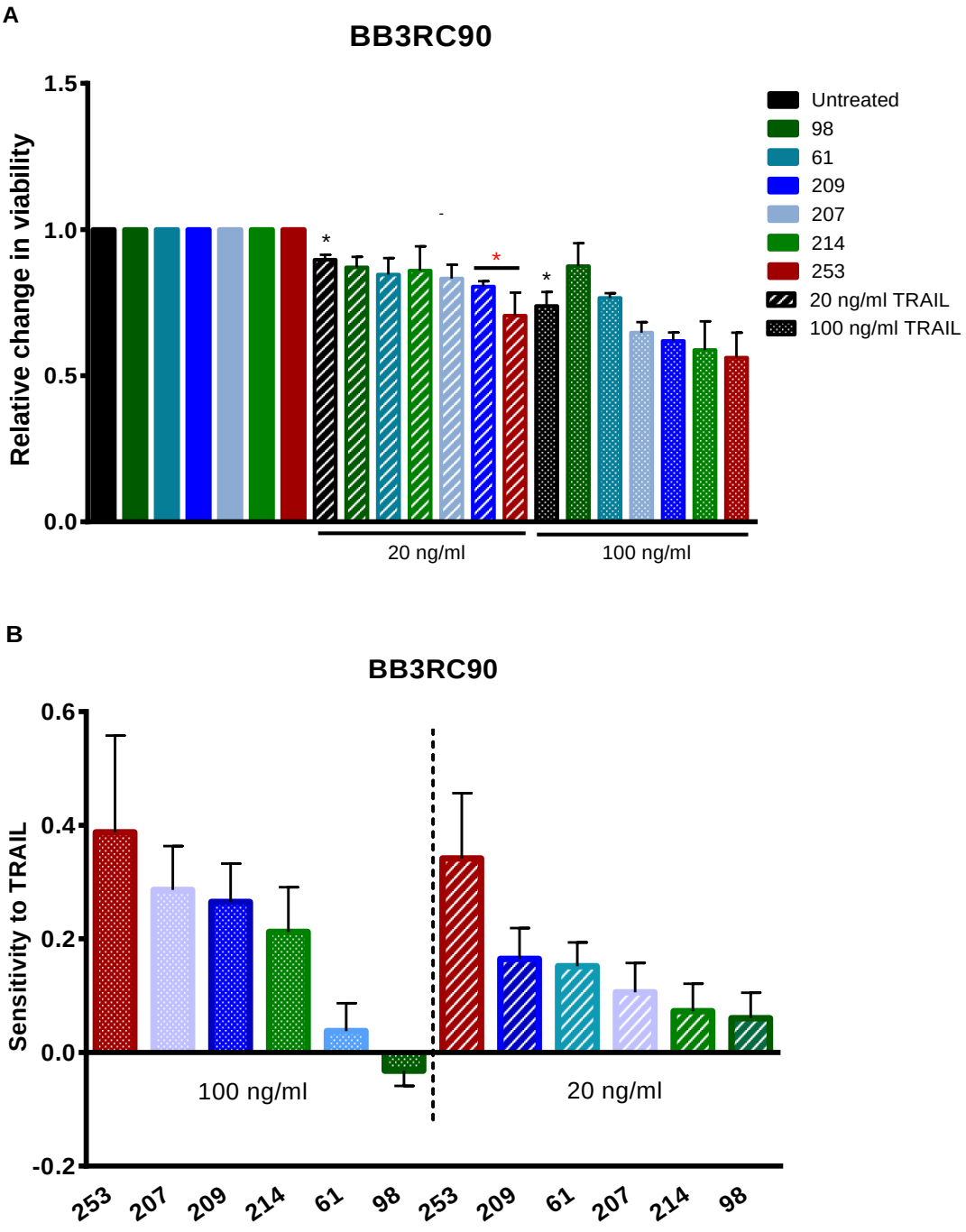

Figure 6.6. Fibroblast-conditioned medium sensitises primary epithelial cells to TRAIL: A. Relative change in viability (cell titre blue assay) following TRAIL, Fibroblasts conditioned medium (CM) and TRAIL/CM treatments. Confluent fibroblasts (98, 213, 153, 214, 61, 148, 168, 206, 207, 209 and 253) were incubated with fresh fibroblast medium for 24 hours to generate CM. Untreated control cells were cultured with only fibroblast medium and treated cells with CM for 24 hours before 20 ng/mL and 100 ng/mL of TRAIL treatment. CM treatment was normalised to the untreated control and TRAIL treatment was normalised to the CM control. n=3 and for 207, 209, 214 and 253 n=4 with 3 internal replicates. | **B.** Waterfall plot of the overall sensitivity to TRAIL. | Bars represent mean +/- SD. (p)-value - significant vs untreated control. *(p) <0.05; **(p)<0.005; ***(p)<0.0005; t-test. * (p)-value - significant vs TRAIL alone.

I

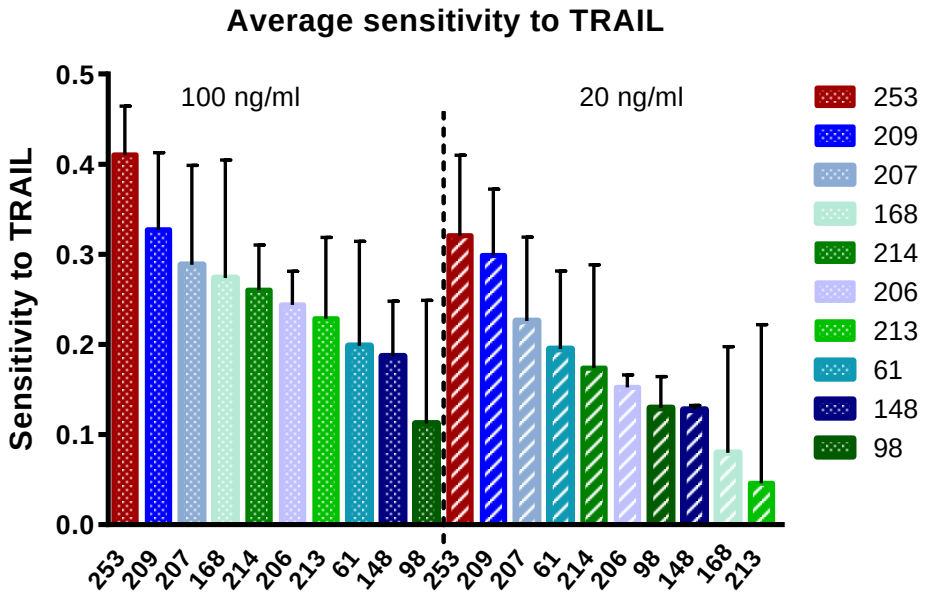

Figure 6.7. Fibroblast-conditioned medium sensitises primary epithelial cells to TRAIL: *relative change in viability (cell titre blue assay) following TRAIL, Fibroblasts conditioned medium (CM) and TRAIL/CM treatments*. Confluent fibroblasts (98, 213, 153, 214, 61, 148, 168, 206, 207, 209 and 253) were incubated with fresh fibroblast medium for 24 hours to generate CM. Untreated control cells were cultured with only fibroblast medium and treated cells with CM for 24 hours before 20 ng/mL and 100 ng/mL of TRAIL treatment. Average sensitivity to TRAIL of BB3RC81, BB3RC90, BB3RC29 and MC-7 cells. | Bars represent mean +/- SD.

6.2.4. Fibroblasts-conditioned medium induced partial EMT-like markers in MCF-7 cells

In the previous section, we have found that CM sensitised cells to TRAIL. We next wished to determine the mechanism of CM induced sensitivity to TRAIL treatment by establishing whether specific markers of EMT were altered following CM treatment. Our laboratory has seen that MDA-MB-231 conditioned medium changes luminal MCF-7 cells into a more mesenchymal-type phenotype: involving upregulation of vimentin and fibronectin; downregulation of E-cadherin and twist but no changes in the EMT-related factors slug and snail (Rhiannon French, unpublished data). An independent study however, reported a stronger relation between slug expression and loss of E-cadherin in breast cancer cell lines (Hajra *et al*., 2002). This latter study reported that MCF-7 cells express E-cadherin with no expression of Slug and MDA-MB-231 cells express Slug with no expression of E-cadherin. To investigate whether EMT markers were upregulated or downregulated by CM factors, MCF-7 cells were treated with CM from several fibroblasts and cells phenotype and gene expression of EMT markers (E-cadherin, N-cadherin, Vimentin, Slug, Snail, IL-6 and IL-8) were assessed.

MCF-7 cells were treated with CM from fibroblasts 98, 61, 214, 207, 209 and 253 for 24 hours and analysed by phase-contrast microscopy to check any changes in morphology (for example change in cell shape). MCF-7 cells did not change in morphology in response to any of the treated samples (Figure 6.8 A). The mRNA expression of specific EMT markers was also analysed in MCF-7 cells and directly compared with the expression of the same markers in fibroblasts 214 and 253. The fibroblasts exhibited lower expression of E-cadherin and increased expression of N-cadherin, Vimentin, Slug, Snail, IL-6 and IL-8 compared to the MCF-7 cells (Figure 6.8 B). This was consistent with MCF-cells exhibiting a luminal phenotype whereas fibroblasts have a mesenchymal phenotype.

MCF-7 cells treated with CM for 24 hours had a lower expression of E-cadherin, N-cadherin and Vimentin compared to untreated cells. Additionally, these cells had higher expression of Slug, Snail, IL-6 and IL-8 compared to control (Figure 6.9 A). Of these markers, IL-6 had the highest

upregulation and Snail had the least compared to the untreated control. CM 98, 214, 207 and 209 induced similar expression of these markers but CM 253 showed lower expression of N-cadherin and this was the only sample with downregulation of IL-8 (Figure 6.9 A). The same experiment was repeated but for 48 hours of CM treatment with CM 209 and CM 253. The gene expression pattern was similar to 24 hours, with downregulation of E-cadherin, N-cadherin and Vimentin; up-regulation of Slug and IL-6 with minimal up-regulation of Snail. IL-8 was downregulated in 209 and in 253 (Figure 6.9 B).

To determine if the changes in E-cadherin gene expression manifested in changes in protein expression, cells were treated with CM for 24 hours and 48 hours and then fixed and stained with E-cadherin antibodies by immunofluorescence. These semi-quantitative experiments failed to confirm that E-cadherin was downregulated by CM or that e-cadherin was redistributed within the tumour cells (Figure 6.10 A and B).

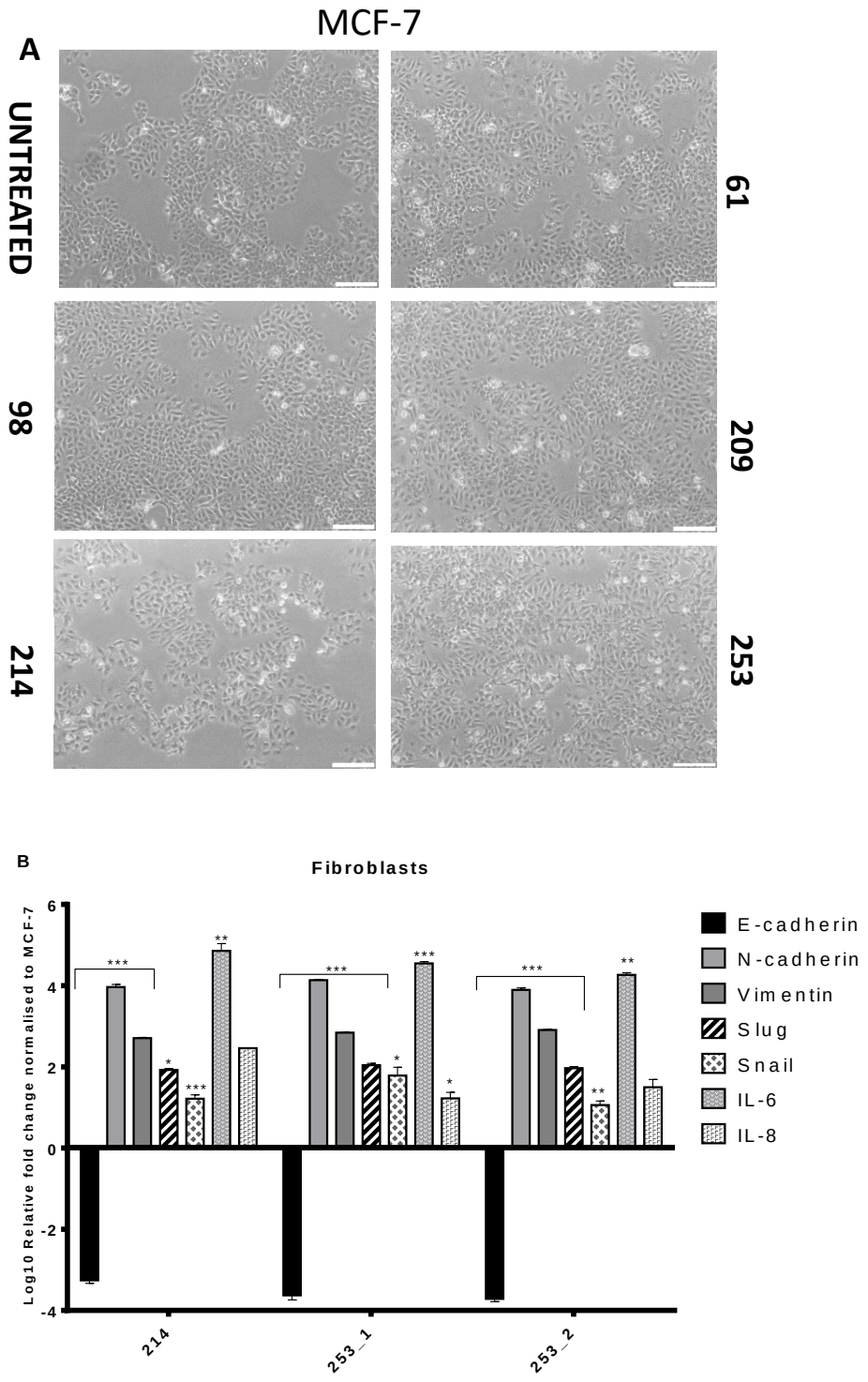

Figure 6.8. Fibroblasts-conditioned medium induced partial EMT-like markers expression in MCF-7 cells. | A. MCF-7 cells were incubated with CM from fibroblasts 98, 214, 207, 209 and 253 for 24 hours. Analysis of MCF-7 cells through a light microscope. Scale bar = 200 µM. | **B**. qPCR: Relative fold change of E-cadherin, N-cadherin, Vimentin, Slug, Snail, IL-6 and IL-8 expression after 24 hours in Fibroblast 214 and CAFS (253_1 and 253_2). Relative fold change was normalised to MCF-7 cells used as a control. | n=1 for 214 and n=2 for 253 (253_1 and 253_2) with 3 internal replicates. Bars represent mean +/- SD and p-value - significant vs MCF-7 control. *(p) <0.05; **(p)<0.005; ***(p)<0.0005; t-test.

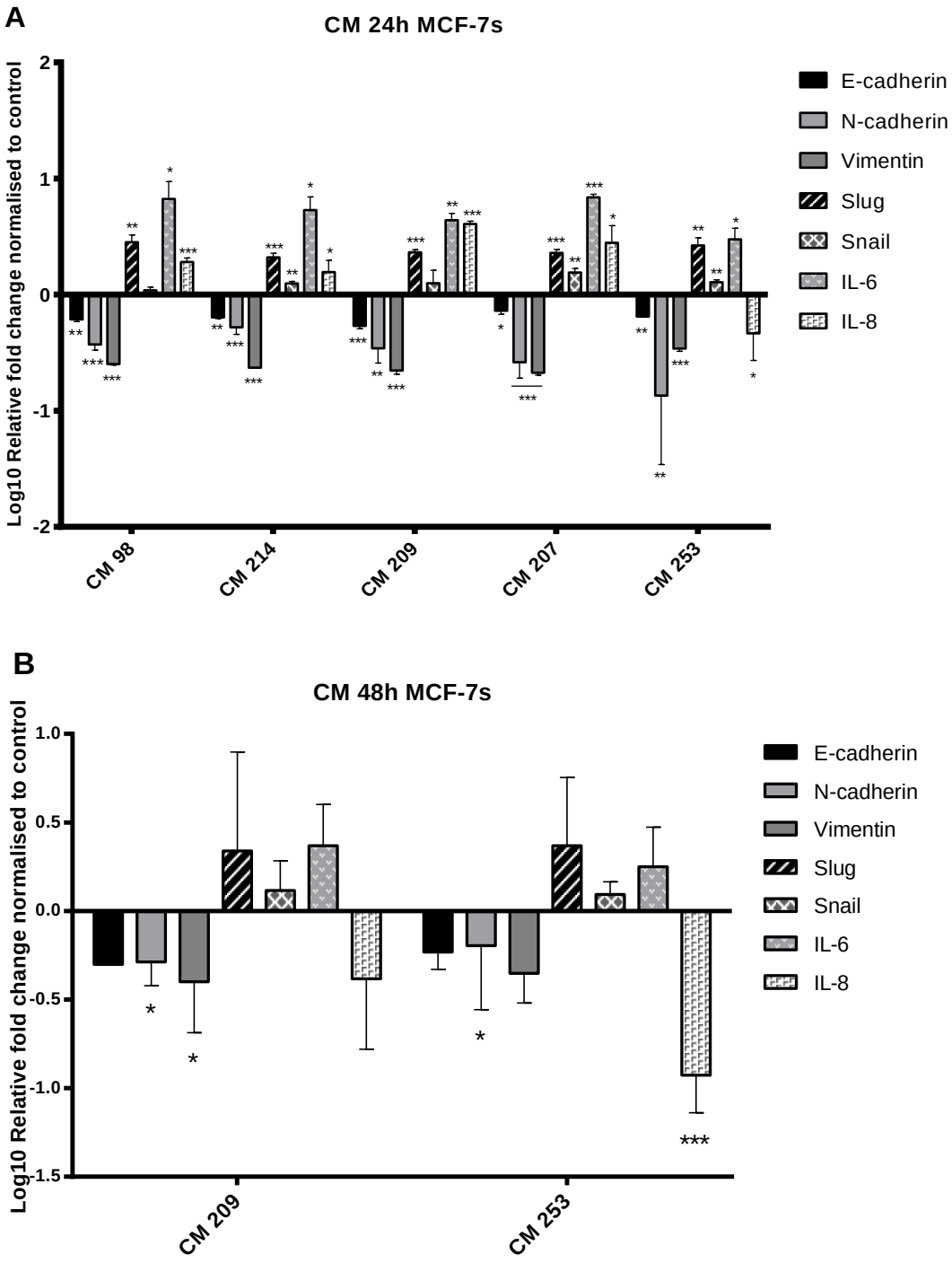

Figure 6.9. Fibroblasts-conditioned medium induced partial EMT-like markers expression in MCF-7 cells. | A. qPCR: Relative fold change of E-cadherin, N-cadherin, Vimentin, Slug, Snail, IL-6 and IL-8 expression after 24 hours and 48 hours of CM treatment normalised to the untreated control using MCF-7 cells were incubated with CM from fibroblasts 98, 214, 207, 209 and 253. |**B.** Same conditions as A but MCF-7 cells were treated with CM for 48 hours. CM 209 represents n=2 and 253 represents n=3. Bars represent mean +/- SD and p-value - significant vs MCF-7 control. *(p) <0.05; **(p)<0.005; ***(p)<0.0005; t-test.

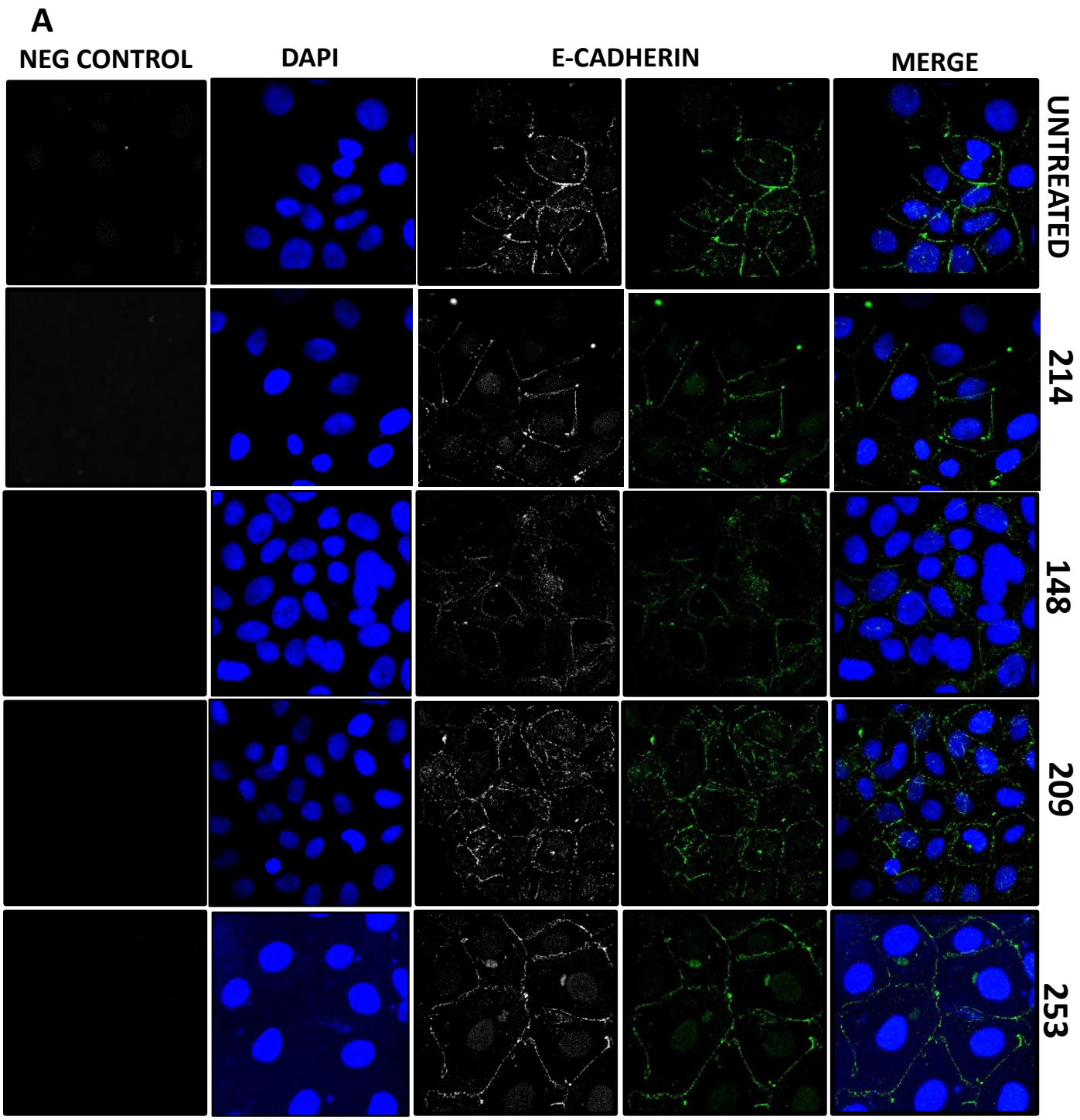

Figure 6.10 A. Fibroblasts-conditioned medium did not change E-cadherin expression in MCF-7 cells. Immunofluorescence: Cells were treated with CM for 24 hours and then fixed and stained with E-cadherin. CM did not change membrane bound E-cadherin. n=1

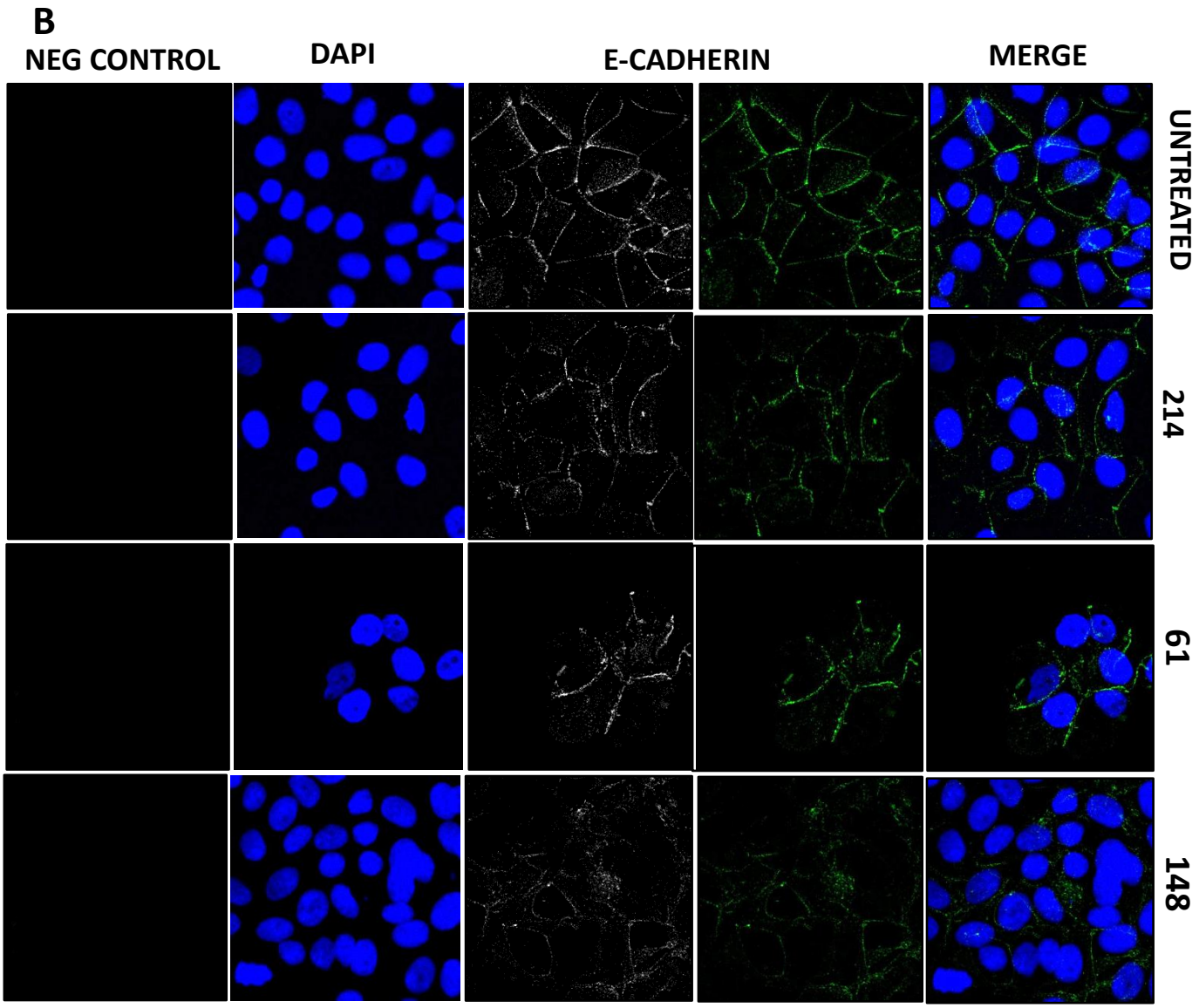

Figure 6.10. B Fibroblasts-conditioned medium did not change E-cadherin expression in MCF-7 cells. Immunofluorescence: Cells were treated with CM for 48 hours and then fixed and stained with E-cadherin. CM did not change membrane bound E-cadherin. n=1

6.2.5. Induction of EMT in MCF-7 cells does not sensitise to TRAIL

We have demonstrated that CM is able to change expression of EMT markers at the mRNA level. However, in order to determine whether it was EMT itself that prompted sensitivity to TRAIL, we wished to independently correlate these changes with TRAIL sensitivity. MCF-7 cells were therefore treated with a EMT-inducing medium which contained: anti-human E-Cadherin, anti-human sFRP-1, anti-human Dkk-1, recombinant human Wnt-5a and recombinant human TGF-β. Cells were treated with this EMT supplement for 96 hours prior 20 ng/mL of TRAIL. Our laboratory has seen that this EMT-inducing medium is able to increase the expression of N-cadherin, Vimentin, Slug and Twist but no change in Snail and E-cadherin in MCF-7 cells (Dan Turnham, unpublished data). Moreover, if this medium is removed from cells, cells undergo a mesenchymal-epithelial transition recovering the original state (Dan Turnham, unpublished data).

Induction of EMT with the EMT-inducing medium had no significant effect on overall cell viability or the ability of the cells to respond to TRAIL (Figure 6.11). Therefore, MCF-7 cells that have undergone conventional EMT retained resistance to TRAIL.

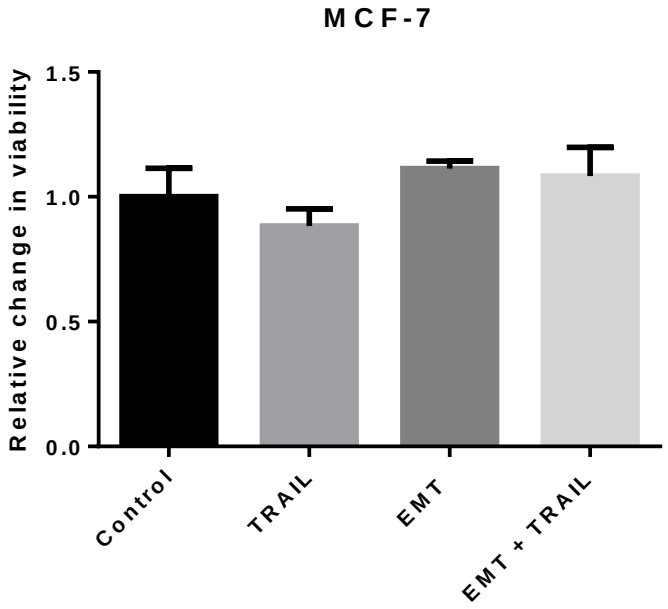

Figure 6.11. Induction of EMT in MCF-7 does not sensitises to TRAIL. *MCF-7 relative change in viability following TRAIL and EMT supplement treatments*. MCF-7 cells were cultured with StemXVivo™ EMT inducing medium supplement that contains EMT inducing factors for 96 hours before 20 ng/ml of TRAIL. After 18 hours, metabolic activity/viability was measured by cell titre blue assay. Graph represents single experiment with 3 internal replicates. Bars stood for mean +/- SD.

6.2.6. Longer treatment with conditioned medium does not sensitise MCF-7 cells to TRAIL

As complete induction of EMT using an EMT-inducing medium over 96 hours did not sensitise cells to TRAIL, we were intrigued to establish whether a 96 hours treatment with CM would result in the same sensitisation to TRAIL seen with 24 hours CM treatment, or whether this prolonged treatment resulted in lack of sensitivity to TRAIL perhaps due to the induction of EMT. To test this, MCF-7 cells were treated with CM from fibroblasts 105, 89, 214 and 61 for 96 hours to mimic the assay performed with the EMT-inducing medium. CM was changed at 72 hours in order to not compromise cells viability. Cells were treated with 100 ng/ml of TRAIL at 24 hours and 96 hours for 18 hours before cell titre blue. As previously seen, 24 hours treatment was able to sensitise MCF-7 cells to TRAIL but a 96 hour treatment was not able to sensitise the same cells (Figure 6.12). Therefore, CM only sensitises cells to TRAIL over a short time-frame.

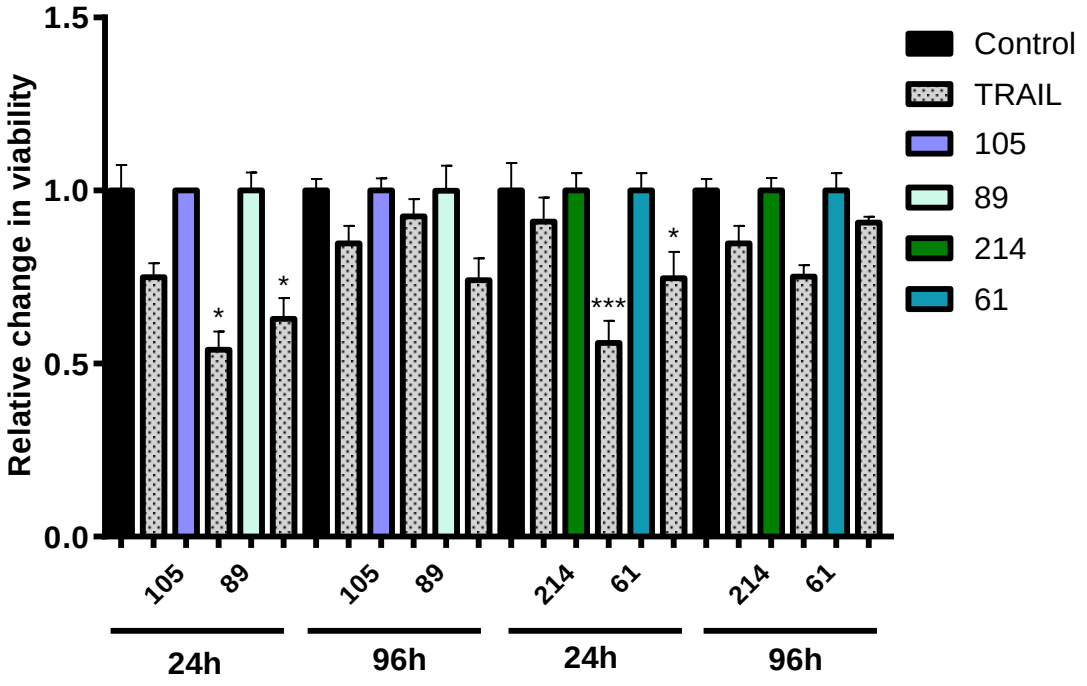

Figure 6.12. Longer treatment with conditioned medium does not sensitise MCF-7 cells to TRAIL: *relative change in viability.* Cell titre blue: MCF-7 cells were plated in 48 well-plates and incubated with fibroblasts CM for 24 hours and 96 hours. CM was changed at 72 hours to not compromise cell viability. At 24 hours and 96 hours cells were treated with 100 ng/mL of TRAIL for 18 hours. Bars represent mean +/- SD of one single experiment with 3 internal replicates. *(p)-value - significant vs TRAIL control: *(p) <0.05; **(p)<0.005; ***(p)<0.0005; t-test.

6.2.7. Fibroblast-conditioned medium has a minimal effect at sensitising breast cancer stem cells to TRAIL

To investigate whether the CM and TRAIL is detrimental to breast cancer stem cells, MCF-7s were incubated with CM medium for 24 hours in adherent conditions, treated with TRAIL for 18 hours. The cells were then passaged into sphere-forming conditions to test whether the treatment was capable of reducing the stem-like population. CM from CAF 209, 214 and 253 with 100 ng/mL of TRAIL was able to slightly decrease sphere number by 4 – 10% (Figure 6.13). TRAIL had a bigger effect with CM from 253, than in sample 209 and 214 which corresponds with the effect of CM/TRAIL seen with bulk MCF-7 cells.

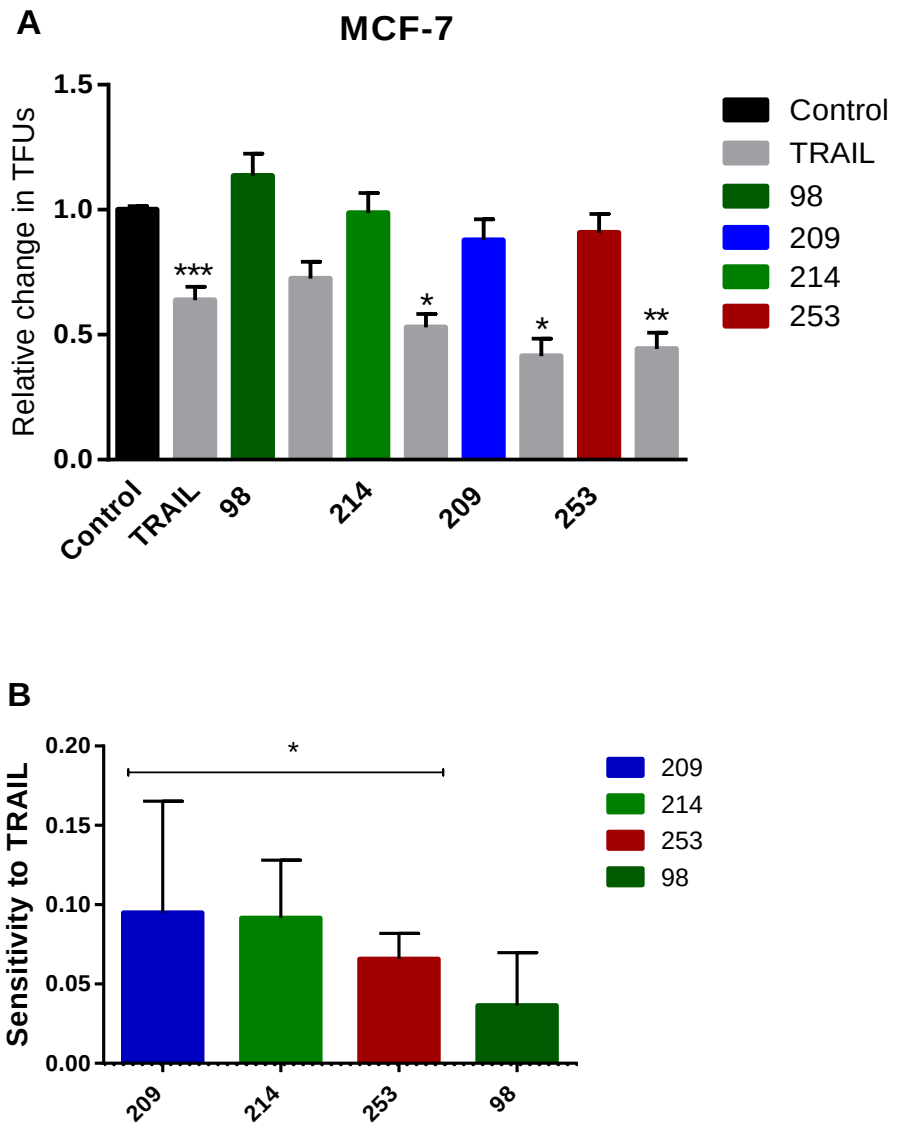

Figure 6.13. Fibroblast-conditioned medium sensitises breast cancer stem cells to TRAIL. | **A.** Relative change in MCF-7 tumoursphere forming units (TFUs) after TRAIL treatment performing tumoursphere assay. MCF-7 cells were plated in 96 well-plates and incubated with fibroblasts-conditioned medium for 24 hours prior 20 ng/mL of TRAIL. 18 hours later, cells were trypsinized and 1000 cells were cultured in low attachment plates. Spheres were counted 10 days after culture (Passage 1) |**B.** Waterfall plot representing verall sensitivity of MCF-7s to TRAIL after CM treatments.| Bars represent mean +/- SD of one single experiment with 4 internal replicates. (p)-value - significant vs untreated control: *(p) <0.05; **(p)<0.005; ***(p)<0.0005; t-test.

6.3. Discussion

In this chapter, we wished to explore the potential link between CAFs, EMT and TRAIL sensitivity or resistance. It has been shown that a mesenchymal-like phenotype is present in cells that are sensitive to TRAIL (Rahman *et al*. 2009, Piggott *et al*., 2011, French *et al*., 2015) but an EMT process is linked to resistance to TRAIL (Wang *et al*., 2014). Our model, tried to use CAFs as an inducer of EMT which is a different approach to that used by Wang *et al*., where an induced resistance to TRAIL resulted in an EMT state.

In this chapter, fibroblasts were co-cultured with MCF-7 cells to investigate whether CAFs sensitised cells to TRAIL. Co-cultures with different CAFs led to a sensitisation of cells to TRAIL (Figure 6.1). To test whether this sensitisation was due to soluble factors, CM was generated from fibroblasts and different cell lines were treated with CM and CM +/- TRAIL. CM and TRAIL experiments led to a similar sensitisation to the co-cultures meaning that this sensitisation does not require direct contact with fibroblasts (Figure 6.2). Therefore, fibroblasts may release soluble factors that may modulate the sensitivity of cells to TRAIL. As previously mentioned, our laboratory has seen that CM from a mesenchymal TRAIL-sensitive cell line resulted in TRAIL-sensitisation in a resistant cell line. Cytokine arrays of the CM detected high expression of IL-8, a well-known EMT marker. Since CAFs release IL-8, this soluble factor may be responsible for increasing the sensitivity to TRAIL. A cytokine array would be helpful in establishing this in the future.

To study what markers were upregulated after CM treatments, gene expression of a panel of well-known EMT-markers were analysed by RT-qPCR. We hypothesised that there would be a switch of luminal to mesenchymal markers and also an upregulation of Slug, Snail, IL-6 and IL-8. In all CM treated cells there was a downregulation of E-cadherin, N-cadherin and Vimentin (Figure 6.9 B). However, this was not confirmed at the protein level for E-cadherin by semi-quantitative immunofluorescence (Figure 6.10). Additionally, the experiment lacks of a positive control for E-cadherin to confirm whether it is actually E-cadherin expressing green fluorescence.

Additionally, CM treatment during 48h resulted in a similar pattern as 24 hours meaning that CM treatment for 24 hours is enough to change those markers and sensitise to TRAIL. Furthermore, there is an upregulation of Slug and IL-6 and maintenance of Snail levels. In regards to IL-8, we were expecting an upregulation of this maker and concordantly it was up-regulated 24 hours after all treatments except after CM 253. Unexpectantly, at 48 hours, IL-8 was downregulated in both CM 209 and CM 253.

A recent study conducted by Fernando *et al*. investigated the role of IL-8 in tumour EMT and demonstrated that directly treating breast epithelial tumour cells with purified, recombinant human IL-8 *in vitro*, significantly decreased E-cadherin expression and increased fibronectin expression in MCF-7 and T47D luminal breast cancer cells (Fernando *et al*., 2017). Since our laboratory has seen a link between TRAIL sensitivity and IL-8 expression in CM, we predicted MCF-7 to express the highest levels of IL-8 after CM 253 treatment, which was the CM that resulted in the highest sensitisation to TRAIL. However, out of the all CMs studied, CM 253 showed to be the least effective at inducing IL-8 expression in MCF-7 meaning this sensitivity was likely not mediated by IL-8.

Additionally, the highest upregulated gene after CM treatment was IL-6. A study has shown that, in human cholangiocarcinoma, IL-6 enhances Mcl-1 expression via an Akt-dependent mechanism, which regulates cellular Mcl-1 expression and therefore disruption of IL-6/Akt signalling sensitises cells to TRAIL cytotoxicity (Kobayashi *et al.,* 2005). If this scenario of IL-6 expression linked to TRAIL resistance exists in breast cancer cells, the IL-6 induced by CAFs is not the factor that drives TRAIL sensitivity in MCF-7 cells.

Our laboratory has experience of treating MCF-7 cells with an EMT-inducing medium for 96 hours and seeing an upregulation of N-cadherin, Vimentin and Slug with no change in E-cadherin and Snail (Figure 6.11). The results using CM at 24 hours and 48 hours were different to the EMT-inducing medium (with the exception of Snail, where the result was similar). MCF-7 treatment with CM for 96 hours did not sensitise cells to TRAIL, which could mean that CM in a longer term could induce the

same traditional EMT changes seen with the EMT-inducing medium resulting in a resistance to TRAIL. However, this 96 hours assay requires additional repeats to confirm this finding – and ultimately one would need to determine the extent of this EMT by molecular analysis.

Thus, currently it is only known that fibroblasts induced a partial EMT (when one or more of the key characteristics of complete-EMT are not exhibited) rather than a complete EMT (when epithelial cells commit to a mesenchymal phenotype), which resulted in a sensitisation of cells to TRAIL.

As it is likely that IL-6, IL-8 and Snail do not mediate TRAIL sensitivity it would be important in the future to study other EMT markers such as: twist; fibronectin; runx, Zeb-1 and Zeb-2 etc., to fully understand the mechanism behind CM and TRAIL sensitivity.

Also in this chapter, the effect of fibroblast-CM on four different breast cancer cell lines was investigated. CM increased the viability of the cells, which could be due to an increase in cell proliferation or prevention of apoptosis. These results corroborate previous studies which have shown that fibroblasts directly modulate tumour growth by secreting factors with oncogenic and mitogenic functions capable of increasing tumour cell proliferation and protecting from apoptosis (Pietras, 2010). Moreover, Majety *et al*. have demonstrated that co-culturing with fibroblasts/CAFs increased the proliferation of several types of cancer cells (Lung, Pancreas, Breast). In addition, they have shown that co-culture induced differential expression of soluble factors in a cancer type-specific manner. For example, epidermal growth-factor was primarily secreted by co-cultures of pancreatic and breast cancer cells whereas hepatocyte growth factor was mainly secreted by lung cancer cells and fibroblasts, and that IL-6 is primarily secreted by the breast cancer co-cultures indicating a cancer-specific pattern in cytokine secretion. Treatment with blocking antibodies against a few factors or their receptors resulted in the inhibition of cancer cell proliferation in the co-cultures. Specifically, blocking IL-6 led to a significant decrease in the survival of BT20 cells that were co-cultured with fibroblasts, demonstrating that the increase in cell proliferation was mediated by IL-6 (Majety *et al*., 2015).

Additionally, another study shows that PI3K/Akt and MAPK/Erk pathways may be the common key pathways by which both normal and cancer fibroblasts regulate cancer cell proliferation. High secretion of one or more cytokines by CAFs (IL-6, IL-8, VEGF, CCL2 (RANTES) and CCL5 (MCP-1)) may potentially mediate the activation of these pathways to induce cancer cell proliferation (Subramaniam *et al*., 2013). These findings agree with our expression data where IL-6 was the highest upregulated gene after CM treatment (Figure 6.9 A and B). However, to complement the viability assay, it would be essential to perform a proliferation assay to measure proliferation in these cells after CM treatment, for example, labelling cells with the proliferation marker ki67. In addition, despite having these promising results, it would be important to test more ratios of Fibroblasts:Epithelial cells in the co-cultures to study the ability of different concentrations of CAFs at sensitising the same number of epithelial cells. It was also seen that fibroblasts from normal tissue or fibroadenomas have less ability of increasing cell metabolic activity/proliferation compared with CAFs (Figure 6.2 E). These findings agree with a study that shows fibroblasts derived from benign endometrial hyperplasia tissues were not able to increase cancer cell proliferation (Subramaniam *et al*., 2013). Additionally, *in vitro* experiments co-culturing MDA-MB-231 breast cancer cells with human CAFs isolated from mammary tissue resulted in an increased proliferation rate with a higher population of tumour cells in S phase compared to tumour cells co-cultured with normal fibroblasts (Peng *et al.,* 2013). In addition, our experiments showed that in two of the four cell lines, an increase in fibroblasts grade was correlated with an increase of cell proliferation (Figure 6.2 A-D).

We have shown that CM treatment led to a sensitisation to TRAIL cytotoxicity in all cell lines tested (Figure 6.3 – 6.7). Overall, fibroblasts 207, 209 and 253 have shown to increase sensitivity of epithelial cells to TRAIL. Interestingly, CM from fibroblasts derived from a benign sample (98) and fibroadenomas (213, 214) were also able to sensitise cells to TRAIL (Figure 6.3 6.7). This may suggest that this TRAIL sensitisation mediated by fibroblasts is not related to a tumour microenvironment but related to factors that normal fibroblasts and CAFs induce a response in epithelial cells.

Several studies have reported a link between CAFs and drug resistance. However, there are experiments linking CAFs to drug sensitivity. One study has shown that mesenchymal stem cells and CAFs increased the cytotoxic effect of a RAF inhibitor on MDA-MB-231 cells by downregulating ERK1/2 phosphorylation and sensitised MCF-7 cells to a mTOR inhibitor. This result showed that CAFs may not contribute to all mechanisms of drug-resistance. However, the potential reason may be attributed to heterogeneity of CAFs in drug response (Dittmer, *et al*. 2011). The CAF 253, which showed to induce the highest sensitivity, was derived from a TAMR sample. As seen in Chapter 5, TAMR cells are particularly sensitive to TRAIL. Additionally, the biopsy 253 (the original sample of CAF 253) was the most susceptive to TRAIL at a stem cell level (Table 6.1), which agrees with the fact that this CAF gives the best sensitisation to TRAIL sensitivity. It has been reported that tamoxifen resistance was related to increased levels of Snail, Vimentin, N-cadherin and decreased levels of E-cadherin, which are considered as EMT characteristics (Liu *et al*., 2013). Our gene expression of MCF-7 cells after CM 253 treatment has partially shown the opposite: downregulation of E-cadherin, Vimentin and N-cadherin and maintenance of Snail levels. Furthermore, a study has shown that mitochondrial activity in epithelial breast cancer cells drives tamoxifen resistance and that mitochondrial inhibition is able to re-sensitise cancer cells to tamoxifen. CAFs induce tamoxifen-resistance by increasing mitochondrial activity in epithelial cancer cells (Martinez-Outschoorn *et al.*, 2011). Additionally, in breast cancer, IL-6 secretion by CAFs promotes tamoxifen resistance through degradation of ER-α (Wang *et al*., 2014). These fibroblasts from the tamoxifen-resistant sample 253 could be able to increase the mitochondrial activity of epithelial cells making them more susceptible to TRAIL. However, to test the previous hypothesis more CAFS from tamoxifen derived samples would be needed.

Several studies have also shown the activation of EMT could induce the generation of the CSC population (Wellner *et al*., 2009). In prostate cancer, CAFs can stimulate EMT and increase the stemness properties of cancer cells through the secretion of MMPs (Giannoni *et al*., 2010). Furthermore, CAFs from breast cancer have been reported to promote the EMT in cancer cells via the

secretion of stromal-derived factor 1 (SDF-1) and TGF-β1 providing additional support, suggesting that CAFs play a crucial role in promoting cancer stemness (Soon *et al*., 2013). Our next step was to investigate whether CM and TRAIL affects the stem cell population. We hypothesised that CM could potentially increase stemness in the bulk population. Therefore, MCF-7 cells were treated with CM in adherent conditions and then passaged into sphere conditions. CM alone did not increase the number of tumourspheres and CM plus TRAIL had a minimal effect on bCSCs (4-10%) (Figure 6.13) Therefore, at least under these conditions, CAFs do not appear to induce a stem/progenitor like state in epithelial cancer cells. Other experiments that could be performed to confirm this finding are colony forming assays and analysis of the stem cell markers ALDH and CD44 after CM/TRAIL treatment. Furthermore, CAFs sensitivity was only tested on cell lines that were ER positive and HER2 negative. Testing CM treatments on a panel of cell lines with different receptor status would be important to find a particular subtype that gives a better senstitisation to TRAIL and also, on cell lines that are resistant to TRAIL at a stem cell level.

CAFs are more genetically stable and proliferate more slowly than cancer cells. As such, fibroblasts or fibroblast secreted factors represent appealing drug targets (Kalluri and Zeisberg, 2006; Lu *et al*., 2009). It would be advantageous to correlate soluble factors released by the fibroblasts with TRAIL sensitivity in order for TRAIL to become a candidate for cancer patients with a particular type of CAFs within the tumour. Another advantage of studying CAFs and TRAIL sensitivity is to try to find a signature correlated to TRAIL sensitivity. Furthermore, a recent study investigated TRAIL-resistance mechanisms in human benign fibroblasts from colon and lung and has shown that these fibroblasts express pro-apoptotic TRAIL receptor DR5 and less expression of DR4. Normal fibroblasts expressed reduced c-myc and caspase-8 activity as compared to TRAIL-sensitive colon cancer cells (Crowder *et al*., 2016). It would be interesting to measure the levels of DR4/DR5 and caspase-8 activity in each of these fibroblasts to correlate these levels with TRAIL response.

In summary, CM treatment resulted in an increase in cell viability in all cell lines tested. Co-culture of fibroblasts with different cell lines and conditioned medium led to a similar sensitisation to TRAIL which suggest that this sensitivity is due to soluble factors released by fibroblasts. This sensitisation to TRAIL was not related to a tumourigenic microenvironment and to a traditional EMT trait. Preliminary data has shown that exposing cells to CM for 96 hours did not sensitise cells to TRAIL cytotoxicity, which could mean that long exposure to CM could result in a full EMT-like phenotype. Fibroblasts derived from a tamoxifen-resistant tumour have shown the highest sensitisation to TRAIL, which mimics the sensitisation of the original sample. These findings support but do not unequivocally prove the importance of the tumour microenvironment in modulating drug responses. In the future, it will be important to perform a more extensive investigation of the soluble factors present in each conditioned medium. We hypothesise that different fibroblasts may release different levels of soluble factors and we wish to find the soluble factors that can lead to the highest sensitisation to TRAIL. In the future, these fibroblasts could function as a biomarker to predict TRAIL responses along with other studies that have demonstrated the ability of a stroma-derived signature to accurately predict disease outcome in breast cancer (Wald *et al.*, 2011; Soon, 2016).

CHAPTER 7

General Discussion

7. General Discussion

7.1. General Discussion

Breast cancer 5-year survival, in the UK, has doubled in the past last 40 years; yet this survival is heavily associated with the stage of the disease at diagnosis. Five-year relative survival in patients is 99% at Stage I but only 15% at Stage IV (Cancer Research UK). Perhaps the most notable improvement in recent years has been the introduction of tamoxifen as the first choice for adjuvant therapy in ER positive patients, especially, for premenopausal women as it decreases breast cancer recurrence and annual mortality rate by 50% and 31%, respectively. However, 20-30% of tumours show resistance to tamoxifen therapy, which either existed prior to the treatment (*de-novo* resistance) or developed during the therapy (acquired tamoxifen resistance) (r*eviewed* in Ali *et al*., 2016). Breast cancer stem cells (bCSCs) have been shown to be responsible for relapse after tamoxifen resistance and metastasis (Singh and Settleman, 2010; Weinberg, 2011; Visvader *et al.,* 2012; Mitra *et al.*, 2015; Simões *et al.,* 2015, Doherty *et al*., 2016). Additionally, endocrine therapies, such as tamoxifen increase the proportion of bCSCs within the tumours (Section 5.2.2; Simões *et al*., 2015). Many signalling pathways also have been reported to be upregulated as a consequence for this resistance to endocrine treatments such as EGFR/HER2, PI3K/AKT; MAPK, mTOR (Oh *et al*., 2001; Campbell *et al*., 2001; Herynk and Fuqua, 2007).

Furthermore, an acquisition of endocrine resistance accompanied by the appearance of mesenchymal-like features has been suggested, which might correlate with an increased predesposition to metastatic disease (Hiscox *et al*., 2006). This mesenchymal-like phenotype was due to an EGFR-driven modulation of the phosphorylation status of beta-catenin, which could contribute to a higher aggressive phenotype and transition towards a mesenchymal phenotype *in vitro* (Hiscox *et al*., 2006). Many drugs have been investigated in order to target cancer cells. One of these drugs is TRAIL that has become an interesting anti-cancer agent that specifically induces apoptosis in cancer cells with no toxicity to normal cells (Ashkenazi *et al*. 1999; Keane *et al*., 1999; Zhang *et al*., 2005), and

also to primary cells as we have demonstrated in Chapter 4 using HMECs (Figure 4.1 – 4.3). Additionally, TRAIL had previously been shown to selectively target breast cancer cell types with a mesenchymal-like phenotype (Rahman *et al*., 2009). This was the rationale behind why our group started to investigate TRAIL sensitivity in breast cancer cells with endocrine resistance as they present with mesenchymal features. Despite TRAIL having demonstrated cytotoxicity in breast cancer cell lines *in vitro,* it has failed numerous clinical trials. However, none of these trials have pre-selected patients based on TRAIL sensitivity (*reviewed* in De Miguel, *et al*., 2016). Therefore on order TRAIL to become a promising drug to the clinic a better stratification of breast cancer is needed.

It was our intention to investigate TRAIL treatment and c-FLIP suppression in primary breast tumours *ex vivo* directly from the clinic and therefore bridge the gap between *in vitro* success of TRAIL treatment and lack of it in patients. These *ex vivo* models better mimic the characteristic features of primary breast cancer (Perou *et al*., 2000; Prat *et al*., 2010). Assays utilising primary cultures can provide important models for the study of breast cancer pathogenesis including metastatic disease, *in vivo* assessment of drug sensitivities and discovery of new therapeutics (Drews-Elger *et al*., 2014). However, in Chapter 3, we have showed that the efficiency of obtaining viable cultures for diagnostic biopsies and surgical samples was 36.7% and 44.5%, respectively. Within these viable samples diagnostic biopsies and surgical samples the successful samples (more than 20 spheres) was 76.5% and 28.9%, respectively (Table 3.2). During this project, it was only possible to test TRAIL treatment in diagnostic biopsies/surgical samples, due to a lack of sufficient viable tissue and lack of propagation in adherent culture. In contrast, we were able to test both c-FLIP suppression and TRAIL in primary breast cancer cells from pleural effusions from patients with metastatic breast cancer. These cells were able to efficiently survive under adherent culture and propagate under tumoursphere conditions.

In Chapter 5, we showed evidence that TRAIL efficiently targets bCSCs in 82% of the endocrine resistant tumours *ex vivo* (Section 5.2.1). To further evaluate TRAIL efficiency in endocrine-resistant

tumours, PDX models were generated to investigate TRAIL efficiency *in vivo*. In the model where the resistance to tamoxifen was acquired *in vivo*, TRAIL administration lead to a significant reduction of tumour size in the tamoxifen-resistant tumours. Additionally, single cells from these tumours showed less ability to form tumourspheres *ex vivo,* demonstrating TRAIL efficiency in eliminating bCSCs *in vivo* (Figure 5.13 A and B). Moreover, an anatrozole-resistant breast sample was transplanted into mice and TRAIL decreased primary tumour size and number and size of metastases (Section 5.2.1 and 5.2.2).

Previous studies have demonstrated increased JNK signalling following the long-term acquisition of resistance to endocrine therapies (Musgrove *et al.,* 2009, Shou *et al*., 2002). Piggott *et al*., demonstrated that one consequence of this JNK activation is the ITCH-dependent destabilisation of the c-FLIP protein which correlates with TRAIL sensitivity both in cell line models *in vitro* and in clinical samples *ex vivo* (Piggott *et al.,* 2018). Therefore, these data suggest that pre-selecting patients with resistance to endocrine treatments could be the solution to TRAIL finally becoming successful in clinical trials for breast cancer patients. Also, these sub-group of patients could be based on sensitivity to TRAIL agonists and investigation of c-FLIP, p-ITCH and/or p-JNK levels in tumours could help specify the selection process (Figure 7.1).

As previously mentioned, TRAIL has been proven to be efficient at targeting bulk and bCSCs in mesenchymal cells that lack ER positivity (Rahman *et al*., 2009, Piggott *et al.*, 2011; *French et al.,* 2015). We have also demonstrated TRAIL efficiency in targeting bCSCs in ER-negative tumours. This sensitivity has been explained by low levels of cytoplasmic c-FLIP and not being able to inhibit the DISC complex and subsequent caspase activation (French *et al*., 2015). However, despite the successes of TRAIL in pre-clinical studies, TRAIL has failed numerous clinical trials for patients with triple negative breast cancer (TNBC). In Chapter 5, we showed evidence that TRAIL could be efficient at targeting recurrent tumours that are ER-negative (Figure 5.8) but have been ER positive in the past and relapsed following acquisition of resistance to endocrine therapies.

There are still 60-70% of patients with the ER-positive breast cancer that potentially will show resistance to TRAIL as a monotherapy. It is established now that the survival factor c-FLIP significantly contributes to bCSCs resistance to TRAIL. Additionally, prevention of bCSCs *de novo* formation is another of the key goals to overcome cancer recurrence. There is preliminary evidence in breast cancer cell lines that c-FLIP plays a role in the transition of cancer cells between stem- and non-stem-like states. This study shows that long-term suppression of c-FLIP results in ablation of *bCSCs de novo* formation from a population devoid of bCSCs (L. Piggott, unpublished data). This has implications for long-term survival of patients receiving cancer stem cell therapies, and suggests that c-FLIP could be considered as an adjuvant therapy in its own right and future studies could include investigation to see whether following bCSC ablation after c-FLIP suppression/TRAIL treatment, prolonged suppression of c-FLIP could inhibit this recurrence of cancer stem cells from non-stem-like states.

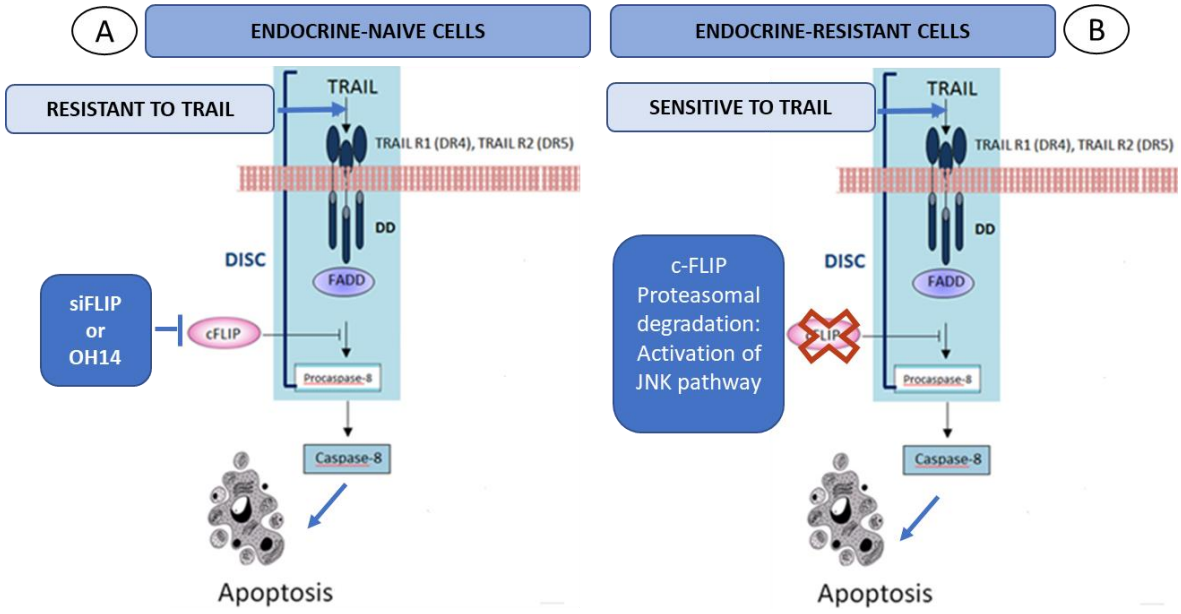

Figure 7.1. Hypothesised mechanism to overcome TRAIL resistance in endocrine-naïve cells and explanation of TRAIL-sensivity in endocrine resistant cells. | A. C-FLIP suppression (siFLIP or OH14) can be used to sensitise cells to TRAIL. **| B.** Endocrine resistant cells are sensitive to TRAIL because there a proteossomal degradation of c-FLIP and therefore c-FLIP is not able to interfere with the DISC formation.

We demonstrated that pharmacological suppression of c-FLIP using OH14 was able to decrease viability and MaSCs in HMECS. However, genetic suppression of c-FLIP (siFLIP) despite decreasing viability did not have a significant effect on viability. This might suggest that OH14 could have off-target effects in normal cells. To test the last theory, OH14 needs to be tested with the pan-caspase inhibitor to test whether is off-target effects or cytotoxicity. Yet, we question if HMECs is the best model for normal breast cells. C-FLIP inhibition could be ideally tested in normal tissues harvested directly from mastectomies or breast reduction as primary cultures, as they are a better model to test compounds in normal tissues directly from patients. Our laboratory has administrated OH14, a c-FLIP inhibitor developed in house, to NSG mice at 10mg/kg for 65 days consecutively (a dose which exhibits tumour efficacy in other tumour types) and there was no toxicity associated to the drug (R. Clarkson, personal communication). More studies are needed to prove safety and efficiency at this dose such experiments on OH14 stability in mouse plasma or data of distribution of the drug metabolism in the mouse. Therefore, our data led us to conclude that c-FLIP inhibition *per se* is not detrimental to normal cells and preliminary data suggests that OH14 might not be detrimental to normal cells *in vivo*.

The combined treatment of c-FLIP suppression and TRAIL treatment affected HMECs viability in bulk and stem cell population having a similar effect in normal and in cancer cells. However, OH14 can display some off-target effects in normal cells or HMECs and therefore it is not the best model for test compounds in normal tissue. Suppressing c-FLIP and TRAIL treatment decreased viability and tumourspheres in primary metastatic tumour cells derived from pleural effusions of patients with metastatic breast cancer. siFLIP sensitised bulk cells to TRAIL in 80% of the samples (roughly 30 -50%) and OH14 sensitised 70% the samples to TRAIL reducing viability by 5– 10%. siFLIP and OH14 sensitised bCSCs to TRAIL in all samples. This result shows robust evidence how this strategy could be applied to patients with metastatic breast cancer. However, in vivo experiments would be key to validate this finding. Additionally, as this dual treatment was not able to eliminate 100% of bCSCs, the treatment could be allied to other conventional treatments already used in the clinic.

The tumour microenvironment has been suggested to promote metastatic disease and the maintenance of a cancer stem-like cell phenotype (Kuperwasser *et al.,* 2004; Wellner *et al*., 2009; Schauer *et al.*, 2011; Kruijf *et al*., 2011). We were intrigued about studies reporting TRAIL sensitivity associated with a mesenchymal phenotype (Rahman *et al*., 2009, Piggott *et al.*, 2011, French *et al*., 2015) and others associating EMT states with TRAIL resistance (Wang *et al.,* 2014). Our laboratory has seen that soluble factors released by a mesenchymal TRAIL-sensitive breast cancer cell line were able to sensitise the resistant cell line MCF-7 to TRAIL (Rhiannon French, unpublished data). Additionally, the development of endocrine therapy resistance in primary breast cancer is associated with poor prognosis by a transition to more aggressive tumour phenotypes that have undergone partial EMT. Therefore, we aimed to test whether EMT is linked to TRAIL resistance or sensitivity. Many studies have shown that cancer associated fibroblasts (CAFs) are able to induce EMT in cancer cells, here, we used CAFs to induce EMT in MCF-7s and thus to study how the tumour microenvironment could modulate sensitivity to TRAIL treatment. In Chapter 6, we have demonstrated that fibroblasts-conditioned medium (CM) was able to sensitise MCF-7 cells and primary metastatic breast samples to TRAIL. However, this sensitisation was not mediated by an EMT state induced by CAFs because an EMT-inducing medium did not sensitise cells MCF-7 cells to TRAIL. Despite studying expression of E-cadherin, N-cadherin, Vimentin, Snail, Slug, IL-6 and IL-8 in MCF-7 after CM treatments, we were not able to associate any of those markers to the TRAIL sensitivity after 24 hours and 48 hours. Additionally, a longer treatment with CM at 96 hours did not sensitise MCF-7 cells to TRAIL, potentially due to the EMT state induced by CAFs, which is supported by literature where they demonstrated that CAFs induces EMT in MCF-7 cells (Soon *et al*., 2013).

Furthermore, CM was able to induce viability of MCF-7 cells compared to the untreated control, perhaps due to increase of proliferation or protection from apoptosis (Figure 6.2; Subramaniam *et al*., 2013). This showed the influence of the tumour microenvironment on cancer cells and implies that drug strategies need to target both stem cells and the tumour microenvironment

as this may be affecting cell plasticity and helping the transition from the non-stem (luminal-like) state to a stem (mesenchymal-like) state. Furthermore, identification of the types of CAFs that can confer this sensitisation to TRAIL, could be applied as a biomarker for TRAIL sensitivity and be beneficial to breast cancer patients.

It is important that in the future we establish a better characterisation of the mechanisms behind the correlation between mesenchymal-state, EMT and TRAIL sensitivity. It is established that mesenchymal cells are sensitive to TRAIL, however, here we find that an EMT state confers resistance to TRAIL. Additionally, acquirement of endocrine resistance is linked to a partial EMT towards a mesenchymal phenotype, which confers TRAIL sensitivity. We propose that only a partial EMT is able to sensitise cells to TRAIL explaining why short exposure with CAFs and CM sensitise cells to TRAIL but longer exposure – and potentially a more 'complete' EMT - confers TRAIL resistance. However, a full characterisation of this partial EMT needs to be elucidated in order to create a panel of factors that promotes sensitivity to TRAIL and therefore be valuable to the clinic (Figure 7.2).

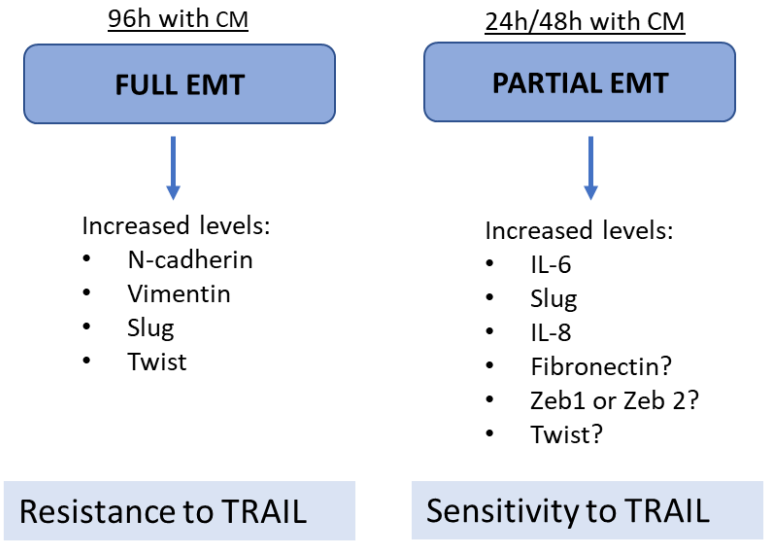

Figure 7.2. Theory behind EMT and TRAIL resistance or sensitivity.

7.2. Work Limitations and Future Work

During this project, TRAIL treatment was only tested in diagnostic biopsies/surgical samples, due to a lack of sufficient viable tissue. Additionally, these samples failed to exhibit the capacity to passage in culture in either adherent or non-adherent culture. Currently, better protocols are needed to improve extraction of single cells from tumours and to prolong life of these cells under culture. Future work could involve generation of breast cancer organoid cultures (using the protocol created by Clevers group; Sachs *et al.,* 2018) with tissue from patients as they are a promising 3D model recapitulating *in vivo* tissue structural organisation, functional differentiation, chemical and mechanical signals (reviewed in Walsh *et al.* 2016).

Furthermore, Cell Titre Blue was the assay choosen to assess cell viability during the last three chapters but another assays should have been performed to detect apoptotic cells, such as: Annexin V; Live/Dead or TUNEL assays. Future experiments could also include proliferation assays (using Ki67 marker) and metabolic assays (MTT).

The tumoursphere assay was performed to assess stem cell activity after TRAIL, siFLIP and OH14 treatments. In this assay, cells capable to survive under anoikis conditions form spheroids and therefore this assay is a readout of stem/progenitor cells within the bulk population (Dontu *et al.,* 2003). It is well known that anoikis resistance is a characteristic of bCSCs and therefore during the last chapters we named these anoikis resistance cells as bCSCs. However, a second passage for some experiments would be needed to confirm the existence of stem cells as only stem cells are able to self-renew. However, when a second passage was performed for some experiments (Section 5.2.1. and 5.2.2.), the second passage confirmed the result obtained after passage one, leading us to speculate that if a second passage would have been performed for every experiment, the result would be similar to the passage one. Moreover, in parallel to every tumoursphere assay, another experiments to assess stemness should be included, for example the analyse of the surrogate stem cell markers ALDH and

CD44. Importantly, the ALDH performed in Section 5.2.7. after OH14 and TRAIL treatments corroborated the readout from the tumoursphere assays.

Another gap in Chapter 4 and 5 was not confirming c-FLIP protein levels after siFLIP treatment but these levels were analysed after thesis submission and published in Piggott *et al*., 2018. C-FLIP protein levels were decreased after siFLIP treatment in the metastatic breast cells BB3RC81, confirming the results obtained for mRNA levels.

Previous studies have demonstrated that c-FLIP survival mechanism at the DISC is primarly medialted by the c-FLIP long isoform (Yerbes *et al.,* 2011, Piggott *et al.,* 2011; Hughes *et al*., 2016). Future experiments could explore the mechanisms of the different c-FLIP isoforms at sensitising primary cells to TRAIL.

We have shown that TRAIL is efficient as a single agent in tumours that have acquired resistance to endocrine therapies, such as to tamoxifen and anastrozole by decreasing bCSCs *in vitro* and *in vivo*. However, TRAIL alone does not fully eliminate the CSC population or completely decreases tumour growth (Section 5.2.2.) and therefore it is not potent enough to prevent relapse in the future. In order to become a reliable candidate to clinical trials, TRAIL needs to be coupled with another existent anti-cancer therapies to completely eliminate CSCs, such as: other endocrine agents, taxanes or platinium agents.

In Chapter 4, we questioned whether HMECs is the best model to test drugs on normal breast cells. C-FLIP inhibition could be ideally tested on normal tissues harvested directly from mastectomies or breast reduction as primary cultures, as they are better model to test compounds in normal tissues directly from patients. Future work would involve OH14 treatments in tissues from breast reductions as tissue from mastectomies may not be considered completely normal tissue. Ideally, OH14 would be tested in normal tissues from the same patients when they undergo surgery for tumour resection.

In chapter 6, the link between EMT and TRAIL sensitivity or resistance was investigated. We proved that fibroblasts can sensitise epithelial cells from breast cancer cell lines to TRAIL but there are

mechanisms behind CAFs and TRAIL sensitivity that we do not fully understand. An important experiment could involve primary tumours with fibroblasts from the same tumour. Then TRAIL treatment could be tested in epithelial cells, with and without the respective stroma component. We would expect that the stroma would sensitise tumour cells to TRAIL in a short manner. It would be also interesting to study whether CAFs from another type of cancer could sensitise breast cancer epithelial cells to TRAIL. We have tested some important EMT markers such as E-cadherin, N-cadherin, Vimentin, Slug, Snail, IL-6 and IL-8. However, a bigger panel of markers would be needed to help to find the responsible mechanism behind CAFs and TRAIL sensitivity, such as: cytokines, fibronectins, Twist, Zeb1 and Zeb2. This big panel of markers could help to define the partial EMT that is responsible for TRAIL sensitivity.

Additionally, it would be interesting to isolate exossomes from the fibroblasts CM. Exosomes are membrane-enclosed vesicles secreted by cells and play complex roles in intercellular communication. Exosomes may act as natural vehicles for delivering protein, mRNA, or microRNA to recipient cells and it is well known that stromal fibroblasts secrete exosomes and these are responsible for drug resistance or promoting metastasis (Green *et al.,* 2016). Future experiments could involve isolation of exossomes from fibroblasts and its' nature confirmed using the exosome marker protein CD81. Then epithelial cells would be treated with exossomes alone, CM with no exossomes and CM containing exossomes to evaluate whether the exossomes could contribute to TRAIL resistance. Additionally, we could also evaluate whether exossomes increase CSC levels and whether blocking exosome release could affect these CSC levels (for example, using the GW4869, a specific inhibitor for neutral sphingomyelinase 2 that regulates packaging of the prion protein into exosomes).

BIBLIOGRAPHY

9. BIBLIOGRAPHY

A

Albertson, D. G. et al. 2003. Chromosome aberrations in solid tumors. *Nat Genet.* 34:369–376

Ali, S. et al. 2016. Molecular mechanisms and mode of tamoxifen resistance in breast cancer. Bioinformation. 12(3):135-139

Al-Hajj, M. et al. 2003. Prospective identification of tumorigenic breast cancer cells. *Proc Natl Acad Sci U S A*, 100, 3983-8.

Allred, D. C. and Medina, D. 2008. The relevance of mouse models to understanding the development and progression of human breast cancer. *Journal of mammary gland biology and neoplasia* 13(3):279-288.

Anderson, W.F. et al. 2002. Estrogen receptor breast cancer phenotypes in the Surveillance, Epidemiology, and End Results database. *Breast cancer research and treatment*.;76:27-36

Ao, A. et al. 2011. Response of estrogen receptor-positive breast cancer tumorspheres to antiestrogen treatments. *PLoS One*, volume 6 , e18810

Apostolou, P. and Fostira, F. 2013. Hereditary breast cancer: the era of new susceptibility genes. *Biomed Res Int*, 2013-747318.

Ashkenazi, A. et al. 1999. Safety and antitumor activity of recombinant soluble Apo2 ligand *J Clin Invest*. 104(2):155-62.

Ashkenazi, A. 2002. Targeting death and decoy receptors of the tumour-necrosis factor superfamily. *Nature reviews* 2(6): 420-430.

Asiedu, M. K. et al. 2011. TGFbeta/ TNF(alpha)-mediated epithelial-mesenchymal transition generates breast cancer stem cells with a claudin-low phenotype. *Cancer Res.* 71, 4707–4719.

B

Baan, R. et al. 2007. Carcinogenicity of alcoholic beverages. *Lancet Oncol,* 8, 292-3.

Bangert, A. et al. 2012. Histone deacetylase inhibitors sensitize glioblastoma cells to TRAIL-induced apoptosis by c-myc-mediated downregulation of cFLIP. *Oncogene*. 1;31(44):4677-88.

Bhowmick, N. A. et al. 2004. Stromal fibroblasts in cancer initiation and progression. *Nature.* 432(7015):332-7.

Bijangi-Vishehsarae, K. et al. 2010. 4-(4-Chloro-2-methylphenoxy)-N hydroxybutanamide (CMH) targets mRNA of the c-FLIP variants and induces apoptosis in MCF-7 human breast cancer cells. *Mol Cell Biochem*. 342(1-2):133-42

Blagodatski et al. 2014. Targeting the Wnt pathways for therapies. *Mol Cell Ther.* 2014; 2: 28. doi: 10.1186/2052-8426-2-28

Bocchinfuso, W.P. and Korach, K.S. 1997. Estrogen receptor residues required for stereospecific ligand recognition and activation. *Mol Endocrinol,* 11, 587-94.

Bonnet, D. and Dick, J. E. 1997. Human acute myeloid leukemia is organized as a hierarchy that originates from a primitive hematopoietic cell. *Nature medicine.* 3(7), 730-737.

Breal, V. 2003. Breast cancer and hormone-replacement therapy in the Million Women Study. *Lancet.*362(9382):419-27.

Britton, K. M. et al. 2011. Cancer stem cells and side population cells in breast cancer and metastasis. *Cancers*; 3:2106–30

Brisken, C. et al. 1998. A paracrine role for the epithelial progesterone receptor in mammary gland development. *Proc Natl Acad Sci U S A,* 95, 5076-81.

C

Campbell, R. A. et al. 2001. Phosphatidylinositol 3-kinase/AKT-mediated activation of estrogen receptor alpha: a new model for anti-estrogen resistance. J Biol Chem, 276, 9817-24.

Carey L. A. 2010. Through a glass darkly: advances in understanding breast cancer biology, 2000-2010. *Clin Breast Cancer*;10:188–195.

Choudhury, S. et al. 2013. Molecular Profiling of Human Mammary Gland Links Breast Cancer Risk to a p27+ Cell Population with Progenitor Characteristics. *Cell Stem Cell.* 3;13(1):117-30.

Chao. Y, et al. 2012. Partial mesenchymal to epithelial reverting transition in breast and prostate cancer metastases. *Cancer Microenviron*;5:19–28.

Cheang, M. C. et al. 2009. Ki67 index, HER2 status, and prognosis of patients with luminal B breast cancer. *J Natl Cancer Inst.* 20;101(10):736-50.

Christgen. M. et al. 2007. Identification of a distinct side population of cancer cells in the Cal-51 human breast carcinoma cell line. *Mol Cell Biochem.* 306:201–212

Clarke, R. et al. 2001. Molecular and pharmacological aspects of antiestrogen resistance. *J Steroid Biochem Mol Biol,* 76, 71-84.

Clevers, H. 2016. Modeling Development and Disease with Organoids. *Cell.* 16;165(7):1586-1597

Collaborative Group on Hormonal Factors in Breast Cancer. 1997. Breast cancer and hormone replacement therapy: collaborative reanalysis of data from 51 epidemiological studies of 52,705 women with breast cancer and 108,411 women without breast cancer. *Lancet*, 350, 1484

Collaborative Group on Hormonal Factors in Breast Cancer. 2001. Familial breast cancer: collaborative reanalysis of individual data from 52 epidemiological studies including 58,209 women with breast cancer and 101,986 women without the disease. *Lancet*, 358, 1389-99

Collaborative Group on Hormonal Factors in Breast Cancer (2002) Breast cancer and breastfeeding: collaborative reanalysis of individual data from 47 epidemiological studies in 30 countries, including 50302 women with breast cancer and 96973 women without the disease. *Lancet*, 360, 187-195

Choi, S. et al. 2014. Lessons from patient-derived xenografts for better in vitro modeling of human cancer. *Adv Drug Deliv Rev.* 79-80:222-37.

Crowder R. N. and El-Deiry W.S., 2012. Caspase-8 regulation of TRAIL-mediated cell death. *Exp Oncol*, 34(3):160-4.

D

Dai, X. et al. 2016. Cancer Hallmarks, Biomarkers and Breast Cancer Molecular Subtypes. *J Cancer.* 7(10): 1281–1294.

Daniel A.R. et al. 2011. Progesterone receptor action: defining a role in breast cancer. *Expert Rev Endocrinol Metab*. 6(3): 359–369.

Daniels, R.A. et al. 2005. Expression of TRAIL and TRAIL receptors in normal and malignant tissues. *Cell Res.* 15(6):430-8.

Day, T. W. et al. 2008. c-FLIP knockdown induces ligand-independent DR5-, FADD-, caspase-8-, and caspase-9-dependent apoptosis in breast cancer cells. *Biochemical Pharmacology* 76(12): 1694-1704.
Day, T. W. et al. 2009. c-FLIP gene silencing eliminates tumor cells in breast cancer xenografts without affecting stromal cells. *Anticancer research* 29(10):3883-3886.

DeLisle, R. K. et al. 2001. Homology modeling of the estrogen receptor subtype beta (ER-beta) and calculation of ligand binding affinities. *J Mol Graph Model*, 20,155-67.

De Miguel, D. et al. 2016. Onto better TRAILs for cancer treatment. *Cell Death Differ.* 23(5): 733–747.

DeOme, K. B. et al. 1959. Development of mammary tumors from hyperplastic alveolar nodules transplanted into gland-free mammary fat pads of female C3H mice. *Cancer Res*;19:515–520.

DeRose et al. 2013. Tumor grafts derived from women with breast cancer authentically reflect tumor pathology, growth, metastasis and disease outcomes. Nature Medicine.; Chapter 14:Unit14.23.

Doherty, M. et al. 2016. Cancer Stem Cell Plasticity Drives Therapeutic Resistance. *Cancers Basel*. 8(1):8

Dontu, G., et al. 2003. Stem cells in normal breast development and breast cancer. *Cell Prolif*. 36(Suppl 1):59–72.

Dontu, G. et al. 2003. In vitro propagation and transcriptional profiling of human mammary stem/progenitor cells. *Genes & Development* 17(10): 1253-1270.

Dontu, G. et al. 2004. Role of Notch signaling in cell-fate determination of human mammary stem/progenitor cells. *Breast cancer research* 6(6): R605-615.

Drews-Elger, K. et al. 2014. Primary breast tumor-derived cellular models: characterization of tumorigenic, metastatic, and cancer-associated fibroblasts in dissociated tumor (DT) cultures. *Breast Cancer Res Treat,* 144(3):503-17 .

Duiker, E. W. et al. 2006. The clinical trail of TRAIL. *European journal of cancer* .42(14): 2233-2240.

E

Eccles, S. A. et al. 2013. Critical research gaps and translational priorities for the successful prevention and treatment of breast cancer *Breast Cancer Research*, 15:R92

Ellis, I. O. et al. 1992. Pathological prognostic factors in breast cancer. II. Histological type. Relationship with survival in a large study with long-term follow-up. *Histopathology*. 20(6):479-89.

Ellis, I. O. et al. 2003. Invasive breast carcinoma. In: Tavassoli FA, Devilee P, editors. Tumours of the Breast and Female Genital Organs. *Lyon: IARC Press*; 2003. pp. 13–59.

Elston, C. W. and Ellis, I.O. 1991. Pathological prognostic factors in breast cancer. I. The value of histological grade in breast cancer: experience from a large study with long-term follow-up. Histopathology.19(5):403-10.

Encarnación, C. A. et al. 1993. Measurement of steroid hormone receptors in breast cancer patients on tamoxifen. *Breast Cancer Res Treat,* 26, 237-46.

F

Farnie, G. et al. 2007. Novel cell culture technique for primary ductal carcinoma in situ: role of Notch and epidermal growth factor receptor signaling pathways. *J Natl Cancer Inst*. 18;99(8):616-27.

Fan, Y. et al. 2015. Upregulation of Fas in epithelial ovarian cancer reverses the development of resistance to cisplatin. *BMB Rep*. 2015;48(1):30–35.

Faridi, J. et al. 2003. Expression of constitutively active Akt-3 in MCF-7 breast cancer cells reverses the estrogen and tamoxifen responsivity of these cells in vivo. Clin Cancer Res, 9, 2933-9.

Fidler, I.J. 2003. Understanding bone metastases: the key to the effective treatment of prostate cancer. *Clin Adv Hematol Oncol.* 1(5):278-9.

Ffrench et al. 2014. Developing ovarian cancer stem cell models: laying the pipeline from discovery to clinical intervention. *Mol Cancer*. 13:262.

Forero-Torres, A. et al. 2015. TBCRC 019: A Phase II Trial of Nanoparticle Albumin-Bound Paclitaxel with or without the Anti-Death Receptor 5 Monoclonal Antibody Tigatuzumab in Patients with Triple-Negative Breast Cancer. 21(12):2722-9.

Fox, E. M., et al. 2012. Abrogating endocrine resistance by targeting ERα and PI3K in breast cancer. *Front Oncol.* 2, 45.

French, R. et al. 2015 Cytoplasmic levels of cFLIP determine a broad susceptibility of breast cancer stem/progenitor-like cells to TRAIL. *Mol Cancer* 14: 209.

Freudenberg, J. A. 2009. The role of HER2 in early breast cancer metastasis and the origins of resistance to HER2-targeted therapies. *Exp Mol Pathol.* 87(1): 1–11.

Fulda, S. et al. 2010. Targeting mitochondria for cancer therapy. *Nat Rev Drug Discov.* 9(6):447–464.

Fuqua, S. A. et al. 2000. A hypersensitive estrogen receptor-alpha mutation in premalignant breast lesions. *Cancer Res,* 60, 4026-9.

G

Garcia-Closas, M. 2006. Clarifying breast cancer risks associated with menopausal hormone therapy. *Lancet Oncol.* 7(11):885-6.

Gasch et al. 2017. Catching moving targets: cancer stem cell hierarchies, therapy-resistance & considerations for clinical intervation. *Molecular Cancer*. 16:43

Gee, J.M., et al. 2005. Epidermal growth factor receptor/HER2/insulin-like growth factor receptor signalling and oestrogen receptor activity in clinical breast cancer. *Endocr Relat Cancer,* 12 Suppl 1:S99-S111.

Giannoni. E. et al. 2010. Reciprocal activation of prostate cancer cells and cancerassociated fibroblasts stimulates epithelialmesenchymal transition and cancer stemness. *Cancer Res*. 70:6945–6956.

Ginestier, C. et al. 2007. ALDH1 is a marker of normal and malignant human mammary stem cells and a predictor of poor clinical outcome. *Cell Stem Cell,* 1, 555-67.

Goncharenko-Khaider, N., et al. 2013. Biological Significance of Apoptosis in Ovarian Cancer: TRAIL Therapeutic Targeting. *Medicine*. Chapter 11.

Gottardis, M. M. and Jordan, V.C. 1988. Development of tamoxifen-stimulated growth of MCF-7 tumors in athymic mice after long-term antiestrogen administration. *Cancer Res*;48:5183–7.

Green, S. and Chambon, P. 1986. A superfamily of potentially oncogenic hormone receptors. *Nature,* 324, 615-7.

Green, T. M. et al. 2015. Breast Cancer-Derived Extracellular Vesicles: Characterization and Contribution to the Metastatic Phenotype. *Biomed Res Int*. 2015: 634865.

Gupta, P.B. et al. 2011. Stochastic State Transitions Give Rise to Phenotypic Equilibrium in Populations of Cancer Cells. *Cell.* 146(4):633-44.

Gupta, G.P. and Massagué, J. 2006. Cancer metastasis: building a framework. *Cell*. 127(4):679-95.

Gustafsson, J. A. 1999. Estrogen receptor beta--a new dimension in estrogen mechanism of action. *J Endocrinol.* 163(3):379-83.

H

Hajra, K. M. et al. 2002. The SLUG zinc-finger protein represses E-cadherin in breast cancer. *Cancer Res.* 62:1613–1618.

Hanahan, D. and Weinberg, R. A. 2000. The hallmarks of cancer. *Cell*. 100(1),. 57-70.

Harrison, H. et al. 2013. Oestrogen increases the activity of oestrogen receptor negative breast cancer stem cells through paracrine EGFR and Notch signalling. *Breast Cancer Res*, 15,R21.

Hartmann L. C. et al. 2005. Benign breast disease and the risk of breast cancer. *N Engl J Med*. (3):229-37.

Hashida, S. et al. 2015. Acquisition of cancer stem cell-like properties in non-small cell lung cancer with acquired resistance to afatinib. *Cancer Sci*;106(10):1377–1384.

Hayes, E. L. and Lewis-Wambi J.S. 2015. Mechanisms of endocrine resistance in breast cancer: an overview of the proposed roles of noncoding RNA. *Breast Cancer Res.* 17; 17:40.

Herschkowitz, J. I. 2007. Identification of conserved gene expression features between murine mammary carcinoma models and human breast tumors. *Genome Biol*. 8(5):R76.

Hiscox, S. et al. 2006. Tamoxifen resistance in MCF7 cells promotes EMT-like behaviour and involves modulation of beta-catenin phosphorylation. *Int J Cancer*; 118(2):290-301.

Howell, A. et al.2002. Fulvestrant, formerly ICI 182,780, is as effective as anastrozole in postmenopausal women with advanced breast cancer progressing after prior endocrine treatment. *J Clin Oncol,* 20, 3396-403.

Howell, A. and Sapunar, F. 2011. Fulvestrant revisited: efficacy and safety of the 500-mg dose. *Clin Breast Cancer,* 11, 204-10.

Hu, S. et al. 1997. A novel family of viral death effector domain-containing molecules that inhibit both CD-95 and tumor necrosis factor receptor-1-induced apoptosis*. J. Biol. Chem*. 272, 9621-9624.

Hu, R. et al. 2011. Androgen receptor expression and breast cancer survival in postmenopausal women. *Clin Cancer Res.* 1;17(7):1867-74.

Hughes, M. A. et al. 2016. Co-operative and Hierarchical binding of c-FLIP and Caspase-8: A unified Model defines how c-FLIP isoforms differentially control cell fate. *Molecular Cell.* 61, 834-849.

Hutcheson, I. R. et al. 2011. Fulvestrant-induced expression of ErbB3 and ErbB4 receptors sensitizes oestrogen receptor-positive breast cancer cells to heregulin β1. *Breast Cancer Res,* 13, R29.

I

Irmler, M. et al. 1997. Inhibition of death receptor signals by cellular FLIP. *Nature*. 388, 190-195.

Inman, J. L. et al. 2015. Mammary gland development: cell fate specification, stem cells and the microenvironment. *Development*. 142(6):1028-42.

Itoh, T., et al. 2005. Letrozole-, anastrozole-, and tamoxifen-responsive genes in MCF-7aro cells: a microarray approach. *Mol Cancer Res,* 3, 203–218.

J

Janik, K. et al. 2016. Efficient and simple approach to in vitro culture of primary epithelial cancer cells. *Biosci Rep*. 36(6): e00423.

Javed, A. and Lteif, A. 2013 Development of the Human Breast. *Semin Plast Surg*. 27(1):5-12.

Jemal, A. and Bray, F. 2011. Global cancer statistics. *Cancer J Clin*, 61, 69-90.

Jiang. et al. 2009. Aldehyde dehydrogenase 1 is a tumor stem cell-associated marker in lung cancer. Mol Cancer Res. 7(3):330–8.

Jolly, M. K. et al. 2017. EMT and MET: necessary or permissive for metastasis? *Mol Oncol.* 11(7): 755–769.

Jung, Y. and Lippard, S. J. 2007. Direct cellular responses to platinum-induced DNA damage. Chem Rev. 107(5):1387–1407.

L

Lakis, S. et al. 2014. The androgen receptor as a surrogate marker for molecular apocrine breast cancer subtyping. *Breast.* 23(3):234-43

Lu, B. et al. 1998. Estrogen receptor-β mRNA variants in human and murine tissues. Mol Cell Endocrinol. 138:199–203

LeBlanc, H. N. and Ashkenazi, A. 2003. Apo2L/TRAIL and its death and decoy receptors. *Cell Death Differ.* 10(1):66-75.

Lee, Y.J. et al. 2012. Molecular mechanism of SAHA on regulation of autophagic cell death in tamoxifen-resistant MCF-7 breast cancer cells. *Int J Med Sci*, 9, 881-93.

Lewis-Wambi, J.S. and Jordan, V.C. 2009. Estrogen regulation of apoptosis: how can one hormone stimulate and inhibit? *Breast Cancer Res*, 11-206.

Liu, Y. et al., 2014. Lack of correlation of stem cell markers in breast cancer stem cells. *Br J Cancer.* 110(8): 2063–2071.

Lopez-Novoa, J. M. and Nieto, M.A. 2009. Inflammation and EMT: an alliance towards organ fibrosis and cancer progression. *EMBO Mol Med*; 1(6–7):303–14

Luo, Y. et al. 2012. ALDH1A Isozymes Are Markers of Human Melanoma Stem Cells and Potential Therapeutic Targets. *Stem Cells*. 30(10): 2100–2113.

K

Kabos, P. et al. 2011. Cytokeratin 5 positive cells represent a steroid receptor negative and therapy resistant subpopulation in luminal breast cancers. *Breast Cancer Res Treat.* 128:45–55

Kalluri, K. and Weinberg, R. 2009. The basics of epithelial-mesenchymal transition. *J Clin Invest*. 119(6): 1420-1428.

Kataoka, T. et al. 2000. The caspase-8 inhibitor FLIP promotes activation of NF-kappaB and Valastyan and Weinberg 2011 Tumor Metastasis: Molecular Insights and Evolving Paradigms *Cell.* 147(2): 275–292

Katayama. et al. 2010. Modulation of Wnt signaling by the nuclear localization of cellular FLIP-L. *J Cell Sci.* 1:23-8

Keane, M. M. et al. 1999. Chemotherapy augments TRAIL-induced apoptosis in breast cell lines. *Cancer Res.* 59(3):734-41.

Key, T. J., et al. 2001. Epidemiology of breast cancer. *Lancet Oncology* 2 133–140.

Key, T. J. et al. 2002. Endogenous sex hormones and breast cancer in postmenopausal women: reanalysis of nine prospective studies. *Journal of the National Cancer Institute* 94 606–616.

Kirkin, V. et al. 2004. The role of Bcl-2 family members in tumorigenesis. *Biochim Biophys Acta*. 1644(2–3):229–249.

Knight, W. A. et al. 1980. Hormone receptors in primary and advanced breast cancer. *Clin Endocrinol Metab,* 9, 361-8.

Kocanova, S. et al. 2010. Ligands specify estrogen receptor alpha nuclear localization and degradation. *BMC Cell Biol,* 10, 11-98.

Kobayashi, S. et al. 2005. Interleukin-6 contributes to Mcl-1 up-regulation and TRAIL resistance via an Akt-signaling pathway in cholangiocarcinoma cells. *Gastroenterology*.128(7):2054-65.

Kordon, E. C. and Smith, G.H (1998). An entire functional mammary gland may comprise the progeny from a single cell. *Development.* 125(10):1921-30.

Korkaya, H. and Malik F. 2013 Breast Cancer Stem Cells: Responsible for Therapeutic Resistance and Relapse*? Breast Cancer Metastasis and Drug Resistance*, 385-398

Krueger, et al. 1999. Cellular FLICE-inhibitory protein splice variants inhibit different steps of caspase-8 activation at the CD95 death-inducing signaling complex *J. Biol. Chem*., 276 (2001), pp. 20633–20640.

Kruyt, F. A. 2008. TRAIL and cancer therapy. *Cancer Lett* 263: 14

Kuiper, G. G. et al. 1996. Cloning of a novel receptor expressed in rat prostate and ovary. *Proc Natl Acad Sci U S A,* 93, 5925-30.

Kumar, R. et al. 1996. Overexpression of HER2 modulates bcl-2, bcl-XL, and tamoxifen-induced apoptosis in human MCF-7 breast cancer cells. *Clin Cancer Res,* 2, 1215-9.

Kuperwasser, C. et al 2004. Reconstruction of functionally normal and malignant human breast tissues in mice. *Proc Natl Acad Sci U S A*. 6;101(14):4966-71.

Kyprianou, N. et al. 1991. Programmed cell death during regression of the MCF-7 human breast cancer following estrogen ablation. *Cancer Res,* 51, 162–166.

L

Lapidot, T. 1994. A cell initiating human acute myeloid leukaemia after transplantation into SCID mice. *Nature*, 367, 645–648.

Li, Q. Q. et al., 2009. Twist1-mediated Adriamycin-induced epithelial-mesencymal transition relates to multidrug resistance and invasive potential in breast cancer cells. *Clin Cancer Res*. 15(8):2657-65.

Liu, S. et al. 2014. Breast Cancer Stem Cells Transition between Epithelial and Mesenchymal States Reflective of their Normal Counterparts. *Stem Cell Reports*. ;2(1):78-91.

Luu, T. H. et al. 2008. A phase II trial of vorinostat (suberoylanilide hydroxamic acid) in metastatic breast cancer: a California Cancer Consortium study. Clin Cancer Res 4(21):7138-7142

M

Ma, S. et al. 2008. CD133+ HCC cancer stem cells confer chemoresistance by preferential expression of the Akt/PKB survival pathway. *Oncogene*. 27(12):1749–1758. doi: 10.1038/sj.onc.1210811.

Madjd, Z. et al. 2009. $CD44^+$ cancer cells express higher levels of the anti-apoptotic protein Bcl-2 in breast tumours. *Cancer Immun*. 9:4.

Malhotra, G. K. et al. 2010. Histological, molecular and functional subtypes of breast cancers. Cancer Biol Ther. 10(10): 955–960.

Malhotra, G. K. et al. 2011 Shared signaling pathways in normal and breast cancer stem cells. *J Carcinog*. 2011; 10:38.

Malin, D. et al. 2011. Enhanced Metastasis Suppression by Targeting TRAIL Receptor 2 in a Murine Model of Triple-Negative Breast Cancer. *Clin Cancer Res*. 17(15):5005-15.

Mallepell, S. et al. 2006. Paracrine signaling through the epithelial estrogen receptor alpha is required for proliferation and morphogenesis in the mammary gland. *Proc Natl Acad Sci U S A,* 103, 2196-201.

Mallini, P. et al. 2013. Epithelial-to-mesenchymal transition: What is the impact on breast cancer stem cells and drug resistance. *Cancer Treat Rev* S0305-7372(13)00197-7

Mani, S. A. et al. 2008. The epithelial-mesenchymal transition generates cells with properties of stem cells. *Cell*.;133:704–715.

Marsden, C. G. et al. 2012. A novel in vivo model for the study of human breast cancer metastasis using primary breast tumor-initiating cells from patient biopsies". *BMC Cancer*. 10;12:10.

Mariani, S. M. et al. 1997. Interleukin 1 beta-converting enzyme related proteases/caspases are involved in TRAIL-induced apoptosis of myeloma and leukemia cells. *The Journal of cell biology* 137(1):221-229.

Martinez-Outschoorn, U.E. et al. 2011. Anti-estrogen resistance in breast cancer is induced by the tumor microenvironment and can be overcome by inhibiting mitochondrial function in epithelial cancer cells. *Cancer Biol Ther*. 15; 12(10): 924–938.

McDonnel,l D. P. and Norris, J.D. 2002. Connections and Regulation of the Human Oestrogen Receptor. *Science* 296, 1642–1964.

McDonnell, D. P. 2006. Mechanism-based discovery as an approach to identify the next generation of estrogen receptor modulators. *FASEB J*, 20, 2432-4.

McGrogan, B. T. et al. 2008. Taxanes, microtubules and chemoresistant breast cancer. *Biochim Biophys Acta*. 1785:96–132

Mawji, I. A. et al. 2007. A chemical screen identifies anisomycin as an anoikis sensitizer that functions by decreasing FLIP protein synthesis. *Cancer Res* 67:8307–8315.

Micalizzi, D. S. et al. 2010. Epithelial–mesenchymal transition in cancer: parallels between normal development and tumor progression. *J Mammary Gland Biol Neoplasia*; 15:117

Michalet, S. and Dijoux-Franca, MG. (2009). ABC transporters and resistance to antibiotics. In: Ahcne B, Jean B, Jacques R, editors. ABC transporters and multidrug resistance. Hoboken, NJ, USA: *Wiley;* pp 177–193.

Miller, W. R. 2003. Aromatase inhibitors: mechanism of action and role in the treatment of breast cancer. *Semin Oncol,* 14, 3-11.

Miller, W.R. and Larionov, A. 2010.Changes in expression of oestrogen regulated and proliferation genes with neoadjuvant treatment highlight heterogeneity of clinical resistance to the aromatase inhibitor, letrozole. *Breast Cancer Res,* 12, R52.

Mitra, A. et al. 2015. EMT, CTCs and CSC in tumor relapse and drug-resistance. *Oncotarget,* ;6:10697–10711. doi: 10.18632/oncotarget.4037.

Moasser, M .M. 2007. The oncogene HER2; Its signaling and transforming functions and its role in human cancer pathogenesis*. Oncogene*. 26(45): 6469–6487. doi: 10.1038/sj.onc.1210477

Moore, N. and Lyle, S. 2011. Quiescent, slow-cycling stem cell populations in cancer: a review of the evidence and discussion of significance. *J Oncol.*

Morel, G. W et al. 2012. EMT inducers catalyze malignant transformation of mammary epithelial cells and drive tumorigenesis towards claudin-low tumors in transgenic mice. *PLoS Genetics* 8 e1002723.

Moreno-Bueno, G. et al. 2008. Transcriptional regulation of cell polarity in EMT and cancer. *Oncogene* 27, 6958–6969.

Moussa, O. et al. 2012. Biomarker discordance: prospective and retrospective evidence that biopsy of recurrent disease is of clinical utility. *Cancer Biomark.* 12:231–239

Moustakas, A. and Heldin, C. H. 2007. Signaling networks guiding epithelial–mesenchymal transitions during embryogenesis and cancer progression. *Cancer Sc*i;10:1512–2034

Mueller, M. M. and Fusenig, N. E. 2004. Friends or foes—bipolar effects of the tumour stroma in cancer. *Nat Rev Cancer* 4:839–849.

Musgrove, E. A. and Sutherland, R.L. 2009. Biological determinants of endocrine resistance in breast cancer. *Nat Rev Cancer*, 9, 631-43.

N

Neve, R. M. et al. 2006. A collection of breast cancer cell lines for the study of functionally distinct cancer subtypes. *Cancer cell* 10(6):515-527.

Nicholson, R. I. et al. 2004. Growth factor-driven mechanisms associated with resistance to estrogen deprivation in breast cancer: new opportunities for therapy. *Endocr Relat Cancer,* 11, 623–641.

O

O'Brien, C. S. et al. 2009. Resistance to endocrine therapy: are breast cancer stem cells the culprits? J *Mammary Gland Biol Neoplasia*, 14, 45-54.

Orimo A and Weinberg RA. 2006. Stromal fibroblasts in cancer: a novel tumor-promoting cell type. *Cell Cycle* 5:1597–1601

Osborne, C. K. et al. 2004. Fulvestrant: an oestrogen receptor antagonist with a novel mechanism of action. *Br J Cancer,* 90 Suppl 1:S2-6.

Osborne, C. K. et al. 2003. Role of the estrogen receptor coactivator AIB1 (SRC-3) and HER-2/neu in tamoxifen resistance in breast cancer. *J Natl Cancer Inst*.; 95:353–61.

Oztürk S., et al. 2012. Cellular FLICE-like inhibitory proteins (c-FLIPs): fine-tuners of life and death decisions. *Exp. Cell Res*., 318, 1324–1331

P

Palena, C. et al., 2012. Influence of IL-8 on the epithelial-mesenchymal transition and the tumour microenvironment. 8(6):713-722.

Papadaky, M. A. et al. 2014. Co-expression of putative stemness and epithelial-to-mesenchymal transition markers on single circulating tumour cells from patients with early and metastatic breast cancer. *BMC Cancer*. 3;14:651.

Pardal, R. et al. 2005. Stem cell self-renewal and cancer cell proliferation are regulated by common networks that balance the activation of proto-oncogenes and tumor suppressors. *Cold Spring Harb Symp Quant Biol*. (70):177–85.

Parkin, D. M. et al. 2011. The fraction of cancer attributable to lifestyle and environmental factors in the UK in 2010. *Br J Cancer,* 6, 105.

Peng, Q. et al. 2013. Biological characteristics and genetic heterogeneity between carcinoma-associated fibroblasts and their paired normal fibroblasts in human breast cancer. *PLoS One.* 8:e60321.

Perou, C. M. et al. 2000. Molecular portraits of human breast tumours. *Nature* 406:747–752

Perou, C. M. et al. 2010. Clinical implementation of the intrinsic subtypes of breast cancer. *Lancet Oncol.* 11(8):718-9;

Perey, L. et al. 2007. Clinical benefit of fulvestrant in postmenopausal women with advanced breast cancer and primary or acquired resistance to aromatase inhibitors: final results of phase II Swiss Group for Clinical Cancer Research Trial (SAKK 21/00). *Ann Oncol,* 18, 64-9.

Phillips, T. M. et al. 2006 The response of CD24(-/low)/CD44+ breast cancer-initiating cells to radiation. *J Natl Cancer Inst*. 98(24):1777-85.

Piggott, L. et al. 2011. Suppression of apoptosis inhibitor c-FLIP selectively eliminates breast cancer stem cell activity in response to the anti-cancer agent, TRAIL *Breast Cancer Res*; 13: R88

Piggott, L. et al. 2018. Acquired resistance of ER- positive breast cancer to endocrine treatment confers an adaptive sensitivity to TRAIL through post-translational downregulation of c-FLIP. *Clin Cancer Res*. pii: clincanres.1381.2017.

Pike, M. C. 1993. Estrogens, progestogens, normal breast cell proliferation, and breast cancer risk. *Epidemiol Rev*. 15(1):17-35.

Pink, J. J. et al. 1997. Cloning and characterization of a 77-kDa oestrogen receptor isolated from a human breast cancer cell line. *Br J Cancer*, 75, 17-27.

Pinto, C. A. et al. 2013. Breast cancer stem cells and epithelial mesenchymal plasticity - Implications for chemoresistance. *Cancer Lett.* 341(1):56-62.

Pitti, R. M. et al. 1996. Induction of apoptosis by Apo-2 ligand, a new member of the tumor necrosis factor cytokine family. *The Journal of biological chemistry* 271(22):12687-12690.

Place, A. E. et al. 2011. The microenvironment in breast cancer progression: biology and implications for treatment. *Breast cancer research* 13(6):227.

Pourreyron, C. et al. 2011. Feeder layers: co-culture with nonneoplastic cells. *Methods Mol Biol.* 731:467-70.

Prat, A. et al. 2010. Phenotypic and molecular characterization of the claudin-low intrinsic subtype of breast cancer. *Breast Cancer Res*, 12, R68.

Ponti, D. et al. 2005. Isolation and in vitro propagation of tumorigenic breast cancer cells with stem/progenitor cell properties. *Cancer research* 65(13):5506-5511.

Q

Quintavalle, C. et al. 2010. c-FLIPL enhances anti-apoptotic Akt functions by modulation of Gsk3β activity. *Cell Death Differ.* 17(12):1908-16.

Rahman, M. et al. 2009. TRAIL induces apoptosis in triple-negative breast cancer cells with a mesenchymal phenotype. Breast Cancer Res Treat 113:217-230.

Reya, T. et al. 2001. Stem cells, cancer, and cancer stem cells. *Nature*, 414, 105–11.

R

Radisky, S. R. and Radisky, D.C. 2010. Matrix Metalloproteinase-Induced Epithelial-Mesenchymal Transition in Breast Cancer. *J Mammary Gland Biol Neoplasia*. 15(2): 201–212.

Rahman, M. et al. 2009. The TRAIL to targeted therapy of breast cancer. *Adv Cancer Res*. 103: 43–73.

Rao, X. et al. 2001. MicroRNA-221/222 confers breast cancer fulvestrant resistance by regulating multiple signaling pathways. *Oncogene*, 30, 1082-97.

Rausch, L. K. et al. 2017. The Linkage between Breast Cancer, Hypoxia, and Adipose Tissue. *Front Oncol.* 7: 211.

Ricardo, S. et al. 2011. Breast cancer stem cell markers CD44, CD24 and ALDH1: expression distribution within intrinsic molecular subtype. *J Clin Pathol*, 64, 937-46.

Riggins, R. B. et al. 2006. Physical and functional interactions between Cas and c-Src induce tamoxifen resistance of breast cancer cells through pathways involving epidermal growth factor receptor and signal transducer and activator of transcription 5b. *Cancer Res,* 66, 7007-15.

Roger, P., et al. 2001. Decreased expression of estrogen receptor beta protein in proliferative preinvasive mammary tumors. *Cancer Res,* 61, 2537-41.

Roodi, N., et al. 1995. Estrogen receptor gene analysis in estrogen receptor-positive and receptor-negative primary breast cancer. *J Natl Cancer Inst*, 87, 446-51.

Russo, J. et al. 1979. Susceptibility of the mammary gland to carcinogenesis: I. Differentiation of the mammary gland as determinant of tumor incidence and type of lesion. *Am J Pathol*, 96, 721-736.

S

Sabnis, G. et al. 2007. Inhibition of the phosphatidylinositol 3-kinase/Akt pathway improves response of long-term estrogen-deprived breast cancer xenografts to antiestrogens. *Clin Cancer Res,* 13, 2751-7.

Sachs, N. et al. 2018. A Living Biobank of Breast Cancer Organoids Captures Disease Heterogeneity. *Cell*. 172(1-2):373-386.e10.

Safa, A. R. et al. 2008. Cellular FLICE-like inhibitory protein (CFLIP): a novel target for cancer therapy Curr Cancer Drug Targets, 8(1):37-46.

Safa, A. R. and Pollok K. E. 2011. Targeting the Anti-Apoptotic Protein c-FLIP for Cancer Therapy. *Cancers*. 3, 1639-1671;

Sasano, H. et al. 1999. Effects of aromatase inhibitors on the pathobiology of the human breast, endometrial and ovarian carcinoma. *Endocr Relat Cancer,* 6, 197–204.

Schauer, I. G. et al. 2011. Cancer-associated fibroblasts and their putative role in potentiating the iniciation and development of epithelial ovarian cancer. *Neoplasia.* 13(5): 393-405.

Seo, S. K. et al. 2011. Histone deacetylase inhibitors sensitize human non-small cell lung cancer cells to ionizing radiation through acetyl p53-mediated c-myc down-regulation. *Journal of thoracic oncology* 6(8):1313-1319.

Shah, N. R. and Wong, T. 2006. Current breast cancer risks of hormone replacement therapy in postmenopausal women. *Expert Opin Pharmacother*. 7(18): 2455–2463.

Shanker, A. et al. 2008. Treating metastatic solid tumors with bortezomib and a tumor necrosis factor-related apoptosis-inducing ligand receptor agonist antibody. *Journal of the National Cancer Institute* 100(9): 649-662.

Shankar, S. et al. 2009. Suberoylanilide hydroxamic acid (Zolinza/vorinostat) sensitizes TRAIL-resistant breast cancer cells orthotopically implanted in BALB/c nude mice. *Mol Cancer Ther*;8:1596-605.

Shaw, F. L. et al. 2012. A detailed mammosphere assay protocol for the quantification of breast stem cell activity J Mammary Gland Biol Neoplasia. 17(2):111-7

Scheel C. et al. 2011. Paracrine and autocrine signals induce and maintain mesenchymal and stem cell states in the breast. Cell, 145, 926–940.

Shen, D. et al. (2012). Cisplatin resistance: a cellular self-defense mechanism resulting from multiple epigenetic and genetic changes. *Pharmacol Rev.* 64(3):706–721.

Shirley, S. and Micheau, O. 2010. Targeting c-FLIP in cancer. Cancer letters.

Siegelin, M.D . and Siegelin, Y. 2011. Brain Tumors – Current and Emerging Therapeutic Strategies, Chapter 13 Novel Therapeutic Venues for Glioblastoma: Novel Rising Preclinical Treatment Medicine*, Oncology*

Simpson, P.T. et al. 2005. Molecular evolution of breast cancer. *J Pathol*, 205, 248-54.

Singh A. and Settleman J. 2010. EMT, cancer stem cells and drug resistance: An emerging axis of evil in the war on cancer. *Oncogene*;29:4741–4751. doi: 10.1038/onc.2010.215.

Slamon, D. J. 1987. Human breast cancer: correlation of relapse and survival with amplification of the HER-2/neu oncogene. *Science.* 9;235(4785):177-82.

Smalley, M. and Ashworth, A. 2003. Stem cells and breast cancer: a field in transit. Nature Reviews Cancer 3, 832-844. Doi:10.1038/nrc1212

Smalley, M. et al., 2007. Regulator of G-protein signalling 2 mRNA is differentially expressed in mammary epithelial subpopulations and over-expressed in the majority of breast cancers. *Breast Cancer Research.* 9(6):R85.

Smalley, M. et al. 2012. Breast cancer stem cells: Obstacles to therapy. *Cancer Lett*, 338, 57-62.

Sokol, E. S. et al. 2015. Growth of human breast tissues from patient cells in 3D hydrogel scaffolds. *Breast Cancer Research.* 128:19.

Song, R. X. and Santen, R.J. 2003. Apoptotic action of estrogen. *Apoptosis,* 8, 55–60.

Soon, P.S. et al. 2013. Breast cancer-associated fibroblasts induce epithelial-to-mesencgymal transition in breast cancer cells. *Endocr Relat. Cancer*. 20(1):1-12- doi10.1530/ERC-12-0227.

Sorlie, T. et al. 2001. Gene expression patterns of breast carcinomas distinguish tumor subclasses with clinical implications. *Proc Natl Acad Sci U S A,* 98, 10869-74.

Sorlie, T. et al. 2003. Repeated observation of breast tumor subtypes in independent gene expression data sets. *Proc Natl Acad Sci U S A*, 100, 8418-23.

Sorlie, T. et al. 2006. Gene expression profiles do not consistently predict the clinical treatment response in locally advanced breast cancer. *Mol Cancer Ther,* 5, 2914-8.

Spaeth, E.L. et al. 2013. Mesenchymal CD44 expression contributes to the acquisition of an activated fibroblast phenotype via TWIST activation in the tumor microenvironment. Cancer Res 73:5347–5359

Speirs, V. 2002. Distinct expression patterns of ER alpha and ER beta in normal human mammary gland. *J Clin Pathol.* 55(5):371-4.

Steeg P. S. 2006. Tumor metastasis: mechanistic insights and clinical challenges. *Nat Med,* 12(8):895-904.

Sternlicht, M.D. 2006. Key stages in mammary gland development: The cues that regulate ductal branching morphogenesis. *Breast Cancer Res.* 8(1): 201.

Straussman R., et al. 2012. Tumour micro-environment elicits innate resistance to RAF inhibitors through HGF secretion. *Nature* 487:500–504

Suetsugu, A. et al. 2013. Imaging exosome transfer from breast cancer cells to stroma at metastatic sites in orthotopic nude-mouse models. *Advanced Drug Delivery Reviews.* 65(3):383–390.

Sun, M. et al. 2015. Enhanced efficacy of chemotherapy for breast cancer stem cells by simultaneous suppression of multidrug resistance and antiapoptotic cellular defense. *Acta Biomater*;28:171–182.

Swerdlow A. J. and Jones M.E. 2007. Ovarian cancer risk in premenopausal and perimenopausal women treated with Tamoxifen: a case–control study. *Br J Cancer*. 96(5): 850–855.

T

Tan, E.Y. et al. 2013. ALDH1 expression is enriched in breast cancers arising in young women but does not predict outcome. *Br J Cancer*. 109:109–113.

Tao, L. et al. 2011. Repression of mammary stem/progenitor cells by p53 is mediated by Notch and separable from apoptotic activity. *Stem cells*. 29(1):119-127.

Takebe, N. et al. 2011. Breast cancer growth and metastasis: interplay between cancer stem cells, embryonic signaling pathways and epithelial-to-mesenchymal transition.*Breast Cancer Res*. 13, 211

Taube J. H. et al. 2010. Core epithelial-to-mesenchymal transition interactome gene-expression signature is associated with claudinlow and metaplastic breast cancer subtypes, Proc. *Natl. Acad. Sci. USA* 107, 15449–15454.

Tentler, J. J. et al. 2012. Patient-derived tumour xenografts as models for oncology drug development. *Nat Rev Clin Oncol.;*9(6):338-50.

Teschendorff, A. E. et al. 2007. Miremadi A, Pinder SE, Ellis IO, Caldas C. An immune response gene expression module identifies a good prognosis subtype in estrogen receptor negative breast cancer. *Genome Biol*. 8:R157

Thiantanawat, A., et al. 2003. Signaling pathways of apoptosis activated by aromatase inhibitors and antiestrogens. *Cancer Res,* 63, 8037–8050.

Thome, M. et al. 1997 Viral FLICE-inhibitory proteins (FLIPs) prevent apoptosis induced by death receptors. *Nature*. 386, 517-521.

Thompson, A. M. et al 2010. Prospective comparison of switches in biomarker status between primary and recurrent breast cancer: the Breast Recurrence In Tissues Study (BRITS). *Breast Cancer Res.* 12(6):R92.

To, K. W.et al. 2015. Vatalanib sensitizes ABCB1 and ABCG2-overexpressing multidrug resistant colon cancer cells to chemotherapy under hypoxia. *Biochem pharmacol*. 97(1);27–37.

Tsai, M. J. and O'Malley, B.W. 1994. Molecular mechanisms of action of steroid/thyroid receptor superfamily members. *Annu Rev Biochem*. 63:451-86.

Turin, I. et al. 2014. In Vitro Efficient Expansion of Tumor Cells Deriving from Different Types of Human Tumor Samples. *Med. Sci.* 2(2), 70-81.

V

Vainio, H. and Bianchini, F. 2002. International Agency for Research on Cancer: Weight Control and Physical Activity. Lyon, France, volume 6 IARC

Valastyan, S. and Weinberg, R.A. 2011. Tumor metastasis: molecular insights and evolving paradigms. *Cell.* 147(2):275-92.

Valent, P. et al. 2012. Cancer stem cell definitions and terminology: the devil is in the details. *Nat Rev Cancer.* 12(11):767-75.

Vandeven, H. and Pensler, J. 2017. Gynecomastia.

Vanharanta, S. and Massague, J. 2013. Origins of Metastatic Traits. *Cancer Cell*. 24(4):410-21

Vargo-Gogola, T. and Rosen, J.M. 2007. Modelling breast cancer: one size does not fit all. *Nature reviews* 7(9):659-672.

Visvader, J. E. 2009. Keeping abreast of the mammary epithelial hierarchy and breast tumorigenesis. *Genes Dev*. 15;23(22):2563-77. doi: 10.1101/gad.1849509.

Visvader J. E. and Lindeman G.J. 2012. Cancer stem cells: Current status and evolving complexities. *Cell Stem Cell*, ;10:717–728.

Visvader, J. E. and Stingl, J. 2014) Mammary stem cells and the differentiation hierarchy: current status and perspectives. *Genes Dev*; 28(11): 1143–1158.

W

Walsh, A.J. et al. 2016. Drug response in organoids generated from frozen primary tumor tissues. *Sci Rep.* 6:18889.

Weigelt B. et al. 2010. Histological types of breast cancer: How special are they? *Molecular Oncology* Volume 4, Issue 3, June 2010, Pages 192–208

Weigelt, B. et al. 2014. Metaplastic breast carcinoma: more than a special type. *Nat. Rev. Cancer* 14, 147–148.

Welch-Reardon, K. M. et al. 2015. A role for partial endothelial-mesenchymal transitions in angiogenesis? *Thromb Vasc Biol.* 35(2): 303–308.

Wellner, U. et al. 2009. The EMT-activator ZEB1 promotes tumorigenicity by repressing stemness-inhibiting microRNAs. *Nat Cell Biol*. (12):1487-95.

Whittle, B. et al. 2015. Patient-derived xenograft models of breast cancer and their predictive power. *Breast Cancer Research* 17:17

Wiley, S. R. et al. 1995. Identification and characterization of a new member of the TNF family that induces apoptosis. *Immunity* 3(6):673-682.

Wu, Y. et al. 2016. Epithelial-Mesenchymal Transition and Breast Cancer. *J Clin Med.* 5(2): 13.

Y

Yang, J. K. 2008 FLIP as an anti-cancer therapeutic target *Yonsei Med J* 49: 19

Yager, J. D. and Davidson, N.E. 2006. Estrogen carcinogenesis in breast cancer. N Engl J Med 19;354(3):270-82.

Yerbes, R. and Lopez-Rivas, A. 2010. Itch/AIP4-independent proteasomal degradation of cFLIP induced by the histone deacetylase binhibitor SAHA sensitizes breast tumour cells to TRAIL*. Investigational new drugs*. 30(2): 541-547.

Yersal O. and Barutca S. 2014. Biological subtypes of breast cancer: Prognostic and therapeutic implications. *World J Clin Oncol*, 5(3): 412–424.

Yu, M. et al. 2013. Reversal of ATP-binding cassette drug transporter activity to modulate chemoresistance: why has it failed to provide clinical benefit? *Cancer Metastasis Rev*. 2013;32(1–2):211–227. doi: 10.1007/s10555-012-9402-8

Yu, M. et al. 2013. Circulating breast tumor cells exhibit dynamic changes in epithelial and mesenchymal composition. *Science.* 339(6119):580-4.

Z

Zang, F. et al. 2014. C-FLIP(L) contributes to TRAIL resistance in HER2-positive breast cancer. *Biochem Biophys Res Commun.* 18;450(1):267-73.

Zhang, Q. et al. 2015.Tumor recurrence and drug resistance properties of side population cells in high grade ovary cancer. *Drug Res*. 2015;65(3):153–157

Zhang, Q. X. et al. 1997. An estrogen receptor mutant with strong hormone-independent activity from a metastatic breast cancer. *Cancer Res*, 57, 1244-9.

Zhang, N., et al. 2008. The long isoform of cellular FLIP is essential for T lymphocyte Proliferation through an NF-κB-independent pathway. *J. Immunol*. 180:5506–5511.